Sedimented Chemosynthetic Ecosystems of the Southern Ocean

James Benjamin Bell

Submitted in accordance with the requirements for the degree of
Doctor of Philosophy

The University of Leeds
Faculty of Earth and Environment
School of Geography

April 2017

The candidate confirms that the work submitted is his own, except where work which has formed part of jointly authored publications has been included. The contribution of the candidate and the other authors to this work has been explicitly indicated below. The candidate confirms that appropriate credit has been given within the thesis where reference has been made to the work of others.

The work in Chapter 3 of the thesis has appeared in publication as follows:

Geochemistry, faunal composition and trophic structure in reducing sediments on the southwest South Georgia margin. *Royal Society Open Science* (2016) **3**; 160284. **James B. Bell**, Alfred Aquilina, Clare Woulds, Adrian G. Glover, Crispin T. S. Little, William D. K. Reid, Laura E. Hepburn, Jason Newton & Rachel A. Mills

Contributions: JBB was responsible for the literature review; geochemical, taxonomic and isotopic analyses; statistical methods; preparation of plots and figures and for preparing all drafts of the manuscript. AA, CW, AGG, WDKR, LEH and RAM were responsible for collection of samples at sea. Additional geochemical data were collected and analysed by AA, LEH and RAM. JBB was assisted in taxonomic analyses by AGG and CTSL and in elemental and isotopic analyses by CTSL, CW and JN. All authors commented on various draft manuscripts and approved the final version. This manuscript was reviewed by Prof. David Pond (Scottish Association for Marine Science) and Prof. Lisa Levin (Scripps Institute of Oceanography).

The work in Chapter 4 of the thesis has appeared in publication as follows:

Macrofaunal ecology of sedimented hydrothermal vents in the Bransfield Strait, Antarctica. *Frontiers in Marine Science* (2016) **3**: 32. 10.3389/fmars.2016.00032. **James B. Bell**, Clare Woulds, Lee E. Brown, Christopher J. Sweeting, William D. K. Reid, Crispin T. S. Little, and Adrian G. Glover

Contributions: JBB was responsible for the literature review; taxonomic data collection; taxonomic and geochemical data analyses; preparation of figures and all drafts of the manuscript. AGG, CW, WDKR and CJS were responsible for

collection of samples at sea. JBB was assisted in taxonomic analyses by CTSL and AGG and in statistical analyses by CW and LEB. All authors commented on various draft manuscripts and approved the final version. This manuscript was reviewed by Dr Americo Montiel (University of Magallanes, Chile) and Dr Daniella Zeppilli (French Research Institute for Exploitation of the Sea).

The work in Chapter 5 of the thesis under review at the time of submitting this thesis, following an invitation from the Associate Editor to submit a revised version. Manuscript first submitted on the 27th of July 2016. Associate Editor decision 7th December 2016. Revised manuscript submitted 20th December 2016.

Hydrothermal activity lowers trophic diversity in Antarctic sedimented hydrothermal vents. *Biogeosciences* (In review) **James B. Bell**, William D. K. Reid, David A. Pearce, Adrian G. Glover, Christopher J. Sweeting, Jason Newton, & Clare Woulds

Contributions: JBB was responsible for the literature review; preparation of isotope samples; analysis of isotopic data; statistical methods; preparation of figures and all drafts of the manuscript. WDKR, DAP, AGG, CJS and CW were responsible for collection of samples at sea. DAP was responsible for 16S sequencing and interpretation of sediment microbial assemblages. JBB was assisted in isotopic data collection by JN and isotopic data analyses by WDKR and CW. All authors commented on various draft manuscripts and approved the final version.

The work presented in Chapter 6 of the thesis was under initial review at the time of submitting this thesis.

Hydrothermal activity, functional diversity and chemoautotrophy are major drivers of seafloor carbon cycling. *Scientific Reports* (In review) **James B. Bell**, Clare Woulds & Dick van Oevelen.

Contributions: JBB was responsible for the literature review; collation of data; designing and implementing model code; statistical methods; preparation of

figures and all drafts of the manuscript. JBB was assisted in model design; implementation and statistical methods by DvO and in data collation by DvO and CW. All authors commented on various draft manuscripts and approved the final version.

Thesis by Alternative Format (TAF) Rationale

As a consequence of the samples having being collected prior to the commencement of the studentship, primary data collection began shortly following the studentship start date. The student was then able to begin preparing manuscripts within one year of starting and the first article submission was accepted in February 2016 (Chapter 4). Subsequent submissions of the second and third data chapters were made in 2016, with chapter 3 accepted in August 2016 and chapter 5 resubmitted in December 2016, following initial reviews. Chapter 6 was in review at the time of submission. This meant that TAF was considered to be the most appropriate option for the thesis and the data chapters are organised with respect to submitted versions of each of the publications (either accepted or in review). Copies (PDFs) of each of the published manuscripts accompany this thesis as well as each having gold open access at their respective journals. Supplementary material is included as appendices on the attached CD. The student has also contributed to several other publications during the studentship, but only publications lead authored by the student that are relevant to this project are given in the thesis below.

Copyright Declaration

Acknowledgements

I am enormously grateful to several people, whose support has been invaluable to me during the last three and a half years. My supervisors; Clare Woulds, Adrian Glover and Lee Brown have supported me throughout my academic development and I have particularly appreciated the repeated opportunities for self-direction and professional development. I have found the project very fulfilling and certainly hope that this won't be the last contribution I make to marine science.

Further to my two main supervisors, I'd also like to thank the numerous other people whom I've been fortunate enough to work with during the course of my PhD: Will Reid; Cris Little; Jason Newton; Karen Bacon; Laura Hepburn; Alfred Aquilina and Rachel Mills. Thanks also to the generous support of my examiners, Andrew Sweetman and Graeme Swindles. In particular, I'd also like to accord special thanks to Dan Jones and Claudia Alt, whose tireless support at the start of my academic career gave me the chance to get started on all this science business. I would also like to gratefully acknowledge the funding support I have received from NERC and the Natural History Museum.

I would also like to thank my lovely wife, Becci, and my two wonderful daughters, Sophie and Emma for reminding me about the other important things in life, and forcing me to have a work-life balance from time to time. Thank you also to my parents, Nick and Alison, who have helped give me the opportunities to be able to have reached this stage. Even more thanks (in no particular order) to the great friends who've helped me on my way: Jess; Alice; Will; Joe; Owen; Scott; Liz; Sarah (F and L); Freddie; Greta; Fernanda; Adriane; Michelle and Annie.

The completion of this thesis represents a major step in my life's ambition to study the biological wonders of the deep ocean. From the age of six, I had already resolved to become a marine biologist and I am proud to able to say that I have accomplished that and incredibly appreciative of those mentioned above who have helped make it happen.

I have published papers and given talks on deep-sea biology, completed a PhD thesis in deep-sea biology, participated in a deep-sea research cruise and even done stand-up comedy about deep-sea biology. I am a deep-sea biologist.

High fives six-year old self

Abstract

Sedimented chemosynthetic ecosystems (SCEs) are complex seafloor environments that combine several potential sources of organic matter. Their physical similarity to the vast soft-sediment habitats on the seafloor means that they can be inhabited by a diverse range of more ubiquitous fauna. This is in stark contrast to ecosystems such as hard substratum hydrothermal vents, which are typically almost totally dominated by a few specialist species. Another characteristic of these ecosystems is that they exhibit diffuse environmental gradients, relating to chemosynthetic production potential and environmental toxicity. Consequently, it is often difficult to determine their spatial extent, and the ecological responses along such gradients. A central theme of the research presented in this thesis has been to determine the role of habitat-structuring processes at two contrasting SCEs in the Atlantic sector of the Southern Ocean. I demonstrate that these environments elicit significant changes in assemblage structure, trophodynamics and carbon cycles. Chemosynthetic activity generally did not constitute a major proportion of the diet of any assemblage, even at the most hydrothermally active sites, but was detected in macrofaunal food webs at very surprising distances (~ 100km) from the (known) sites of active venting. This research illustrates and examines the impacts that these environments can have upon a range of ecological processes and raises questions about the full extent and significance of chemosynthetic organic matter production in seafloor ecosystems.

Acronyms used in this thesis

Note: Model shorthand used in linear inverse modelling study (Chapter 6) given in Table 6.6.3a.

ACC	–	Antarctic Circumpolar Current
AMI	–	Average Mutual Information
ANOVA	–	Analysis of Variance
ANR	–	*Antimora rostrata*, reference material used in SIA
AOM	–	Anaerobic Oxidation of Methane
AXE	–	The Axe, Bransfield Strait
BOV	–	Bransfield Off-Vent/ Off-Axis
CAR	–	R package, 'Companion to Applied Regression'
cFCI	–	Corrected Finn's Cycling Index
ChEsSo	–	Chemosynthetically-driven Ecosystems South of the Polar Front, NERC Consortium Grant
CMBSF	–	Centimetres below seafloor
CoV	–	Coefficient of Variation
CTJ	–	Chile Triple Junction
dCr	–	Range in Carbon isotopic values
DIC	–	Dissolved Inorganic Carbon
dNr	–	Range in Nitrogen isotopic values
DOC	–	Dissolved Organic Carbon
EK	–	East Kilbride Node, NERC LSMSF
ESR	–	East Scotia Ridge, Southern Ocean
FAME	–	Fatty acid methyl ester
GC-C-IRMS	–	Gas Chromatography Combustion Isotope Ratio Mass Spectrometry
GLM	–	Generalized Linear Model
HI	–	Hydrothermal Index
HR1	–	Hook Ridge Site 1, Bransfield Strait
HR2	–	Hook Ridge Site 2, Bransfield Strait
HSD	–	Tukey's Honestly Significant Difference Test
ICP	–	Inductively coupled plasma (absorption spectroscopy)

JC	–	RRS *James Cook* (see also JC55)
JR	–	RRS *James Clark Ross* (see also JR224)
LIM	–	Linear Inverse Model/ Modelling
LSMSF	–	NERC Life Sciences Mass Spectrometry Facility
MDC	–	Methane-derived Carbon (see also Methane-derived Organic Matter (MDOM))
MDS	–	Multi-Dimensional Scaling
MTE	–	Metabolic Theory of Ecology
MUFA	–	Mono-Unsaturated Fatty Acid
NERC	–	Natural Environment Research Council
OBIS	–	Ocean Biogeographic Information System
OM	–	Organic Matter
PERMANOVA	–	Permutational Analysis of Variance
PLFA	–	Phospholipid Fatty Acid
PUFA	–	Poly-unsaturated Fatty Acid
POC	–	Particulate Organic Carbon
rTCA	–	Reverse Tri-Carboxcylic Acid cycle
SCOC	–	Sediment Community Oxygen Consumption
SEA	–	Standard Elliptical Area
SEA.B	–	Bayesian Standard Elliptical Area
SEAc	–	Sample size corrected Standard Elliptical Area
SG	–	South Georgia
SHV	–	Sedimented Hydrothermal Vent
SIA	–	Stable Isotope Analysis
SIAR	–	R package, 'Stable Isotope Analysis in R' (see also mixSIAR)
SIMPROF	–	Similarity Profile Routine
SPE	–	Solid Phase Extraction
SPP	–	Surface Primary Productivity
TA	–	Total Hull Area
TAF	–	Thesis by Alternative Format
TDF	–	Trophic Discrimination Factor (see also Trophic Enrichment Factor)
TOC	–	Total Organic Carbon
TOS	–	Total Organic Sulphur

TS1	–	The Three Sisters Site 1, Bransfield Strait
TS2	–	The Three Sisters Site 2, Bransfield Strait
TST	–	Total System Throughput
VEGAN	–	R package ‘Vegetation Analysis in R’
WAP	–	West Antarctic Peninsula
XRD	–	X-Ray Diffraction/ Diffractometer

Table of Contents

Table of Figures and Tables

Chapter 1: Introduction

Chemosynthetic activity, the use of reduced chemicals as an energy source for the creation of organic matter, is globally widespread in seafloor ecosystems and has significant impacts upon biodiversity, trophodynamics and nutrient cycling. There is a diverse range of sedimented chemosynthetic ecosystems (SCEs) on the seafloor, including cold seeps, hydrothermal vents and mud volcanoes. These ecosystems are particularly interesting places to study benthic ecology as they are physically similar to background deep-sea sediments but also provide chemosynthetic substrates that support in situ production. This creates significant potential for species overlap between these ecosystems and background areas, unlike hard substratum chemosynthetic ecosystems such as high-temperature hydrothermal vents. Recent research has highlighted the lack of knowledge about ecosystem function in these environments, their extent and how they influence gradients in biodiversity and trophodynamics between chemosynthetic ecosystems and background deep-sea sediments (Bernardino et al. 2012, Levin et al. 2016a). In addition to being important components of regional biodiversity, deep-sea chemosynthetic ecosystems also provide a number of important ecosystem services, such as oceanic iron fertilisation (Aquilina et al. 2014) or suppression of atmospheric methane emissions. In this thesis, I focus upon ecological differences associated with the supply of chemosynthetic substrates to two soft sediment seafloor ecosystems in the Southern Ocean. There is a pressing need to study these ecosystems, which are likely to come under increasing anthropogenic pressure in the future, either from direct impacts (from mining or hydrocarbon extraction) or indirect influences (e.g. climate change driven shifts in pH or temperature). The aim of the present project is to establish how benthic communities respond to environmental differences in and around sedimented chemosynthetic ecosystems in the Southern Ocean.

1.1 *Sedimented hydrothermal vents*

Hydrothermal vents were first discovered in 1977 along the East Pacific Rise (Corliss & Ballard 1977) and have since become recognised to be almost ubiquitous

along plate boundaries in the global ocean. All hydrothermal vents are essentially powered by a largely sub-seafloor convective cell whereby seawater percolates to several kilometres beneath the seafloor (Jannasch & Mottl 1985, Gage & Tyler 1991). Within the crust, seawater becomes heated and undergoes several physico-chemical processes (such as thermochemical sulphate reduction), thereby maturing into hydrothermal fluid (Kawagucci et al. 2013). Once heated, this fluid becomes very buoyant and vents through cracks in the crust or sedimented basins and is expelled into deep-sea bottom waters. The hydrothermal fluid is laden with a cocktail of chemosynthetic substrates, including hydrogen, methane, hydrogen sulphide and certain heavy metals (Bernardino et al. 2012), which in turn can support dense and diverse assemblages of vent-associated microbes and metazoa.

High-temperature, hard substrate hydrothermal vents are characterised by hydrothermal fluid venting from mineralized chimneys at temperatures often in excess of 250˚C. Sedimented hydrothermal vents (SHVs) however occur when hydrothermal fluid flows through marine sediments, creating an environment of high porosity, warm (usually ~10 – 100˚C) sediments that can be more enriched in chemosynthetic substrates like hydrogen sulphide or methane than high-temperature vents (Bernardino et al. 2012). This is because hydrothermal activity increases the thermal degradation rate of sediment organic matter, which accelerates production of these thermogenic substrates (Whiticar & Suess 1990). Sedimented vents are thought to form either through seismic activity creating faults beneath a sedimented basin through which hydrothermal fluid can vent (Gebruk et al. 2000), or as previously high-temperature vent systems that become buried, leaving remnants of mineralized chimneys (Klinkhammer et al. 2001, Reid et al. invited review in prep.). SHVs can occur as independent systems (Klinkhammer et al. 2001) or associated with high-temperature vents as peripheral hydrothermal sediment (Southward et al. 2001, Sweetman et al. 2013) (Figure 1.1a).

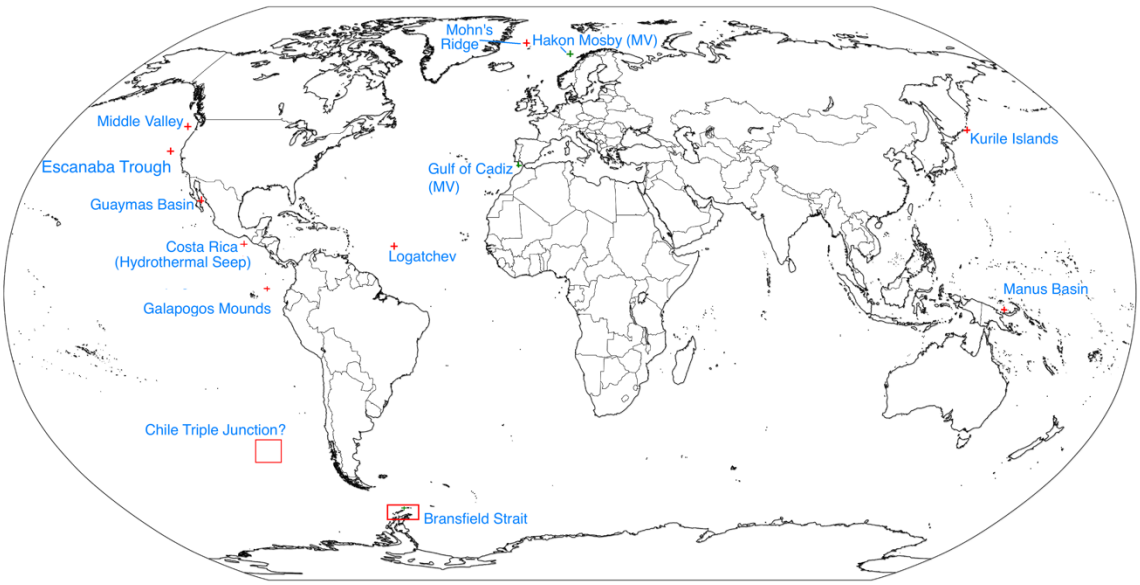

Figure 2.1a – Distribution of known sedimented hydrothermal vent systems and mud volcanoes (MV).

Sedimented vents can support a diverse range of fauna, including both vent endemic species that host chemosynthetic microbial endosymbionts, as well as more ubiquitous deep-sea benthos (Southward et al. 2001, Sahling et al. 2005, Levin et al. 2009, Sweetman et al. 2013, Bell et al. 2016d). The combination of in situ production, temperature differences and the habitat structure creates ecological differences expressed along a gradient of environmental distance, relating to the tolerance of local benthos to sediment toxicity and the importance of food availability (Bernardino et al. 2012, Bell et al. 2016d). In SHVs where surface primary production can be high, the supply of in situ productivity may be less important than at SHVs in less productive seas (Bernardino et al. 2012). Similarly, the supply of hydrothermal fluid can vary widely and so the potential for chemosynthetic production is thus controlled by extrinsic factors that place limits upon the distribution and activity of vent-endemic megafauna or microbial aggregations.

1.2 *Cold Seeps & Reducing Sediments*

Cold seeps have a similar selection of chemosynthetic substrates to SHVs but these substrates are supplied through the dissociation of sub-seafloor deposits of gas

hydrates. At suitable temperatures and pressures, methane is stored in a chemical matrix called a clathrate (Kastner et al. 1998), which per unit volume can store in excess of 160 times the amount methane, compared with the atmosphere (Kvenvolden 1993). Dissociation of this methane from its hydrate causes methane to be supplied to seafloor ecosystems, where it can be metabolized through various processes, such as anaerobic oxidation of methane (AOM). This process is coupled with sulphate reduction, which in turn increases the supply of hydrogen sulphide to these sediments. The result is methane and sulphide rich sediments, which can support populations of chemosynthetic microbes and seep-endemic fauna. This process also increases porewater bicarbonate concentration, giving rise to precipitations of carbonates, ranging from small, localised crusts (Bell et al. 2016b) to large carbonate blocks or pavements (Levin et al. 2015, Levin et al. 2016b).

Since the supply of methane is diffuse within the sediment, it is often difficult to determine the extent of individual seep ecosystems. Although patches of microbial mat or seep-endemic fauna (e.g. *Lamellibrachia* spp. Polychaeta: Siboglinidae) may end abruptly, it is likely that wide areas of peripheral sediments still receive sufficient methane flux to make them geochemically distinct from both the area of focussed methane flow but also background sediments with no methane supply (Bernardino et al. 2012, Levin et al. 2016a). Although fauna in these environments do not have to contend with the temperature stress associated with sediment hydrothermalism, the sulphidic sediments may still provide physiological barriers to colonisation and it is usually the case that a subset of the regional generalist fauna are likely to occupy methane-rich sediments, causing shifts in community composition along gradients of methane flux (Bernardino et al. 2012, Levin et al. 2013, Bell et al. 2016b, Levin et al. 2016a). Just as in other chemosynthetic ecosystems, these ecological gradients are also inevitably influenced by other factors, including depth, latitude and biogeography.

In future climate scenarios, where rising oceanic temperatures are likely to increase the rate at which methane hydrates dissociate, the activity and extent of such ecosystems may increase (Bell 2014, Bell et al. 2016b). This has considerable implications for species distribution and biodiversity, since many of the more

generalist regional fauna of a particular area may be unable to colonise areas of methane flux. The result may be substantial shifts in species distribution and community composition across wide areas of the seafloor. Temperate or high latitude continental shelf regions are likely to be the most vulnerable to these changes, since they are among the areas with the greatest potential for sub-seafloor methane storage (Wood & Jung 2008). Without detailed study of a range of methane-enriched ecosystems in multiple areas of the global ocean, it is very difficult to estimate the kinds of differences that may result from this climactic change. Increased marine methane emissions will also cause a positive feedback loop leading to further temperature increase, as methane is a potent greenhouse gas. Biological suppression of these emissions is considerable, with the majority of methane at the seafloor currently being sequestered as methane-derived carbon (MDC) in microbial or metazoan tissue rather than being released into the surface ocean and atmosphere. Cold seep communities are therefore providers of an important ecosystem service in regulating the atmosphere and global climate.

1.3 *The Southern Ocean*

The Southern Ocean, owing to its relative isolation from the majority of the global ocean has the potential to elicit significant biogeographic differences in resident vent or seep fauna (Rogers et al. 2012) as well as background fauna (Clarke & Crame 1992, Clarke 2008, Clarke & Crame 2010). The Antarctic Circumpolar Current (ACC) creates a permanent frontal system that extends from the surface waters to full ocean depth, separating Antarctic waters from relatively warm seas in the Pacific, Indian and Atlantic Oceans. This hydrographic barrier poses a significant barrier to the transfer of pelagic larva, and some taxa such as decapods are intolerant to the low temperatures of the Southern Ocean (Marsh et al. 2015). In addition to the differences in temperature, the Southern ocean is also geologically complex, with the Scotia back-arc basin having recently separated from the Chile Ridge (~ 20 MYA) and become isolated from the near-continuous ocean ridge system (Breitsprecher & Thorkelson 2009, Vérard et al. 2012, Roterman et al. 2013). The combination of hydrographic and geological processes make the Southern Ocean a unique setting for both generalist fauna or those endemic to vents and seeps. High-temperature

hydrothermal vent fields along the East Scotia Ridge represent a distinct biogeographic province from vents in other areas of the global ocean (Marsh et al. 2012, Rogers et al. 2012), raising questions about the faunal composition of other known chemosynthetic ecosystems in the Southern Ocean. These ecosystems include cold seeps and peripheral methane-rich sediments (Hauquier et al. 2011, Tyler et al. 2011, Römer et al. 2014, Bell et al. 2016b), whale falls (Amon et al. 2013) and sedimented hydrothermal vents (Dählmann et al. 2001, Klinkhammer et al. 2001, Bell et al. 2016c, Bell et al. 2016d). Hydrothermal vents are crucial to species distribution in the Southern ocean as most benthos are adapted to water temperatures between -1.5 and 0˚C (Klinkhammer et al. 2001, Rogers et al. 2012) and relatively sensitive to fluctuations in temperature (Clarke et al. 2009). Thus, the temperature increase associated with hydrothermal venting may prove crucial to Southern Ocean biogeography, and is likely to have very noticeable impacts upon assemblage structure and trophodynamics.

1.4 *Chemosynthesis*

Chemosynthesis is the means by which reduced chemicals are used as an energy source to facilitate the fixation of organic matter. It was first suggested by the Ukrainian microbiologist, Sergei Winogradsky, on the basis of some laboratory experiments with the thiotrophic bacterium *Beggiatoa* spp. (a common resident in seep and vent environments) (Winogradsky 1887, Schwedt et al. 2011). This mechanism was not demonstrated in the deep-sea until around 100 years later (Jannasch & Mottl 1985), but has since become recognised as a dominant source of organic matter for several seafloor environments, including hydrothermal vents, hydrocarbon seeps, mud volcanoes and large organic falls (Dubilier et al. 2008, German et al. 2011, Levin et al. 2016a).

Chemosynthetic reaction pathways are often considered in terms of their substrate (e.g. sulphide oxidation or sulphate reduction). These reactions each depend upon the chemical energy contained within the bonds of various reduced compounds and in certain settings can be cyclical (e.g. sulphate reduction produces sulphide, which in turn can fuel sulphide oxidation).

$$A) \quad H_2S + 2O_2 \rightarrow H_2SO_3^- + e^- + energy$$

$$B) \quad SO_4^{2-} + CH_4 \rightarrow HCO_3^- + HS^- + H_2O + energy$$

$$C) \quad 2O_2 + CH_4 \rightarrow CO_2 + H_2O + energy$$

Equations 1.4a – Common chemosynthetic reaction mechanisms: A) Sulphide oxidation; B) Anaerobic oxidation of methane and C) Aerobic oxidation of methane.

At hydrothermal vents, the relative importance of these pathways depends heavily on the composition of the hydrothermal fluid and the function of the resident microbial assemblages (which to some degree reflects the nature of the fluid composition). At cold seeps and in reducing sediments, chemosynthetic production is predominately through methane and sulphide oxidation (aerobic and anaerobic), with the rate relating to the sediment oxygenation and the supply of methane (and sulphate in the case of AOM).

There a number of enzymatic reaction mechanisms by which chemosynthesis can occur (Hugler et al. 2011) but in principle, they are fairly similar. Electrons from reduced compounds like hydrogen sulphide or methane are used to power the electron transport chain, in place of electrons liberated from water in photosynthesis, which depends upon the energy in light. The most common enzymatic pathways are the reverse tricarboxcylic acid (rTCA) and the Calvin-Benson-Bassham (CBB) cycles (Hugler & Sievert 2011, Reid et al. invited review in prep.) but there are also a number of other possible routes (e.g. Wood-Ljungdahl) that are generally limited to a much smaller subset of chemoautotrophs (Hugler & Sievert 2011).

In seafloor chemosynthetic environments, locally produced organic matter can be made available to metazoan food webs through several means, including: endosymbiosis (e.g. Siboglinid polychaetes); episymbiosis (e.g. Anomuran decapods) and consumption of free-living bacteria (e.g. in colonial ‘mats’) at or below the seafloor. Sedimented systems are of particular interest as they represent less of a physical barrier to background fauna than do ecosystems like hard substratum

vents (Bernardino et al. 2012) but it is still not clear how effectively chemosynthetic activity is able to subsidise local food webs, especially among non-specialist taxa, and on what spatial scales (Levin et al. 2016a).

1.5 *Stable Isotope Ecology*

Stable isotopes (non-radioactive elements with a range of atomic masses) have become widely used in ecology as measures of biological activity and behaviour (Fry 2006). Stable isotopes are useful because of the way that specific reaction pathways alter the ratios between 'heavy' and 'light' isotopes in biological systems. For instance, the ratio between ^{15}N and ^{14}N ($\delta^{15}N$) generally increases during the transfer of organic matter between producer and consumer (predominately through amino acids). This is because trans-amination occurs as the consumer assimilates proteins and amino acids, which discriminates against the heavier isotope, causing a shift in the isotope ratio. Nitrogen isotopes are valuable as discriminators of trophic level, particularly when analysed at the level of different amino acid $\delta^{15}N$ signatures (Chikaraishi et al. 2009) but it is also necessary to have isotopes that are able to discriminate between different food sources. Carbon ($^{13}C/\ ^{12}C$) and sulphur ($^{34}S/\ ^{32}S$) isotope ratios are widely used for this purpose since they are minimally affected by transfer between different trophic levels and therefore stay relatively representative of the original isotope ratio of the food source. Ultimately, all food sources originate from some organic matter fixation pathway, either chemosynthetic or photosynthetic, and the different enzymatic pathways each have a specific impact upon carbon or sulphur isotope ratios. For example, the CBB cycle, a widely used respiration pathway (in both chemo- and photosynthesis) influences the isotope ratio of the carbon source (CO_2) by 11 – 29 ‰, depending upon the specific form of the enzyme involved (Reid et al., in prep). Further to the variation associated with specific reaction mechanisms, isotopic signatures are also strongly influenced by the isotope ratios of the inorganic sources (e.g. vent fluid or seawater DIC) (Walker et al. 2008). In this way, different sources of organic matter can exhibit a range of isotope ratios and, when coupled with nitrogen, provides a framework for determining the diet and trophic position of an individual or species. However, the variability that is inherent in isotope ratios is still a significant source of uncertainty

in applying these techniques. Isotope ratios are fractionated at a number of points during synthesis, transfer and uptake of organic matter and each of these processes has an associated change (± a certain amount). Kinetic isotope fractionation depends upon a range of factors, including the substrate concentration, reaction temperature and the specific reaction process involved (Habicht & Canfield 1997, Canfield 2001). These differences, commonly called trophic discrimination factors (TDFs) or trophic enrichment factors, are responsible for considerably increasing the range of isotope ratios that can by exhibited by an individual or species, even if the target organism is maintaining consistent diet and behaviour (which is in itself rarely a valid assumption) and that the spatio-temporal variation in isotopic signatures of each food source is well characterised.

Process/ Cycle	Major Enzyme	$\delta^{13}C$ shift range (‰)
Calvin-Benson-Bassham	RubisCO Form I	11 - 29
	RubisCO Form II	18 – 23
Reverse Tricarboxylic Acid	Various	2 – 13
Wood-Ljundahl/ Reductive Acetyl-CoA	COdehydrogenase, Acetyl-CoA synthase	2.7 – 8.0 (*Archaeoglobales*) 4.8 – 26.7 (Methanogens)
3-Hydroxypropionate/ 4-Hydroxybutyrate Cycle	4-hydroxybutyryl-CoA dehydratase	0.2 – 3.8
Dicarboxylate/4-Hydroxybutyrate	Various	0.2 – 3.8

Table 1.5 – Isotopic shift ranges associated with different organic matter fixation pathways known from chemosynthetic systems. CBB and rTCA are thought the major means of chemoautotrophy at seafloor chemosynthetic ecosystems (House et al. 2003, Berg et al. 2010, Hugler & Sievert 2011, Reid et al. invited review in prep.).

Stable isotope mixing models have recently become powerful tools for estimating dietary contribution. However, since each food source is generally associated with a specific TDF, they are heavily sensitive to uncertainty in these factors and thus their

use may be compromised where sufficient information is unavailable (Phillips & Gregg 2003, Phillips et al. 2014). Therefore, researchers are recognising the need to develop more detailed techniques to address this uncertainty. One approach is to measure as many of the TDFs and their associated variability as possible but this requires laboratory controlled diet experiments and in cases where the fauna are almost totally unknown (such as the deep-sea), this is generally not a practical solution. This also requires that the laboratory conditions adequately replicate the in situ conditions and this may be difficult, or even impossible, to validate. These models are also not able to discriminate between sources whose isotopic signatures overlap (Phillips et al., 2014).

An alternative approach is to use statistical tools that directly incorporate known uncertainty (Soetaert & van Oevelen 2008, van Oevelen et al. 2009). Linear Inverse Modelling (LIM) is one such means to address the sort of uncertainty that is common in deep-sea ecosystem studies and can be used to estimate the rate of energy or carbon transfer between different components of an ecosystem (van Oevelen et al. 2011a, van Oevelen et al. 2011b, van Oevelen et al. 2012). In a LIM, a wider range of data sources than just stable isotopic data are used, including biomass, growth and respiration rates and supply of OM. These data collectively act to constrain the range of allowable flow rates between given compartments (e.g. detritus to deposit feeder) to what should eventually become a range of ecologically sensible values, within the model's a-priori solution space. The solution space is a N-dimensional construct (where N is the number of possible flows) and represents the total allowable range of values into which a single model solution can fit. The resultant model is then sampled within this space multiple times to generate a probability distribution (so-called likelihood approach) of the parsimonious flow values for each flow.

1.6 *Aims & Objectives*

There remain substantial questions about how chemosynthetic production influences the composition and dynamics of seafloor communities, particularly in the Southern Ocean. This project aims to determine the role of environmental

factors in structuring microbial and faunal characteristics in and around sedimented chemosynthetic ecosystems in two contrasting systems in the Atlantic sector of the Southern Ocean. Using a suite of techniques, including geochemical, taxonomic, molecular and isotopic analyses, this thesis will attempt to take a holistic and comprehensive view of these ecosystems, answering questions such as:

1. How does geochemical variability influence the structure of biological assemblages?
2. How crucial are sedimented chemosynthetic ecosystems in determining regional biodiversity and species distribution in the Southern Ocean?
3. How effectively does chemosynthetic production subsidise the diet of endemic and background fauna?
4. What is the impact of sediment hydrothermalism upon seafloor biogeochemical cycles?
5. How do Southern Ocean SCEs compare to similar systems across the globe?

In addition to these research questions, I will also attempt to place SCEs in the context of future planetary changes and anthropogenic impacts and identify key areas for future improvement. By considering the role of SCEs in modulating patterns in Southern Ocean biodiversity and biogeochemical cycles, we can begin to gain an understanding of the vulnerability of their resident fauna to future change and start to evaluate their candidacy for protected status.

Chapter 2: Materials & Methods

2.1 *Study sites*

This project used samples collected during RRS *James Cook* cruise 55 (JC55) in Jan-Feb 2011 (Tyler et al. 2011). During this cruise, a number of sedimented sites were visited in two areas of the Southern Ocean; the Bransfield Strait and South Georgia. This work is part of the ChEsSo (Chemosynthetically driven ecosystems south of the polar front) NERC consortium project) (Figure 2.1a).

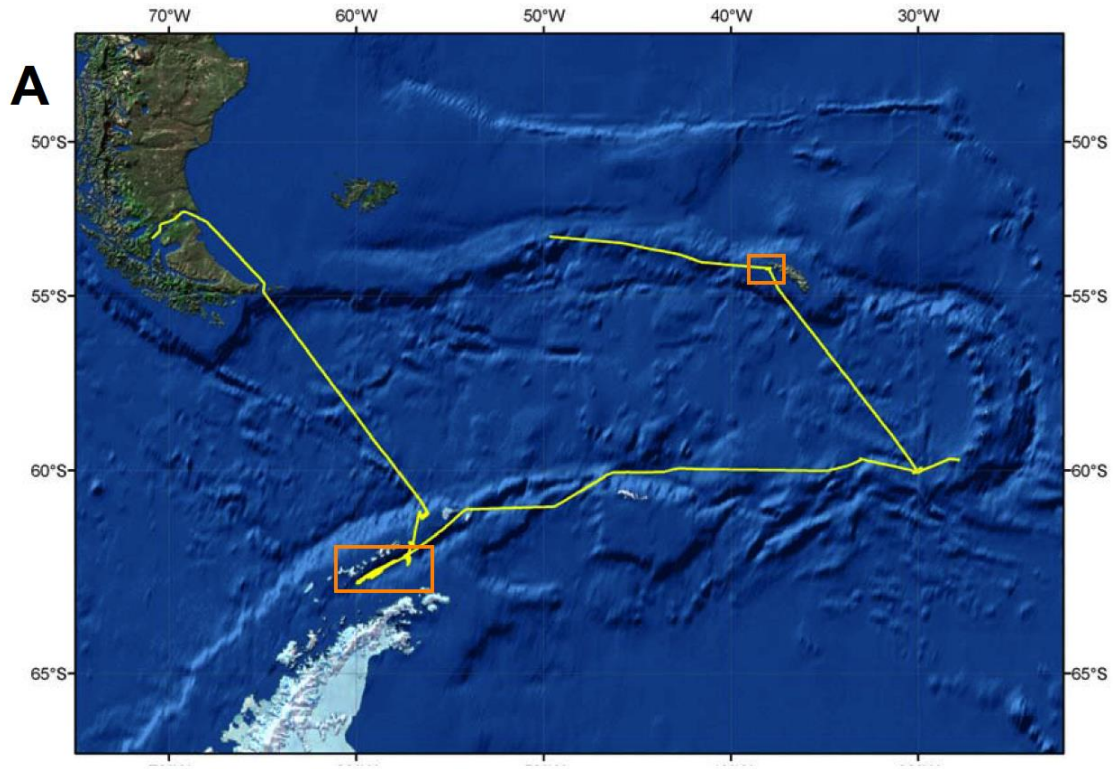

Figure 2.1 b – Cruise track of JC55. Areas of interest for this thesis are highlighted in orange boxes (Figure 1A from Tyler et al. (2011)).

2.1.1 *The Bransfield Strait*

The Bransfield Strait is a slow spreading basin located between the West Antarctic Peninsula and the South Shetland Islands. Along the central basin axis, there are several volcanic edifices, one of which host hydrothermal activity (Dählmann et al. 2001, Klinkhammer et al. 2001, Aquilina et al. 2013). At this site (Hook Ridge), there were remnants of mineral vent chimneys indicating past venting temperatures in

excess of 250˚C (Klinkhammer et al. 2001) but that had apparently since become sedimented. No vent-endemic megafauna were observed but there were extensive areas of chemosynthetic bacterial mat and populations of a macrofaunal species of siboglinid tubeworm (*Sclerolinum contortum*) have been observed at Hook Ridge (Sahling et al. 2005, Aquilina et al. 2013, Georgieva et al. 2015), indicating a potential for chemosynthetic trophic support. However, the Bransfield Strait experiences some of the greatest particle sinking rates across the entire Southern ocean (Wefer & Fischer 1991, Kim et al. 2005), potentially undermining the significance of locally produced organic matter. In these studies, we visited two sites of variable hydrothermal activity at Hook Ridge, as well as several sites where hydrothermal activity was not detected (Tyler et al. 2011). Hydrothermal advection rates, and the flux of chemosynthetic substrates varied widely around Hook Ridge (Aquilina et al. 2013, Aquilina et al. 2014) but hydrothermal products, in the form of thermogenic methane, were also detected throughout the basin (Whiticar & Suess 1990, Aquilina et al. 2013).

2.1.2 *South Georgia*

During a fisheries survey (Belchier et al. 2004), a site of potential methane seepage was identified on the South Georgia continental margin. Sulphidic sediments and metastable authigenic carbonates were discovered at around 250m depth. This area was revisited during RRS *James Cook cruises* 42 and 55 (Rogers et al. 2010, Tyler et al. 2011) during which gravity core and megacore samples were collected for geochemical and faunal analyses (Table 3.4.1 b).

2.2 *Sample collection and analysis*

Megacore samples (0 – 10 cmbsf) were collected from the South Georgia continental margin (Figure 3.3a). In the Bransfield Strait, samples were collected from the volcanic edifices (Hook Ridge, the Three Sisters and the Axe), as well as an off-axis site at a similar depth along the basin margin (Figure 4.4.2a). Core samples were sliced into 0 – 5 and 5 – 10 cmbsf partitions, sieved over a 300μm sieve and

preserved in either 80% ethanol or 10% buffered formalin in seawater. At each site, except the Axe, 3 – 6 replicate deployments were collected from each site. Several cores from each deployment were pooled into single samples, since replicate cores within each deployment are pseudoreplicates.

Geochemical analyses were predominately conducted by researchers at the National Oceanography Centre in Southampton (See methods in Aquilina et al. 2013, Aquilina et al. 2014, Bell et al. 2016b), although some analyses (such as organic carbon profiles) were completed as part of this project (Bell et al. 2016b, Bell et al. 2016d).

2.2.1 *Faunal assemblage data*

Fauna were sorted and counted under a dissecting microscope, using a higher power stereomicroscope or a scanning electron microscope where necessary to describe specific features. Samples were initially picked and sorted to family or class level at the Natural History Museum by George Hallam and Elisa Naeme (University of Leeds), and revised and refined during this project. Annelid and bivalve specimens were sorted to species level and other, less abundant macrofaunal taxa were sorted to family level or higher. To prevent over-estimation of annelid density, only 'complete' specimens (i.e. those with intact heads) were counted, since these taxa can fragment easily during collection and curation. Putative species identities were cross-referenced with taxonomic keys and the Ocean Biogeographic Information System (OBIS) (Fauchald 1977, Fauchald & Jumars 1979, Barnard & Karaman 1991, Beesley et al. 2000, Poore 2001, Kilgallen 2007, Rozemarjin et al. 2011, Reed et al. 2013, Jumars et al. 2015). Representative oligochaete and bivalve specimens were reviewed by expert taxonomists; Christer Erséus (University of Gothenburg) and P Graham Oliver (National Museum of Wales, Cardiff) respectively to confirm species identities. Several of the oligochaete morphospecies were putatively new species but this could not be confirmed as subsequent attempts to sequence their CO1 genes (at University of Gothenburg) failed, likely owing to sub-optimal preservation conditions.

There were a number of morphospecies that could not be assigned confidently to known species identities, suggesting that they may have represented new species. Consideration was given to whether the student should describe these but it was decided that the time required to formally describe a new species was not in the best interest of the project, which has predominately focussed more upon ecological trends, rather than the autecology or morphology of specific taxa. The student contributed data, material and imagery to the description of *Sclerolinum contortum* from Hook Ridge, though this was lead by a colleague at the NHM (Georgieva et al. 2015).

2.2.2 *Stable isotopic sampling*

A combination of bulk and compound-specific stable isotope analyses (SIA) were utilised in this project for carbon, nitrogen and sulphur isotopes. All bulk SIA was conducted at the East Kilbride node of the NERC Life Sciences Mass Spectrometry Centre (EK), including samples of fauna and sediment organic matter. These analyses were supported by the NERC LSMSF steering committee. Compound-specific analyses of phospholipid fatty acids (PLFAs) were conducted at the James Hutton Institute in Aberdeenshire. The formal preparation and analytic procedures for both bulk and compound-specific SIA are detailed in each of the subsequent chapters where necessary. For bulk SIA, samples were submitted as individuals where possible, but low sample dry mass often meant that individuals had to be pooled to permit reliable and precise measurements of isotopic signatures. Specimens were not acidified for the main analyses because; a) sample mass was limiting in most cases and spatial replication was selected over measurement precision and b) preliminary experiments at EK indicated that acidification of annelid and peracarid specimens did not reliably reduce error in carbon isotope measurements but impacted upon nitrogen and sulphur measurements.

2.2.3 *Image analysis*

During JC55, the towed video camera 'SHRIMP' (Seabed High-Resolution Imaging Platform) was deployed at several sites (Hook Ridge, The Three Sisters and South

Georgia) (Tyler et al. 2011). Video imagery from each site was extracted from the original tapes and still frames (JPEGs) were produced (at a rate of 1 frame per second) and were checked visually according to a selection criteria (concerning area of seafloor covered, suspended sediment cover and image quality) to eliminate unsuitable images (Bell et al. 2016a). These still frames were used to create image mosaics, as well as for counting megafaunal morphospecies visible on the seafloor at each site. Here we define megafauna as those species visible and identifiable from seafloor video imagery (Gage & Tyler 1991). The identities of the morphospecies were cross-referenced with Agassiz trawl samples collected in the Bransfield Strait (Tyler et al. 2011). Image data, coupled with area-dry weight relationships from physical samples, were used to estimate faunal biomass in the Bransfield Strait for use as stock sizes in the LIM chapter. A minimum of 150m^2 was analysed from both Hook Ridge sites and from the Three Sisters. This coverage was a balance between proximity to the coring sites and a total area large enough to elucidate community patterns. The Three Sisters data were used as to estimate megafaunal biomass at the off-vent site, since SHRIMP tows were not conducted at this site during JC55.

2.2.4 *Statistical analyses*

Unless explicitly detailed, all analyses were completed in the R statistical environment (R Core Team 2013), using packages listed in the methods section of each chapter (Anderson 2001, Soetaert & van Oevelen 2008, Fox & Weisberg 2011, Baselga et al. 2013, Oksanen et al. 2013, Parnell & Jackson 2013, Whitaker & Christmann 2013).

Chapter 3: Geochemistry, faunal composition and trophic structure in reducing sediments on the southwest South Georgia margin

Royal Society Open Science 160284

James B. Bell[1, 2]*, Alfred Aquilina[3], Clare Woulds[1], Adrian G. Glover[2], Crispin T. S. Little[4], William D. K. Reid[5], Laura E. Hepburn[3], Jason Newton[6] & Rachel A. Mills[3]

[1]School of Geography & Water@Leeds, University of Leeds, LS2 9JT, UK
[2]Natural History Museum, Cromwell Rd, London SW7 5BD, UK
[3]Ocean and Earth Sciences, National Oceanography Centre, University of Southampton, Southampton SO14 3ZH, UK
[4]School of Earth and Environment, University of Leeds, Leeds, LS2 9JT, UK
[5]Ridley Building, School of Biology, Newcastle University, NE1 7RU, UK
[6]NERC Life Sciences Mass Spectrometry Facility, SUERC, East Kilbride G75 0QF, UK

Keywords: Methane; Southern Ocean; Ecology; Assemblage composition; Trophodynamics; Authigenic carbonates

3.1 Abstract

Despite a number of studies in areas of focussed methane seepage, the extent of transitional sediments of more diffuse methane seepage, and their influence upon biological communities is poorly understood. We investigated an area of reducing sediments with elevated levels of methane on the South Georgia margin around 250 m depth and report data from a series of geochemical and biological analyses. Here the geochemical signatures were consistent with weak methane seepage and the role of sub-surface methane consumption was clearly very important, preventing gas emissions into bottom waters. As a result, the contribution of methane-derived carbon to the microbial and metazoan food webs was very limited, although sulphur isotopic signatures indicated a wider range of dietary contributions than was apparent from carbon isotope ratios. Macrofaunal assemblages had high dominance and were indicative of reducing sediments, with many taxa common to other similar environments and no seep endemic fauna, indicating transitional assemblages. Also similar to other cold seep areas, there were samples of authigenic carbonate but rather than occurring as pavements or sedimentary concretions, these carbonates were restricted to patches on the shells of *Axinulus antarcticus* (Bivalvia, Thyasiridae), which is suggestive of microbe-metazoan interactions.

3.2 Introduction

Cold seeps are discontinuous areas of methane and hydrogen sulphide seepage and are widespread in both shallow and deep water (Klauda & Sandler 2005, Naehr et al. 2007). There has been much interest in submarine methane deposits, both for their potential as an energy source but also the threat posed to the climate by the potential release of this potent greenhouse gas (Klauda & Sandler 2005, Wright & Schaller 2013). Thus, the fate of methane in marine sediments is an area of interest for wider climate science (Hinrichs & Boetius 2002, Krüger et al. 2005, Knab et al. 2008). Areas of methane seepage are commonly identifiable by high levels of dissolved methane, bubble plumes/ gas flares or bottom simulating reflectors (Lodolo et al. 1993, Geletti & Busetti 2011, Hart et al. 2011, Römer et al. 2014). High latitude continental shelf regions are areas with potentially widespread methane

storage, particularly in the Arctic and Southern Oceans, where the presence of methane reservoirs has been confirmed or inferred at a number of sites (Kvenvolden et al. 1987, Lodolo et al. 1993, Lodolo et al. 2002, Wood & Jung 2008, Larter et al. 2009, Rogers et al. 2010, Geletti & Busetti 2011, Hauquier et al. 2011, Tyler et al. 2011, Römer et al. 2014). Since methane can provide a basis for chemosynthesis, this has clear implications for biogeochemical cycles and the range of available habitats and biodiversity in the polar oceans (Levin 2005). Methane-enriched, reducing sediments are part of a continuum between cold seeps and background sediments in the deep-sea (Levin et al. 2016a) and may support transitional faunal assemblages. Research into faunal composition and trophic structure in these settings is very limited and here we present for the first time a comprehensive study of geochemical and faunal characteristics of reducing sediments from the Southern Ocean.

Sediments that host an active methane flux to bottom water are often places of elevated biomass and abundance of deep-sea benthos (Levin 2005, Levin & Mendoza 2007, Thurber et al. 2010), representing important, localised sources of organic matter for benthic food webs. Such sediments are characterised by elevated methane and hydrogen sulphide concentrations. Sulphide is produced through sulphate reduction during anaerobic oxidation of methane (AOM) (Habicht & Canfield 1997, Hinrichs et al. 1999, Boetius et al. 2000, Boetius & Suess 2004) and can in turn supply reduced chemical species for chemosynthetic reaction pathways that depend upon sulphide oxidation (Levin et al. 2003, Levin 2005, Levin et al. 2006, Levin et al. 2013). Methane-derived carbon (MDC) is an important metabolic resource at high activity seeps (Levin & Michener 2002, Levin 2005, Levin et al. 2009, Thurber et al. 2010, Levin et al. 2013), but the influence of methane-enriched sediments upon trophic structure in areas of lower methane flux is comparatively unknown. MDC is commonly associated with very low $\delta^{13}C$ signatures (typically -100 to -40 ‰) compared with other sources of organic matter (typically >-30 ‰) (Levin & Michener 2002, Levin & Mendoza 2007). AOM can also yield very low $\delta^{34}S$ signatures as a result of sulphate reduction making stable isotope analysis (SIA) an ideal tool to estimate the extent of MDC utilisation (Habicht & Canfield 1997). Carbon ($\delta^{13}C$: $\delta^{12}C$) and sulphur ($\delta^{34}S$: $\delta^{32}S$) isotope ratios do not fractionate much

between trophic levels and so are useful in detecting differences in food source partitioning. Nitrogen ($\delta^{15}N$: $\delta^{14}N$) isotope ratios provide information on trophic level of individuals or species within a food web as its isotopic signature is increased (~3 ‰ but can vary widely) during the transfer of proteins from source to consumer (Peterson 1999, Canfield 2001, Levin & Michener 2002). Phospholipid Fatty Acids (PLFAs) can also provide useful insights into the relative abundance and isotopic signatures of certain bacterial biomarkers (Boschker et al. 1998, Boschker & Middelburg 2002, Colaço et al. 2007). These compounds degrade quickly following death and so can provide a useful insight into recent microbial activity.

Highly active seeps, typically identified as areas with gas flares or dense aggregations of seep-endemic fauna, have been studied in a number of areas (Dando et al. 1994, Levin 2005, Levin & Mendoza 2007, Thurber et al. 2010, Bernardino et al. 2012). However, the extent, ecology and biogeochemistry of sediments with elevated levels of methane but are not sufficiently deep (Sahling et al. 2003) or methane-enriched to support seep-endemic fauna, is not clear. It is possible that, through ocean warming, submarine methane hydrate deposits, which are globally widespread (Wood & Jung 2008, Piñero et al. 2013) will gradually destabilise as bottom temperatures increase, further increasing the extent of such environments (Pohlman et al. 2013). This investigation of the geochemical and biological processes in methane-enriched sediments provides a basis for estimating possible future ecological scenarios.

3.3 Aims and Hypotheses

Around the sub-Antarctic island of South Georgia (54˚S), numerous cold seep sites have been identified in fjords along the northern margin (Römer et al. 2014), (Figure 3.3a). We present a combined geochemical and faunal study of reducing sediments on the SW South Georgia margin, surveyed during two separate expeditions in 2010 and 2011 (Rogers et al. 2010, Tyler et al. 2011) in order to investigate the role of reducing conditions in marine sediment and its impact upon faunal communities with a view to addressing the following hypotheses: 1) faunal community composition is controlled by the extent of reducing conditions, 2) methane-derived

carbon is a significant basal component of the food web and 3) sediments on the South Georgia margin show geochemical signatures consistent with methane seepage.

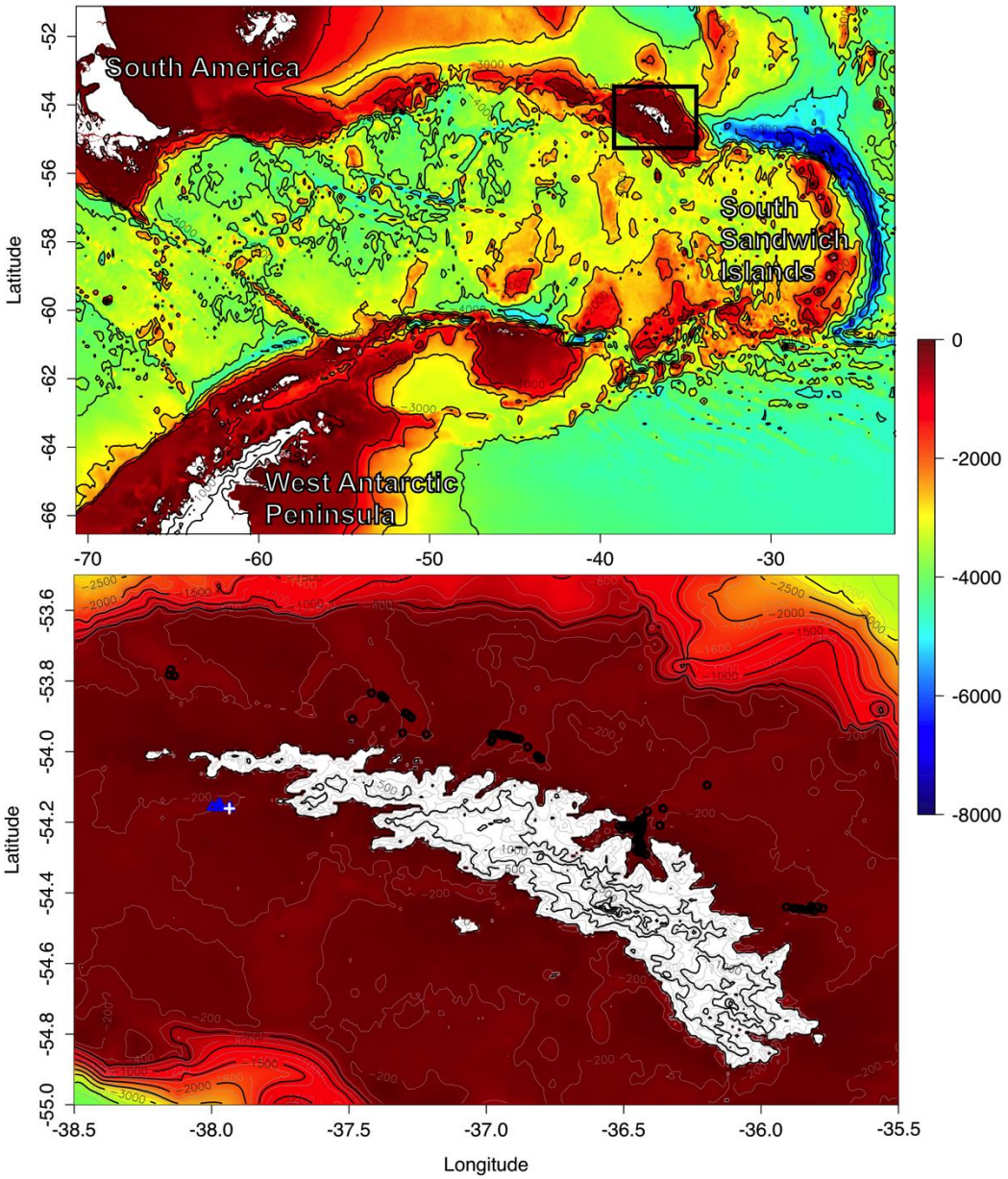

Figure 3.3a – Map of Sampling Locations around South Georgia. Blue triangles indicate JC42 & JC55 sampling stations. Black circles indicate positions of gas flares (Römer et al. 2014) and the white cross shows the location of recovered ikaite crystals (Belchier et al. 2004). Bathymetry data from GEBCO.

3.4 Methods

3.4.1 *Sampling*

An area of potential methane seepage was originally identified on the SW South Georgia margin (Belchier et al. 2004). During a routine fisheries survey, friable samples of what were initially identified as methane hydrate were recovered from a trawl of sulphidic sediments at around 250 m depth (Figure 3.3a; Belchier et al. 2004). Upon closer inspection, and cross-referencing with environmental conditions, it became apparent that these samples were not methane hydrate but were in fact the metastable authigenic carbonate ikaite (Belchier & Larter, pers. comms. See Figure 3.4.1a). The presence of authigenic carbonates, such as ikaite, is sometimes associated with methane seepage (Greinert & Derkachev 2004, Naehr et al. 2007, Levin et al. 2015) and the area was identified as a site of interest for the study of Southern ocean marine chemosynthetic ecosystems, though unfortunately the ikaite crystals quickly degraded after recovery and could not be preserved. During the 'Chemosynthetic Ecosystems South of the Polar Front' research programme, the area was visited during two separate expeditions: RRS *James Cook* 42 (JC42, Jan-Feb 2010) & 55 (JC55, Jan-Feb 2011). We report data from sediment geochemistry samples, taken during JC42 and JC55 (Rogers et al. 2010, Tyler et al. 2011), and faunal samples taken during JC55 (Tyler et al. 2011). We visited 3 stations on the southwest South Georgia margin (Table 3.4.1a) at around 250 m depth, distributed over an area of approximately 7 km^2.

Cruise	Station	Sub-station	Latitude	Longitude	Depth (m)	Faunal Preservation	Use(s)
JC42	02_03	1	-54.1575	-37.9761	257	N/A	Geochemistry
JC55	111	1	-54.1575	-37.9761	257	N/A	Dissolved O_2, PLFAs
	112	1	-54.1575	-37.9761	257	6% Form.	Quant. Macrofauna, Geochemistry, XRD
	113	2	-54.1580	-37.9345	247	80 % Etoh	Macrofaunal SIA, Geochemistry, XRD
	117	3	-54.1475	-37.9717	254	6% Form.	Quant. Macrofauna, Geochemistry, Dissolved O_2
	118	2	-54.1580	-37.9344	247	6% Form.	Quant. Macrofauna, XRD
	119	2	-54.1580	-37.9344	248	80 % Etoh	Macrofaunal SIA
	120	2	-54.1580	-37.9344	248	6% Form.	Quant. Macrofauna, XRD
	121	2	-54.1580	-37.9344	248	6% Form.	Quant. Macrofauna
	122	2	-54.1580	-37.9344	248	80 % Etoh	Macrofaunal SIA, XRD

Table 3.4.1 b – Positions (degrees & decimal minutes), depths and usage of JC42 Gravity core and JC55 megacore deployments on the SW South Georgia Margin. 3 – 4 cores pooled per deployment for quantitative macrofauna. XRD = X-Ray Diffraction, SIA = Stable Isotope Analysis, PLFA = Phospholipid Fatty Acids.

Figure 3.4.1a – Images of seafloor of survey region from towed video platform and crystals of Ikaite recovered (Belchier et al. 2004). Crystal image courtesy of Mark Belchier. Red laser dots 10cm apart.

3.4.2 *Fauna*

Fauna were all sampled during JC55 using a Bowers-Connelly dampened megacorer fitted with eight 10cm diameter tubes (Gage & Bett 2005). Between 1 and 6 deployments were taken from each site (Table 3.4.1a) giving a total area quantitatively sampled of ~1490 cm^2. Between 3 and 4 individual cores were pooled from each corer deployment, as cores from the same deployment are pseudoreplicates (Bell et al. 2016b). Material retained on a 300 µm sieve was either preserved directly in 10 % formalin (in buffered seawater) for quantitative community analyses or live sorted and subsequently preserved in 80 % ethanol for on-board photographic documentation and stable isotope analysis. All faunal

samples were sorted under a dissecting microscope to either species/ morphospecies level (annelid and bivalve taxa) or higher levels for low abundance taxa (e.g. family level for peracarid crustaceans). Species identities were cross-referenced with the Ocean Biogeographic Information System (OBIS).

3.4.3 *Stable Isotopes*

A combination of dual- ($\delta^{13}C$ & $\delta^{15}N$, 91 samples) and tri- ($\delta^{13}C$, $\delta^{15}N$ & $\delta^{34}S$, 35 samples) isotope techniques was used to describe isotopic signatures of 29 species/ morphospecies of macrofauna, sediment organic matter content and profiles of sediment organic carbon. The number of faunal samples submitted for C/N and C/N/S analyses were representative of 88 and 92 % of the total faunal abundance respectively, including the 12 most abundant taxa (1 – 10 replicates per taxa depending upon abundance/ availability of sample mass). Specimens submitted for isotope analyses were pooled if necessary to achieve a specified optimal mass (C/N = 0.7 mg ± 0.5, C/N/S = 2.5 mg ± 0.5). Where possible, individual specimens were submitted as separate samples in order to preserve variance structure within populations (Parnell et al. 2010, Jackson et al. 2011) but in some cases, low sample mass meant individuals had to be pooled (e.g. oligochaetes). Specimens were dried for a minimum of 24 hours at 50°C and weighed in mg (correct to 3 d.p.) into ultra-clean tin capsules and stored in a desiccator whilst awaiting SIA.

Sub-samples of sediment were taken from two cores (112 & 117; Table 3.4.1a) for organic carbon profiles and freeze-dried. Sediment samples (~ 1 mg) were acidified using 6M HCl to remove inorganic carbon. Thus $\delta^{13}C$ analyses were acquired from sediment organic carbon (with the carbon content used to calculate percentage organic carbon). Surface samples of freeze-dried sediment from each site (0 – 1 cmbsf) were also analysed for C/N/S isotopes (untreated for N/S and acidified with 6M HCl for C) (Pohlman et al. 2013).

Only specimens preserved in ethanol were used for SIA in an attempt to regulate the influence of preservation effects. As a result, only faunal specimens from the SE of

the study area could be analysed for isotopic signatures (Table 3.4.1a). Specimens had any attached sediment removed prior to SIA and specimens with carbonate structures (i.e. bivalves) were physically removed from their shells. However, given the low sample mass available and the deleterious effects of acid upon nitrogen and sulphur ratios (Connolly & Schlacher 2013), these could not feasibly be acidified. The vast majority of the species that occurred in sufficient abundance for SIA were annelid taxa with no carbonate structures. A pilot study confirmed that acidification had little impact upon $\delta^{13}C$ measurements and it was considered more appropriate to preserve the integrity of nitrogen and sulphur isotope signatures (Connolly & Schlacher 2013, Bell et al. 2016a) at the expense of a small increase in error for carbon isotope measurements. There are usually substantial differences in signatures of methanotrophic and photosynthetic C-fixation pathways, making mixed diets clearly detectable even with an additional $\delta^{13}C$ error. $\delta^{34}S$ measurements were also available to aid interpretation of diet.

All bulk elemental analyses were completed at the East Kilbride Node of the Natural Environment Research Council Life Sciences Mass Spectrometry Facility in 2015. Samples were analysed by continuous flow isotope ratio mass spectrometer using a Vario-Pyro Cube elemental analyser (Elementar), coupled with a Delta Plus XP isotope ratio mass spectrometer (Thermo Electron). Each of the runs of C/N and C/N/S isotope analyses used laboratory standards (Gelatine and two amino acid-gelatine mixtures) as well as the international standard USGS40 (glutamic acid). C/N/S measurements used the internal standards (MSAG2: (Methanesulfonamide/ Gelatine and Methionine) and the international silver sulphide standards IAEA-S1, S2 and S3. All isotope measurements included samples of freeze-dried, powdered *Antimora rostrata* (ANR), an external reference used in other studies of chemosynthetic ecosystems (Reid et al. 2013, Bell et al. 2016a). This standard was used to monitor instrumental variation between runs, instruments and studies. Machine error for ANR measurements was 0.09, 0.35 and 0.93 for $\delta^{13}C$; $\delta^{15}N$ and $\delta^{34}S$ respectively. Measurements of ANR were similar to previous studies, excepting $\delta^{15}N$ from the tri-isotope run and so these data were discarded. Stable isotope ratios are all reported in delta (δ) per mille (‰) notation, relative to international standards: V-PDB ($\delta^{13}C$); Air ($\delta^{15}N$) and V-CDT ($\delta^{34}S$).

3.4.4 *PLFAs*

Phospholipid fatty acid (PLFA) analyses were completed at the James Hutton Institute, University of Aberdeen using 3.38 g of freeze-dried surface (0 – 1 cm) sediment from megacore deployment 111 (Table 3.4.1a) following the procedure detailed in Main et al. (2015), which we summarise below. Lipids were extracted following a method adapted from (Bligh 1959), using a single phase mixture of chloroform: methanol: citrate buffer (1:2:0.8 v-v:v). Lipids were fractionated using 6 ml ISOLUTE SI SPE columns, preconditioned with 5 ml chloroform. Freeze-dried extract was taken up in 400 µL of chloroform, vortex mixed twice and allowed to pass through the column. Columns were washed in chloroform and acetone (eluates discarded) and finally 10 ml of methanol. Methanol eluates were collected in vials, allowed to evaporate under a N_2 atmosphere and frozen at -20 ˚C.

PLFAs were derivitised with methanol to produce fatty acid methyl esters (FAMEs). Samples were taken up in 1 mL of 1:1 (v:v) mixture of methanol and toluene. 1 mL of 0.2 M KOH (in methanol) was added with a known quantity of the C19 internal standard (nonadecanoic acid), vortex mixed and incubated at 37 ˚C for 15 min. After cooling to room temperature, 2 mL of isohexane: chloroform (4:1 v:v), 0.3 mL of 1 M acetic acid and 2 mL of deionized water was added to each vial. The solution was mixed and centrifuged and the organic phase transferred to a new vial and the remaining aqueous phase was mixed and centrifuged again to further extract the organic phase, which was combined with the previous. The organic phases were evaporated under a N_2 atmosphere and frozen at -20 ˚C.

Samples were taken up in isohexane to perform gas chromatography-combustion-isotope ratio mass spectrometry (GC-C-IRMS). The quantity and $\delta^{13}C$ values of individual FAMEs were determined using a GC Trace Ultra with combustion column attached via a GC Combustion III to a Delta V Advantage isotope ratio mass spectrometer (Thermo Finnigan, Bremen). The $\delta^{13}C$ values (‰) of each FAME were calculated with respect to a CO_2 monitoring gas, traceable to IAEA reference material NBS 19 TS-Limestone. Measurement of the Indiana University reference material

hexadecanoicacid methyl ester (certified $\delta^{13}C_{VPDB}$ 30.74 ± 0.01‰) gave a value of 30.91 ± 0.31‰ (mean ± sd, n=51).

Combined areas of all mass peaks (m/z 44, 45 and 46), following background correction, were collected for each FAME. These areas, relative to the internal C19 standard, were used to quantify abundance of each FAME and related to the PLFAs from which they are derived (Thornton et al. 2011). Compounds were compared with previous studies to identify biomarkers of specific bacterial processes or groups (Kohring et al. 1994, Kharlamenko et al. 1995, Pranal et al. 1996, Boschker et al. 1998, Pond et al. 1998, Colaço et al. 2007, Comeault et al. 2010, Dijkman et al. 2010, Kunihiro et al. 2014, Pond et al. 2014). Bacterial biomass was calculated using transfer functions from the total mass of four PLFAs (i14:0, i15:0, a15:0 and i16:0), estimated at 14 % of total PLFA biomass. PLFA biomass is estimated at 5.6 % of total bacterial biomass (Boschker & Middelburg 2002).

3.4.5 *Geochemistry sampling*

A gravity core (ca. 200 cm long) was retrieved during JC42 from a water depth of 257 m (JC_42_02_03; Table 3.4.1a). This was divided into 50 cm long sections using a circular saw on board, and a nylon wire was used to split each section in two vertically: one half was used for analysis and the other was archived at -20˚C. During JC55, sediment samples were collected using a Bowers & Connelly Megacorer (Gage & Bett 2005) equipped with multiple polycarbonate tubes (10 cm diameter). These sediment cores (18 – 27 cm in length) were retrieved from three sites at water depths of 247 – 257 m (Table 3.4.1a). Gravity core sections and sampled megacores were immediately transferred into a glove bag under oxygen-free (N_2 atmosphere) and temperature-controlled conditions (ca. 4 to 6˚C). Gravity core sections were subsampled with a clean spatula at intervals of 5 – 10 cm. Sampled megacores were manually extruded (at intervals of 1 – 2 cm) into a polycarbonate ring and sectioned using a PTFE sheet that was cleaned with de-ionised water between samples. Bottom water temperatures were 1.2˚C.

3.4.6 *Geochemistry Analysis*

Dissolved methane in sediment samples was measured as soon as possible after core collection using the headspace vial method (Reeburgh 2007). In brief, open-ended, graduated plastic syringes were used to measure an aliquot (3 ml) of wet sediment, which was then extruded into a 20 ml glass vial, followed by 5.0 ml of 1.0 M NaOH to terminate microbial activity. The vial was crimped shut, shaken vigorously for several minutes and left to stand for more than 1 hr. The headspace was then sampled by syringe and the methane was analysed by GC-FID (Agilent 7890A).

Sediment porosity was calculated from the loss of water after drying the sediment at 60˚C assuming densities of 2.6 and 1.025 g cm^{-3} for the sediment and pore fluid, respectively (Sahling et al. 2005).

Shipboard determinations of dissolved oxygen content in the upper sediment were carried out on a dedicated core from two sites (Table 3.4.1a). A Unisense OX50 micro-sensor was calibrated between O_2-saturated and anoxic seawater solutions with temperature and salinity equivalent to bottom waters. Unisense micro-profiling apparatus and SensorTrace PRO software resolved oxygen content at 100 and 200 µm intervals down-core. Oxygen profiles were later surface-normalised to bottom water values determined from water samples taken from deployments near the seafloor to convert to µmol kg^{-1}.

Pore water was separated from the sediment matrix by centrifugation at 12,000 G at 4 ˚C for 10 minutes under N_2; the supernatant fluids were filtered under N_2 through disposable 0.2 µm cellulose nitrate membrane syringe filters (Whatman, UK). Filtered pore waters were divided for H_2S, total alkalinity (TA), dissolved sulphate, and dissolved metals (including Fe and Mn). H_2S, TA and dissolved sulphate were determined onboard and samples for dissolved metal analysis were acidified (pH <2) by adding 2 µl of concentrated HCl (UpA, Romil) per 1ml of sample, pending analysis at the National Oceanography Centre, Southampton. Elemental abundances in porewaters were determined by ICP-atomic absorption spectroscopy (Perkin Elmer Optima 4300DV). Instrument precision was better than 2 % and

measurements of an artificial seawater standard (CRM-SW) were within 1 % of the recommended values.

Total alkalinity and H_2S were measured immediately following pore water extraction: TA by titrating against 0.10 M HCl while bubbling nitrogen through the sample (Ivanenkov & Lyakhin 1978) and H_2S using standard photometric procedures based on formation of methylene blue (Grasshoff et al. 1999). Sulphate was measured by ion chromatography (Dionex ICS2500), with reproducibility better than 2% (determined by repeat analysis of a seawater standard).

3.4.7 *XRD Analyses*

During sorting, it was noted that the valves of *Axinulus antarcticus* (Bivalvia: Thyasiridae; Zelaya, 2010) were often partially coated in deposits of yellow, superficially amorphous material, typically close to the antero-dorsal margin. To determine the composition of these deposits, samples were scraped off the shells of the specimens and analysed using an X-Ray Diffractometer (XRD). Two samples of these deposits were submitted, as well as one of freeze-dried sediment as a control (Table 3.4.1a). Owing to an instrument failure, the first shell deposit sample was analysed using a different instrument to the second shell deposit sample and sediment sample. The first shell deposit sample was analysed using a Bruker D8 diffractometer and a Lynx eye detector. The remaining samples were analysed using a Philips PW1050 diffractometer and a point detector. Both systems used a $\theta/ -2\theta$ goniometer and Cu K α-1 radiation.

3.4.8 *Statistical Analyses*

The following analyses were conducted in the R environment (R Core Team 2013), using the Vegan library (v2.0-8) (Oksanen 2013) unless otherwise specified. Only quantitatively preserved cores were used in assemblage composition analyses. Abundance data from quantitative cores was standardised to individuals per square metre. Community composition from these sites were compared to the composition of Antarctic shelf sediments and cold seep sites in the Pacific (Levin et al. 2010, Neal

et al. 2011, Grupe et al. 2015) using the metaMDS and PERMANOVA routine (999 permutations) (Anderson 2001). Estimated species richness (100 individuals, 999 permutations) was calculated in EstimateS (v9.1.0) (Colwell 2013).

3.5 Results

3.5.1 *Faunal Community Composition*

A total of 4413 animal specimens were counted. Polychaetes dominated all samples (49 – 70 %) with oligochaetes (15 – 34 %) and bivalves (10 – 12 %) accounting for most of the remaining taxa. The most abundant species was *Aphelochaeta glandaria* (Polychaeta: Cirratulidae; Blake, 1996) (1 556 ind. counted, up to 14 420 ind. m^2), but also occurring in significant abundances were *Tubificoides* sp. (Oligochaeta: Tubificidae; Lastočkin, 1937) (500 ind. counted, up to 8 531ind. m^2), *Psamathe fauveli* (Polychaeta: Hesionidae; Averincev, 1962) (664 ind. counted, up to 5 178 ind. m^2) and *Axinulus antarcticus* (Bivalvia) (456 ind. counted, up to 3 756 ind. m^2). Many specimens of *A. antarcticus* had an unidentified hydrozoan attached to the dorsal margin. These hydrozoan specimens fragmented and detached from their hosts and as such their abundance could not be quantified.

Alpha diversity and estimated species richness were qualitatively similar in all deployments (Table 3.5.1a). Sub-station 1 had the greatest proportion of oligochaetes (34 %, compared with 15 – 22 % elsewhere) and the lowest proportion of polychaetes (49 %, compared with 64 – 70 % elsewhere). No significant differences were observed in the composition between each of the substations (PERMANOVA, $F = 0.79$, $p = 0.795$).

JC55 Station	Sub-station	Ind. counted	Ind. m^2	Species	Diversity (H')	Est. species richness (n=100) (±S.D.)
112	1	798	25 402	40	2.27	16.81 (2.55)
117	3	828	35 142	43	2.38	17.60 (2.56)
118	2	990	31 513	45	2.18	17.57 (2.43)
120	2	804	25 593	34	2.18	15.85 (2.24)
121	2	993	31 609	41	2.36	18.23 (2.36)

Table 3.5.1a – Faunal abundance, diversity and species richness of macrofauna from quantitatively sampled cores. Proportion of individuals counted to total density varied as a result of different numbers of pooled cores between deployments.

3.5.2 *Isotopic analyses*

Since only ethanol-preserved specimens were used for isotopic measurements, all faunal samples were from the second sub-station (Table 3.4.1a). Measurements of $\delta^{13}C$ ranged from -26.37 to -15.87 ‰ across all faunal samples (mean: -19.55 ‰ ± S.D. 1.48). $\delta^{15}N$ values ranged from 4.20 – 12.40 ‰ (mean: 8.28 ‰ ± S.D. 1.68) (Figure 3.5.2a). Sediment organic material had low $\delta^{15}N$ values (5.87 ‰ ± 0.91), indicating that it was the base of the food chain for most species. Several species also had a low $\delta^{15}N$ signature similar to sediment organic matter (Figure 3.5.2b), suggesting an additional ^{15}N-depleted source of organic nitrogen. All faunal $\delta^{34}S$ signatures were less than that of surface sediment OM (14.03 ‰ ± 0.12) and varied widely ($\delta^{34}S$ mean: 4.25 ‰ ± S.D. 5.13, range: -9.36 – 14.11 ‰), indicating at least two sources of organic sulphur (Figure 3.5.2c).

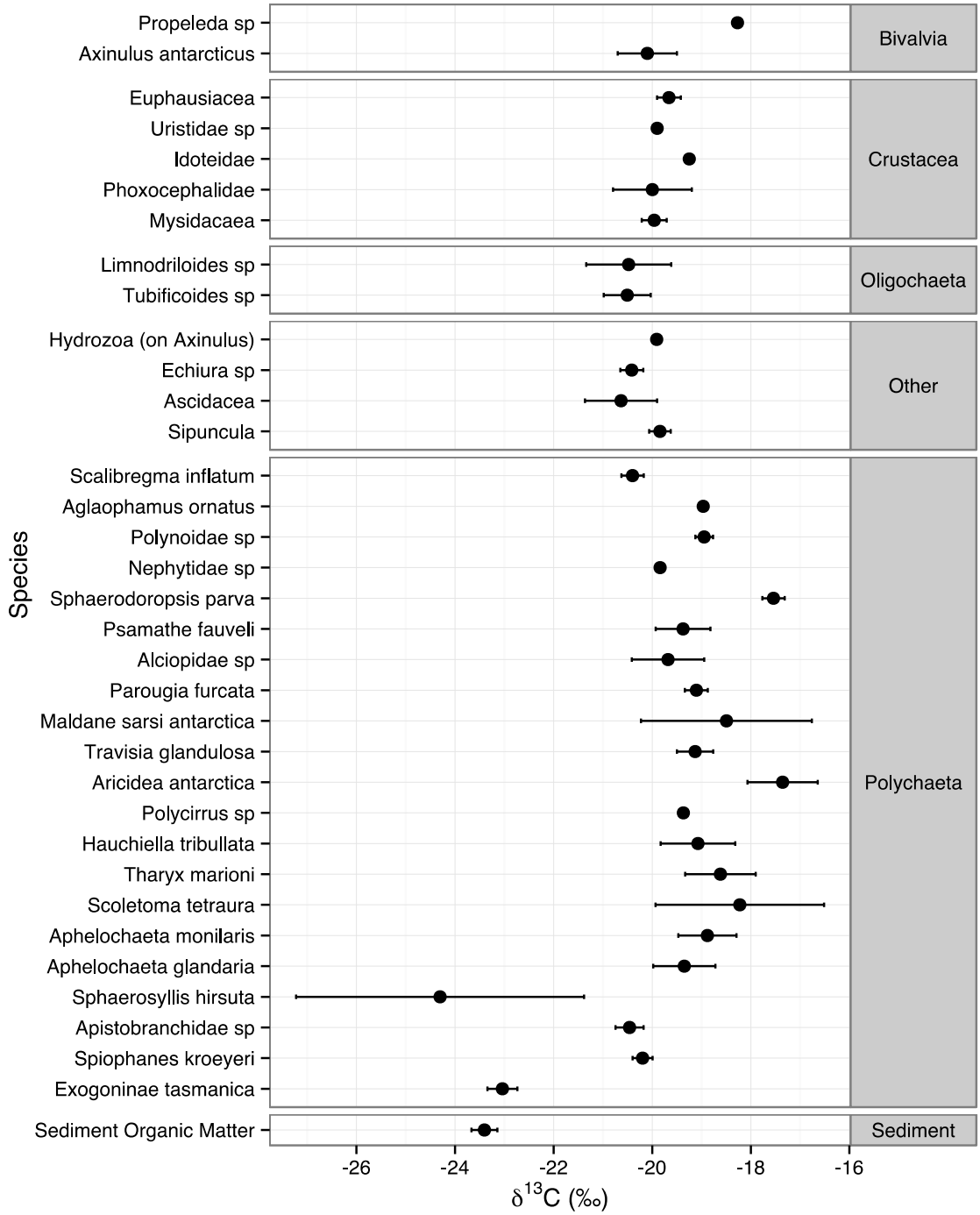

Figure 3.5.2a – Species and sediment organic matter $\delta^{13}C$ ± 1 S. D., grouped by higher taxa.

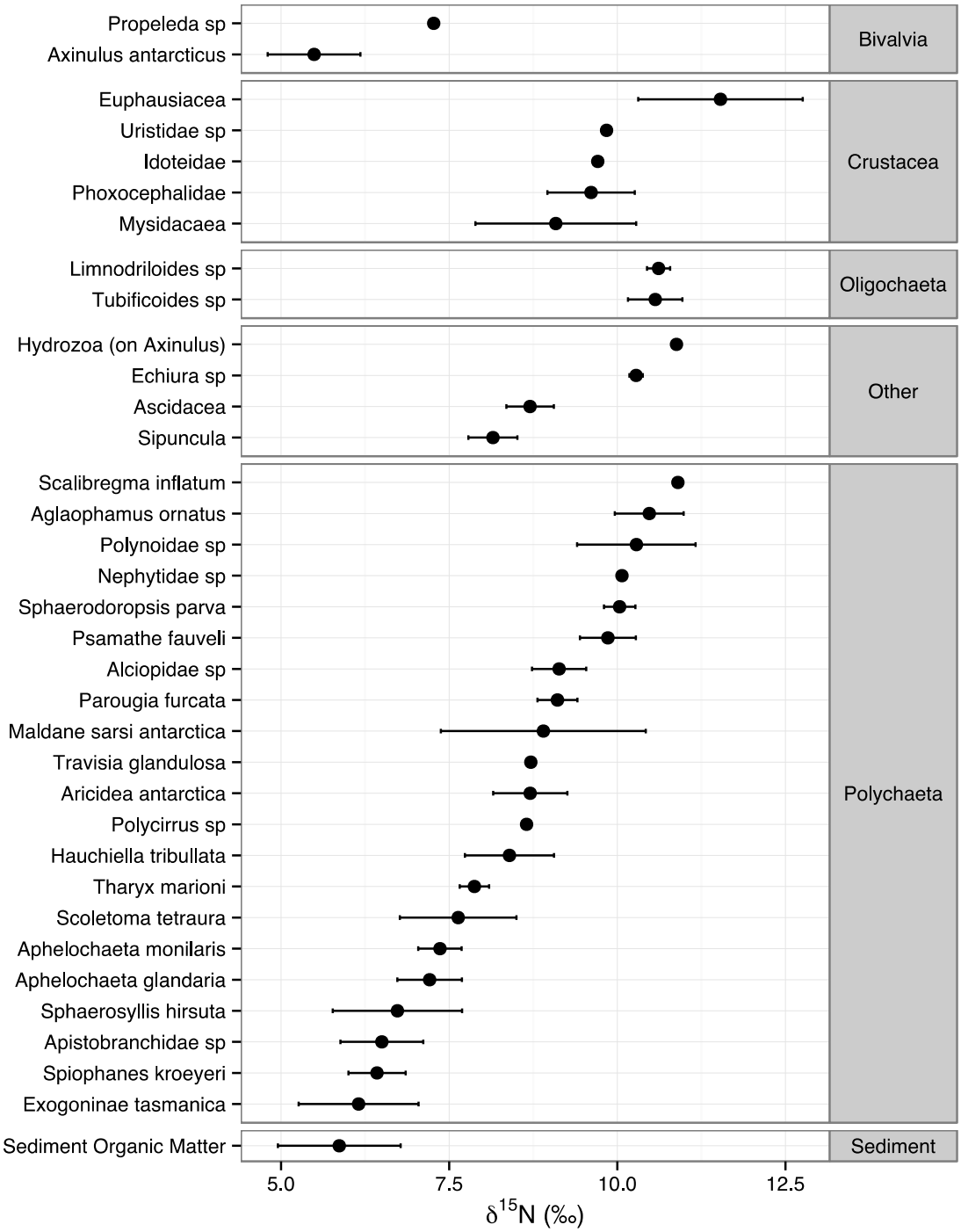

Figure 3.5.2b – Species and sediment organic matter $\delta^{15}N \pm 1$ S. D., grouped by higher taxa.

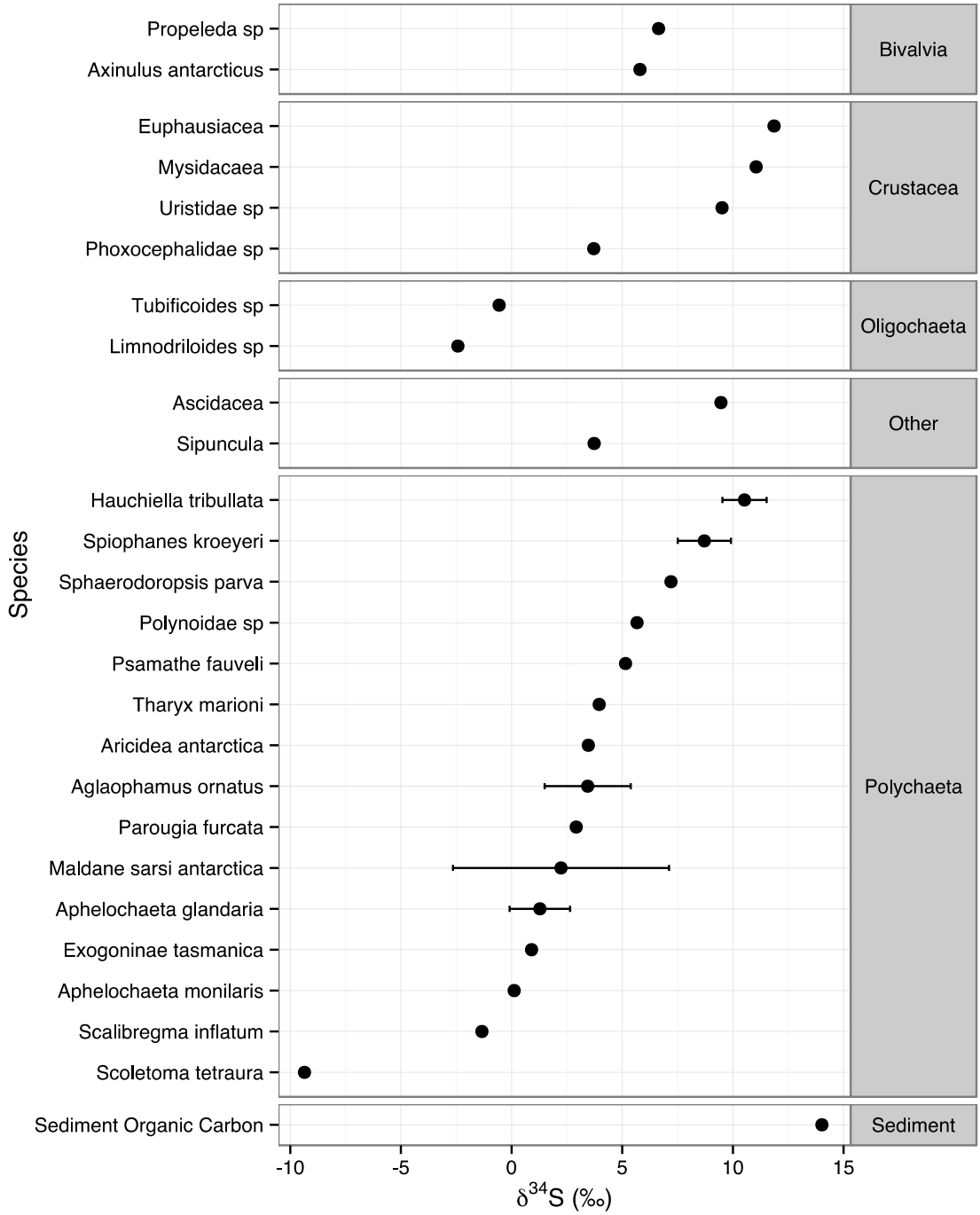

Figure 3.5.2c – Faunal & Sediment organic matter $\delta^{34}S \pm 1$ S. D., grouped by higher taxa.

3.5.3 *PLFAs*

A total of 34 compounds were identified, ranging in concentration between 0.006 – 1.637 μg per g freeze-dried sediment. These were comprised of 15 saturated fatty acids (SFAs), 14 mono-unsaturated fatty acids (MUFAs) and 5 poly-unsaturated fatty acids (PUFAs). Most of the compounds occurred in low abundance (16 < 1 % of total, 29 < 5 %). The most abundant PLFAs were: C16:0 (1.637 μg per g sediment, 16.56 % of total); C16:1ω7c (1.509 μg per g, 15.39 %); C18:1ω(10 or 11) (1.301 μg per g, 13.51 %) and C18:1ω7 (1.188 μg per g, 12.34 %). Carbon isotopic signatures of PLFAs ranged between -45.60 and -23.85 ‰ ($\delta^{13}C$ mean -31.17 ‰). Bacterial total biomass was estimated from the concentration of i14:0, i15:0, ai15:0 and i16:0 at 113.14 μg per g sediment (115.97 μg per cm^3).

3.5.4 *Geochemistry*

Overall, down-core profiles are characterised by distinct geochemical zones indicative of early diagenesis (Figure 3.5.4a). A rapid down-core decrease in dissolved oxygen concentrations occurred in the top 0 – 2 cm, consistent with aerobic oxidation of organic material. Beneath the oxic layer (> 1 – 2 cmbsf; Figure 3.5.4a), in the manganiferous and ferruginous zones, concentrations of dissolved Mn and Fe were elevated, reaching maximum concentrations of 2.4 μmol kg^{-1} and 110 μmol kg^{-1} respectively at station 112. This is consistent with dissimilatory Fe and Mn reduction by microbial activity during organic matter remineralisation. Organic carbon content was consistent downcore, ranging between 1.40 – 1.92 %. Organic carbon $\delta^{13}C$ also did not show downcore changes (Figure 3.5.4a), varying by only ~1 ‰ throughout the entire profile.

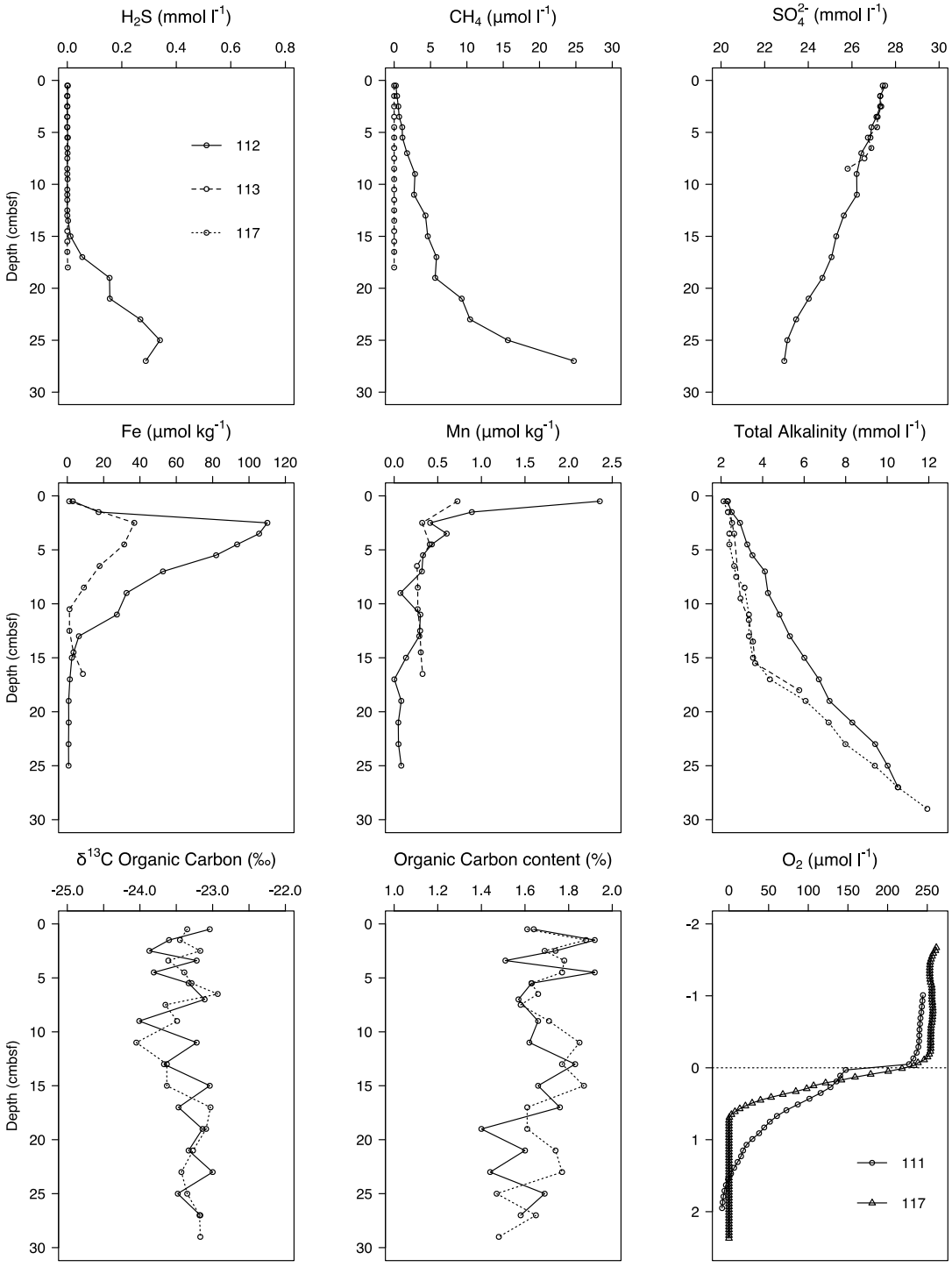

Figure 3.5.4 b - JC55 Megacore profiles. Legend as upper-left for all plots except oxygen (bottom-right)

Pore water concentrations of sulphate decreased down core from the sediment surface, with concomitant increase in sulphide and total alkalinity in both the short megacores (Figure 3.5.4a) and the deeper gravity core samples (Figure 3.5.4b). The rapid increase in dissolved methane with depth, as observed as megacores JC55 112

& 117 below 20 cmbsf (Figure 3.5.4a), and particularly in deeper sections of the gravity core (~ 140 – 160 cmbsf), are indicative of methane production at depth (Figure 3.5.4b).

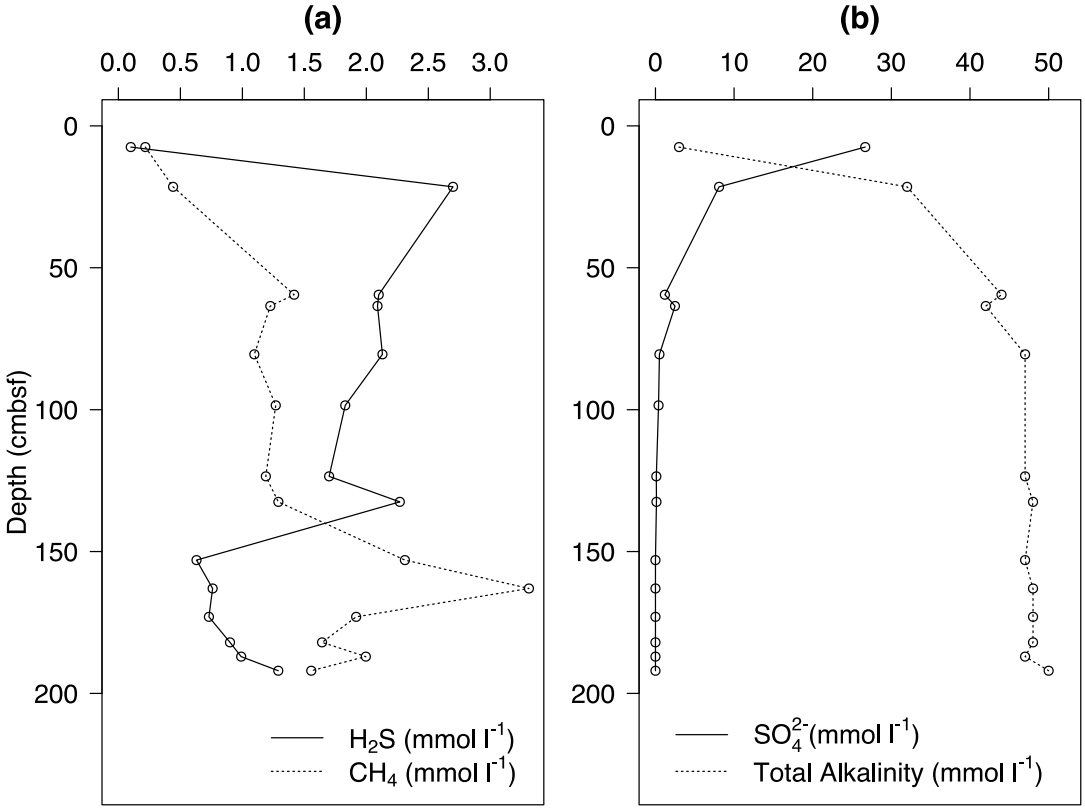

Figure 3.5.4b – JC42 Gravity core profiles. X scale varies

3.5.5 *Authigenic carbonates*

XRD analysis of the superficially amorphous, brittle, yellow deposit on the valves of *Axinulus antarcticus* determined that these deposits were comprised predominately of the carbonates, aragonite and dolomite. A reference sample of freeze-dried sediment did not contain either of these carbonates and the strongest signal was of quartz. One shell deposit sample also contained small signals from mica and chlorite, presumably a contamination from surrounding sediment. Although the carbonate deposits were generally located on specific areas of shell (towards the dorsal margin), they were not consistent in shape and area, indicating that they were not precipitated as part of shell growth.

3.6 Discussion

3.6.1 *Community composition*

Cirratulid polychaetes were by far the most numerous of any macrofaunal family, comprising 27 – 45 % of abundance. Although a cosmopolitan family of deep-sea polychaetes (source: OBIS), their presence has also been documented at several seeps (Levin & Mendoza 2007, Levin et al. 2010, Bernardino et al. 2012, Levin et al. 2015), as well as oxygen minimum zones (Levin et al. 2010) and a sedimented vent in the Bransfield Strait (Bell et al. 2016b). The presence, and high abundance, of tubificid oligochaetes and thyasirid bivalves could be indicative of reducing conditions as both of these families are known from other methane seeps (Dando & Spiro 1993, Dando et al. 1994, Fujiwara et al. 2001, Giere & Krieger 2001, Oliver & Sellanes 2005, Oliver & Holmes 2006, Engel 2007, Bernardino et al. 2012).

No differences were observed in assemblage composition between sites, indicating that the geochemical differences apparent in Fig. 5 were insufficient to influence assemblage structure. The density of *Aphelochaeta* spp., *Axinulus antarcticus* and tubificid oligochaetes accounted for 62 – 72 % of the total and were consistently highly dominant, indicative of reducing conditions at all sites (Bernardino et al. 2012), supporting our suggestion of macrofaunal assemblages structured by sediment geochemistry. Faunal assemblages were compared with others from the West Antarctic Peninsula (WAP) and from seeps in the Pacific (Levin et al. 2010, Neal et al. 2011, Grupe et al. 2015). Assemblage composition was clearly different, at class/ order level to the WAP and Pacific margin seeps (Permanova, $p = 0.001$; Figure 3.6.1a) (Neal et al. 2011). Polychaetes were the dominant class at the WAP and South Georgia (71.3 and 64.1 % respectively) but the South Georgia assemblages contained much higher proportions of oligochaetes and bivalves. Species-level discriminated polychaete assemblages from the WAP (Neal et al. 2011) showed very high dominance (26 – 70 %) of a single spionid species, *Aurospio foodbancsia* (Mincks et al. 2009) in contrast to the dominance of cirratulid polychaetes in South Georgia samples. Spionid polychaetes were comparatively

absent from our sites (0.66 % of total abundance, ~1 % of polychaetes), represented almost entirely by *Spiophanes kroeyeri*. Samples from comparable depths (300 – 500 m) around the South Sandwich Islands (Kaiser et al. 2008) were different to the South Georgia assemblages, being instead dominated by molluscs and malacostracans, with annelids comprising a relatively small component of the assemblages. These samples, whilst not directly comparable owing to differences in sampling techniques (collected by epibenthic sled, as opposed to megacoring), provide evidence of differences between South Georgia and other shelf areas of the East Scotia back-arc basin at several taxonomic levels and support the suggestion that these sediments represent a continuum between seep and background sediments.

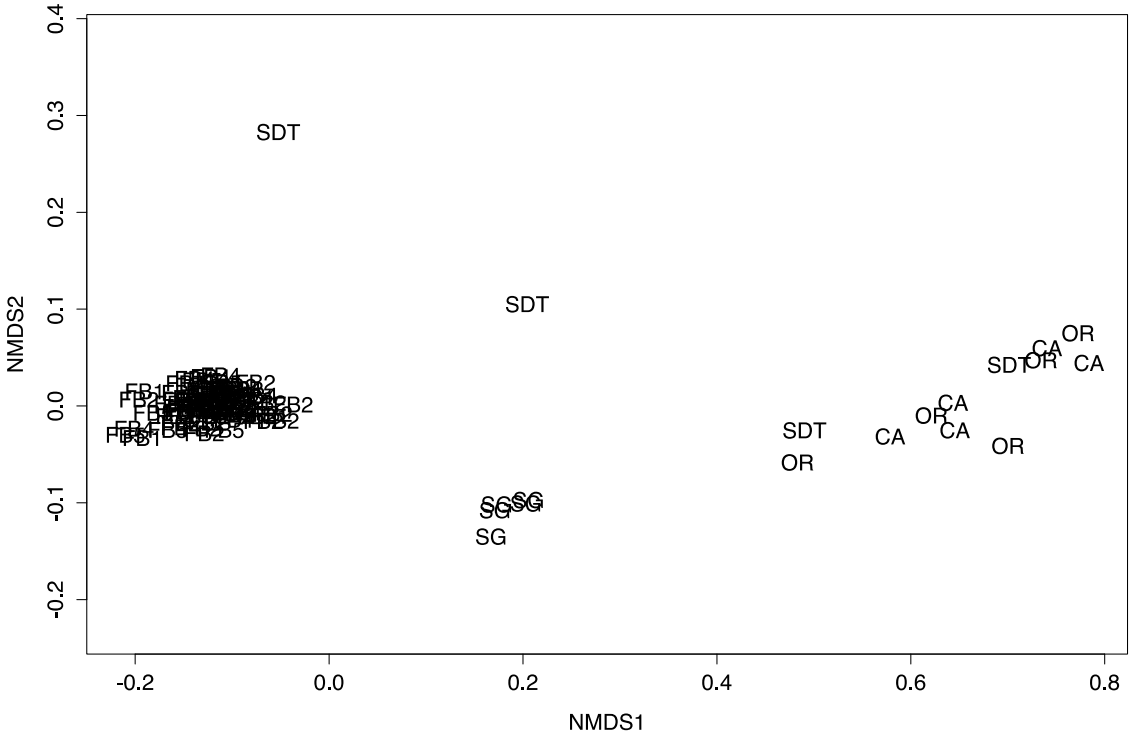

Figure 3.6.1a – Class/ Order level MDS plot of South Georgia macrofauna composition compared to cold seep and background sediments. CA = California margin seeps (Levin et al. 2010); FB = FoodBancs (very tightly clustered), West Antarctic Peninsula (Neal et al. 2011); OR = Oregon margin seeps (Levin et al. 2010); SDT = San Diego Trough seeps (Grupe et al. 2015); SG = South Georgia (this study).

Remotely operated vehicles were deployed during JC42 (ROV *Isis*) and JC55 (Seabed High Resolution Imaging Platform) and undertook visual surveys of areas of interest,

as identified by ship-board echo sounders (EK60) and elevated methane levels in the water column, but no aggregations of microbial mat or seep endemic fauna were observed (Rogers et al. 2010, Tyler et al. 2011). Cold seep sites in the Sea of Okhotsk were also not inhabited by seep-endemic fauna shallower than 370m depth (Sahling et al. 2003) and so absence of seep-endemic fauna from South Georgia sediments may reflect depth-related patterns in assemblage structure or a lack sufficient concentrations of chemosynthetic substrate.

3.6.2 *Trophic Structure and Carbon Sources*

Most metazoan isotope ratios were characteristic of sediment organic matter ($\delta^{13}C_{org}$ -23.40 ‰), which is presumed to be predominately surface-derived OM, with limited in situ production. Estimates of the $\delta^{13}C$ signatures of surface POC at this latitude approximately range between -29 and -24 ‰ (Young et al. 2013). Even in A*xinulus antarcticus*, where authigenic carbonates suggestive of AOM were directly observed, $\delta^{13}C$ signatures of tissue were not indicative of assimilation of MDC (mean $\delta^{13}C$ -20.10 ‰, Figure 3.5.2a). The lack of a strong MDC signal in metazoan tissue indicates that methanotrophy was not a significant contributor to the macrofaunal food web and we suggest that the methane flux was insufficient to support dense aggregations of methanotrophic bacteria at the sediment surface. This is similar to Californian seep sediments (depth 520 m) where macrofauna had an estimated 0 – 5 % dietary contribution of MDC (Levin & Michener 2002). It is probable that, given the relatively high concentration of sulphate in the upper layers of the sediment and the relatively high rate of methane depletion between 20 – 30 cmbsf (Figure 3.5.4a), the majority of AOM activity occurred deeper than the range of the metazoans sampled here (0 – 10 cmbsf). This is consistent with the absence of microbial mats or aggregations of seep-endemic fauna observed during video transects of the area (Larter et al. 2009, Rogers et al. 2010, Tyler et al. 2011). The sub-surface depletion of methane concentration (Figure 3.5.4a) emphasises the role of microbial processes in subsurface methane cycling, limiting potential atmospheric emissions.

Polychaetes of the order Phyllodocida (e.g. alciopids, hesionids, nephtyids and polynoids) were among the taxa with the highest $\delta^{15}N$ values (> 9 ‰, Figure 3.5.2b), indicating that these taxa occupied a higher trophic level. These taxa are all characterised by high activity (large locomotory structures) and mouthparts capable of a predatory lifestyle. However, syllids (*Sphaerosyllis hirsuta* and *Exogoninae (parexogone) tasmanica*) that also possess morphology adapted to carnivory, did not have the same $\delta^{15}N$ enrichment (mean 6.12 ‰) and also had low $\delta^{13}C$ and $\delta^{34}S$ values (Figure 3.5.2a; Figure 3.5.2c). This suggests that these taxa might have derived some of their organic matter from bacterial MDC, consistent with relatively low $\delta^{13}C$ and $\delta^{15}N$ values (Levin et al. 2009, Thurber et al. 2010). *Sphaerosyllis* and *Exogoninae* are common on carbonates at Costa Rica (Levin et al. 2015) and Hydrate Ridge seeps (Levin et al. 2016b) and in Chile Margin hydrothermal sediments (Thurber, Levin unpublished).

Interestingly, some of the highest $\delta^{15}N$ values belonged to tubificid oligochaetes (mean 10.58 ‰ ±S.D. 0.28, Figure 3.5.2b) and an unidentified species of echiuran (mean 10.28 ‰ ±S.D. 0.01, Figure 3.5.2b), consistent with observations of a morphologically similar species of echiuran at a sediment-hosted hydrothermal vent in the Bransfield strait (Bell et al. 2016a). This may indicate selective feeding strategies that favour OM that had been recycled by microbial activity, resulting in a relatively high trophic level. A visual inspection of gut content of tubificid oligochaetes (400x magnification) did not identify any remains that could be attributed to specific food sources.

Sulphur isotope ratios were the most variable of the isotopic data, suggesting diverse feeding strategies between and within taxa (Figure 3.5.2c). Faunal and sediment $\delta^{34}S$ (Mean ± S.D. 4.25 ± 5.13 & 14.03 ‰ ± 0.12 respectively) were also lower than might be expected of non-methane-enriched sediments (18 – 20 ‰ (Reid et al. 2012)), indicating the influence of a relatively ^{34}S-poor source. Low $\delta^{34}S$ values are associated with microbial AOM (Habicht & Canfield 1997, Canfield 2001) as sulphate reduction, which results in low $\delta^{34}S$ signatures, co-occurs with methane oxidation. This suggests that microbial MDC was a component of the macrofaunal food web. Variability in $\delta^{34}S$ signatures was unsupported by carbon isotopic

measurements, which showed relatively little variation and there is a clear disparity between carbon and sulphur isotope composition. This highlights the importance of using multiple stable isotope analysis to elucidate trophodynamics. The disparity between sulphur and carbon isotopic measurements could have resulted from differences in carbon and sulphur processing within the biota or as a result of the highly variable isotopic fractionation associated with sulphate-sulphide exchanges (sulphate reduction and sulphide oxidation) (Canfield 2001). Additionally, it is possible that the relative contribution of AOM to total organic carbon and total organic sulphur may have been different and thus contributing to the differences in ranges observed, though this cannot be assessed from the available data.

Sediment organic carbon $\delta^{13}C$ was generally lighter than most of the faunal measurements (difference in means $\delta^{13}C$ of 3.90 ‰) (Figure 3.5.2a) and may have been a mix of surface-derived material and MDC. The relatively heavy faunal signatures probably resulted from a preservation/ treatment effect rather than an additional, unknown source of organic matter. Isotopic shifts may have arisen from ethanol preservation or the fact that sediment organic carbon samples were acidified but faunal samples were not. Untreated sediment samples had $\delta^{13}C$ values that were 0.66 ‰ greater than acidified sediment samples (Reid et al. 2012). Only faunal samples preserved in ethanol were selected to minimise any faunal preservation effects between different samples. However, ethanol preservation can still impact faunal signatures (Barrow et al. 2008) although this effect can be very variable. A review of isotope shifts associated with preservation effects demonstrated that storing samples in >70 % ethanol significantly increased or decreased carbon isotopic signatures in 4 of 8 published studies. Nitrogen isotopic signatures were significantly affected in 3 out of 5 published studies. Given the variable response to ethanol preservation, it is difficult to correct isotopic signatures but it is likely that preservation effects may have artificially altered some individual faunal isotopic signatures.

3.6.3 *PLFAs*

Although it can be difficult to ascribe PLFAs to specific microbial groups or processes, some compounds are indicative of certain groups (Kharlamenko et al. 1995), especially when they occur in high relative abundance. For example, although the abundant PLFAs C16:1ω7c and C18:1ω7 may be synthesised by a number of groups, including phytoplankton and bacteria (Dijkman et al. 2010, Kunihiro et al. 2014), they occurred in very high abundance in symbiont-bearing species at hydrothermal vents and seeps and are linked to sulphide oxidation (Pranal et al. 1996, Fang et al. 2006, Li et al. 2007, Van Gaever et al. 2009, Riou et al. 2010, Thurber et al. 2013). PLFAs attributed to sulphate reduction and sulphide oxidation at seeps (Li et al. 2007) accounted for 9.3 and 27.7 % of the total abundance respectively. Biomarkers specific to phytoplankton groups, like 20:5ω3 in diatoms (Miyatake et al. 2014), occurred in relatively low abundance (~ 5 % of the total) though this is not to say that the contribution of photosynthetically-derived OM was this low, since other PLFAs are likely to have come from phytoplankton (Dijkman et al. 2010, Miyatake et al. 2014). Photosynthetic PLFAs will also have decayed during sinking and are inevitably under-estimated in such samples.

MUFAs in particular are associated with cold seeps (Kharlamenko et al. 1995, Fang et al. 2006, Colaço et al. 2007, Comeault et al. 2010) and three of the four most abundant FAs were MUFAs, collectively accounting for 41.24 % of the total composition. Whilst these FAs may not be exclusive to methanotrophic bacteria (Dijkman et al. 2010), their high relative abundance is evidence of active (or very recently active) methanotrophy in the upper layers of sediment (0 – 1 cm). Carbon isotopic signatures of PLFAs were generally quite similar to those of reducing sediments in the Gulf of Mexico (Cifuentes & Salata 2001). MUFA $\delta^{13}C$ ranged between -30.73 to -24.55 ‰ suggesting either a very heavy source of methane (compared with biogenic methane), or that these FAs were produced from a combination of methanotrophy and heterotrophic metabolism. Methane with similarly heavy isotopic values is more commonly associated with a hydrothermal origin (Reeves et al. 2011), hence it is unlikely that methane was the sole source of carbon in MUFAs without a very substantial metabolic fractionation effect.

3.6.4 *Geochemistry*

Sulphate showed a steep decline between 0 – 50 cmbsf (Figure 3.5.4b) and there was a concomitant increase in H_2S and alkalinity indicating sulphate reduction was active at these depths. The fact that the sulphate depletion was accompanied by an increase in porewater methane concentrations with depth suggests that anaerobic oxidation of methane may have been active. The sulphate depletion is relatively rapid compared to methane-containing slope sediments on the Norwegian, Gulf of Mexico, Chilean and Argentine margins, where complete depletion of sulphate did not occur above 100, 250, 350 and 400 cmbsf respectively (Hensen et al. 2003, Treude et al. 2005, Coffin et al. 2008, Knab et al. 2008). These sites generally had comparable or higher methane concentrations below the sulphate reduction zone to the South Georgia shelf. These porewater profiles were similar to other sediments where AOM has been directly observed but the approximate depth of complete sulphate depletion was shallower on the South Georgia shelf than elsewhere (Hensen et al. 2003, Coffin et al. 2008, Knab et al. 2008). Sediments with little to no methane flux showed very little decline in porewater sulphate concentrations in the top 5 m of sediment (Hensen et al. 2003). Oxygen penetration depth (Figure 3.5.4a) was less than 2 cmbsf, suggesting that aerobic oxidation of methane was probably very limited.

Despite a relatively steep depletion in methane concentrations between ~20-30 cmbsf, we did not observe a change in the $\delta^{13}C$ of sediment organic carbon (Figure 3.5.4a) that might have resulted from significant rates of methanotrophy. This was likely owing to the small quantities of porewater methane relative to the total mass of organic carbon. We estimate that, if entirely converted into POC, this amount of methane would only have changed the $\delta^{13}C_{org}$ by between 10^{-2} and 10^{-14} ‰ in each core section, depending upon the isotopic signature of the methane which was unknown, but estimated between approximately -80 and -50 ‰ (Whiticar 1999). This potential change is far less than is observable, given the variability in the data and is comparable to $\delta^{13}C_{org}$ profiles at Gulf of Mexico cold seeps (Joye et al. 2004).

3.6.5 *Authigenic carbonates*

Authigenic carbonates have been widely documented at methane seeps, since AOM increases the concentration of bicarbonate in pore waters (Figure 3.5.4a; Figure 3.5.4b) and favours in situ precipitation (Habicht & Canfield 1997, Kharlamenko et al. 2001, Lichtschlag et al. 2010, Deusner et al. 2014, Bell et al. 2016a). Carbonate production at methane seeps can result in several different forms, both low- and high-Mg content, including calcite, aragonite, dolomite and ikaite (Van Lith et al. 2003, Naehr et al. 2007, Magalhães et al. 2012, Levin et al. 2015, Mazzini et al. 2015) and samples of ikaite were previously found on the SW South Georgia margin (Belchier et al. 2004). Our observations were of small, localised carbonate crusts on the shells of *Axinulus antarcticus*, but not on other bivalve species or in the ambient sediment from the area. These observations are in contrast with previous descriptions of large carbonate precipitations within the sediment reported at other seeps (Suess et al. 1982, Vasconcelos et al. 1995, Stakes et al. 1999, Greinert et al. 2002, Greinert & Derkachev 2004, Naehr et al. 2007).

Exterior calcification or encrusting material is known from other bivalve species. For example, some species in the family Veneridae precipitate μm-scale, needle-shaped, aragonite formations on their periostracum (Vasconcelos et al. 1995, Feng & Roberts 2010). Lucinid species, known from chemosynthetic ecosystems, can also precipitate unusual periostracal features, as arrays of scales (Glover & Taylor 2010). Inspection of *A. antarcticus* and other bivalve species present (e.g. *Propeleda* sp. Nuculanidae) under a scanning electron microscope did not reveal similar structures (S4).

Mineral deposits have also been associated with *Montacuta ferruginosa* (Montagu, Montacutidae), in this case a phosphorus-rich ferric mineral that forms part of an epibiotic biofilm (Taylor et al. 2004). These deposits were attributed to a γ-proteobacterial community, utilising iron and were not linked to methanotrophy or AOM, but were similar to hydrothermal vent communities (Gillan et al. 1998, Gillan & De Ridder 2001, 2004). Microbial compositional data were not available here but given the elevated levels of methane, the AOM-associated carbonates present and

the low $\delta^{34}S$ signature of *Axinulus* (relative to sediment), it seems likely that these precipitates were also microbially mediated (Gillan et al. 1998). We suggest that *A. antarcticus* feeding behaviour enhances local fluid flow and thus favours precipitation of carbonates, potentially facilitated by a consortium of anaerobic methanotrophic bacteria (Vasconcelos et al. 1995).

3.7 Conclusions

Macrofaunal assemblage composition was indicative of reducing conditions but the incorporation of methane-derived carbon was apparently very limited to both microbial and metazoan assemblages, similar to off-seep and near-seep areas from other studies. We highlight a disparity between carbon and sulphur isotopic measurements that emphasises the need to use multiple isotopes in the study of trophodynamics in chemosynthetic ecosystems. Geochemical signatures were consistent with weak methane seepage and we demonstrate the role of sub seafloor methane consumption, preventing methane emissions into the bottom water.

3.8 Author Contributions

Conceived and executed the sampling programme at sea: AA, CW, AGG, WDKR, LEH & RAM. Geochemical analyses: AA, LEH, RAM & JBB. Taxonomic analyses: JBB, AGG & CTSL. Isotopic analyses: JBB, CW, WDKR & JN. Elemental analyses: CTSL & JBB. Statistical methods: JBB. Wrote the paper: JBB & AA. Produced plots: JBB. Commented on and approved the paper: JBB, AA, CW, AGG, CTSL, WDKR, LEH, JN & RAM.

3.9 Funding

This work was funded by the NERC ChEsSo consortium (Chemosynthetically-driven Ecosystems South of the Polar Front, NERC Grant NE/DOI249X/I). CW was supported by a bursary from Antarctic Science Ltd. JBB was funded by a NERC PhD Studentship (NE/L501542/1). Isotopic analyses were funded by the NERC Life Sciences Mass Spectrometry Facility (EK246-01/15).

3.10 Acknowledgements

The authors would like to thank the following for their support in this work. We thank the Masters and Crews of RRS *James Clark Ross* cruise 224 and RRS *James Cook* cruises 042 and 055 for technical support and the Cruise Principal Scientific Officers; Professor Alex Rogers and Professor Paul Tyler. We also thank the editor and anonymous reviewers for their valuable contributions and assistance. We gratefully acknowledge taxonomic contributions from P Graham Oliver and Christer Erséus. We also thank: Christopher Sweeting for his assistance in preparing the mass spectrometry grant application and curation of the megafaunal samples; Lesley Neve for the processing and analysis of XRD samples and Barry Thornton for processing and analysis of PLFA samples.

3.11 References

Anderson MJ (2001) A new method for non-parametric multivariate analysis of variance. Austral Ecology 26:32-46

Barrow Lindy M, Bjorndal Karen A, Reich Kimberly J (2008) Effects of Preservation Method on Stable Carbon and Nitrogen Isotope Values. Physiological and Biochemical Zoology 81:688-693

Belchier M, Purves M, Marlow T, Szlakowski J, Collins M, Hawkins S, Mitchell R, Xavier J, Black A (2004) FPRV *Dorada* cruise DOSG04: South Georgia Groundfish Survey, 6th January - 10th February 2004. A report to the Government of South Georgia and the South Sandwich Islands

Bell JB, Reid WDK, Pearce DA, Glover AG, Sweeting CJ, Newton J, Woulds C (2016a) Hydrothermal activity lowers trophic diversity in Antarctic sedimented hydrothermal vents. Biogeosciences Discussions

Bell JB, Woulds C, Brown LE, Little CTS, Sweeting CJ, Reid WDK, Glover AG (2016b) Macrofaunal ecology of sedimented hydrothermal vents in the Bransfield Strait, Antarctica. Frontiers in Marine Science 3:32

Bernardino AF, Levin LA, Thurber AR, Smith CR (2012) Comparative Composition, Diversity and Trophic Ecology of Sediment Macrofauna at Vents, Seeps and Organic Falls. Plos ONE 7:e33515

Bligh EG (1959) A rapid method of total lipid extration and purification. Canadian Journal of Biochemistry and Phsiology 37:911-917

Boetius A, Ravenschlag K, Schubert CJ, Rickert D, Widdel F, Gieseke A, Amman R, Jørgensen BB, Witte U, Pfannkuche O (2000) A marine microbial consortium apparently mediating anaerobic oxidation of methane. Nature 407:623-626

Boetius A, Suess E (2004) Hydrate Ridge: a natural laboratory for the study of microbial life fueled by methane from near-surface gas hydrates. Chemical Geology 205:291-310

Boschker HT, Middelburg JJ (2002) Stable isotopes and biomarkers in microbial ecology. FEMS Microbiology Ecology 40:85-95

Boschker HT, Nold SC, Wellsbury P, Bos D, de Graaf W, Pel R, Parkes RJ, Cappenberg TE (1998) Direct linking of microbial populations to specific biogeochemical processes by 13C-labelling of biomarkers. Nature 392:801-805

Canfield DE (2001) Isotope fractionation by natural populations of sulfate-reducing bacteria. Geochimica Et Cosmochimica Acta 65:1117-1124

Cifuentes LA, Salata GG (2001) Significance of carbon isotope discrimination between bulk carbon and extracted phspholipid fatty acids in selected terrestrial and marine environments. Organic Geochemistry 32:613-621

Coffin R, Hamdam L, Plummer R, Smith J, Gardner J, Hagen R, Wood W (2008) Analysis of methane and sulfate flux in methane-charged sediments from the Mississippi Canyon, Gulf of Mexico. Marine and Petroleum Geology 25:977-987

Colaço A, Desbruyères D, Guezennec J (2007) Polar lipid fatty acids as indicators of trophic associations in a deep-sea vent system community. Marine Ecology 28:15-24

Colwell RK (2013) *EstimateS*: Statistical estimation of species richness and shared species from samples. Version 9. Persistent URL <purloclcorg/estimates>

Comeault A, Stevens CJ, Juniper SK (2010) Mixed photosynthetic-chemosynthetic diets in vent obligate macroinvertebrates at shallow hydrothermal vents on Volcano 1, South Tonga Arc - evidence from stable isotope and fatty acid analyses. Cahiers De Biologie Marine 51:351-359

Connolly RM, Schlacher TA (2013) Sample acidification significantly alters stable isotope ratios of sulfur in aquatic plants and animals. Marine Ecology Progress Series 493:1-8

Dando PR, Bussmann I, Niven SJ, O'Hara SCM, Schmaljohann R, Taylor LJ (1994) A methane seep area in the Skagerrak, the habitat of the pogonophore *Siboglinum poseidoni* and the bivalve mollusc *Thyasira sarsi*. Marine Ecology Progress Series 107:157-167

Dando PR, Spiro B (1993) Varying nutritional dependence of the thyasirid bivalves Thyasira sarsi and T. equalis on chemo-autotrophic symbiontic bacteria, demonstrated by isotope ratios of tissue carbon and shell carbonate. Marine Ecology Progress Series 92:151-158

Deusner C, Holler T, Arnold GL, Bernasconi SM, Formolo MJ, Brunner B (2014) Sulfur and oxygen isotope fractionation during sulfate reduction coupled to anaerobic oxidation of methane is dependent on methane concentration. Earth and Planetary Science Letters 399:61-73

Dijkman NA, Boschker HTS, Stal LJ, Kromkamp JC (2010) Composition and heterogeneity of the microbial community in a coastal microbial mat as revealed by the analysis of pigments and phospholipid-derived fatty acids. Journal of Sea Research 63:62-70

Engel AS (2007) Observations on the biodiversity of sulfidic karst habitats. Journal of Cave and Karst Studies 69:187-206

Fang J, Shizuka A, Kato C, Schouten S (2006) Microbial diversity of cold-seep sediments in Sagami Bay, Japan, as determined by 16S rRNA gene and lipid analyses. FEMS Microbiol Ecol 57:429-441

Feng D, Roberts HH (2010) Initial results of comparing cold-seep carbonates from mussel- and tubeworm-associated environments at Atwater Valley lease block 340, northern Gulf of Mexico. Deep Sea Research Part II: Topical Studies in Oceanography 57:2030-2039

Fujiwara Y, Kato C, Masui N, Fujikura K, Kojima S (2001) Dual symbiosis in the cold-seep thyasirid clam Maorithyas hadalis from the hadal zone in the Japan Trench, western Pacific. Marine Ecology Progress Series 214:151-159

Gage JD, Bett BJ (2005) Deep-sea benthic sampling. In: Holmes NA, McIntyre AD (eds) Methods for the study of the marine benthos. Blackwell Scientific Publications, Oxford

Geletti R, Busetti M (2011) A double bottom simulating reflector in the western Ross Sea, Antarctica. Journal of Geophysical Research 116:B04101

Giere O, Krieger J (2001) A triple bacterial endosymbiosis in a gutless oligochaete (Annelida): ultrastructural and immunocytochemical evidence. Invertebrate Biology 120:41-49

Gillan DC, De Ridder C (2001) Accumulation of a ferric mineral in the biofilm of Montacuta ferruginosa (Mollusca, Bivalvia). Biomineralization, bioaccumulation, and inference of paleoenvironments. Chemical Geology 177:371-379

Gillan DC, De Ridder C (2004) Iron encrustation of the bivalve Montacuta ferruginosa. Journal of the Marine Biological Association of the United Kingdom 84:1213-1214

Gillan DC, Speksnijder AGCL, Zwart G, De Ridder C (1998) Genetic Diversity of the Biofilm Covering Montacuta ferruginosa (Mollusca, Bivalvia) as Evaluated by Denaturing Gradient Gel Electrophoresis Analysis and Cloning of PCR-Amplified Gene Fragments Coding for 16S rRNA. Applied Environmental Microbiology 64:3464-3472

Glover EA, Taylor JD (2010) Needles and pins: acicular crystalline periostracal calcification in venerid bivalves (Bivalvia: Veneridae). Journal of Molluscan Studies 76:157-179

Grasshoff L, Ehrhardt M, Kremling K, Anderson L (1999) Methods of Seawater Analysis. Wiley-VCH, Weinheim

Greinert J, Bollwerk SM, Derkachev A, Bohrmann G, Suess E (2002) Massive barite deposits and carbonate mineralization in the Derugin Basin, Sea of Okhotsk: precipitation processes at cold seep sites. Earth and Planetary Science Letters 203:165-180

Greinert J, Derkachev A (2004) Glendonites and methane-derived Mg-calcites in the Sea of Okhotsk, Eastern Siberia: implications of a venting-related ikaite/glendonite formation. Marine Geology 204:129-144

Grupe BM, Krach ML, Pasulka AL, Maloney JM, Levin LA, Frieder CA (2015) Methane seep ecosystem functions and services from a recently discovered southern California seep. Marine Ecology 36:91-108

Habicht KS, Canfield DE (1997) Sulfur isotope fractionation during bacterial sulfate reduction in organic-rich sediments. Geochimica Et Cosmochimica Acta 61:5351-5361

Hart PE, Pohlman JW, Lorenson TD, Edwards BD Beaufort Sea Deep-Water Gas Hydrate Recovery from a Seafloor Mound in a region of widespread BSR occurrence. Proc Proceedings of the 7th International Conference on Gas Hydrates

Hauquier F, Ingels J, Gutt J, Raes M, Vanreusel A (2011) Characterisation of the nematode community of a low-activity cold seep in the recently ice-shelf free Larsen B area, Eastern Antarctic Peninsula. PLoS One 6:e22240

Hensen C, Zabel M, Pfeifer K, Schwenk T, Kasten S, Riedinger N, Schulz HD, Boetius A (2003) Control of sulfate pore-water profiles by sedimentary events and the significance of anaerobic oxidation of methane for the burial of sulfur in marine sediments. Geochimica et Cosmochimica Acta 67:2631-2647

Hinrichs KU, Boetius A (2002) The anaerobic oxidation of methane: new insights in microbial ecology and biogeochemistry. In: Wefer G, Billett D, Jorgensen BB, Schluter M, van Weering T (eds) Ocean Margin Systems. Springer, Heidelberg

Hinrichs KU, Hayes JM, Sylva SP, Brewer PG, DeLong EF (1999) Methane-consuming archaebacteria in marine sediments. Nature 398:802-805

Ivanenkov V, Lyakhin Y (1978) Determination of total alkalinity in seawater. In: Borodovsky OK, Ivanenkov V (eds) Methods of hydrochemical investigations in the ocean. Nauka Publishing House, Moscow

Jackson AL, Inger R, Parnell AC, Bearhop S (2011) Comparing isotopic niche widths among and within communities: SIBER - Stable Isotope Bayesian Ellipses in R. The Journal of animal ecology 80:595-602

Joye SB, Boetius A, Orcutt BN, Montoya JP, Schulz HN, Erickson MJ, Lugo SK (2004) The anaerobic oxidation of methane and sulfate reduction in sediments from Gulf of Mexico cold seeps. Chemical Geology 205:219-238

Kaiser S, Barnes DKA, Linse K, Brandt A (2008) Epibenthic macrofauna associated with the shelf and slope of a young and isolated Southern Ocean island. Antarctic Science 20

Kharlamenko VI, Kiyashko SI, Imbs AB, Vyshvartzev DI (2001) Identification of food sources of invertebrates from the seagrass Zostera marina community using carbon and sulfur stable isotope ratio and fatty acid analyses. Marine Ecology Progress Series 220:103-117

Kharlamenko VI, Zhukova NV, Khotimchenko SV, Svetashev VI, Kamenev GM (1995) Fatty-acids as markers of food sources in a shallow-water hydrothermal ecosystem (Kraternaya Bight, Yankich island, Kurile Islands). Marine Ecology Progress Series 120:231-241

Klauda JB, Sandler SI (2005) Global Distribution of Methane Hydrate in Ocean Sediment. Energy & Fuels 19:459-470

Knab NJ, Cragg BA, Borowski C, Parkes RJ, Pancost R, Jørgensen BB (2008) Anaerobic oxidation of methane (AOM) in marine sediments from the Skagerrak (Denmark): I. Geochemical and microbiological analyses. Geochimica et Cosmochimica Acta 72:2868-2879

Kohring L, Ringelberg D, Devereuk R, Stahl DA, Mittelman MW, White DC (1994) Comparison of phylogenetic relationships based on phospholipid fatty acid profiles and ribosomal RNA sequence similarities among dissimiltory sulfate-reducing bacteria. Fems Microbiology Letters 119:303-308

Krüger M, Treude T, Wolters H, Nauhaus K, Boetius A (2005) Microbial methane turnover in different marine habitats. Palaeogeography, Palaeoclimatology, Palaeoecology 227:6-17

Kunihiro T, Veuger B, Vasquez-Cardenas D, Pozzato L, Le Guitton M, Moriya K, Kuwae M, Omori K, Boschker HT, van Oevelen D (2014) Phospholipid-derived fatty acids and quinones as markers for bacterial biomass and community structure in marine sediments. PLoS One 9:e96219

Kvenvolden KA, Golan-Bac M, Rapp JB (1987) Hydrocarbon Geochemistry of Sediments Offshore from Antarctica: Wilkes Land Continental Margin. CPCEMR Earth Science Series 5A:205-213

Larter RD, Tyler PA, Connelly DP, Copley J, Rogers A, Bennett SA, Flouquet CFA, Graham AG, Hilario A, Ramirez-Llodra EZ, Beaton AD, Owsianka DR, Afanasayev V, Cooper JSP, Mason PJ, Wilis DD (2009) RRS James Clark Ross Cruise JR224: Chemosynthetically-driven Ecosystems South of the Polar Front consortium programme. BODC Cruise Report

Levin LA (2005) Ecology of Cold Seep Sediments: Interactions of Fauna with flow, chemistry and microbes. Oceanography and Marine Biology: An Annual Review 43:1-46

Levin LA, Baco AR, Bowden D, Colaço A, Cordes E, Cunha MR, Demopoulos A, Gobin J, Grupe B, Le J, Metaxas A, Netburn A, Rouse GW, Thurber AR, Tunnicliffe V, Van Dover C, Vanreusel A, Watling L (2016a) Hydrothermal Vents and Methane Seeps: Rethinking the Sphere of Influence. Frontiers in Marine Science 3:72

Levin LA, Mendoza GF (2007) Community structure and nutrition of deep methane-seep macrobenthos from the North Pacific (Aleutian) Margin and the Gulf of Mexico (Florida Escarpment). Marine Ecology 28:131-151

Levin LA, Mendoza GF, Gonzalez JP, Thurber AR, Cordes EE (2010) Diversity of bathyal macrofauna on the northeastern Pacific margin: the influence of methane seeps and oxygen minimum zones. Marine Ecology 31:94-110

Levin LA, Mendoza GF, Grupe BM (2016b) Methane seepage effects on biodiversity and biological traits of macrofauna inhabiting authigenic carbonates. Deep Sea Research Part II: Topical Studies in Oceanography

Levin LA, Mendoza GF, Grupe BM, Gonzalez JP, Jellison B, Rouse G, Thurber AR, Waren A (2015) Biodiversity on the Rocks: Macrofauna Inhabiting Authigenic Carbonate at Costa Rica Methane Seeps. PLoS One 10:e0131080

Levin LA, Mendoza GF, Konotchick T, Lee R (2009) Macrobenthos community structure and trophic relationships within active and inactive Pacific hydrothermal sediments. Deep Sea Research Part II: Topical Studies in Oceanography 56:1632-1648

Levin LA, Michener RH (2002) Isotopic evidence for chemosynthesis-based nutrition of macrobenthos: The lightness of being at Pacific methane seeps. Limnology and Oceanography 47:1336-1345

Levin LA, Ziebis W, Mendoza GF, Bertics VJ, Washington T, Gonzalez J, Thurber AR, Ebbed B, Lee RW (2013) Ecological release and niche partitioning under stress: Lessons from dorvilleid polychaetes in sulfidic sediments at methane seeps. Deep-Sea Research Part II-Topical Studies in Oceanography 92:214-233

Levin LA, Ziebis W, Mendoza GF, Growney VA, Tryon MD, Brown KM, Mahn C, Gieskes JM, Rathburn AE (2003) Spatial heterogeneity of macrofauna at northern

California methane seeps: influence of sulfide concentration and fluid flow. Marine Ecology Progress Series 265:123-139

Levin LA, Ziebis W, Mendoza GF, Growney-Cannon V, Walther S (2006) Recruitment response of methane-seep macrofauna to sulfide-rich sediments: An in situ experiment. Journal of Experimental Marine Biology and Ecology 330:132-150

Li Y, Peacock A, White D, Geyer R, Zhang C (2007) Spatial patterns of bacterial signature biomarkers in marine sediments of the Gulf of Mexico. Chemical Geology 238:168-179

Lichtschlag A, Felden J, Brüchert V, Boetius A, de Beer D (2010) Geochemical processes and chemosynthetic primary production in different thiotrophicmats of the Håkon Mosby Mud Volcano (Barents Sea). Limnology & Oceanography 55:931-949

Lodolo E, Camerlenghi A, Brancolini G (1993) A bottom simulating relefector on the South Shetland margin, Antarctic Pensinsula. Antarctic Science 5:207-210

Lodolo E, Camerlenghi A, Madrussani G, Tinivella U, Rossi G (2002) Assessment of gas hydrate and free gas distribution on the South Shetland margin (Antarctica) based on multichannel seismic reflection data. Geophysical Journal International 148:103-119

Magalhães VH, Pinheiro LM, Ivanov MK, Kozlova E, Blinova V, Kolganova J, Vasconcelos C, McKenzie JA, Bernasconi SM, Kopf AJ, Díaz-del-Río V, González FJ, Somoza L (2012) Formation processes of methane-derived authigenic carbonates from the Gulf of Cadiz. Sedimentary Geology 243-244:155-168

Main CE, Ruhl HA, Jones DOB, Yool A, Thornton B, Mayor DJ (2015) Hydrocarbon contamination affects deep-sea benthic oxygen uptake and microbial community composition. Deep Sea Research Part I: Oceanographic Research Papers 100:79-87

Mazzini A, Svensen H, Planke S, Forsberg CF, Tjelta TI (2015) Pockmarks and methanogenic carbonates above the giant Troll gas field in the Norwegian North Sea. Marine Geology

Mincks SL, Dyal PL, Paterson GLJ, Smith CR, Glover AG (2009) A new species of Aurospio(Polychaeta, Spionidae) from the Antarctic shelf, with analysis of its ecology, reproductive biology and evolutionary history. Marine Ecology 30:181-197

Miyatake T, Moerdijk-Poortvliet TCW, Stal LJ, Boschker HTS (2014) Tracing carbon flow from microphytobenthos to major bacterial groups in an intertidal marine sediment by using an in situ13C pulse-chase method. Limnology and Oceanography 59:1275-1287

Naehr TH, Eichhubl P, Orphan VJ, Hovland M, Paull CK, Ussler W, Lorenson TD, Greene HG (2007) Authigenic carbonate formation at hydrocarbon seeps in continental margin sediments: A comparative study. Deep Sea Research Part II: Topical Studies in Oceanography 54:1268-1291

Neal L, Mincks Hardy SL, Smith CR, Glover AG (2011) Polychaete species diversity on the West Antarctic Peninsula deep continental shelf. Marine Ecology Progress Series 428:119-134

Oksanen J (2013) Multivariate Analysis of Ecological Communities in R: vegan tutorial. cranr-projectorg Vegan: Community Ecology Package

Oliver PG, Holmes AM (2006) New species of Thyasiridae (Bivalvia) from chemosynthetic communities in the Atlantic Ocean. Journal of Conchology 39:175-183

Oliver PG, Sellanes J (2005) New species of Thyasiridae from a methane seepage area off Concepción, Chile. Zootaxa 1092:1-20

Parnell AC, Inger R, Bearhop S, Jackson AL (2010) Source partitioning using stable isotopes: coping with too much variation. PLoS One 5:e9672

Peterson BJ (1999) Stable isotopes as tracers of organic matter input and transfer in benthic food webs: A review. Acta Oecologica-International Journal of Ecology 20:479-487

Piñero E, Marquardt M, Hensen C, Haeckel M, Wallmann K (2013) Estimation of the global inventory of methane hydrates in marine sediments using transfer functions. Biogeosciences 10:959-975

Pohlman JW, Riedel M, Bauer JE, Canuel EA, Paull CK, Lapham L, Grabowski KS, Coffin RB, Spence GD (2013) Anaerobic methane oxidation in low-organic content methane seep sediments. Geochimica et Cosmochimica Acta 108:184-201

Pond DW, Bell MV, Dixon DR, Fallick AE, Segonzac M, Sargent JR (1998) Stable-Carbon-Isotope Composition of Fatty Acids in Hydrothermal Vent Mussels Containing Methanotrophic and Thiotrophic Bacterial Endosymbionts. Applied and environmental microbiology 64:370-375

Pond DW, Tarling GA, Mayor DJ (2014) Hydrostatic pressure and temperature effects on the membranes of a seasonally migrating marine copepod. PLoS One 9:e111043

Pranal V, FialaMedioni A, Guezennec J (1996) Fatty acid characteristics in two symbiotic gastropods from a deep hydrothermal vent of the west Pacific. Marine Ecology Progress Series 142:175-184

R Core Team (2013) R: A Language and environment for statistical computing. R Foundation for Statistical Computing, Vienna, Austria http://www.R-project.org/.

Reeburgh WS (2007) Oceanic methane biogeochemistry. Chemical Reviews 107:486-513

Reeves EP, Seewald JS, Saccocia P, Bach W, Craddock PR, Shanks WC, Sylva SP, Walsh E, Pichler T, Rosner M (2011) Geochemistry of hydrothermal fluids from the PACMANUS, Northeast Pual and Vienna Woods hydrothermal fields, Manus Basin, Papua New Guinea. Geochimica Et Cosmochimica Acta 75:1088-1123

Reid WDK, Sweeting CJ, Wigham BD, Zwirglmaier K, Hawkes JA, McGill RAR, Linse K, Polunin NVC (2013) Spatial Differences in East Scotia Ridge Hydrothermal Vent Food Webs: Influences of Chemistry, Microbiology and Predation on Trophodynamics. Plos One 8

Reid WDK, Wigham BD, McGill RAR, Polunin NVC (2012) Elucidating trophic pathways in benthic deep-sea assemblages of the Mid-Atlantic Ridge north and south of the Charlie-Gibbs Fracture Zone. Marine Ecology Progress Series 463:89-103

Riou V, Bouillon S, Serrão Santos R, Dehairs F, Colaço A (2010) Tracing carbon assimilation in endosymbiotic deep-sea hydrothermal vent Mytilid fatty acids by ^{13}C-fingerprinting. Biogeosciences 7:2591-2600

Rogers AD, Alker BJ, Aquilina A, Clarke A, Connelly DP, Copley J, Dinley J, German C, Graham AG, Green D, Hawkes JA, Hepburn L, Huvenne VA, James R, Linse K, Marsh L, Reid WDK, Roterman CN, Sweeting CJ, Thatje S, Zwirglmaier K (2010) RRS James Cook Cruise 42: Chemosynthetic Ecosystems of the Southern Ocean. Cruise Report

Römer M, Torres M, Kasten S, Kuhn G, Graham AGC, Mau S, Little CTS, Linse K, Pape T, Geprägs P, Fischer D, Wintersteller P, Marcon Y, Rethemeyer J, Bohrmann G (2014) First evidence of widespread active methane seepage in the Southern

Ocean, off the sub-Antarctic island of South Georgia. Earth and Planetary Science Letters 403:166-177

Sahling H, Galkin SV, Salyuk A, Greinert J, Foerstel H, Piepenburg D, Suess E (2003) Depth-related structure and ecological significance of cold-seep communities - a case study from the Sea of Okhotsk. Deep-Sea Research Part I-Oceanographic Research Papers 50:1391-1409

Sahling H, Wallman K, Dählmann A, Schmaljohann R, Petersen S (2005) The physicochemical habitat of *Sclerolinum sp.* at Hook Ridge hydrothermal vent, Bransfield Strait, Antarctica. Limnology & Oceanography 50:598-606

Stakes DS, Orange DL, D. PJ, Salamy KA, Maher N (1999) Cold-seeps and authigenic carbonate formation in Monterey Bay, California. Marine Geology 159:93-109

Suess E, Balzer W, Hesse K-F, Müller PJ, Ungerer CA, Wefer G (1982) Calcium Carbonate Hexahydrate from Organic-Rich Sediments of the Antarctic Shelf: Precursors of Glendonites. Science 216:1128-1130

Taylor JD, Glover EA, Peharda M, Bigatti G, Ball AD (2004) Extraordinary flexible shell sculpture; the structure and formation of calcified periostracal lamellae in Lucina pensylvanica (Bivalvia: Lucinidae). Malacologia 46:277-294

Thornton B, Zhang Z, Mayes RW, Högberg MN, Midwood AJ (2011) Can gas chromatography combustion isotope ratio mass spectrometry be used to quantify organic compound abundance? Rapid Communications in Mass Spectrometry 25:2433-2438

Thurber AR, Kröger K, Neira C, Wiklund H, Levin LA (2010) Stable isotope signatures and methane use by New Zealand cold seep benthos. Marine Geology 272:260-269

Thurber AR, Levin LA, Rowden AA, Sommer S, Linke P, Kröger K (2013) Microbes, macrofauna, and methane: A novel seep community fueled by aerobic methanotrophy. Limnology and Oceanography 58:1640-1656

Treude T, Niggemann J, Kallmeyer J, Wintersteller P, Schubert CJ, Boetius A, Jørgensen BB (2005) Anaerobic oxidation of methane and sulfate reduction along the Chilean continental margin. Geochimica et Cosmochimica Acta 69:2767-2779

Tyler PA, Connelly DP, Copley JT, Linse K, Mills RA, Pearce DA, Aquilina A, Cole C, Glover AG, Green DR, Hawkes JA, Hepburn L, Herrera S, Marsh L, Reid WD, Roterman CN, Sweeting CJ, Tate A, Woulds C, Zwirglmaier K (2011) RRS *James Cook*

cruise JC55: Chemosynthetic Ecosystems of the Southern Ocean. BODC Cruise Report

Van Gaever S, Moodley L, Pasotti F, Houtekamer M, Middelburg JJ, Danovaro R, Vanreusel A (2009) Trophic specialisation of metazoan meiofauna at the Häkon Mosby Mud Volcano: fatty acid biomarker isotope evidence. Marine Biology 156:1289-1296

Van Lith Y, Warthmann R, Vasconcelos C, McKenzie JA (2003) Sulphate-reducing bacteria induce low-temperature Ca-dolomite and high Mg-calcite formation. Geobiology 1:71-79

Vasconcelos C, McKenzie JA, Bernasconi SM, Grujic D, Tien AJ (1995) Microbial mediation as a possible mechanism for natural dolomite formation at low temperatures. Nature 377:220-222

Whiticar MJ (1999) Carbon and Hydrogen isotope systematics of bacterial formation and oxidation of methane. Chemical Geology 161:291-314

Wood WT, Jung WY Modeling the extent of the Earth's methane hydrate cryosphere. Proc Proceedings of the 6th International Conference on Gas Hydrates

Wright JD, Schaller MF (2013) Evidence for a rapid release of carbon at the Palaeocene-Eocene thermal maximum. Proceedings of the National Academy of Sciences of the United States of America 110:15908-15913

Young JN, Bruggeman J, Rickaby REM, Erez J, Conte M (2013) Evidence for changes in carbon isotopic fractionation by phytoplankton between 1960 and 2010. Global Biogeochemical Cycles 27:505-515

Chapter 4: Macrofaunal ecology of sedimented hydrothermal vents in the Bransfield Strait, Antarctica

Frontiers in Marine Science **3** March 2016
http://dx.doi.org/10.3389/fmars.2016.00032

James B. Bell[1, 2]*, Clare Woulds[1], Lee E. Brown[1], Christopher J. Sweeting[3], William D. K. Reid[4], Crispin T. S. Little[5], and Adrian G. Glover[2]

[1]School of Geography and Water@Leeds, University of Leeds, Leeds, LS2 9JT, UK.
[2]Life Sciences, Natural History Museum, London, SW7 5BD UK
[3] Ridley Building, School of Marine Science and Technology, Newcastle University, NE1 7RU, UK
[4]Ridley Building, School of Biology, Newcastle University, NE1 7RU, UK
[5]School of Earth and Environment, University of Leeds, Leeds, LS2 9JT, UK

Keywords: Chemosynthetic; Southern Ocean; Environmental Distance; Deep-sea; Ecology; Sedimented

4.1 Abstract

Sedimented hydrothermal vents, where hot, mineral-rich water flows through sediment, are poorly understood globally, both in their distribution and the ecology of individual vent fields. We explored macrofaunal community ecology at a sediment-hosted hydrothermal vent in the Southern Ocean. This is the first such study of these ecosystems outside of the Pacific and the furthest south (62˚S) of any vent system studied. Sedimentary fauna were sampled in four areas of the Bransfield Strait (Southern Ocean), with the aim of contrasting community structure between vent and non-vent sites. Macrofaunal assemblages were clearly distinct between vent and non-vent sites, and diversity, richness and density declined towards maximum hydrothermal activity. This variation is in contrast to observations from similar systems in the Pacific and demonstrates the influence of factors other than chemosynthetic primary productivity in structuring infauna at deep-sea vent communities. Vent endemic fauna had limited abundance and were represented by a single siboglinid species at hydrothermally active areas, meaning that that the majority of local biota were those also found in other areas. Several taxa occupied all sampling stations but there were large differences in their relative abundances, suggesting communities were structured by niche variation rather than dispersal ability.

4.2 Introduction

Deep-sea hydrothermal vent fields are under imminent threat from mineral extraction (Petersen et al. 2004, Van Dover 2010), creating an imperative to understand these environments so that their inhabitants may be effectively conserved. Size, distribution and faunal composition of sediment-hosted hydrothermal vents (SHVs) in particular are poorly understood globally. At SHVs, and in some diffuse venting areas around high-temperature vents, hydrothermal fluid mixes with ambient seawater beneath the seafloor (Bemis et al. 2012) and, in terms of oceanic heat flux, may be more significant than high temperature vents (Larson et al. 2015). The mixing of the hydrothermal fluid with ambient seawater means that it cools too slowly to precipitate mineral structures, creating an

environment comprised of hot (generally 10 – 100˚C above ambient), high porosity sediment, typically with high levels of hydrogen sulphide, methane and reduced metals, such as iron and manganese (Levin et al. 2009, Bernardino et al. 2012, Aquilina et al. 2013, Urich et al. 2014). The vast majority of deep-sea hydrothermal vent research has focused on high-temperature vents, which are typically dominated by vent endemic species (e.g. Rogers et al. 2012). In contrast, there have been only a handful of ecological studies at SHVs (Grassle et al. 1985, Grassle & Petrecca 1994, Kharlamenko et al. 1995, Levin et al. 2009, Levin et al. 2012, Sweetman et al. 2013) and none from the Southern Ocean. Hydrothermal sites in the Bransfield Strait (Southern Ocean) potentially provide a stepping stone between chemosynthetic communities in the Atlantic, Indian and Pacific Oceans (Rogers et al. 2012, Roterman et al. 2013) as well as providing an interesting site to explore how ambient deep Southern Ocean benthos respond to reducing environments.

Sediment-hosted vents support communities of chemosynthetic primary producers; free-living, colonial or symbiotic. SHVs thus have direct implications for the wider faunal community, through both in situ organic matter production and the environmental toxicity associated with hydrothermalism (Levin et al. 2009, Bernardino et al. 2012). The relative physical similarity of SHV (compared with high-temperature vents) to non-hydrothermal environments allows more scope for opportunistic interactions between vent endemic fauna and more common deep-sea fauna with profound impacts upon community structure in both macro- and meiofaunal species (Zeppilli et al. 2011, Bernardino et al. 2012, Zeppilli et al. 2015). Bernardino et al. (2012) proposed a conceptual model of how macrofaunal community characteristics (such as abundance and diversity) respond to gradients in environmental toxicity and organic matter (OM) availability at SHVs. These models are consistent with models of non-chemosynthetic macrofaunal response to gradients in pollution and organic enrichment (Pearson & Rosenberg 1978) and the intermediate disturbance hypothesis (Connell 1978). Maximum biodiversity is predicted at intermediate levels of toxicity and productivity (Connell 1978), where higher niche or environmental diversity potentially facilitates higher diversity (Bernardino et al. 2012, Gollner et al. 2015, McClain & Schlacher 2015). However, high species dominance/low diversity in deep-sea macrofauna is generally rare

(McClain & Schlacher 2015), and often characteristic of reducing or highly disturbed environments (Netto et al. 2009). The models further suggest that the proportion of background fauna generally declines towards a community dominated by vent-endemic species (Bernardino et al. 2012). These changes emulate a distance-decay model (Nekola & White 1999, McClain et al. 2011, McClain et al. 2012), but one accelerated by the rapid change in environmental conditions (sub-km scale), where dispersal limitations are superseded by habitat selection.

Towards the region of greatest hydrothermal flux, it was also hypothesised that increased supply of chemosynthetic substrates would support larger populations of vent endemic species and greater OM production rates, in turn enhancing local abundance or biomass (Bernardino et al. 2012). However, there is conflicting evidence as to whether SHV enrich macrofaunal abundance, suggesting that other factors (e.g. supply of other sources of OM or environmental stress) may also be important (Grassle et al. 1985, Grassle & Petrecca 1994, Levin et al. 2009). The importance of local environmental factors in structuring communities of SHVs remains a key unknown, particularly for non-Pacific SHVs that have not previously been studied quantitatively. The lack of quantitative ecology from SHVs outside the Pacific severely limits our understanding of these ecosystems.

Sedimented hydrothermal systems have been identified in the Bransfield Strait, but ecological investigations have not yet been reported. The only other hydrothermal vent system reported in the Southern Ocean is a high-temperature, hard substratum vent (Rogers et al. 2012), which are not directly comparable to the Bransfield Strait SHVs. The Strait (Figure 4.4.2a) harbours deep (1050 m) sediment-hosted vents (Klinkhammer et al. 2001, Aquilina et al. 2013) as well as episodic shallow water venting around Deception Island (Somoza et al. 2004). In spite of the wide ranges in temperature in recent geological history (Clarke & Crame 1992, 2010), some Southern Ocean biota are sensitive to small (ca. 2 – 3˚C) temperature perturbations (Barnes & Peck 2008, Clarke et al. 2009). Typical seafloor temperature in the Bransfield Strait is around -1.5˚C (Bohrmann et al. 1998, Clarke et al. 2009), compared with estimates of 25 – 50˚C at hydrothermally active areas (Dählmann et al. 2001, Klinkhammer et al. 2001, Aquilina et al. 2013). This raises questions as to

the ability of Southern Ocean benthos to colonise areas of hydrothermal activity and suggests that it may be crucial to species distribution in the Bransfield Strait.

4.3 Aims & Hypotheses

The aim of the present study is to show how hydrothermalism influences infaunal communities in the Bransfield Strait. We present macrofaunal assemblage data and critically evaluate conceptual models of SHV ecology, (Bernardino et al. 2012) adding perspectives from high-latitude SHVs. The following hypotheses were explored: 1) Hydrothermally active sites will support a greater macrofaunal density than background sites due to increased OM availability 2) Macrofaunal diversity will be different between areas with or without active hydrothermalism; 3) Abundance of vent endemic species (*Sclerolinum contortum* (Georgieva et al. 2015)) will be highest in areas of moderate hydrothermal activity, as suggested by Sahling et al. (2005). We also explore the influence of environmental gradients upon community composition and results are quantitatively compared to Bernardino et al. (2012)'s conceptual models of abundance, diversity and proportions of vent endemic fauna, using a measure of environmental distance.

4.4. Materials and Methods

4.4.1 *Ethics statement*

In accordance with the Antarctic Act (1994) and the Antarctic Regulations (1995), necessary permits (S5-4/2010) were acquired from the South Georgia and South Sandwich Islands Government.

4.4.2 *Sample Collection and Processing*

The Bransfield Strait is located between the West Antarctic Peninsula and the South Shetland Islands. Two subaerial volcanoes (Deception and Bridgeman Islands) divide the Strait into three sub-basins, the central of which hosts several volcanic edifices: Hook Ridge; the Three Sisters and the Axe (Whiticar & Suess 1990,

Bohrmann et al. 1998, Dählmann et al. 2001, Klinkhammer et al. 2001, Aquilina et al. 2013) (Figure 4.4.2a). At Hook Ridge, remnants of a high temperature mineral chimney venting shimmering water were seen during a video survey (Aquilina et al. 2013) and hot, sulphidic sediments have been recovered (Dählmann et al. 2001, Klinkhammer et al. 2001). Of the four study areas visited in the Bransfield Strait during *RRS James Cook* cruise 55 (Figure 4.4.2a) only Hook Ridge was found to be hydrothermally active and cores from different areas of the ridge were subject to fluid advection rates of 9 – 34 cm yr^{-1} (Aquilina et al. 2013). Sediments from the off-vent site, the Three Sisters and the Axe showed no signatures consistent with active hydrothermalism.

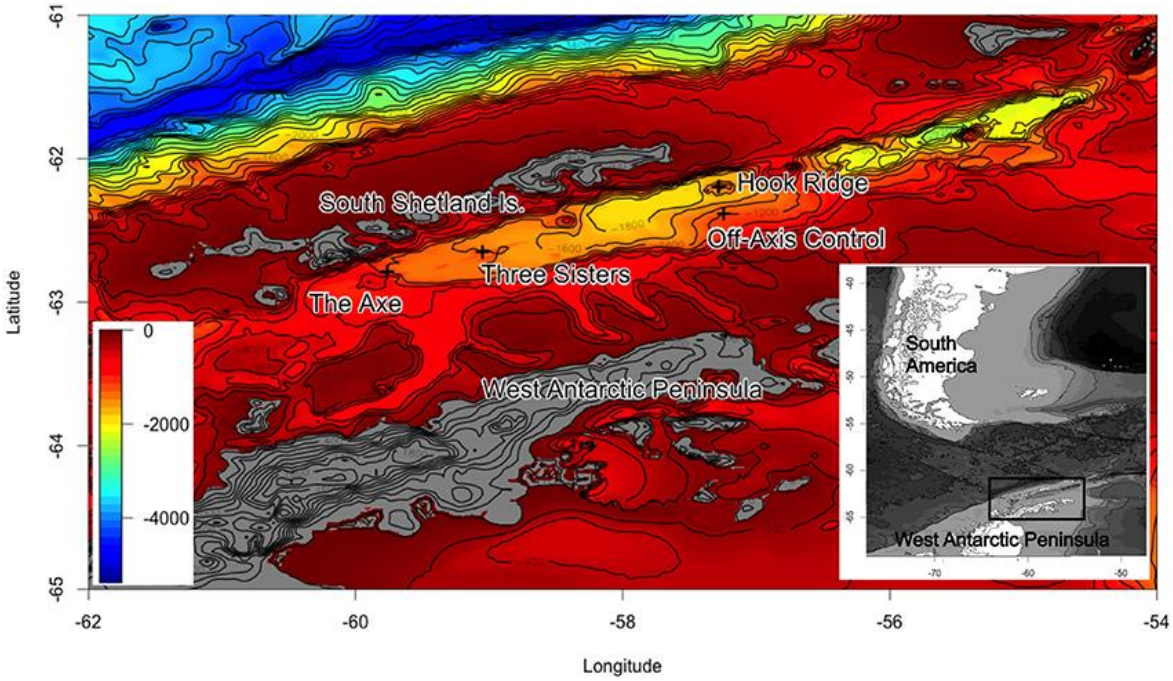

Figure 4.4.2a: Bathymetric charts of the Bransfield Strait (30 arc-second grids constructed using GEBCO bathymetry) showing sampling locations during JC055. Latitude and longitude given as degrees and decimal minutes.

Samples were collected in January 2011, aboard RRS *James Cook* cruise 55 (Tyler et al. 2011). Following bathymetric and water column surveys to identify the source of venting (see Aquilina et al. 2013), replicate corer deployments were made (3 – 6 per site except at the Axe). All samples were collected using a Bowers and Connelly dampened megacorer (Gage & Bett 2005), from each of the three raised edifices in the central basin, and one off-axis/ off-vent control site (Figure 4.4.2a; Table 4.4.2a). A single deployment was made at the Axe, owing to shallow sediment coverage and

the absence of water column signals indicative of hydrothermal activity (Aquilina et al. 2013). From each deployment, multiple 10cm diameter sediment cores were collected. Samples from individual cores from the same deployment were pooled into single samples, as cores from the same deployment are pseudoreplicates.

Hydrothermally Active?	Site	Site code	# of replicate deployments	Latitude	Longitude	Depth (m)
No	Control Site (off-vent)	BOV	4	-62.384	-57.244	1150
Yes (9 cm yr^{-1})	Hook Ridge Site 1	HR1	6	-62.197	-57.298	1174
Yes (34 cm yr^{-1})	Hook Ridge Site 2	HR2	6	-62.192	-57.278	1054
No	Three Sisters Site 1	TS1	1	-62.654	-59.033	1121
No	Three Sisters Site 2	TS2	2	-62.655	-59.050	1311
No	The Axe	AXE	1	-62.787	-59.762	1024

Table 4.4.2a – List of sampling locations and # of deployments. Position reported as degrees and decimal minutes. Geochemical data and hydrothermal flux rates from published literature (Aquilina et al. 2013, Aquilina et al. 2014).

Cores were sliced into upper (0-5cm) and lower (5-10cm) partitions and were passed through a 300µm sieve to extract macrofauna (e.g. Levin et al. 2009). Differences between upper and lower core partitions were only analysed where there were measureable hydrothermal differences between each partition. Fauna were preserved in either 80% ethanol or 10% buffered formalin in seawater. In the laboratory, macrofauna were sorted to highest possible taxonomic level using a dissecting microscope. All annelid and bivalve specimens were sorted to species or

morphospecies level, with other taxa sorted to family or higher. Incomplete specimens (those without heads) were not counted, to prevent over-estimating their density. Feeding modes were determined by morphology, and validated against taxonomic keys (Fauchald 1977, Fauchald & Jumars 1979, Barnard & Karaman 1991, Beesley et al. 2000, Smirnov 2000, Poore 2001, Kilgallen 2007, Rozemarjin et al. 2011, Reed et al. 2013, Jumars et al. 2015), the Ocean Biogeographic Information System (OBIS) and studies from similar areas/ environments that have conducted stable isotope analyses (Fauchald & Jumars 1979, Mincks et al. 2008, Levin et al. 2009).

Samples of freeze-dried sediment were acidified (6M HCl) to remove inorganic carbon and then analysed for carbon content. Samples were analysed at EK using a continuous flow isotope ratio mass spectrometer using a Vario-Pyro Cube elemental analyser (Elementar), coupled with a Delta plusXP mass spectrometer (Thermo Electron).

4.4.3 *Statistical Analyses*

The lack of replicates taken from the Axe and TS1 meant that it was excluded from any permutational analyses aimed at discriminating differences by site. Abundance per deployment was standardised to give abundance per m^2. Unless otherwise specified, all subsequent analyses were conducted in the R environment (R Core Team 2013).

4.4.4 *Species Diversity and Richness*

Calculations of diversity and richness were made from species-level discriminated fauna only (annelids and bivalves only). Shannon-Wiener diversity (H') was calculated in VEGAN (v2.0-8) (Oksanen et al. 2013) for whole deployments and individual vertical core partitions. Species-accumulation curves and shared species were calculated using EstimateS (v9.1.0) (Gotelli & Colwell 2001, Colwell et al. 2012, Colwell 2013). Individual-based species-accumulation curves (999 permutations) were constructed from species level data for each of the sites (n=100). Pairwise

shared species were calculated from abundance data summed by site using the abundance-based Chao-Sørenson index (Chao et al. 2005) to reduce under-sampling bias given the inconsistent number of replicate deployments per site.

4.4.5 *Community Structure*

Untransformed community composition data were used to create a Bray-Curtis similarity matrix and visualised using the metaMDS method in VEGAN (Oksanen et al. 2013). Significant structure within the data was tested with a similarity profile routine (SIMPROF, 10 000 permutations, average linkage) using the clustsig package (v1.0) (Clarke et al. 2006, Clarke et al. 2008, Whitaker & Christmann 2013). Similarity between sites was compared using permutational ANOVA (PERMANOVA, 999 permutations) (Anderson 2001), using site as a factor. The validity of PERMANOVA was checked using the PERMDISP test for homogeneity of variance (betadisper & anova in Vegan), since PERMANOVA is sensitive to multivariate dispersion (Anderson 2001). No differences between sites were observed (ANOVA: F-value; 0.535, df = 16; $P > 0.05$).

4.4.6 *Environmental variables*

To compare the relative influence of hydrothermal fluids at different sites, and to test the theoretical model suggested by Bernardino et al. (2012), a proxy index for hydrothermal activity (the Hydrothermal Index – HI) was developed. Sites with comparable levels of relevant environmental parameters were considered to be likely to be more similar in faunal characteristics than those with greater differences (Bernardino et al. 2012, McClain et al. 2012, Gollner et al. 2015). This approach is analogous to the 'Glaciality index' (Brown et al. 2010) and 'benthic index' (Robertson et al. 2015) that have shown how various biological trends in separate systems can be explained by collating environmental parameters.

A single core profile from each site (except TS1) of geochemical data were available and initial selection criteria were based upon results of an envfit visualization (Oksanen et al. 2013) that identified influential (e.g. H_2S) and co-linear species (e.g.

Cl^- and SO_4^{2-}). Environmental data were not available from every site used for ecological analyses, hence more conventional ordination techniques (e.g. CCA) were not possible, which would also not have permitted comparisons with conceptual models as presented here. Temperature profiles were not available for inclusion. Biologically and hydrothermally relevant parameters were selected for the index, comprised of two chemosynthetic substrates (H_2S and CH_4), and an indicator of temperature changes and hydrothermal flux (Cl^-). Low chlorinity (relative to seawater) is characteristic of hydrothermal fluid and so the reciprocal for Cl^- concentration was given as a proxy for hydrothermal fluid input (Ginsburg et al. 1999, Aquilina et al. 2013, Larson et al. 2015).

Down core geochemical profiles from pore fluid data (Aquilina et al. 2013) were split into upper and lower partitions, as per the faunal samples (Supplement 4-3). Pore fluid concentrations of H_2S, CH_4 and Cl^- were averaged into 0- 5cm and 5-10 cm below seafloor (b.s.f.) sections. Concentrations of each were then normalised to the mean value (i.e. mean = zero) for each component (thus each was equally weighted) and the sum for each site was given as the HI (two values per site, one per partition). Initially, faunal variation between upper and lower core partitions at non-hydrothermally active sites contributed the majority of the residual error, although relationships between HI and abundance and diversity were still significant (GLM, $df = 1$, $p < 0.05$). Since the hydrothermal index focuses upon the relationship between faunal characteristics and hydrothermalism, variation between upper and lower partitions of non-hydrothermally active sites was excluded from subsequent analyses.

Three statistical models were developed to determine the extent that HI could explain patterns in diversity, density and species richness. Data (mean values for each site) were fitted to generalized linear models using the glm and Anova functions in the CAR package (v2.0-18) (Fox et al. 2013). Normality tests (Shapiro-wilk) were run on each of the responses and used to inform selection of distribution for the models. Diversity data were fitted to a Gaussian model. Count data (abundance and species richness) were fitted to Poisson models but residual deviance exceeded degrees of freedom, indicating over-dispersion, so the models

were corrected using a quasi-Poisson dispersion factor (Dobson 1990, Dobson & Barnett 2008).

4.5 Results

4.5.1 *Abundance and community composition*

A total of 2,320 individuals (73 – 780 ind. per site), of 81 macrofaunal taxa (25 – 50 per site) were collected. Fifty-one polychaete species, from thirty-two families represented the most abundant taxon (981 individuals). Peracarid crustaceans were the second most abundant taxon (755 ind. from 18 families), followed by oligochaetes (402 ind. from two families). Sites were dominated numerically by polychaetes (41 – 56 % by abundance), except at Hook Ridge and the Axe where peracarids, mostly isopods, dominated (41 – 55 %) (Figure 4.5.1a). Oligochaetes were very abundant at the control site (37 % of abundance) and relatively rare elsewhere (6 – 18 %). The dominant feeding group (Figure 4.5.1a) was generally comprised of carnivores/ scavengers at Hook Ridge (44 – 56 %) and motile deposit feeders dominated at non-Hook Ridge sites (42 – 78 %). Functional composition of taxa varied significantly (Pearson's $\chi^2 = 178.37$, $p < 0.01$) and was dissimilar between all pairwise comparisons ($p < 0.05$).

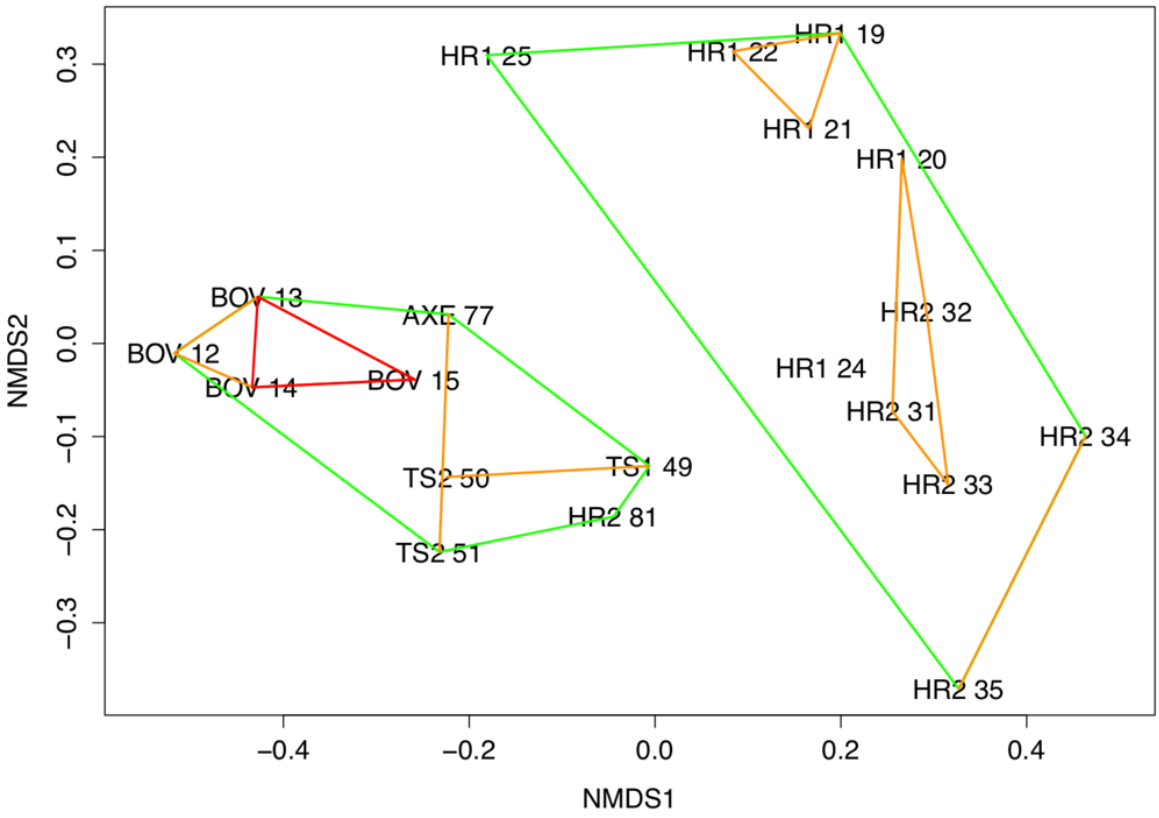

Figure 4.5.1a – Multidimensional scaling ordination with ordinal hulls. Ordinal hulls based on Manhattan distance computed during cluster analysis. Hulls indicate areas of < 0.7 dissimilarity (green), < 0.5 (blue) and < 0.3 (red). 2-D stress = 0.13. Site numbers refer to deployments (Table 1), using whole core data

The most abundant morphospecies groups present in the Bransfield strait were idoteid isopods at Hook Ridge 1 (2022 ind. m^2 S.E. ± 752) and *Limnodriloides* sp. B (Oligochaeta: Naididae) at the control site (1958 ind. m^2 S.E. ± 510) although the dominance of the Isopoda may have reflected the coarser taxonomic resolution used (Supplement 4-1). The most abundant polychaete species in the Bransfield strait was *Aricidea antarctica* (Paraonidae, Hartmann-Schröder and Rosenfeldt, 1988), comprising 23 % of total macrofaunal density at the control site (1313 ind. m^2 S.E.± 269) but generally occurring in low relative abundances of 1 – 5 % elsewhere.

Community composition was significantly different between all sites (PERMANOVA, $F = 3.359$, $df = 4$, $p < 0.01$) (Figure 4.5.1b) and clearly distinguished the Hook Ridge sites from the other, non-hydrothermally-active areas (SIMPROF, $p = 0.05$). Relative

abundances of annelid and peracarid taxa were the main discriminators in assemblage structure between vent and non-vent conditions. Deployment 81 at Hook Ridge 2 was significantly different to other Hook Ridge sites (Figure 4.5.1a; SIMPROF, p = 0.05) and reflected the relative lack of terebellids (Polychaeta) and isopods and increased abundance of naidid oligochaetes at HR2 81, giving it an assemblage more characteristic non Hook-Ridge sites, particularly the control site were naidids were highly abundant.

	Site					
	BOV	HR1	HR2	TS1	TS2	AXE
Replicates	4	6	6	1	2	1
Total no. of individuals	777	780	317	73	241	132
Total no. of species	50	33	34	25	40	34
Diversity (H') (± S.E.)	2.15 (±0.07)	1.33 (±0.06)	1.49 (±0.26)	2.50	2.24 (±0.13)	2.89
Mean species richness (± S.E.)	22.75 (±1.49)	6.83 (±1.01)	5.67 (±1.20)	17	20 (±3.00)	26
Est. Species Richness (n=100) (±S.D.)	20.71 (±3.56)	16.43 (±2.45)	20.38 (±2.52)	33.91 (±3.77)	25.46 (±3.45)	31.06 (±3.02)
Mean Density (ind. m^2) (± S.E.)	6438 (± 425)	6474 (± 1698)	1826 (± 241)	2953	4456 (± 1120)	3820
Organic Carbon (weight %)	1.35	1.35	0.97	n.d.	1.40	n.d.

Table 4.5.1a – Species diversity and mean and estimated richness (for species-level discriminated fauna only), total density and organic carbon levels in the Bransfield Strait. BOV = Bransfield Off-Vent; HR1 = Hook Ridge 1; HR2 = Hook Ridge 2; TS1 = Three Sisters; TS2 = Three Sisters 2 and AXE = The Axe

Hook Ridge 1 and the control site had the greatest mean macrofaunal density (Table 4.5.1a). At Hook Ridge, macrofaunal density ranged widely, including the most

(deployment 25: 14324 ind. m^2) and least (deployment 35: 1061 ind. m^2) densely populated sites across the whole Strait. Whilst elevated faunal density was observed in the immediate vicinity of a patch of siboglinids (deployment 25), mean density was similar between non-hydrothermally active sites (5180 ind. m^2, S.E.± 580, n=12) and Hook Ridge (4150 ind. m^2, S.E. ± 1077, n=9) (Wilcoxon rank sum test, W = 25, p = 0.08) (Figure 4.5.1b).

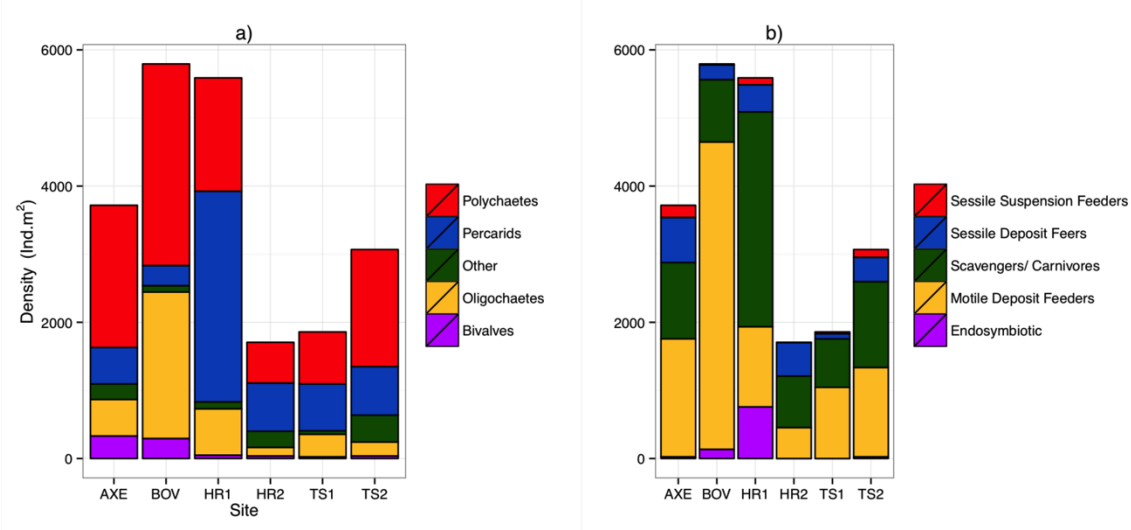

Figure 4.5.1b – Comparative density (ind. m^{-2}) of a) major taxa and b) functional groups by site for whole core data.

4.5.2 *Species Richness and Diversity*

Individual-based estimates of species richness, grouped by site, showed that the Three Sisters and the Axe were the most species rich sites and that Hook Ridge 1 was the least species rich (Table 4.5.1a). The Hook Ridge sites had the lowest mean diversity, consistent with a higher proportion of endemic species and a more reducing environment. Mean shared species between sites was 53 % with the highest being between the two Hook Ridge sites (82 %). The non-Hook Ridge sites shared between 18 – 77 % of their species with the lowest shared species between the control site BOV and Three Sisters 1 (18 %).

4.5.3 *Vent Endemic Species*

Siboglinid polychaetes were found at Hook Ridge 1 (*S. contortum*) and the control site, Three Sisters and the Axe (*Siboglinum* sp.). Complete specimens of both siboglinid species never co-occurred (Supplement 4-1) but fragments (sections of tube, with or without body tissue fragments) of *S. contortum* were found at all sites. Siboglinids occurred in low abundances (0 – 71 individuals with heads per deployment) and were never the dominant functional group at any site (0 – 14 % of total abundance per site) (Figure 4.5.1a). Complete specimens of *S. contortum* were counted in two deployments from Hook Ridge 1 only (HR1: 21 and 25, 1 and 70 ind. respectively) and ranged in abundance between 32 – 4520 ind. m^2, comprising 14 % of total faunal abundance at Hook Ridge 1. Owing to the high proportion of *S. contortum* at Hook Ridge 1 deployment 25 (31 % of abundance compared with 0 – 1 % elsewhere), this deployment was distinct from all others (SIMPROF, $p = 0.05$) (Figure 4.5.1b). The patchy or limited distribution of *S. contortum* meant that replicates within the same site showed considerable variation in proportions of vent endemic species. *Siboglinum* sp. occurred in its highest abundance at the control site (2 % of fauna, 64 – 159 ind. m^2).

4.5.4 *Environmental drivers of community composition*

The HI was elevated at both Hook Ridge sites (particularly site 2), relative to other areas of the Bransfield Strait (Table 4.5.4a). HI was highest in downcore sections (5 – 10 cm below seafloor (b.s.f)) from Hook Ridge (0.44 – 4.02) and was always higher than in upper cores (0 – 5 cm b.s.f.) (Table 4.5.4a). HI was greater at Hook Ridge 2 than Hook Ridge 1 and Hook Ridge 1 upper partition had comparable levels of HI to off-vent sites. Mean diversity, species richness and density was fitted to values of HI for each site (1 or 2 partitions per site, Table 4.5.4b), using generalized linear models. Mean diversity, species richness and density all significantly declined with increasing HI (GLM: $p < 0.05$, R^2 0.38 – 0.52; Figure 4.5.4a, Table 4.5.4b). Ecological distance was also consistent with environmental distance (PERMANOVA: $p < 0.001$;).

Sites		Geochemical parameter (±S.E.)			
		H_2S (µmol L^{-1})	CH_4 (µmol L^{-1})	Cl^- (mmol L^{-1})	Hydrothermal Index (±S. E.)
BOV	0-5cm	0.00 -	0.00 -	545.0 (± 0.58)	-1.33 (± 0.33)
	5-10cm	0.00 -	0.00 -	547.7 (± 1.86)	Omitted
HR1	0-5cm	0.00 -	0.29 (± 0.03)	546.1 (± 0.77)	-1.05 (± 0.24)
	5-10cm	0.00 -	1.65 (± 1.67)	540.3 (± 1.31)	0.44 (± 0.24)
HR2	0-5cm	0.71 (± 0.45)	1.72 (± 0.48)	515.6 (± 4.70)	0.94 (± 0.15)
	5-10cm	0.85 (± 0.79)	4.64 (± 1.43)	498.6 (± 0.97)	4.02 (± 0.40)
TS2	0-5cm	0.00 -	0.00 -	561.1 (± 5.51)	-1.40 (± 0.26)
	5-10cm	0.00 -	0.00 -	550.0 (± 3.22)	Omitted
AXE	0-5cm	0.21 (± 0.35)	0.00 -	543.8 (± 2.61)	-1.11 (± 0.25)
	5-10cm	0.00 -	0.00 -	542.8 (± 0.30)	Omitted

Table 4.5.4a – Mean concentrations of four geochemical parameters (binned into upper and lower partitions) used to calculate the hydrothermal index (Data from Aquilina et al. 2013, Aquilina et al. 2014). BOV = Bransfield Off-Vent Control; HR1 = Hook Ridge 1; HR2 = Hook Ridge 2; TS2 = Three Sisters 2 (No data for TS1) and AXE = The Axe. See accompanying papers (Aquilina et al. 2013, Aquilina et al. 2014) for full downcore profiles

Response	GLM family	p,	L-Ratio	adj. R^2
Diversity (H')	Gaussian (link = "identity")	< 0.05	4.65	0.38
Species Richness	Quasi-Poisson (link = "log")	< 0.01	10.55	0.43
Density	Quasi-Poisson (link = "log")	< 0.001	15.02	0.52

Table 4.5.4b – Results of generalized linear models for various biotic measures with hydrothermal index (HI).

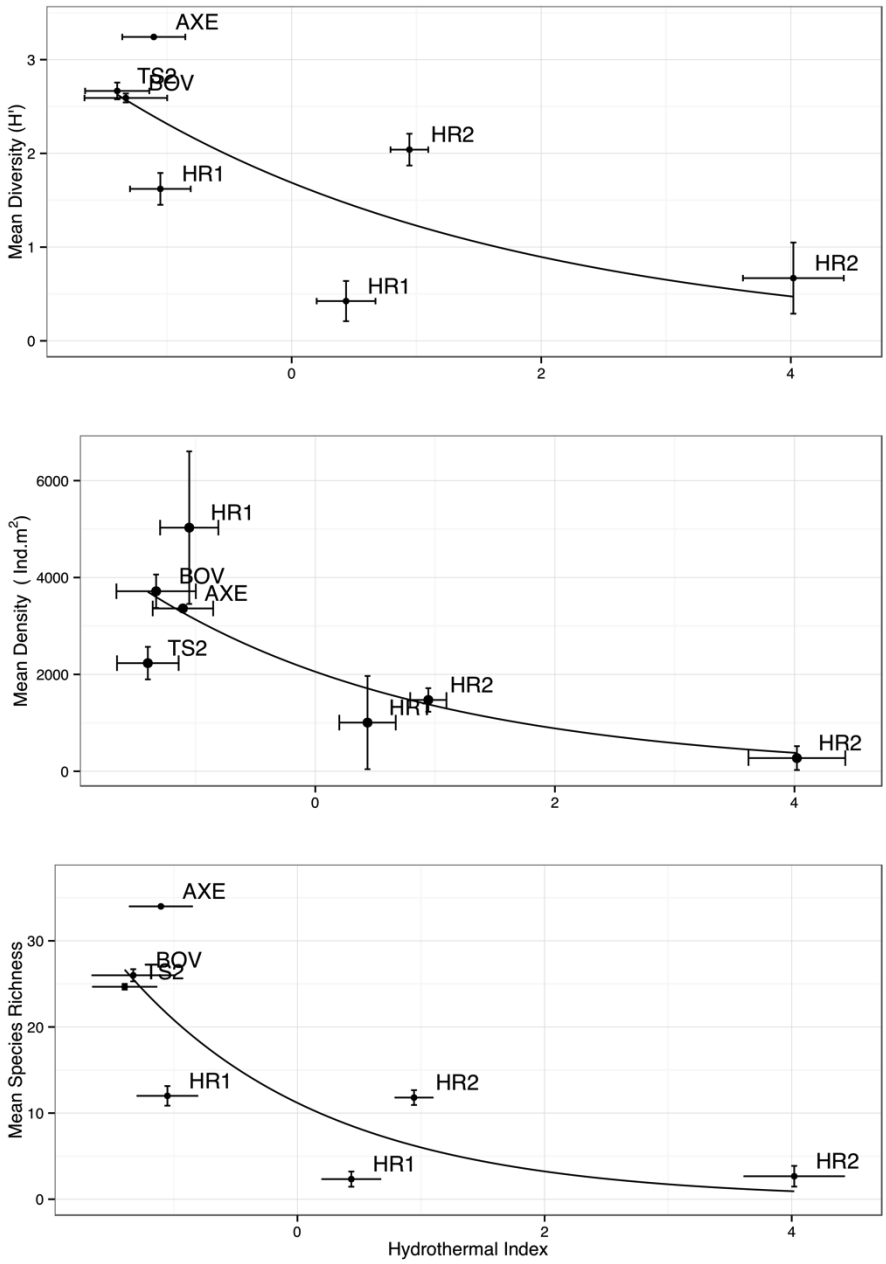

Figure 4.5.4a – Comparison of 'hydrothermal index' with mean diversity, abundance (m^2) and species richness (using data from partitioned cores). Higher HI indicates greater levels of hydrothermal activity. Error bars denote ±1 S.E.

4.6 Discussion

4.6.1 *Controls on faunal diversity*

Diversity was lower at hydrothermally active sites and declined exponentially towards the greatest levels of HI (Figure 4.5.4a; Table 4.5.4b), owing to the increased environmental toxicity creating unfavourable conditions for the majority of local fauna and the general absence of vent-endemic species. Whilst diversity was influenced by environmental distance ($p < 0.05$, Table 4.5.4b), the relationship observed differed from the Bernardino et al. (Bernardino et al. 2012) model in that it was maximal under background conditions and decreased towards greater hydrothermal influence, rather than maximal diversity occurring in areas of intermediate hydrothermal activity (Figure 4.5.4a). The conceptual model of Bernardino et al. (2012) does not encompass the high biodiversity typical of deep-sea macrofauna, resulting in a disagreement with our observations (Figure 4.6.1a). Therefore we accept hypothesis 2 and suggest that the proposed increase and subsequent decrease of diversity (Figure 4.6.1a) with increasing hydrothermal influence (Bernardino et al. 2012) does not capture the high background biodiversity common in the deep-sea (Rex & Etter 2010, Chown 2012) (Figure 4.6.1a).

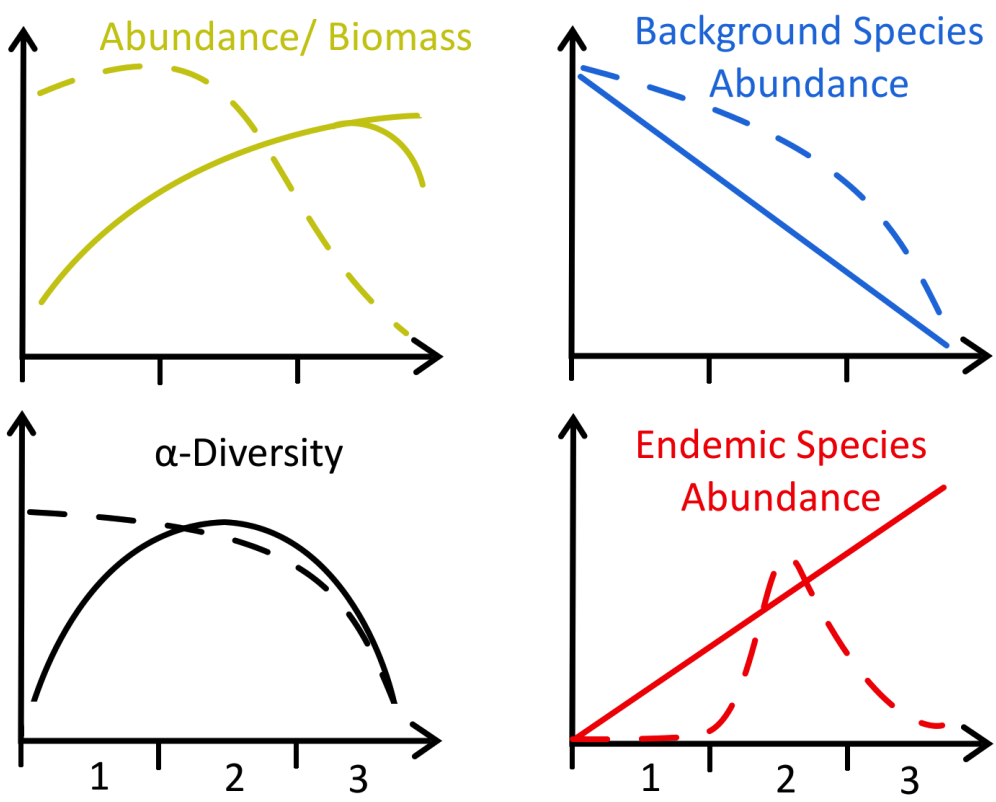

Figure 4.6.1a – Schematic of four faunal trends in diffuse hydrothermal vents, adapted from Bernardino et al. (2012) (solid lines) to include Southern Ocean data (dashed lines). Axes labels refer to three distinct regions of the Bransfield Strait identified by this study with reference to previous work (Sahling et al. 2005, Aquilina et al. 2013): 1 = No hydrothermal activity (i.e. Control, Three Sisters and the Axe), 2 = Moderate hydrothermal activity (i.e. Hook Ridge 1, optimal *S. contortum* habitat) and 3 = Higher hydrothermal activity, unsuitable for most fauna.

Species accumulation curves from the Bransfield Strait, elsewhere in the Southern Ocean and Pacific SHV (Grassle & Petrecca 1994, Flach & Heip 1996, Levin et al. 2009, Neal et al. 2011) show that species richness was higher in background/ inactive sediments than at active vents (Figure 4.6.1b), which is consistent with lower diversity at active vents (Figure 4.6.1b). The Bransfield Strait SHV was generally more species rich than vents from the Manus Basin and comparable to NE Pacific vents at Middle Valley (Figure 4.6.1b) (Levin et al. 2009). The SHV at Middle Valley (2406 – 2411m) is notably deeper than either the Bransfield vents (1054 – 1320m) or the Manus Basin (1430 – 1634m), suggesting that depth does not exert a

consistent effect upon species richness, or abundance (Levin et al. 2009). Around the high temperature vents at the East Pacific Rise however, macrofaunal species richness peaked at intermediate levels of environmental stress (Gollner et al. 2015). This suggests that relationships between environmental gradients and macrofaunal communities may differ between different types of hydrothermal vent. At high temperature vents, meiofaunal taxa showed a similar pattern in species richness to that present here (Gollner et al. 2015), illustrating differences between taxa and environmental settings. Species richness was also generally lower in the Bransfield strait when compared with the West Antarctic shelf seas (Figure 4.6.1b) (Neal et al. 2011) although it should be noted that these samples were from sites ~500m shallower and measure only polychaete species richness.

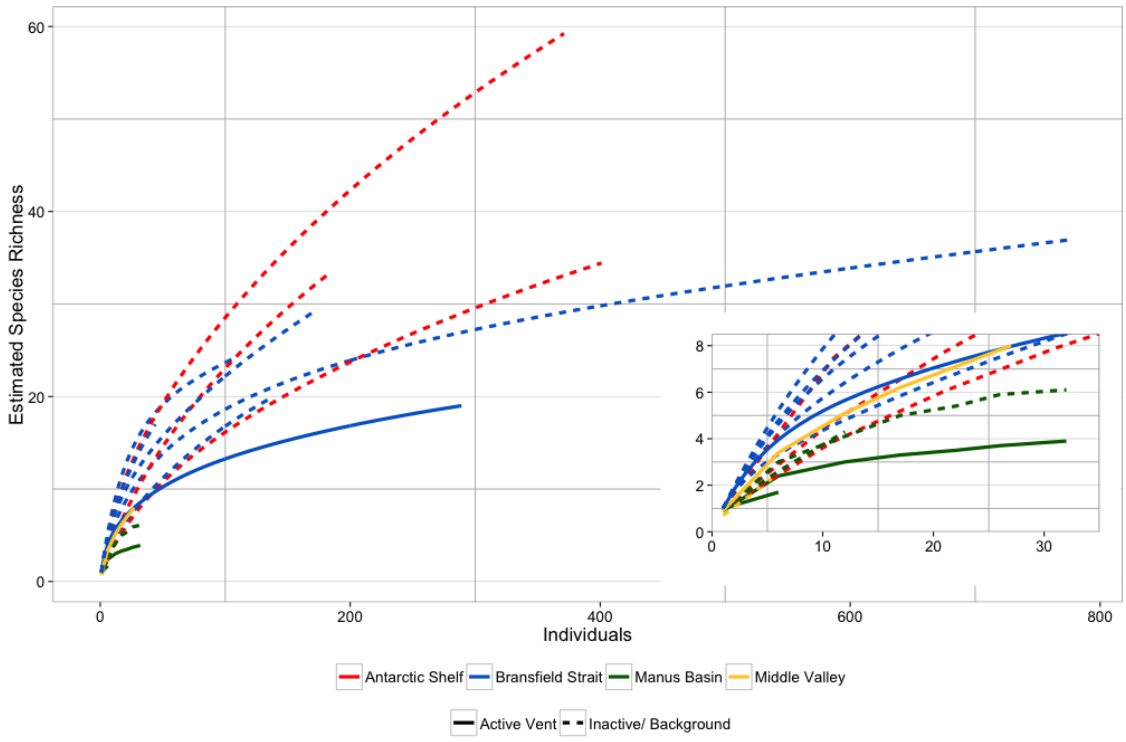

Figure 4.6.1b – Comparative individual-based species accumulation curves between Bransfield Strait sites (this study) and literature values for other diffuse hydrothermal vents (Grassle et al. 1985, Levin et al. 2009) and typical bathyal sediments of the West Antarctic Peninsula (Neal et al. 2011). Data from the West Antarctic Peninsula are for polychaete species richness only.

4.6.2 *Controls on faunal density*

Macrofaunal density declined towards areas of highest hydrothermal advection (Figure 4.5.4a; Figure 4.6.1b). Thus our data did not support our hypothesis that hydrothermal vents support increased faunal density in the Bransfield Strait (hypothesis 1). Mean density was higher at non-hydrothermally active sites in the Bransfield Strait than at Hook Ridge (Figure 4.5.1b), driven mainly by the low faunal density at Hook Ridge 2, the site with the highest fluid advection rates (Aquilina et al. 2013). Environmental stress at Hook Ridge 2 may explain the low faunal abundance (Sahling et al. 2005), presumably reflecting the increased stress associated with elevated temperature or environmental toxicity (Figure 4.5.4a). Bacterial mats were present at Hook Ridge 2 (Aquilina et al. 2013) but no complete specimens of vent endemic species were found.

It is likely that the relationship in density between SHV and local background areas depends upon toxicity at the vents (Levin et al. 2013), the amount of in-situ primary productivity and the availability of other sources of OM. In previous studies of comparable systems, macrofaunal density was not consistently enriched by the presence of hydrothermal flux, and has been observed to be both higher and lower than nearby inactive or background sediments (Grassle et al. 1985, Levin et al. 2009) (Figure 4.6.2a). Temperate or Polar latitude deep-sea SHVs (a.k.a. 'Hot muds') with relatively high surface primary productivity (SPP) (Middle Valley or Bransfield Strait) tend to have lower densities than in nearby background sediments (Grassle et al. 1985, Levin et al. 2009), but where SPP is lower (e.g. Manus basin), density may be higher at SHV (Grassle et al. 1985, Levin et al. 2009) (Figure 4.6.2a). Export production and surface primary productivity is high in the Bransfield Strait (Wefer & Fischer 1991, Kim et al. 2005), thus any extra chemosynthetic OM production may not be as significant to local fauna compared with deeper vents, or vents in less productive seas (Tarasov et al. 2005, Levin et al. 2009).

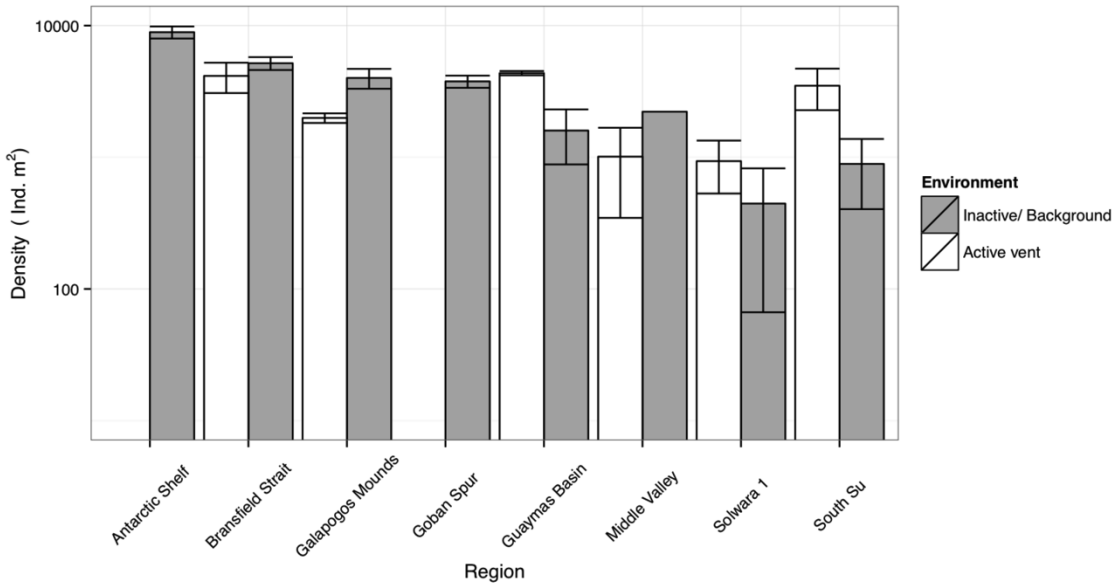

Figure 4.6.2a – Comparative macrofaunal densities between Bransfield Strait sites (this study) and literature values for other diffuse hydrothermal vents (Grassle et al. 1985, Levin et al. 2009) and typical bathyal sediments of the West Antarctic Peninsula (polychaetes only) (Neal et al. 2011) and Goban spur, NE Atlantic (Flach & Heip 1996). Error bars denote ± 1 S.E.

Whilst these data do not fit Bernardino et al. (2012)'s model (Figure 4.6.1a), we suggest that trends in density are much more dependent upon regional factors (e.g. export production or temperature sensitivity of local benthos (Clarke et al. 2009)). The scope for regional variation means that for other systems, where SPP is lower (e.g. Manus Basin) or in-situ production higher (e.g. Middle Valley Clam beds), the existing model applies (Levin et al. 2009, Bernardino et al. 2012). Local OM production rates are also clearly important and areas of dense populations of vent-endemic megafauna (e.g. Clam beds at Middle Valley) can also enrich local macrofaunal density (Levin et al. 2009) but such habitats were not observed in the Bransfield Strait. At the basin scale, our observations do not agree with the model of increasing macrofaunal abundance towards vent (Figure 4.6.1a), but at small scales (i.e. between Hook Ridge 1 replicates) there is a potential increase in faunal abundance and biomass associated with moderate levels of hydrothermal activity.

Deployment 25, from Hook Ridge 1, had both the highest vent-endemic and total faunal density. This suggests that chemosynthetic trophic support may have been

enhancing local density and biomass, particularly for scavengers like crustaceans. However, the effect was clearly quite spatially limited as other sites at Hook Ridge had a much lower faunal abundance, suggesting that in situ OM production was patchily distributed at a scale of 10s of metres (the estimated likely seabed separation of replicate deployments). This is consistent with sediment-hosted vents in the Arctic Ocean, which found limited macrofaunal utilisation of chemosynthetically-derived OM, even within sediment-hosted vent fields (Sweetman et al. 2013). This kind of fine scale structuring of communities is consistent with other SHV (Bernardino et al. 2012). Elsewhere at Hook Ridge (particularly Hook Ridge 2), abundance per deployment was lower or similar to non-vent sites (Table 4.5.1a), leading to the increase in abundance observed (Figure 4.5.4a).

Levels of organic carbon in surface sediment measured from Bransfield Strait sites (Table 4.5.1a; Yoon et al. 1994, Aquilina et al. 2014) showed that Hook Ridge (0.25 – 1.35 wt% organic C) was comparable, to the control site (0.75 – 1.35 wt % organic C) and the Three Sisters (1.40 wt % organic C, Table 4.5.1a), which suggests that chemosynthetic activity was not augmenting available organic matter. It is possible that the relatively high density of scavengers at Hook Ridge 1 increased turnover rates of available organic matter (Rowe et al. 1990), potentially masking local OM production. However, this should have resulted in increased macrofaunal biomass at Hook Ridge, which was not observed in either annelids or peracarids (Supplement 4-2). It is also possible that additional organic carbon produced at Hook Ridge 1 is largely retained in *Sclerolinum* tissue rather than being released into the sediment. It might be expected that the local OM production at SHV could enrich biomass, through increased food availability (Bernardino et al. 2012). However, in the Bransfield Strait, it seems that either environmental conditions at active vents deter background fauna or that local production of chemosynthetically derived organic matter is insufficient to encourage interaction between endemic and background species (or both). Bottom water temperature in the Bransfield Strait is around -1.5˚C (Clarke et al. 2009), compared with estimates of temperature at Hook Ridge (~24 – 48˚C (Dählmann et al. 2001, Petersen et al. 2011)). This may indicate that temperature variation at Southern Ocean SHVs is more significant than in other

areas of the deep-sea. Another factor that may structure Bransfield vent communities is the relative isolation of the Southern ocean caused by the Antarctic Circumpolar Current (ACC) (Clarke et al. 2009, Neal et al. 2011). The ACC may have resulted in an impoverished community of vent-obligate or vent-tolerant fauna, relative to other SHVs where high temperature vents are in close proximity (e.g. Guaymas or Middle Valley).

4.6.3 *Siboglinid autecology*

Although Hook Ridge 2 had the greatest hydrothermal advection rates (Aquilina et al. 2013), available sulphide was probably too low to support populations of *S. contortum* (Sahling et al. 2005) and was much lower than at Hook Ridge 1 (0 – 6 μmol L^{-1} and 0 – 160 μmol L^{-1} respectively, (Aquilina et al. 2013)). Sulphide concentrations at both sites were low for the typical range of sulphide concentrations expected at sediment-hosted vents (1.5 – 8 mM (Bernardino et al. 2012)). Patterns in *S. contortum* density is consistent with Sahling et al. (2005) who concluded that *S. contortum* favoured areas of sulphide concentration of around 100 – 150 μmol L^{-1}, relatively low for SHV, and that in areas of higher hydrothermal influence, higher temperatures or the formation of siliceous surface crusts (Dählmann et al. 2001, Klinkhammer et al. 2001) made conditions unsuitable. There were no complete specimens (i.e. specimens with heads) of *S. contortum* or any other vent endemic species at Hook Ridge 2, but there were densities of *S. contortum* fragments similar to those at Hook Ridge 1 (0 – 1401 ind. m^2). Video imagery also revealed patches of bacterial mat across Hook Ridge suggesting that there was at least patchy chemosynthetic activity across a wide area (Aquilina et al. 2013, Georgieva et al. 2015). It is probable that the differences in density of *S. contortum* between the two sites is driven by either sulphide availability (Aquilina et al. 2013), temperature (Sahling et al. 2005), or both.

Ecological and geochemical (Aquilina et al. 2013) observations from across the Bransfield Strait support dividing the basin into three sub-regions, previously identified around Hook Ridge by Sahling et al. (2005) based on differences in *S. contortum* density, hydrothermal advection and sulphide availability, in support of

hypothesis 3 (Figure 4.6.1a): 1) background areas of no hydrothermal activity (e.g. Control); 2) areas of moderate hydrothermal activity supporting populations of *S. contortum* (Hook Ridge 1); and 3) areas of higher hydrothermal activity with no vent endemic fauna (Hook Ridge 2). Siliceous crusts were observed in areas of higher hydrothermal advection at Hook Ridge (Sahling et al. 2005, Aquilina et al. 2013) corresponding to, or possibly resulting in, areas of absence of *S. contortum* (Sahling et al. 2005, This Study). However, sulphide availability was quite variable at areas of siliceous crust, ranging between ~120 – 330 μmol L^{-1} (Sahling et al. 2005) and 0 – 6 μmol L^{-1} (Aquilina et al. 2013). Sulphide may either have been limiting (Aquilina et al. 2013) or prohibitively toxic (Sahling et al. 2005) in areas of higher hydrothermal activity and is likely crucial in structuring *S. contortum* populations. The apparently limited habitat niche favoured by *S. contortum*, and the lack of any other vent endemic species (e.g. vesicomyid clams) conflicts with the Bernardino et al. model suggestion (Bernardino et al. 2012) that the proportion of vent endemic species should increase towards venting sites (Fig. 4.6.1a). This likely reflects a combination between the physiological constraints of *S. contortum* and the absence of a wider diversity of vent endemic species, illustrating the oceanographic and physiological restrictions that underpin communities of Southern Ocean benthos (Clarke et al. 2009, Chown 2012).

Based on previous estimates of *S. contortum* density at Hook Ridge of up to 800 ind. m^2 (Sahling et al. 2005), it was suggested that *S. contortum* tubes act as conduits, significantly increasing supply of dissolved iron and manganese to overlying waters by allowing them to bypass oxic sediment and thus avoid precipitation (Aquilina et al. 2014). *S. contortum* density in this study (up to 4520 ind. m^2) was much higher than previous estimates (Sahling et al. 2005), demonstrating that population size varies widely in time and or space. Our observations suggest that the capacity of *S. contortum* to support pore fluid to bottom water exchange of dissolved metals may be more than originally estimated (Aquilina et al. 2014). Empty tubes may also facilitate transfer as suggested (Aquilina et al. 2014), and these were certainly far more numerous than complete specimens (up to 19 226 frag. m^2). However, empty tubes commonly contained tissue fragments or sediment or were much shorter than

complete specimens, potentially reducing their capacity to support fluid exchange. It is also unclear how long these fragments last or how quickly they are produced.

The presence of *Siboglinum* sp. at the non-Hook Ridge sites may suggest that these areas could have hosted some chemosynthetic activity (Juniper et al. 1992, Dando et al. 1994, Thornhill et al. 2008). *Siboglinum fjordicum* shows a similar endosymbiont composition to that of *Oligobrachia mashikoi*, a putative methanotroph (Thornhill et al. 2008, Cordes et al. 2010). However, *Siboglinum* spp. are also known from non-chemosynthetic sediments, potentially subsisting on dissolved organic matter (George 1976, Southward et al. 1979, Shields & Blanco-Perez 2013) and so are not necessarily indicative of active chemosynthesis. Methane was detected in sediment cores from the control site (deeper than 10cm b.s.f. (Aquilina et al. 2013)), which had the greatest abundance of *Siboglinum* and was not hydrothermally influenced. It is therefore suggested that *Siboglinum* sp. at the control site were utilizing thermogenic hydrocarbons, such as those observed elsewhere in Bransfield Strait sediments (Whiticar & Suess 1990). It is likely that the production rate of these hydrocarbons is increased by the heat flux associated with hydrothermal activity (Whiticar & Suess 1990), illustrating a potential indirect dependence upon hydrothermalism amongst some fauna. However, methane was not detected at the Three Sisters, which also hosted a small *Siboglinum* sp. population, suggesting that other OM sources are also possible.

4.6.4 *Hydrothermal Activity*

The hydrothermal index echoed geochemical variability (Aquilina et al. 2013, Aquilina et al. 2014) and treated environmental variability as coherent, rather than a series of isolated parameters (Sahling et al. 2005) permitting quantitative assessment of faunal responses (Dauwe & Middelburg 1998, Brown et al. 2010). Ordination techniques were used to select model parameters but the spatial resolution of the environmental data was limited which did not facilitate the use of more established ordination analysis (e.g. BIO-ENV Clarke & Ainsworth 1993). However, given the ship-time cost and pressure for large-scale environmental surveys of the deep sea to establish reference baselines to monitor anthropogenic

and climate related changes in community composition, applied analytical techniques need to be developed where concurrent environmental sampling is poor. We propose that this approach, which can be adapted to any marine or aquatic habitat, can provide and support insights into establishing the influence of environmental gradients on faunal distribution. Here, we use it to test the conceptual models of Bernardino et al. (2012) and identify previously unknown trends in abundance and diversity that may be subject to regional as well as environmental factors.

One parameter missing from HI is temperature, for which data were unavailable. In the Southern Ocean, where benthos are relatively sensitive to temperature fluctuations (Barnes & Peck 2008, Clarke et al. 2009), it is likely that the relatively hot conditions presented by SHVs represented a significant deterrent to background fauna. However, in Guaymas basin macrofaunal assemblages, concentrations of sulphide and methane were found to be drivers of compositional differences and temperature was not a significant factor (Portail et al. 2015). In the absence of temperature data, chlorinity profiles were used. Chloride depletion has been previously used as a proxy for the relative amounts of hydrothermal fluid present (Aquilina et al. 2013) and was considered proportional to temperature (Ginsburg et al. 1999). There are estimates of seafloor temperature at Hook Ridge from previous studies, of 25 – 48.5 ˚C (Bohrmann et al. 1998, Dählmann et al. 2001) but downcore temperature profiles have not been measured. Although chlorinity is believed an acceptable proxy (Ginsburg et al. 1999, Aquilina et al. 2013), future multi-parameter indices for hydrothermal activity in SHV should consider incorporating temperature if possible.

4.6.5 *Controls on faunal distribution and community structure*

Environmental distance, represented by the changing influence of hydrothermal activity (Aquilina et al. 2013), clearly influenced assemblage structure. Diversity, abundance and species richness all declined (GLM: $p = < 0.05, < 0.001$ & < 0.01 respectively) towards the area of highest hydrothermal flux (Figure 4.5.4a; Table 4.5.4b). This demonstrates a clear response of faunal assemblages to environmental

stress and habitat partitioning, being more similar in regions of similar environmental conditions (Bernardino et al. 2012), rather than simple structuring in response to dispersal ability.

Since non-hydrothermally active sites did not exhibit strong variation in the selected geochemical parameters between upper and lower partitions, faunal variation downcore at non-vent sites was not relevant to the amount of hydrothermal flux. Therefore, to separate the influence of hydrothermalism from expected downcore variability, only data for upper partitions were used from non-vent sites (Table 4.5.4a). It should be noted however that expected gradients, particularly in abundance, between upper and lower partitions will have contributed some of the model fit in a manner consistent with non-hydrothermally influenced sites.

The relatively rapid changes at HI levels of < 0 (indicated by the increased gradient, Figure 4.5.4a) suggests a fairly narrow transition zone between background or vent-tolerant assemblages and those that favour hydrothermal conditions (Figure 4.5.4a), with relatively little overlap in dominant taxa (Figure 4.5.1a). Zonation in faunal distribution at hydrothermal vents is common, often associated with competition, environmental distance and availability of biogenic habitat (Levin et al. 2009, Bernardino et al. 2012, Levin et al. 2012, Marsh et al. 2012) and is analogous to more general disturbance gradients (Pearson & Rosenberg 1978).

Proportions of different functional groups varied significantly between sites suggesting that niche variation, rather than geographical separation, was the dominant driver in the compositional differences observed (Nekola & White 1999, McClain et al. 2012). For example, the motile deposit feeder *Aricidea antarctica* (Annelida, Paraonidae) occurred at all sites and was highly abundant at the control site but only minimally abundant elsewhere. Similarly, sessile deposit feeding terebellids (*Polycirrus* sp.) occurred in much higher relative density at Hook Ridge 2 (15 % of abundance) than elsewhere in the Strait (0 – 5 %). *Polycirrus medusa* (Annelida, Terebellidae, Grube, 1850) is known from a sediment-hosted vent in the Arctic (Sweetman et al. 2013), and 'Ampharetid beds' are not uncommon in vent or seep environments (Bernardino et al. 2012), consistent with the relatively high

density and biomass of terebellids at Hook Ridge 2. Patterns in terebellomorph polychaete at SHVs may represent similar mechanisms driving assemblage structure and habitat selection such as competition or tolerance to toxic environments. The majority (81 %) of peracarids were found at Hook Ridge, demonstrating a clear preference to hydrothermally active sites, in comparison to annelids, for which only 19 % of individuals counted were found at Hook Ridge sites. Hydrothermally-influenced sites were more suitable for scavengers and sessile deposit feeders, whilst sites without hydrothermal influence were more favoured by motile deposit feeders.

The fact that many of the more numerous taxa were found at all sites demonstrates that their distribution was not limited by dispersal ability. Communities in the Bransfield Strait had a much higher proportion of species conserved across the basin than in other bathyal settings. For example, macroinvertebrates from the Monterey Canyon (McClain et al. 2011) experienced a reduction in shared species of 50 % over ~7.5 km, compared to around 100 km in this study (classic Sørenson distance, presence-absence data). The relatively high conservation of species throughout the basin coupled with the changes in community structure observed between sites, further suggests that functional diversity, rather than dispersal ability, was very important in structuring local assemblages.

Overall, Pacific and Southern Ocean sedimented vents share a number of higher taxa (e.g. Peracarids (isopods and tanaids) and polychaetes (terebellomorph and nereidid) (Grassle et al. 1985, Levin et al. 2009), but their relative abundances are quite variable. Pacific vent communities are distinct between eastern and western sites (Bernardino et al. 2012), in part reflecting geographic isolation. Eastern Pacific vents had a comparatively low abundance of peracarid crustaceans (relative to western Pacific and Bransfield Strait SHV) and tended to be more dominated by polychaete species characteristic of reducing environments (e.g. dorvilleids) (Grassle et al. 1985, Grassle & Petrecca 1994, Levin et al. 2009). Vent endemic fauna at sediment-hosted vents at the Chile Triple Junction (CTJ) (Thurber et al., unpublished data, cited in Levin et al., 2012) were also only represented by siboglinid polychaetes, as with the Bransfield Strait vents and it is likely, given their

proximity, that the Bransfield vents are most similar to vents at the CTJ. Macrofauna from shallower sites around the South Shetland Islands were also numerically dominated by polychaetes, as with non-Hook Ridge areas of the Bransfield Strait, and structured in part by habitat (substratum) availability (Arnaud et al. 1998). These observations are semi-quantitative however, and include a wider range of size classes than analysed here so were not directly comparable.

4.7 Conclusions

In this first community-ecology study of a sediment-hosted hydrothermal vent in the Southern Ocean we have shown that sediment-hosted hydrothermalism strongly influences infaunal communities in the deep Bransfield Strait. We assessed variation in macrofaunal communities along environmental distance gradients. Populations of vent endemic fauna, represented by a single species, had limited distribution but changes in macrofaunal community structure were still clearly evident between active vent and background sediments. The distribution of *S. contortum*, relative to sediment geochemistry, was consistent with previous observations (Sahling et al. 2005), supporting our hypothesis. Diversity, species richness and density were all lower at hydrothermally active sites than in background sediments, confirming hypothesis two but rejecting hypothesis one We have identified several ways in which faunal trends for Bransfield Strait SHVs differ from generalized trends derived from other SHVs (Bernardino et al. 2012). Potential factors driving these differences include: physiological stress (Levin et al. 2013); other sources of OM (Wefer & Fischer 1991, Palmer & Totterdell 2001, Kim et al. 2005) undermining the significance of locally produced OM, and sensitivity to environmental conditions of Southern Ocean benthos (Barnes & Peck 2008).

4.8. Conflict of Interest Statement and Funding Disclosure

This work was supported entirely by UK Natural Environment Research Council (NERC) grants. All authors declare that there are no conflicts of interest arising from the work outlined in this manuscript. NERC staff were not involved in the decision to publish. JBB was funded by a (NERC) PhD Studentship (NE/L501542/1). This work

was also funded by the NERC ChEsSo consortium (Chemosynthetically-driven Ecosystems South of the Polar Front, NERC Grant NE/DOI249X/I).

4.9 Author Contributions

The authors have made the following declarations about their contributions. Conceived, designed and executed sampling programme: AG, CW, WR and CS. Data collection and taxonomy: JB, AG and CL. Performed analyses: JB and LB, Designed Hydrothermal Index: JB, LB and CW. Literature review: JB. Wrote the paper: JB, CW. Prepared figures: JB. Commented on the paper: JB, CW, LB, CL, CS, WR and AG

4.10 Acknowledgements

We are grateful to the Master and Crew of RRS *James Cook* cruise 055 for technical support and the Cruise Principal Scientific Officer Professor Paul Tyler. We gratefully acknowledge taxonomic contributions from P Graham Oliver and Christer Erséus and geochemical data and insight provided by Laura Hepburn, Alfred Aquilina and Rachel Mills.

4.11 References

Anderson MJ (2001) A new method for non-parametric multivariate analysis of variance. Austral Ecology 26:32-46

Aquilina A, Connelly DP, Copley JT, Green DR, Hawkes JA, Hepburn L, Huvenne VA, Marsh L, Mills RA, Tyler PA (2013) Geochemical and Visual Indicators of Hydrothermal Fluid Flow through a Sediment-Hosted Volcanic Ridge in the Central Bransfield Basin (Antarctica). Plos One 8:e54686

Aquilina A, Homoky WB, Hawkes JA, Lyons TW, Mills RA (2014) Hydrothermal sediments are a source of water column Fe and Mn in the Bransfield Strait, Antarctica. Geochimica et Cosmochimica Acta 137:64-80

Arnaud PM, López CM, Olaso I, Ramil F, Ramos-Esplá AA, Ramos A (1998) Semi-quantitative study of macrobenthic fauna in the region of the South Shetland Islands and the Antarctica Peninsula. Polar Biology 19:160-166

Barnard JL, Karaman GS (1991) The families and genera of marine gammaridean Amphipoda (except marine gammaroids). Part 2. Records of the Australian Museum, Supplement 13:419-866

Barnes DKA, Peck LS (2008) Vulnerability of Antarctic shelf biodiversity to predicted regional warming. Climate Research 37:149-163

Beesley PL, Ross GJB, Glasby C (2000) Polychaetes & Allies: The Southern Synthesis. *Fauna of Australia Vol. 4A Polychaeta, Myzostomida, Pogonophora, Echiura, Spincula*. CSIRO, Melbourne

Bemis K, Lowell R, Farough A (2012) Diffuse Flow On and Around Hydrothermal Vents at Mid-Ocean Ridges. Oceanography 25:182-191

Bernardino AF, Levin LA, Thurber AR, Smith CR (2012) Comparative Composition, Diversity and Trophic Ecology of Sediment Macrofauna at Vents, Seeps and Organic Falls. Plos ONE 7:e33515

Bohrmann G, Chin C, Petersen S, Sahling H, Schwarz-Schampera U, Greinert J, Lammers S, Rehder G, Daehlmann A, Wallmann K, Dijkstra S, Schenke HW (1998) Hydrothermal activity at Hook Ridge in the Central Bransfield Basin, Antarctica. Geo-Marine Letters 18:277-284

Brown LE, Milner AM, Hannah DM (2010) Predicting river ecosystem response to glacial meltwater dynamics: a case study of quantitative water sourcing and glaciality index approaches. Aquatic Sciences 72:325-334

Chao A, Chazdon RL, Colwell RK, Shen T-J (2005) A new statistical approach for assessing similarity of species composition with incidence and abundance data. Ecology Letters 8:148-159

Chown SL (2012) Antarctic Marine Biodiversity and Deep-Sea Hydrothermal Vents. Plos Biology 10

Clarke A, Crame JA (1992) The Southern Ocean Benthic Fauna and Climate Change: A Historical Perspective. Philosophical Transactions of the Royal Society B-Biological Sciences 338:299-309

Clarke A, Crame JA (2010) Evolutionary dynamics at high latitudes: speciation and extinction in polar marine faunas. Philosophical transactions of the Royal Society B-Biological sciences 365:3655-3666

Clarke A, Griffiths HJ, Barnes DKA, Meredith MP, Grant SM (2009) Spatial variation in seabed temperatures in the Southern Ocean: Implications for benthic ecology and biogeography. Journal of Geophysical Research 114:1-11

Clarke KR, Ainsworth M (1993) A method of linking multivariate community structure to environmental variables. Marine Ecology Progress Series 92:205-219

Clarke KR, Somerfield PJ, Chapman MG (2006) On resemblance measures for ecological studies, including taxonomic dissimilarities and a zero-adjusted Bray–Curtis coefficient for denuded assemblages. Journal of Experimental Marine Biology and Ecology 330:55-80

Clarke KR, Somerfield PJ, Gorley RN (2008) Testing of null hypotheses in exploratory community analyses: similarity profiles and biota-environment linkage. Journal of Experimental Marine Biology and Ecology 366:56-69

Colwell RK (2013) *EstimateS*: Statistical estimation of species richness and shared species from samples. Version 9. Persistent URL <purloclcorg/estimates>

Colwell RK, Chao A, Gotelli NJ, Lin SY, Mao CX, Chazdon RL, Longino JT (2012) Models and estimators linking individual-based and sample-based rarefaction, extrapolation and comparison of assemblages. Journal of Plant Ecology 5:3-21

Connell JH (1978) Diversity in tropical rain forests and coral reefs. Science 199:1302-1310

Cordes EE, Becker EL, Hourdez S, Fisher CR (2010) Influence of foundation species, depth, and location on diversity and community composition at Gulf of Mexico lower-slope cold seeps. Deep Sea Research Part II: Topical Studies in Oceanography 57:1870-1881

Dählmann A, Wallman K, Sahling H, Sarthou G, Bohrmann G, Petersen S, Chin CS, Klinkhammer GP (2001) Hot vents in an ice-cold ocean: Indications for phase separation at the southernmost area of hydrothermal activity, Bransfield Strait, Antarctica. Earth and Planetary Science Letters 193:381-394

Dando PR, Bussmann I, Niven SJ, O'Hara SCM, Schmaljohann R, Taylor LJ (1994) A methane seep area in the Skagerrak, the habitat of the pogonophore *Siboglinum poseidoni* and the bivalve mollusc *Thyasira sarsi*. Marine Ecology Progress Series 107:157-167

Dauwe B, Middelburg JJ (1998) Amino acids and hexsoamines as indicators of organic matter degradation state in North Sea sediments. Limnology & Oceanography 43:782-798

Dobson AJ (1990) An Introduction to Generalized Linear Models. Chapman & Hall, London

Dobson AJ, Barnett A (2008) An Introduction to Generalized Linear Models. Chapman & Hall, Boca Raton, FL

Fauchald K (1977) The Polychaete Worms: Definitions and Keys to the Orders, Families and Genera, Natural History Museum of Los Angeles County

Fauchald K, Jumars PA (1979) The Diet of Worms: A Study of Polychaete Feeding Guilds. Oceanography and Marine Biology: An Annual Review 17:193-284

Flach E, Heip C (1996) Vertical distribution of macrozoobenthos within the sediment on the continental slope of the Goban Spur area (NE Atlantic). Marine Ecology Progress Series 141:55-66

Fox J, Weisberg S, Adler D, Bates D, Baud-Bovy G, Ellison S, Firth D, Friendly M, Gorjanc G, Graves S, Heiberger R, Laboissiere R, Monette G, Murdoch D, Nilsson H, Ogle D, Ripley B, Venables W, Zeileis A, R Core Team (2013) Companion to Applied Regression. cranr-projectorg

Gage JD, Bett BJ (2005) Deep-sea benthic sampling. In: Holmes NA, McIntyre AD (eds) Methods for the study of the marine benthos. Blackwell Scientific Publications, Oxford

George JD (1976) Ecology of the Pogonophore, *Siboglinum fiordicum* Webb, in a shallow-water fjord community. In: Keegan BF, Boaden PJS, Ceidigh PO (eds) Biology of Benthic Organisms: 11th European Symposium on Marine Biology. Elsevier, Galway

Georgieva M, Wiklund H, Bell JB, Eilersten MH, Mills RA, Little CTS, Glover AG (2015) A chemosynthetic weed: the tubeworm *Sclerolinum contortum* is a biploar, cosmopolitan species. BMC Evolutionary Biology 15:280

Ginsburg GD, Milkov AV, Soloviev VA, Egorov AV, Cherkashev GA, Vogt PR, Crane K, Lorenson TD, Khutorsky MD (1999) Gas hydrate accumulation at the Håkon Mosby Mud Volcano. Geo-Marine Letters 19:57-67

Gollner S, Govenar B, Fisher CR, Bright M (2015) Size matters at deep-sea hydrothermal vents: different diversity and habitat fidelity patterns of meio- and macrofauna. Marine Ecology Progress Series 520:57-66

Gotelli NJ, Colwell RK (2001) Quantifying biodiversity: procedures and pitfalls in the measurement and comparison of species richness. Ecological Letters 4:379-391

Grassle JF, Brown-Leger LS, Morse-Porteous L, Petrecca RF, Williams I (1985) Deep-Sea Fauna of Sediments in the Vicinity of Hydrothermal Vents. Bulletin of the Biological Society of Washington 6:443-452

Grassle JF, Petrecca RF (1994) Soft-sediment hydrothermal vent communities of Escanaba Trough. In: Zierenberg RA, Reiss CA (eds) Geological, hydrothermal, and biological studies at Escanaba Trough, Gorda Ridge, offshore Northern California. US Geological Survey, Denver, CO

Jumars PA, Dorgan KM, Lindsay SM (2015) Diet of worms emended: an update of polychaete feeding guilds. Annual review of marine science 7:497-520

Juniper SK, Jonasson IR, Tunnicliffe V, Southward AJ (1992) Influence of tube building polychaete on hydrothermal chimney mineralization. Geology 20:895-898

Kharlamenko VI, Zhukova NV, Khotimchenko SV, Svetashev VI, Kamenev GM (1995) Fatty-acids as markers of food sources in a shallow-water hydrothermal ecosystem (Kraternaya Bight, Yankich island, Kurile Islands). Marine Ecology Progress Series 120:231-241

Kilgallen NH (2007) Taxonomy of the Lysianassoidea of the Northeast Alantic and Mediterranean: An Interactive Identification Key and Studies on Problematic Groups. PhD Thesis

Kim D, Kim D-Y, Park J-S, Kim Y-J (2005) Interannual variation of particle fluxes in the eastern Bransfield Strait, Antarctica: A response to the sea ice distribution. Deep Sea Research Part I: Oceanographic Research Papers 52:2140-2155

Klinkhammer GP, Chin CS, Keller RA, Dahlmann A, Sahling H, Sarthou G, Petersen S, Smith F (2001) Discovery of new hydrothermal vent sites in Bransfield Strait, Antarctica. Earth and Planetary Science Letters 193:395-407

Larson BI, Houghton JL, Lowell RP, Farough A, Meile CD (2015) Subsurface conditions in hydrothermal vents inferred from diffuse flow composition, and models of reaction and transport. Earth and Planetary Science Letters 424:245-255

Levin LA, Mendoza GF, Konotchick T, Lee R (2009) Macrobenthos community structure and trophic relationships within active and inactive Pacific hydrothermal sediments. Deep Sea Research Part II: Topical Studies in Oceanography 56:1632-1648

Levin LA, Orphan VJ, Rouse GW, Rathburn AE, Ussler W, III, Cook GS, Goffredi SK, Perez EM, Waren A, Grupe BM, Chadwick G, Strickrott B (2012) A hydrothermal seep on the Costa Rica margin: middle ground in a continuum of reducing ecosystems. Proceedings of the Royal Society B-Biological Sciences 279:2580-2588

Levin LA, Ziebis W, Mendoza GF, Bertics VJ, Washington T, Gonzalez J, Thurber AR, Ebbed B, Lee RW (2013) Ecological release and niche partitioning under stress: Lessons from dorvilleid polychaetes in sulfidic sediments at methane seeps. Deep-Sea Research Part II-Topical Studies in Oceanography 92:214-233

Marsh L, Copley JT, Huvenne VAI, Linse K, Reid WDK, Rogers AD, Sweeting CJ, Tyler PA (2012) Microdistribution of Faunal Assemblages at Deep-Sea Hydrothermal Vents in the Southern Ocean. PloS ONE 7:e48348

McClain CR, Nekola JC, Kuhnz L, Barry JP (2011) Local-scale faunal turnover on the deep Pacific seafloor. Marine Ecology Progress Series 422:193-200

McClain CR, Schlacher TA (2015) On some hypotheses of diversity of animal life at great depths on the sea floor. Marine Ecology:12288

McClain CR, Stegen JC, Hurlbert AH (2012) Dispersal, environmental niches and oceanic-scale turnover in deep-sea bivalves. Philosophical transactions of the Royal Society B-Biological sciences 279:1993-2002

Mincks SL, Smith CR, Jeffreys RM, Sumida PYG (2008) Trophic structure on the West Antarctic Peninsula shelf: Detritivory and benthic inertia revealed by δ13C and δ15N analysis. Deep Sea Research Part II: Topical Studies in Oceanography 55:2502-2514

Neal L, Mincks Hardy SL, Smith CR, Glover AG (2011) Polychaete species diversity on the West Antarctic Peninsula deep continental shelf. Marine Ecology Progress Series 428:119-134

Nekola JC, White PS (1999) The distance decay of similarity in biogeography and ecology. Journal of Biogeography 26:867-878

Netto SA, Gallucci F, Fonseca G (2009) Deep-sea meiofauna response to synthetic-based drilling mud discharge off SE Brazil. Deep Sea Research Part II: Topical Studies in Oceanography 56:41-49

Oksanen J, Blanchet GG, Kindt R, Legendre P, Minchin PR, O'Hara RB, Simpson GL, Solymos P, Stevens HH, Wagner H (2013) Package 'vegan'. cranr-projectorg

Palmer JR, Totterdell IJ (2001) Production and export in a global ocean ecosystem model. Deep Sea Research Part I: Oceanographic Research Papers 48:1169-1198

Pearson TH, Rosenberg R (1978) Macrobenthic succession in relation to organic enrichment and pollution of the marine environment. Oceanography and Marine Biology: An Annual Review 16:229-311

Petersen JM, Zielinski FU, Pape T, Seifert R, Moraru C, Amann R, Hourdez S, Girguis PR, Wankel SD, Barbe V, Pelletier E, Fink D, Borowski C, Bach W, Dubilier N (2011) Hydrogen is an energy source for hydrothermal vent symbioses. Nature 476:176-180

Petersen S, Herzig PM, Schwarz-Schampera U, Hannington MD, Jonasson IR (2004) Hydrothermal precipitates associated with bimodal volcanism in the Central Bransfield Strait, Antarctica. Mineralium Deposita 39:358-379

Poore GCB (2001) Isopoda Valvifera: Diagnoses and Relationships of the Families. Journal of Crustacean Biology 21:205-230

Portail M, Olu K, Escobar-Briones E, Caprais JC, Menot L, Waeles M, Cruaud P, Sarradin PM, Godfroy A, Sarrazin J (2015) Comparative study of vent and seep macrofaunal communities in the Guaymas Basin. Biogeosciences 12:5455-5479

R Core Team (2013) R: A language and environment for statistical computing. R Foundation for Statistical Computing, Vienna, Austria

Reed AJ, Morris JP, Linse K, Thatje S (2013) Plasticity in shell morphology and growth among deep-sea protobranch bivalves of the genus *Yoldiella*

(Yoldiidae) from contrasting Southern Ocean regions. Deep Sea Research Part I: Oceanographic Research Papers 81:14-24

Rex MA, Etter RJ (2010) Deep-Sea Biodiversity: Pattern and Scale. Harvard University Press, Cambridge, MA

Robertson BP, Gardner JPA, Savage C (2015) Macrobenthic–mud relations strengthen the foundation for benthic index development: A case study from shallow, temperate New Zealand estuaries. Ecological Indicators 58:161-174

Rogers AD, Tyler PA, Connelly DP, Copley JT, James R, Larter RD, Linse K, Mills RA, Garabato AN, Pancost RD, Pearce DA, Polunin NVC, German CR, Shank T, Boersch-Supan PH, Alker BJ, Aquilina A, Bennett SA, Clarke A, Dinley RJJ, Graham AGC, Green DRH, Hawkes JA, Hepburn L, Hilario A, Huvenne VAI, Marsh L, Ramirez-Llodra E, Reid WDK, Roterman CN, Sweeting CJ, Thatje S, Zwirglmaier K (2012) The Discovery of New Deep-Sea Hydrothermal Vent Communities in the Southern Ocean and Implications for Biogeography. PLoS Biology 10:e1001234

Roterman CN, Copley JT, Linse KT, Tyler PA, Rogers AD (2013) The biogeography of the yeti crabs (Kiwaidae) with notes on the phylogeny of the Chirostyloidea (Decapoda: Anomura). Proceedings of the Royal Society B-Biological Sciences 280

Rowe GT, Sibuet M, Deming J, Tietjen T, Khripounoff A (1990) Organic carbon turnover time in deep-sea benthos. Progress in Oceanography 24:141-160

Rozemarjin K, Christoffer S, Anders KJ, Endre W (2011) Ecology of twelve species of Thyasiridae (Mollusca: Bivalvia). Mar Pollut Bull 62:786-791

Sahling H, Wallman K, Dählmann A, Schmaljohann R, Petersen S (2005) The physicochemical habitat of *Sclerolinum sp.* at Hook Ridge hydrothermal vent, Bransfield Strait, Antarctica. Limnology & Oceanography 50:598-606

Shields MA, Blanco-Perez R (2013) Polychaete abundance, biomass and diversity patterns at the Mid-Atlantic Ridge, North Atlantic Ocean. Deep Sea Research Part II: Topical Studies in Oceanography 98B:315-325

Smirnov RV (2000) *Sclerolinum contortum*. In: Read G, Fauchald K (eds) World Polychaeta database. http://www.marinespecies.org/polychaeta/aphia.php?p=taxdetails&id=129130

Somoza L, Martínez-Frías J, Smellie JL, Rey J, Maestro A (2004) Evidence for hydrothermal venting and sediment volcanism discharged after recent short-lived volcanic eruptions at Deception Island, Bransfield Strait, Antarctica. Marine Geology 203:119-140

Southward A, J., Southward EC, Brattegard T, Bakke T (1979) Further Experiments on the value of Dissolved Organic Matter as Food for *Siboglinum fjiordicum* (Pogonophora). Journal of Marine Biological Asociation of the United Kingdom 59:133-148

Sweetman AK, Levin LA, Rapp HT, Schander C (2013) Faunal trophic structure at hydrothermal vents on the southern Mohn's Ridge, Arctic Ocean. Marine Ecology Progress Series 473:115

Tarasov VG, Gebruk AV, Mironov AN, Moskalev LI (2005) Deep-sea and shallow-water hydrothermal vent communities: Two different phenomena? Chemical Geology 224:5-39

Thornhill DJ, Wiley AA, Campbell AL, Bartol FF, Teske A, Halanych KM (2008) Endosymbionts of *Siboglinum fjordicum* and the Phylogeny of Bacterial Endosymbionts in Siboglinidae (Annelida). Biological Bulletin 214:135-144

Tyler PA, Connelly DP, Copley JT, Linse K, Mills RA, Pearce DA, Aquilina A, Cole C, Glover AG, Green DR, Hawkes JA, Hepburn L, Herrera S, Marsh L, Reid WD, Roterman CN, Sweeting CJ, Tate A, Woulds C, Zwirglmaier K (2011) RRS *James Cook* cruise JC55: Chemosynthetic Ecosystems of the Southern Ocean. BODC Cruise Report

Urich T, Lanzen A, Stokke R, Pedersen RB, Bayer C, Thorseth IH, Schleper C, Steen IH, Ovreas L (2014) Microbial community structure and functioning in marine sediments associated with diffuse hydrothermal venting assessed by integrated meta-omics. Environ Microbiol 16:2699-2710

Van Dover CL (2010) Mining seafloor massive sulphides and biodiversity: what is at risk? ICES Journal of Marine Science 68:341-348

Wefer G, Fischer G (1991) Annual primary production and export flux in the Southern Ocean from sediment trap data. Marine Chemistry 35:597-613

Whitaker D, Christmann M (2013) Package 'clustsig'. cranr-projectorg

Whiticar MJ, Suess E (1990) Hydrothermal hydrocarbon gases in the sediments of the King George Basin, Bransfield Strait, Antarctica. Applied Geochemistry 5:135-147

Yoon HI, Han MW, Park BK, Oh JK, Chang SK (1994) Depositional environment of near-surface sediments, King George Basin, Bransfield Strait, Antarctica. Geo-Marine Letters 14:1-9

Zeppilli D, Mea M, Corinaldesi C, Danovaro R (2011) Mud volcanoes in the Mediterranean Sea are hot spots of exclusive meiobenthic species. Progress in Oceanography 91:260-272

Zeppilli D, Vanreusel A, Pradillon F, Fuchs S, Mandon P, James T, Sarrazin J (2015) Rapid colonisation by nematodes on organic and inorganic substrata deployed at the deep-sea Lucky Strike hydrothermal vent field (Mid-Atlantic Ridge). Marine Biodiversity 45:489-504

Chapter 5: Hydrothermal activity lowers trophic diversity in Antarctic sedimented hydrothermal vents

Biogeosciences (In review)

James B. Bell[1,2]*, William D. K. Reid[3], David A. Pearce[4], Adrian G. Glover[2], Christopher J. Sweeting[5], Jason Newton[6], & Clare Woulds[1]

[1]School of Geography& Water@Leeds, University of Leeds, LS2 9JT, UK.
[2]Life Sciences Dept., Natural History Museum, Cromwell Rd, London SW7 5BD, UK
[3]Ridley Building, School of Biology, Newcastle University, NE1 7RU, UK
[4]Applied Sciences, Northumbria University, Newcastle, NE1 8ST, UK
[5]Ridley Building, School of Marine Science and Technology, Newcastle University, NE1 7RU, UK
[6]NERC Life Sciences Mass Spectrometry Facility, SUERC, East Kilbride G75 0QF, UK

Keywords: Stable Isotopes; Trophic Niche; Sedimented; Hydrothermal; Southern Ocean; Microbial; 16S; PLFA

5.1 Abstract

Sedimented hydrothermal vents are those in which hydrothermal fluid is discharged through sediments and are among the least studied deep-sea ecosystems. We present a combination of microbial and biochemical data to assess trophodynamics between and within hydrothermally active and off-vent areas of the Bransfield Strait (1050 – 1647m depth). Microbial composition, biomass and fatty acid signatures varied widely between and within vent and non-vent sites and provided evidence of diverse metabolic activity. Several macrofaunal species showed diverse feeding strategies and occupied different trophic positions in vent and non-vent areas. Stable isotope values of consumers were generally not consistent with feeding structure morphology. Niche area and the diversity of microbial fatty acids reflected trends in species diversity and was lowest at the most hydrothermally active site. Faunal utilisation of chemosynthetic activity was relatively limited but was detected at both vent and non-vent sites as evidenced by carbon and sulphur isotopic signatures, suggesting that hydrothermal activity can affect trophodynamics over a much wider area than previously thought.

5.2 Introduction

5.2.1 *Sedimented Hydrothermal Vents*

As a result of subsurface mixing between hydrothermal fluid and ambient seawater within the sediment, sedimented hydrothermal vents (SHVs, a.k.a. Sediment-hosted hydrothermal vents), such as Middle Valley or the Guaymas Basin in the Pacific, are more similar to non-hydrothermal deep-sea habitats than they are to high temperature, hard substratum vents (Bemis et al. 2012, Bernardino et al. 2012). This creates opportunities for non-specialist, soft-sediment fauna to colonise areas of chemosynthetic organic matter production, potentially offering an important metabolic resource in the nutrient-limited deep-sea (Levin et al. 2009, Dowell et al. 2016). To take advantage of this resource, fauna must overcome the environmental stress associated with high-temperature, acidic and toxic conditions at SHVs (Levin et al. 2013, Gollner et al. 2015). The combination of elevated toxicity and in-situ organic matter (OM) production results in a different complement of ecological niches between vents and background conditions that elicits compositional changes along a productivity-toxicity gradient (Bernardino et al. 2012, Gollner et al. 2015, Bell et al. 2016b). Hydrothermal sediments offer different relative abundances of chemosynthetic and photosynthetic organic matter, depending upon supply of surface-derived primary productivity, which may vary with depth and latitude, and levels of hydrothermal activity (Tarasov et al. 2005). In shallow environments (< 200 m depth), where production of chemosynthetic and photosynthetic organic matter sources can co-occur, consumption may still favour photosynthetic OM over chemosynthetic OM as this does not require adaptions to environmental toxicity (Kharlamenko et al. 1995, Tarasov et al. 2005, Sellanes et al. 2011). The limited data concerning trophodynamics at deep-sea SHVs indicate that diet composition varies widely between taxa, ranging between 0 – 87 % contribution from chemosynthetic OM (Sweetman et al. 2013). Thus, understanding of the significance of chemosynthetic activity in these settings is very limited.

Sedimented hydrothermal vents host diverse microbial communities (Teske et al. 2002, Weber & Jørgensen 2002, Dhillon et al. 2003, Kallmeyer & Boetius 2004,

Teske et al. 2014, Dowell et al. 2016). Microbial communities are a vital intermediate between hydrothermal fluid and metazoan consumers, and thus their composition and isotopic signatures are of direct relevance to metazoan food webs. The heat flux associated with hydrothermal activity provides thermodynamic benefits and constraints to microbial community assembly (Kallmeyer & Boetius 2004, Teske et al. 2014) whilst accelerating the degradation of organic matter, giving rise to a wide variety of compounds, including hydrocarbons and organic acids (Martens 1990, Whiticar & Suess 1990, Dowell et al. 2016). Microbial aggregations are commonly visible on the sediment surface at SHVs (Levin et al. 2009, Aquilina et al. 2013, Sweetman et al. 2013, Dowell et al. 2016). However, active communities are also distributed throughout the underlying sediment layers, occupying a wide range of geochemical and thermal niches (reviewed by Teske et al. 2014). This zonation in microbial function and composition is very strong and has been extensively studied in Guaymas basin hydrothermal sediments. Sedimented chemosynthetic ecosystems may present several sources of organic matter to consumers (Bernardino et al. 2012, Sweetman et al. 2013, Yamanaka et al. 2015) and the diverse microbial assemblages can support a variety of reaction pathways, including methane oxidation, sulphide oxidation, sulphate reduction and nitrogen fixation (Teske et al. 2002, Dekas et al. 2009, Frank et al. 2013, Jaeschke et al. 2014, Wu et al. 2014, Inskeep et al. 2015, McKay et al. 2015). Phospholipid fatty acid (PLFA) analysis can be used to describe recent microbial activity and $\delta^{13}C$ signatures (Kharlamenko et al. 1995, Boschker & Middelburg 2002, Yamanaka & Sakata 2004, Colaço et al. 2007, Jaeschke et al. 2014). Although it can be difficult to ascribe a PLFA to a specific microbial group or process, high relative abundances of certain PLFAs can be strongly indicative of chemoautotrophy (Yamanaka & Sakata 2004, Colaço et al. 2007, Bell et al. 2016a), and can support an understanding of microbial ecosystem function in hydrothermal sediments (e.g. in western pacific vents, see Yamanaka & Sakata 2004).

Macrofaunal assemblages of the Bransfield SHVs were strongly influenced by hydrothermal activity (Bell et al. 2016b). Bacterial mats were widespread across Hook Ridge, where variable levels of hydrothermal activity were detected (Aquilina et al. 2013). Populations of siboglinid polychaetes (*Sclerolinum contortum* and

Siboglinum sp.), were found at Hook Ridge and non-hydrothermally active sites (Sahling et al. 2005, Georgieva et al. 2015, Bell et al. 2016b). These species are known to harbour chemoautotrophic endosymbionts (Schmaljohann et al. 1990, Gebruk et al. 2003, Thornhill et al. 2008, Eichinger et al. 2013, Rodrigues et al. 2013). Stable isotope analysis (SIA) is a powerful tool to assess spatial and temporal patterns in faunal feeding behaviour and has been used to study trophodynamics and resource partitioning in other SHVs, predominately in the Pacific (Southward et al. 2001, Yamanaka & Sakata 2004, Levin et al. 2009, Soto 2009, Levin et al. 2012, Sweetman et al. 2013, Portail et al. 2016). Stable isotopic analyses provide inferential measures of different synthesis pathways and can elucidate a wide range of autotrophic or feeding behaviours. Stable isotopic signatures are indicators of different synthesis pathways and can elucidate a wide range of feeding behaviours and organic matter production. Carbon and sulphur isotopes are used here to delineate food sources and nitrogen is used as a measure of trophic position (Fry et al. 1991, Levin & Michener 2002, Reid et al. 2013). The signature of source isotope ratios ($\delta^{13}C$ & $\delta^{34}S$) is influenced by the isotopic ratio of the chemical substrate, and the fractionation associated with the metabolic process involved and thus, different fixation pathways elicit different isotopic signatures, even when they utilise the same source (e.g. DIC) (Fry et al. 1991). Possible $\delta^{13}C$ isotopic values of sources in the Bransfield Strait include: ~-40 ‰ for thermogenic methane; ~-27 ‰ for suspended particulate matter or ~-15 ‰ for ice algae (Whiticar & Suess 1990, Mincks et al. 2008, Henley et al. 2012, Young et al. 2013). As an example, *Siboglinum* spp. can use a range of resources, including methane or dissolved organic matter (Southward et al. 1979, Schmaljohann et al. 1990, Thornhill et al. 2008, Rodrigues et al. 2013), making SIA an ideal way in which to examine resource utilisation in these settings (Levin et al. 2009, Soto 2009). We also apply the concept of an isotopic niche (Layman et al. 2007) whereby species or community trophic activity is inferred from the distribution of stable isotopic data in two or three dimensional isotope space.

5.2.2 *Hypotheses*

We used a combination of microbial diversity data based sequencing and compound specific isotopic analyses and bulk isotopic data from sediment, microbial, macro- and megafaunal samples to investigate resource utilisation, niche partitioning and trophic structure at vent and background sites in the Bransfield Strait to test the following hypotheses: 1) Siboglinid species subsist upon chemosynthetically-derived OM; 2) Chemosynthetic organic matter will be a significant food source at SHVs; 3) Stable isotope signatures will reflect a-priori functional designations defined by faunal morphology and 4) Fauna will have distinct niches between vents and background areas.

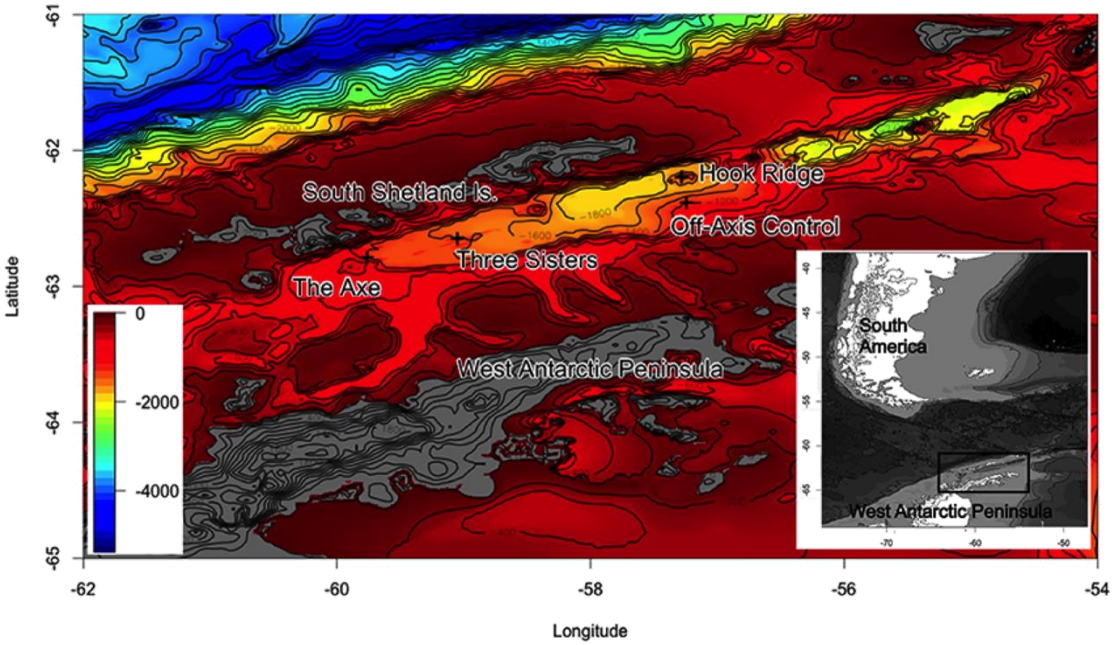

Figure 5.3.1a – Sampling sites (after Bell et al. 2016b)

5.3 Materials and Methods

5.3.1 *Sites and Sampling*

Samples were collected; during RRS *James Cook* cruise JC55 in the austral summer of 2011 (Tyler et al. 2011), from three raised edifices along the basin axis (Hook Ridge, the Three Sisters and The Axe), (Figure 5.3.1a) and one off-axis site, in the Bransfield Strait (1024 – 1311m depth). We visited two sites of variable hydrothermal activity (Hook Ridge 1 and 2) and three sites where hydrothermal activity was not detected (Three Sisters, the Axe and an Off-Axis site) (Aquilina et al. 2013). Of the two hydrothermal sites, Hook Ridge 2 was had higher hydrothermal fluid advection rates and pore fluid temperature but lower concentrations of sulphide and methane (Table 5.3.1a) (Dählmann et al. 2001, Aquilina et al. 2013, Aquilina et al. 2014).

Site	Depth (m)	Hydrothermally active?	References
The Axe (AXE)	1024	No	(Dählmann et al. 2001, Klinkhammer et al. 2001, Sahling et al. 2005, Aquilina et al. 2013, Aquilina et al. 2014, Bell et al. 2016b)
Off-Vent (BOV)	1150	No	
Three Sisters (TS)	1311	No	
Hook Ridge 1 (HR1)	1174	Low activity (9 cm yr^{-1})	
Hook Ridge 2 (HR2)	1054	High Activity (34 cm yr^{-1})	

Table 5.3.1a – Site descriptions and associated references

Samples were collected with a series of megacore deployments, using a Bowers & Connelly dampened megacorer (1024 – 1311m depth) and a single Agassiz trawl at Hook Ridge (1647m depth). With the exception of salps, all microbial and faunal samples presented here were from megacore deployments. For a detailed description of the megacore sampling programme and macrofaunal communities, see Bell et al. (2016b). Sampling consisted of 1 – 6 megacore deployments per site, with 2 – 5 tubes pooled per deployment (Bell et al. 2016b). Cores were sliced into 0 – 5cm and 5 – 10cm partitions and macrofauna were retained on a 300 µm sieve. Residues were preserved in either 80 % ethanol or 10 % buffered formalin initially and then stored in 80% ethanol after sorting (Bell et al. 2016b). Fauna were sorted to species/

morphospecies level (for annelid and bivalve taxa); family level (for peracarids) and higher levels for less abundant phyla (e.g. echiurans). Salps were collected using an Agassiz trawl and samples were immediately picked and frozen at -80 ˚C and subsequently freeze-dried.

5.3.2 *Microbiology Sequencing*

Samples of surface sediment (0 – 1 centimeters below seafloor (cmbsf)) were taken from megacores the two Hook Ridge sites and the off-axis site and frozen (-80˚C). DNA was extracted from the sediment by Mr DNA (Shallowater, TX, USA) using an in-house standard 454 pipeline. The resultant sequences were trimmed and sorted using default methods in Geneious (v.9.1.5 with RDP v.2.8 and Krona v.2.0) and analysed in the Geneious '16 Biodiversity Tool' (https://16s.geneious.com/16s/help.html) (Wang et al. 2007, Ondov et al. 2011, Biomatters 2014).

5.3.3 *Phospholipid Fatty Acids*

Samples of 3 – 3.5 g of freeze-dried sediment from Hook Ridge 1 & 2, the off-vent site and the Three Sisters were analysed at the James Hutton Institute (Aberdeen, UK) following the procedure detailed in Main et al. (2015), which we summarise below. Samples were from the top 1 cm of sediment for all sites except Hook Ridge 2 where sediment was pooled from two core slices (0 – 2 cm), due to sample mass limitations. Lipids were extracted following a method adapted from Bligh (1959), using a single phase mixture of chloroform: methanol: citrate buffer (1:2:0.8 v-v:v). Lipids were fractionated using 6 ml ISOLUTE SI SPE columns, preconditioned with 5 ml chloroform. Freeze-dried material was taken up in 400 µL of chloroform; vortex mixed twice and allowed to pass through the column. Columns were washed in chloroform and acetone (eluates discarded) and finally 10 ml of methanol. Eluates were collected, allowed to evaporate under a N_2 atmosphere and frozen (-20 ˚C).

PLFAs were derivitised with methanol and KOH to produce fatty acid methyl esters (FAMEs). Samples were taken up in 1 mL of 1:1 (v:v) mixture of methanol and toluene. 1 mL of 0.2 M KOH (in methanol) was added with a known quantity of the C19 internal standard (nonadecanoic acid), vortex mixed and incubated at 37 ˚C for 15 min. After cooling to room temperature, 2 mL of isohexane: chloroform (4:1 v:v), 0.3 mL of 1 M acetic acid and 2 mL of

deionized water was added to each vial. The solution was mixed and centrifuged and the organic phase transferred to a new vial and the remaining aqueous phase was mixed and centrifuged again to further extract the organic phase, which was combined with the previous. The organic phases were evaporated under a N_2 atmosphere and frozen at -20 ˚C.

Samples were taken up in isohexane to perform gas chromatography-combustion-isotope ratio mass spectrometry (GC-C-IRMS). The quantity and $\delta^{13}C$ values of individual FAMEs were determined using a GC Trace Ultra with combustion column attached via a GC Combustion III to a Delta V Advantage isotope ratio mass spectrometer (Thermo Finnigan, Bremen). The $\delta^{13}C_{VPDB}$ values (‰) of each FAME were calculated with respect to a reference gas of CO_2, traceable to IAEA reference material NBS 19 TS-Limestone. Measurement of the Indiana University reference material hexadecanoic acid methyl ester (certified $\delta^{13}C_{VPDB}$ -30.74 ± 0.01‰) gave a value of 30.91 ± 0.31‰ (mean ± sd, n=51). Combined areas of all mass peaks (m/z 44, 45 and 46), following background correction, were collected for each FAME. These areas, relative to the internal C19:0 standard, were used to quantify the 34 most abundant FAMEs and related to the PLFAs from which they are derived (Thornton et al. 2011).

Bacterial biomass was calculated using transfer functions from the total mass of four PLFAs (i14:0, i15:0, a15:0 and i16:0), estimated at 14 % of total bacterial PLFA, which in turn is estimated at 5.6 % of total bacterial biomass (Boschker & Middelburg 2002).

5.3.4 *Bulk Stable Isotopes*

All bulk isotopic analyses were completed at the East Kilbride Node of the Natural Environment Research Council Life Sciences Mass Spectrometry Facility. Specimens with carbonate structures (e.g. bivalves) were physically decarbonated and all specimens were rinsed in de-ionised water (e.g. to remove soluble precipitates such as sulphates) and cleaned of attached sediment before drying. Specimens dried for at least 24 hours at 50˚C and weighed (mg, correct to 3 d.p.) into tin capsules and stored in a desiccator whilst awaiting SIA. Samples were analysed by continuous flow isotope ratio mass spectrometer using a Vario-Pyro Cube elemental analyser (Elementar), coupled with a Delta Plus XP isotope ratio mass spectrometer (Thermo Electron). Each of the runs of CN and CNS isotope analyses used laboratory standards (Gelatine and two amino acid-gelatine mixtures) as well as the international standard USGS40

(glutamic acid). CNS measurements used the internal standards (MSAG2: (Methanesulfonamide/ Gelatine and M1: Methionine) and the international silver sulphide standards IAEA-S1, S2 and S3. All sample runs included samples of freeze-dried, powdered *Antimora rostrata* (ANR), an external reference material used in other studies of chemosynthetic ecosystems (Reid et al. 2013, Bell et al. 2016a), used to monitor variation between runs and instruments (Supplement 5-1). Instrument precision (S.D.) for each isotope measured from ANR was 0.42 ‰, 0.33 ‰ and 0.54 ‰ for carbon, nitrogen and sulphur respectively. The reference samples were generally consistent except in one of the CNS runs, which showed unusual $\delta^{15}N$ measurements (Supplement 5-1), so faunal $\delta^{15}N$ measurements from this run were excluded as a precaution. Stable isotope ratios are all reported in delta (δ) per mil (‰) notation, relative to international standards: V-PDB ($\delta^{13}C$); Air ($\delta^{15}N$) and V-CDT ($\delta^{34}S$).

A combination of dual- ($\delta^{13}C$ & $\delta^{15}N$, 319 samples) and tri-isotope ($\delta^{13}C$, $\delta^{15}N$ & $\delta^{34}S$, 83 samples) techniques was used to describe bulk isotopic signatures of 43 species of macrofauna (35 from non-vent sites, 19 from vent sites and 11 from both), 3 megafaunal taxa and sources of organic matter. Samples submitted for carbon and nitrogen (CN) analyses were pooled if necessary to achieve an optimal mass of 0.7 mg (± 0.5 mg). Where possible, individual specimens were kept separate in order to preserve variance structure within populations but in some cases, low sample mass meant individuals had to be pooled (from individuals found in replicate deployments). Optimal mass for Carbon-Nitrogen-Sulphur (CNS) measurements was 2.5 mg (± 0.5 mg) and, as with CN analyses, specimens were submitted as individual samples or pooled where necessary. Samples of freeze-dried sediment from each site were also submitted for CNS analyses (untreated for NS and acidified with 6M HCl for C). Acidification was carried out by repeated washing with acid and de-ionised water.

Specimens were not acidified. A pilot study, and subsequent results presented here, confirmed that the range in $\delta^{13}C$ measurements between acidified (0.1M and 1.0M HCl) was within the untreated population range, in both polychaetes and peracarids and that acidification did not notably or consistently reduce $\delta^{13}C$ standard deviation (Table 5.3.4a). In the absence of a large or consistent treatment effect, the low sample mass, (particularly for CNS samples) was dedicated to increasing replication and preserving integrity of $\delta^{15}N$ & $\delta^{34}S$ measurements instead of separating carbon and nitrogen/ sulphur samples (Connolly & Schlacher 2013).

Formalin and ethanol preservation effects can both influence the isotopic signature of a sample (Fanelli et al. 2010, Rennie et al. 2012). Taxa that had several samples of each preservation method from a single site (to minimise intra-specific differences) were examined to determine the extent of isotopic shifts associated with preservation effects (Table 5.3.4a). Carbon and nitrogen isotopic differences between ethanol and formalin preserved samples ranged between 0.07 – 1.38 ‰ and 0.40 – 1.96 ‰ respectively. Differences across all samples were not significant (Paired t-test, $\delta^{13}C$: t = 2.10, df = 3, p = 0.126 and $\delta^{15}N$: t=1.14, df = 3, p = 0.337). Given the unpredictable response of isotopic signatures to preservation effects (which also cannot be extricated from within-site, intraspecific variation) it was not possible to correct isotopic data (Bell et al. 2016a). This contributed an unavoidable, but generally quite small, source of error in these measurements.

Isotope	Species	Idoteidae	*Polycirrus* sp.	*Aphelochaeta glandaria*	Phyllodocida sp.
	Treatment	0.1M HCl	0.1M HCl	0.1M HCl	1.0M HCl
$\delta^{13}C$ (‰)	Difference in mean	1.59	0.18	0.41	0.90
	σ untreated	0.72	0.30	0.2	0.50
	σ treated	0.67	0.33	0.23	0.16
	Population range	2.86	3.04	2.72	-
$\delta^{15}N$ (‰)	Difference in mean	0.92	0.17	0.10	0.88
	σ untreated	0.22	0.30	0.19	0.35
	σ treated	1.00	0.18	0.15	0.34
	Population range	3.42	4.57	5.75	-
$\delta^{34}S$ (‰)	Difference in mean	-	-	0.36	1.13
	σ untreated	-	-	0.44	0.82
	σ treated	-	-	0.68	1.39
	Population range	-	-	2.32	-

Table 5.3.4a – Differences in isotopic values and standard deviation (σ) of ethanol preserved fauna sampled during JC55 in response to acid treatment, compared with population ranges of untreated samples. Phyllodocida sp. was a single large specimen, used only as part of preliminary experiments.

5.3.5 *Statistical Analyses*

All analyses were completed in the R statistical environment (R Core Team 2013). Carbon and nitrogen stable isotopic measurements were divided into those from vent or non-vent sites and averaged by taxa and used to construct a Euclidean distance matrix (Valls et al. 2014). This matrix was used to conduct a similarity profile routine (SIMPROF, 10 000 permutations, p = 0.05, Ward linkage) using the clustsig package (v1.0) (Clarke et al. 2008, Whitaker & Christmann 2013) to test for significant structure within the matrix. The resulting cluster assignations were compared to a-priori feeding groups (Bell et al. 2016b) using a Spearman Correlation Test (with 9 999 Monte Carlo resamplings) using the coin package (v1.0-24) (Hothorn et al. 2015). Isotopic signatures of species sampled from both vent and non-vent sites were also compared with a one-way ANOVA with Tukey's HSD pairwise comparisons (following a Shapiro-Wilk normality test).

Mean faunal measurements of $\delta^{13}C$ & $\delta^{15}N$ were used to calculate Layman metrics for each site (Layman et al. 2007), sample-size corrected standard elliptical area (SEAc) and Bayesian posterior draws (SEA.B, mean of 10^5 draws ± 95% credibility interval) in the SIAR package (v4.2) (Parnell et al. 2010, Jackson et al. 2011). Differences in SEA.B between sites were compared in mixSIAR. The value of p given is the proportion of ellipses from group A that were smaller in area than those from group B (e.g. if p = 0.02, then 2% of posterior draws from group A were smaller than the group B mean) and is considered to be a semi-quantitative measure of difference in means (Jackson et al. 2011).

5.4 Results

5.4.1 *Differences in microbial composition along a hydrothermal gradient*

A total of 28,767, 35,490 and 47,870 sequences were obtained from the off-axis site and the vent sites, Hook Ridge 1 and 2, respectively. Bacteria comprised almost the entirety of each sample, with Archaea being detected only in the Hook Ridge 2 sample (< 0.01 % of sequences). Hook Ridge 1 was qualitatively more similar to the off-axis site than Hook Ridge 2. Both HR1 (vent) and BOV (non-vent) were dominated by Proteobacteria (48 % and 61 % of reads respectively; Figure 4.5.1a), whereas Flavobacteriia dominated Hook Ridge 2 (43 %, 7 – 12 % elsewhere) with Proteobacteria accounting for a smaller percentage of sequences (36 %; Figure 5.4.1a). By sequence abundance, Flavobacteriia were the most clearly disparate group between Hook Ridge 2 and the other sites. Flavobacteriia were comprised of 73 genera at Hook Ridge 2, 60 genera at BOV and 63 genera at HR1, of which 54 genera were shared between all sites. Hook Ridge 2 had 15 unique flavobacteriial genera but these collectively accounted for just 0.9 % of reads, indicating that compositional differences were mainly driven by relative abundance, rather than taxonomic richness.

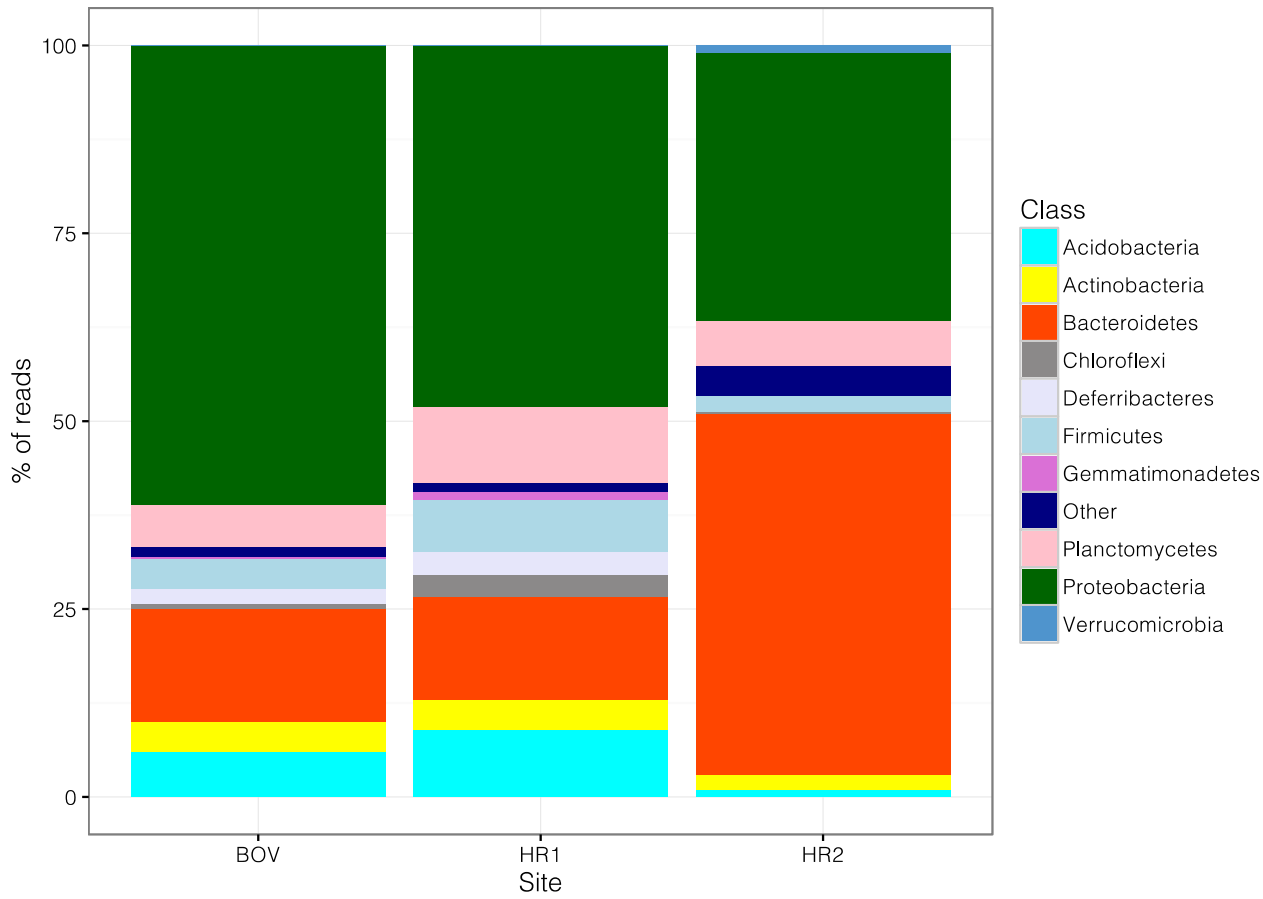

Figure 5.4.1a – Microbial composition (classes) at the off-vent/ off-axis site (BOV) and the two Hook Ridge sites (HR1 and HR2). Archaea excluded from figure as they only accounted for 0.008 % of reads at HR2 and were not found elsewhere.

The most abundant genus from each site was *Arenicella* at BOV and HR1 (7.1 % and 5.2 % of reads respectively) and *Aestuariicola* at HR2 (6.9 % of reads). The four most abundant genera at both BOV and HR1 were *Arenicella* (γ-proteobacteria), *Methylohalomonas* (γ-proteobacteria), *Pasteuria* (Bacilli) & *Blastopirellula* (Planctomycetacia), though not in the same order, and accounted for 17.2 % and 16.0 % of reads respectively. The four most abundant genera at HR2, accounting for 20.2 % of reads were *Aestuariicola*, *Lutimonas, Maritimimonas* & *Winogradskyella* (all Flavobacteriia). The genera *Arenicella* and *Pasteuria* were the most relatively abundant across all sites (2.2 % – 7.1 % and 1.7 % – 5.0 % of reads respectively).

5.4.2 *Microbial fatty acids*

A total of 37 sedimentary PLFAs were identified across all sites, in individual abundances ranging between 0 % – 26.4 % of total PLFA (Table 5.4.2a; Supplement 5-3). All lipid samples were dominated by saturated and mono-unsaturated fatty acids (SFAs and MUFAs), comprising 91 % – 94 % of PLFA abundance per site. The most abundant PLFAs at each site were 16:0 (15.7 % – 26.4 %), 16:1ω7c (11.5 % – 20.0 %) and 18:1ω7 (4.8 % – 16.9 %; Table 5.4.2a). PLFA profiles from each of the non-vent sites sampled (Off-axis and the Three Sisters, 33 and 34 PLFAs respectively) were quite similar (Table 5.4.2a) and shared all but one compound (16:1ω11c, present only at the non-vent Three Sisters site). Fewer PLFAs were enumerated from Hook Ridge 1 and 2 (31 and 23 respectively), including 3 PLFAs not observed at the non-vent sites (br17:0, 10-Me-17:0 & 10-Me-18:0), which accounted for 0.5 % – 1.2 % of the total at these sites. Hook Ridge 2 had the lowest number of PLFAs and the lowest total PLFA biomass of any site, though this was due in part to the fact that this sample had to be pooled from the top 2 cm of sediment (top 1cm at other sites). Bacterial biomass was highest at Hook Ridge 1 and ranged 85 mg C m^{-2} – 535 mg C m^{-2} (Table 5.4.2a).

PLFA carbon isotopic signatures ranged -56 ‰ to -20 ‰ at non-vent sites and -42 ‰ to -8 ‰ at vent sites (Table 5.4.2a). Weighted average $\delta^{13}C$ values were quite similar between the non-vent sites and Hook Ridge 1 (-30.5 ‰ and -30.1 ‰ respectively), but were heavier at Hook Ridge 2 (-26.9 ‰; Table 5.4.2a). Several of the PLFAs identified had a large range in $\delta^{13}C$ between samples (including 16:1ω11t $\delta^{13}C$ range = 17.2 ‰ or 19:1ω8 $\delta^{13}C$ range = 19.1 ‰), even between the non-vent sites (e.g. 18:2ω6, 9, $\Delta\delta^{13}C$ = 24.36; Table 5.4.2a). Of the 37 PLFAs, 7 had a $\delta^{13}C$ range of > 10 ‰ but these were comparatively minor and individually accounted for 0 % – 4.9 % of total abundance. Average $\delta^{13}C$ range was 6.3 ‰ and a further 11 PLFAs had a $\delta^{13}C$ range of > 5 ‰, including some of the more abundant PLFAs, accounting for 36.8 ‰ – 46.6 % at each site. PLFAs with small $\delta^{13}C$ ranges (< 5 ‰) accounted for 44.6 % – 54.4 % of total abundance at each site.

	Bransfield Off-Vent			Middle Sister			Hook Ridge 1			Hook Ridge 2			Range
PLFA	nM per g	%	$\delta^{13}C$ (‰)	nM per g	%	$\delta^{13}C$ (‰)	nM per g	%	$\delta^{13}C$ (‰)	nM per g	%	$\delta^{13}C$ (‰)	$\delta^{13}C$ (‰)
i14:0	0.03	0.12	-22.1	0.02	0.09	-28.0	0.11	0.22	-15.7	0.10	0.80	-28.8	-13.1
14:0	0.80	3.04	-31.2	0.83	3.43	-30.9	3.25	6.63	-32.7	0.80	6.40	-29.6	-3.1
i15:0	0.76	2.89	-28.6	0.76	3.13	-28.1	2.02	4.13	-29.7	0.40	3.20	-28.1	-1.7
a15:0	1.06	4.03	-28.4	1.06	4.39	-27.7	2.68	5.48	-29.1	0.90	7.20	-28.9	-1.4
15:0	0.30	1.13	-29.3	0.19	0.77	-29.8	0.50	1.01	-29.0	0.30	2.40	-28.3	-1.5
i16:1	0.11	0.44	-31.4	0.02	0.10	-20.3	0.22	0.45	-27.6	0.00	0.00	n.d.	-11.1
16:1w11c	0.00	0.00	n.d.	0.06	0.24	-23.1	0.04	0.09	-17.4	0.00	0.00	n.d.	-5.7
i16:0	0.34	1.30	-28.5	0.30	1.24	-27.8	0.64	1.31	-29.4	0.20	1.60	-28.8	-1.6
16:1w11t	0.78	2.98	-24.4	0.66	2.75	-25.0	2.40	4.91	-25.8	0.30	2.40	-8.7	-17.2
16:1w7c	3.98	15.19	-28.9	3.37	13.95	-28.1	11.50	23.50	-29.2	2.50	20.00	-22.9	-6.3
16:1w5c	1.12	4.27	-34.1	0.96	3.99	-34.0	2.23	4.55	-31.2	0.30	2.40	-24.3	-9.7
16:0	4.29	16.37	-31.1	3.80	15.73	-30.0	7.70	15.75	-31.8	3.30	26.40	-29.3	-2.5
br17:0	0.00	0.00	n.d.	0.00	0.00	n.d.	0.14	0.28	-22.9	0.00	0.00	-15.8	-7.2
10-Me-16:0	0.46	1.77	-28.5	0.45	1.87	-29.0	0.97	1.98	-30.3	0.20	1.60	-41.3	-12.8
i17:0	0.08	0.32	-33.2	0.20	0.84	-29.8	0.00	0.00	n.d.	0.00	0.00	n.d.	-3.4
a17:0	0.25	0.97	-31.9	0.21	0.87	-31.3	0.35	0.72	-29.0	0.20	1.60	-28.6	-3.4

12-Me-16:0	0.25	0.94	-32.92	0.21	0.86	-31.59	0.33	0.68	-28.60	0.10	0.80	-28.23	-4.7
17:1w8c	0.13	0.50	-34.08	0.11	0.44	-31.27	0.27	0.55	-27.14	0.10	0.80	-27.23	-6.9
17:0cy	0.33	1.26	-36.20	0.27	1.10	-32.83	0.63	1.30	-32.30	0.20	1.60	-27.66	-8.5
17:0	0.15	0.56	-39.96	0.08	0.33	-50.39	0.15	0.30	-40.03	0.20	1.60	-30.81	-19.6
10-Me-17:0	0.00	0.00	n.d.	0.00	0.00	n.d.	0.05	0.10	-34.98	0.00	0.00	n.d.	0.00
18:3w6,8,13	0.67	2.55	-34.64	0.69	2.87	-33.83	1.22	2.50	-31.16	0.50	4.00	-29.04	-5.6
18:2w6,9	0.12	0.46	-27.81	0.09	0.36	-52.17	0.38	0.77	-29.96	0.30	2.40	-26.65	-25.5
18:1w9	1.13	4.30	-29.96	1.33	5.50	-29.90	1.70	3.47	-29.64	0.40	3.20	-25.58	-4.4
18:1w7	4.42	16.85	-29.01	3.84	15.91	-29.07	5.44	11.12	-29.87	0.60	4.80	-24.74	-5.1
18:1w(10 or 11)	2.33	8.88	-30.12	2.26	9.36	-29.93	2.09	0.88	-31.89	0.00	1.60	n.d.	-2.0
18:0	0.66	2.50	-30.60	0.54	2.22	-30.62	0.68	4.27	-29.42	0.30	0.00	-29.86	-1.2
19:1w6	0.03	0.12	-23.45	0.03	0.12	-30.05	0.06	1.39	-26.21	0.00	2.40	n.d.	-6.6
10-Me-18:0	0.00	0.00	n.d.	0.00	0.00	n.d.	0.14	0.12	-25.36	0.00	0.00	n.d.	0.00
19:1w8	0.11	0.42	-56.57	0.17	0.69	-37.46	0.22	0.29	-41.19	0.00	0.00	n.d.	-19.1
19:0cy	0.20	0.77	-35.55	0.20	0.83	-34.80	0.40	0.45	-30.47	0.10	0.00	-28.70	-6.9
20:4(n-6)	0.14	0.55	-39.95	0.20	0.83	-34.07	0.00	0.81	n.d.	0.00	0.80	n.d.	-5.9
20:5(n-3)	0.41	1.57	-37.99	0.30	1.23	-39.28	0.00	0.00	n.d.	0.00	0.00	n.d.	-1.3

20:1(n-9)	0.42	1.60	-31.5	0.41	1.71	-33.7	0.00	0.00	n.d.	0.00	0.00	n.d.	-2.2
22:6(n-3)	0.22	0.83	-34.1	0.43	1.77	-30.0	0.00	0.00	n.d.	0.00	0.00	n.d.	-4.2
22:1(n-9)	0.10	0.39	-31.3	0.10	0.41	-29.9	0.00	0.00	n.d.	0.00	0.00	n.d.	-1.4
24:1(n-9)	0.03	0.12	-28.7	0.02	0.07	-29.7	0.00	0.00	n.d.	0.00	0.00	n.d.	-1.0
Total	26.23			24.15			48.50			12.30			
Average	0.71		-30.5	0.65		-30.1	1.31		-30.3	0.33		-26.9	
		mg C m^{-2}	**$\delta^{13}C$ (‰)**		**mg C m^{-2}**	**$\delta^{13}C$ (‰)**		**mg C m^{-2}**	**$\delta^{13}C$ (‰)**		**mg C m^{-2}**	**$\delta^{13}C$ (‰)**	
Bacterial Biomass		134.50	-26.8		197.12	-26.4		534.55	-26.6		85.45	-23.2	

Table 5.4.2a – PLFA profiles from freeze-dried sediment (nM per g dry sediment). PLFA names relate to standard notation (i = iso; a = anti-iso; first number = number of carbon atoms in chain; ω = double bond; Me = methyl group). N.P. = Not present in sample. Total PLFA $\delta^{13}C$ measurements weighted by concentration Bulk bacterial $\delta^{13}C$ estimated from average conversion factor ($\delta^{13}C$ in PLFA depleted compared to bulk bacterial biomass by 3.7 ‰ (Boschker and Middelburg, 2002). No data = n.d.

5.4.3 *Description of bulk isotopic signatures*

Most faunal isotopic signatures were within a comparatively narrow range ($\delta^{13}C$: -30 ‰ to -20 ‰, $\delta^{15}N$: 5 ‰ to 15 ‰ and $\delta^{34}S$: 10 ‰ to 20 ‰) and more depleted isotopic signatures were usually attributable to siboglinid species (Figure 5.4.3a). *Siboglinum* sp. (found at all non-vent sites) had mean $\delta^{13}C$ and $\delta^{15}N$ values of -41.4 ‰ and -8.9 ‰ respectively and *Sclerolinum contortum* (predominately from Hook Ridge 1 but found at both vent sites) had values of -20.5 ‰ and -5.3 ‰ respectively. Some non-endosymbiont bearing taxa (e.g. macrofaunal neotanaids from the off-axis site and megafaunal ophiuroids at Hook Ridge 2) also had notably depleted $\delta^{15}N$ signatures (means -3.6 ‰ to 2.6 ‰ respectively; Figure 5.4.3a).

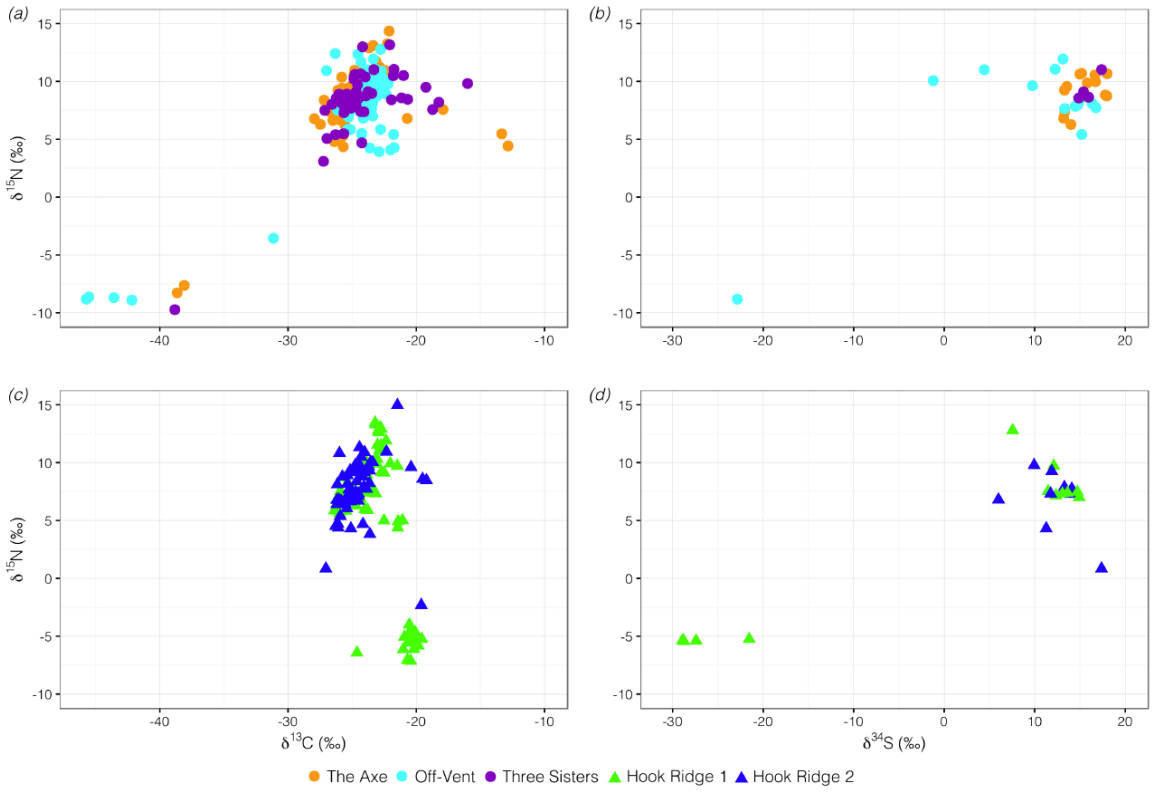

Figure 5.4.3a – Carbon-Nitrogen and Sulphur-Nitrogen biplots for bulk isotopic signatures of benthos, separated into non-vent (top) and vent sites (bottom).

Isotopic signatures of sediment organic matter were similar between vents and non-vents for $\delta^{13}C$ and $\delta^{15}N$ but $\delta^{34}S$ was significantly greater at non-vent sites ($p < 0.05$, Table 5.4.3a; Figure 5.4.3b). Variability was higher in vent sediments for all isotopic

signatures. Faunal isotopic signatures for $\delta^{13}C$ and $\delta^{34}S$ ranged much more widely than sediment signatures and indicate that sediment organics were a mixture of two or more sources of organic matter. A few macrofaunal species had relatively heavy $\delta^{13}C$ signatures that exceeded -20 ‰ that suggested either a heavy source of carbon or marine carbonate in residual exoskeletal tissue, particularly for peracarids (~ 0 ‰). Samples of pelagic salps from Hook Ridge had mean values for $\delta^{13}C$ of -27.4 ‰ (± 0.88) and $\delta^{34}S$ of 21.5 ‰ (± 0.74).

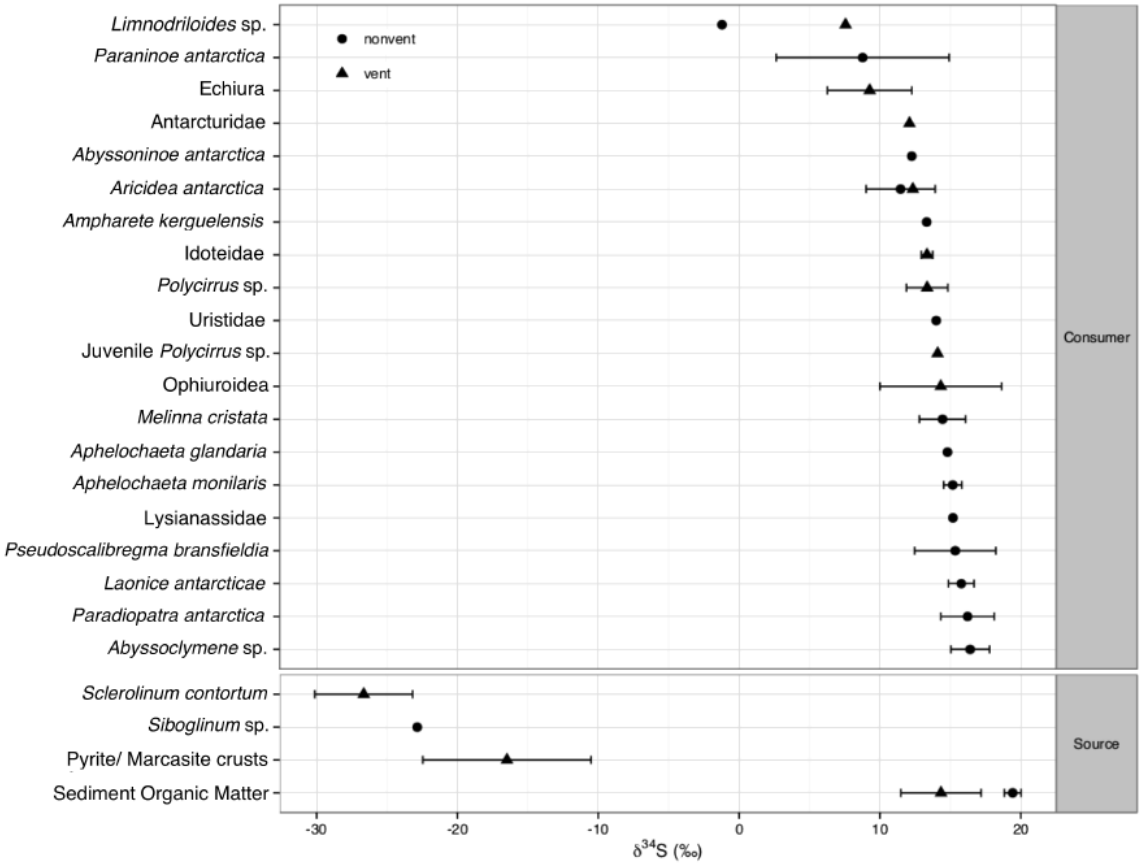

Fig. 5.4.3b – Plot of $\delta^{34}S$ measurements by discriminated by species and habitat (vent/ non-vent ± 1 s.d.). Data for $\delta^{34}S$ in crusts from Petersen et al. (2004)

Isotope	Vents ‰ (± S.D.)	Non-Vent ‰ (± S.D.)	Different? (T-Test, df = 3)
$\delta^{13}C$	-26.22 (± 0.41)	-25.80 (± 0.26)	No
$\delta^{15}N$	5.73 (± 0.71)	5.00 (± 0.30)	No
$\delta^{34}S$	14.34 (± 2.85)	19.43 (± 0.59)	Yes (T = 3.49, p < 0.05)

Table 5.4.3a – Mean isotopic signatures of sediment organic matter.

5.4.4 *Comparing macrofaunal morphology and stable isotopic signatures*

Averaged species isotopic data were each assigned to one of four clusters (SIMPROF, p = 0.05; Supplement 5-5). No significant correlation between a-priori (based on morphology) and a-posteriori clusters (based on isotopic data) was detected (Spearman Correlation Test: Z = -1.34; N = 43; p = 0.18). Clusters were mainly discriminated based on $\delta^{15}N$ values and peracarids were the only taxa to be represented in all of the clusters, indicating high trophic diversity.

Several taxa found at both vent and non-vent sites were assigned to different clusters between sites. A total of eleven taxa were sampled from both vent and non-vent regions, of which four were assigned to different clusters at vent and non-vent sites. Neotanaids (Peracarida: Tanaidacea) had the greatest Euclidean distance between vent/ non-vent samples (11.36), demonstrating clear differences in dietary composition (Figure 5.4.4a). All other species were separated by much smaller distances between regions, which ranged 0.24 to 2.69. Raw $\delta^{13}C$ and $\delta^{15}N$ values were also compared between vent and non-vent samples for each species (one-way ANOVA with Tukey HSD pairwise comparisons). Analysis of the raw data indicated that $\delta^{13}C$ signatures were different for neotanaids only and $\delta^{15}N$ were different for neotanaids and an oligochaete species (*Limnodriloides* sp.) (ANOVA, p < 0.01, Figure 5.4.4a).

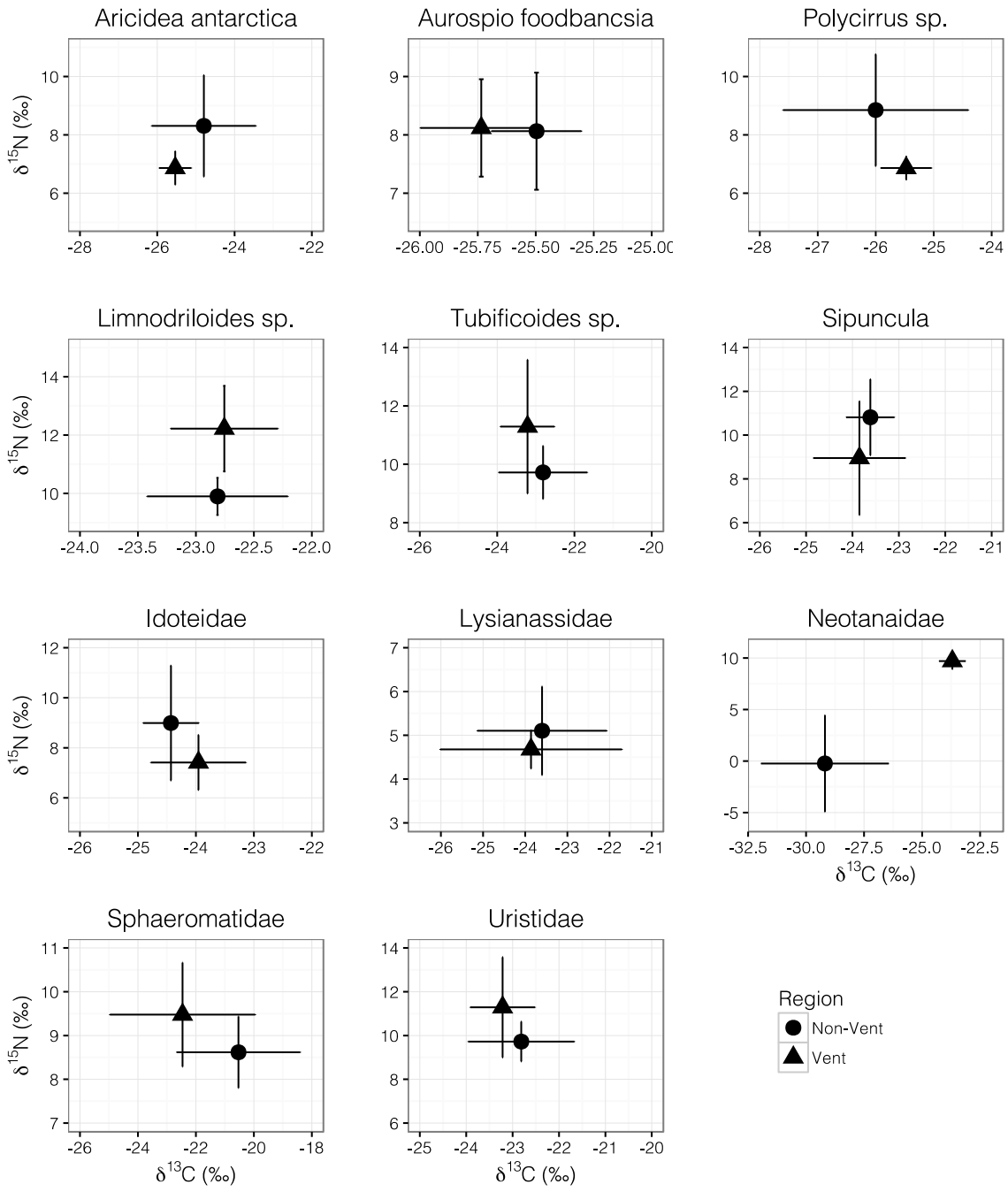

Figure 5.4.4a – Biplot of CN isotopic data from species sampled both at vents and non-vent background regions. Mean ± standard deviation, X-Y scales vary

5.4.5 *Community-level trophic metrics*

All site niches overlapped (mean = 50 %, range = 30 – 82 %) and the positions of ellipse centroids were broadly similar for all sites (Table 4.5.4a; Figure 5.4.5a). Vent site ellipse areas were similar but significantly smaller than non-vent ellipses (SEA.B, n = 10^5, p = < 0.05). There were no significant differences in ellipse area between any of the non-vent sites. Ranges in carbon sources (dCr) were higher for non-vent sites (Table 5.4.5a) indicating a greater trophic diversity in background conditions. Nitrogen range (dNr, Table 5.4.5a) was similar between vents and non-vents suggesting a similar number of trophic levels within each assemblage. All site ellipses had broadly similar eccentricity, ranging 0.85 – 0.97 (Table 5.4.5a). However the angle of the long axis (theta) was different between vent and non-vent sites (-1.43 to 1.55 radians at Hook Ridge, 0.67 to 0.86 radians at non-vent sites). Range in nitrogen sources was more influential at vent sites with *Sclerolinum contortum*, which had low $\delta^{15}N$ signatures, had similar to $\delta^{13}C$ to non-endosymbiont bearing taxa. The strongly depleted $\delta^{13}C$ measurements of *Siboglinum* sp. meant that ellipse theta was skewed more towards horizontal (closer to zero) for non-vent sites.

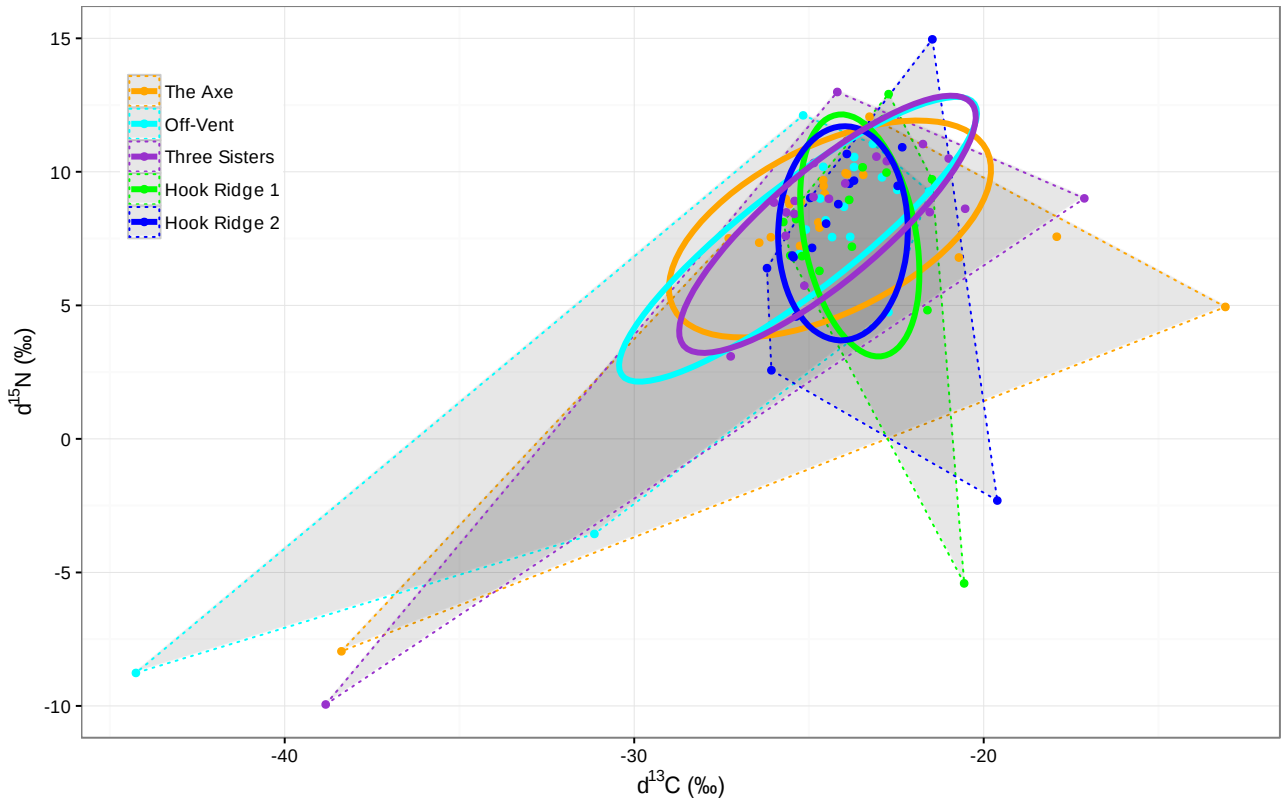

Figure 5.4.5a – Faunal isotopic signatures (mean per species), grouped by site with total area (shaded area marked by dotted lines) and sample-size corrected standard elliptical area (solid lines).

	Ellipse						Centroid						NND		
Site	SEAc (‰²)	SEA.B (‰²)	Cred. (95% ± ‰²)	TA (‰²)	Θ	E	$\delta^{13}C$ (‰)	$\delta^{15}N$ (‰)	$\delta^{34}S$ (‰)	dNr (‰)	dCr (‰)	dSr (‰)	CD	Mean	S.D.
The Axe	49.27	45.00	19.93	161.64	0.67	0.85	-24.4	7.9		20.02	25.29		3.59	1.76	4.17
Off-Vent	39.81	36.52	16.82	139.12	0.81	0.97	-25.3	7.5	8.1	20.88	22.70	38.83	4.34	2.13	3.88
Three Sisters	35.46	32.61	14.71	110.24	0.86	0.95	-24.5	8.0		22.94	21.71		3.85	1.93	3.78
Hook Ridge 1	23.10	20.66	11.17	42.59	-1.43	0.94	-23.5	7.6	5.4	18.32	5.18	40.35	3.30	1.64	2.60
Hook Ridge 2	23.38	21.08	10.73	61.79	1.55	0.89	-24.0	7.7		17.27	6.59		3.17	1.52	2.03
Mean															
Non-Vent	41.51	38.04	17.15	137.00	0.78	0.92	-24.7	7.8		21.28	23.23		3.93	1.94	3.94
Vent	23.24	20.87	10.95	52.19	0.10	0.91	-23.8	7.7		17.80	5.88		3.23	1.58	2.31

Table 5.4.5a – Ellipse Area & Layman Metrics of benthos by site. SEAc = Sample-sized corrected standard elliptical area; SEA.B = Bayesian estimate of standard elliptical area; TA = Total hull area; E = Eccentricity; dNr = Nitrogen range; dCr = Carbon range; dSr = Sulphur range; CD = Centroid distance; NND = Nearest Neighbour Difference. Note: dSr reported only for Hook Ridge 1 and the off-vent site since $\delta^{34}S$ values of siboglinids were only measured from these sites; hence dSr at other sites would be a considerable underestimate. As $\delta^{34}S$ values were comparatively under-representative, these values were not used in calculation of any other metric.

5.5 Discussion

5.5.1 *Microbial signatures of hydrothermal activity*

PLFA profiles between the off-axis site and the Three Sisters indicated similar bacterial biomass at each of these non-vent sites and that bacterial biomass varied much more widely at Hook Ridge (Table 5.4.2a). The Hook Ridge 2 sample is not directly comparable to the others as it was sampled from sediment 0 – 2 cmbsf (owing to sample mass availability), though organic carbon content, hydrogen sulphide flux and taxonomic diversity were all lower at this site and may support suggestion of a lower overall bacterial biomass (Aquilina et al. 2013, Bell et al. 2016b). The very high bacterial biomass at Hook Ridge 1 suggests a potentially very active bacterial community, comparable to other hydrothermal sediments (Yamanaka & Sakata 2004) but $\delta^{13}C$ was qualitatively similar to non-vent sites, implying that chemosynthetic activity was comparatively limited, or that the isotopic signatures of the basal carbon source (e.g. DIC) and the fractionation associated with FA synthesis resulted in similar $\delta^{13}C$ signatures. It should also be noted that there remains unknown variability in the bulk carbon isotope data resulting from the possible preservation effects from formalin or ethanol. Hook Ridge 1 PLFA composition was intermediate between non-vent sites and Hook Ridge 2 (Supplement 5-3) but the sequence composition was quite similar between Hook Ridge 1 and the off-axis site (Figure 5.4.1a). A small number of the more abundant PLFAs had notable differences in relative abundance between vent/ non-vent sites (Table 3). For example, 16:1ω7, which has been linked to sulphur cycling pathways (Colaço et al. 2007) comprised 14.0 % – 15.2 % of abundance at non-vent sites and 20.0 % – 23.5 % at vent sites. However 18:1ω7, also a suggested PLFA linked to thio-oxidation (Colaço et al. 2007) occurred in lower abundance at vent sites (4.8 % – 11.1 %) than non-vent sites (15.9 % – 16.9 %). Our results further suggest that chemosynthetic activity was relatively limited since, although there were differences in microbial isotopic signatures of chemosynthetic activity, these were not necessarily consistent between different PLFAs. For example, of the PLFAs that have been linked to chemosynthesis, 16:1ω7 was more abundant at the vent sites but 18:1ω7 was more abundant at the non-vent sites.

Several PLFAs had isotopic signatures that varied widely between sites, demonstrating differences in fractionation and/ or source isotopic signatures. The heaviest PLFA $\delta^{13}C$ signatures were associated with Hook Ridge sites and were quite variable (e.g. 16:1ω11t at HR2, $\delta^{13}C$ = -8.7 ‰, ~-24 ‰ to -25 ‰ elsewhere). This provides strong evidence of isotopic differences in the sources or fractionation by the metabolic pathways used to synthesise these FAs. However, bacterial fractionation of organic matter can have substantial variation in $\delta^{13}C$ signatures, depending upon variability in the composition (e.g. C: N ratios) of the source (Macko & Estep 1984), which makes it difficult to elucidate the specific nature of the differences in substrates between sites. Heavier carbon isotopic signatures (> -15 ‰) are generally associated with rTCA cycle carbon fixation (Hayes 2001, Hugler & Sievert 2011, Reid et al. 2013), suggesting that this pathway was active at this site, albeit at probably quite low rates. Conversely, many of the lightest $\delta^{13}C$ signatures (e.g. 19:1ω8, -56.6 ‰, off-axis site) were associated with the non-vent sites. Although 19:1ω8 has not been directly associated with a particular bacterial process (Koranda et al. 2013, Dong et al. 2015), it is quite similar in structure to 19:1ω7, produced by the sulphate reducing *Desulfovibrio* (Nichols et al. 1986) and there were several genera present within the *Desulfovibrionales* at the off-vent site that may have been responsible. *Siboglinum* isotopic data demonstrates that methanotrophy was probably occurring at these sites, and these depleted PLFA isotopic signatures provides further evidence of methanotrophy, in free-living sedimentary bacteria. Chemotrophic bacterial sequences, such as *Blastopirellula* (Schlesner 2015) or *Rhodopirellula* (Bondoso et al. 2014) were found at all sites in relatively high abundance, suggesting widespread and active chemosynthesis, though the lack of a particularly dominant bacterial group associated with chemosynthetic activity suggested that the supply of chemosynthetic OM was likely relatively limited.

Some PLFAs also had marked differences in $\delta^{13}C$ signatures, even where there was strong compositional similarity between sites (i.e. the non-vent sites). This suggested that either there were differences in the isotopic values of inorganic or organic matter sources or that different bacterial metabolic pathways were active.

Between the non-vent sites, these PLFAs included PUFAs and MUFAs (Poly- and Mono-unsaturated fatty acids) such as 18:2ω6, 9 ($\Delta\delta^{13}C$ 24.4 ‰) and 19:1ω8 ($\Delta\delta^{13}C$ 19.1 ‰). Differences in PLFA $\delta^{13}C$ between Hook Ridge sites also ranged widely, with the largest differences being associated with PLFAs such as 16:1ω11t ($\Delta\delta^{13}C$ 17.2 ‰) and 10-Me-16:0 ($\Delta\delta^{13}C$ 11.0 ‰). A number of fatty acids have been linked to chemoautotrophy, such as 10-Me-16:0 (*Desulfobacter* or *Desulfocurvus,* Sulphate reducers) and 18:1ω7 (Yamanaka & Sakata 2004, Colaço et al. 2007, Klouche et al. 2009, Boschker et al. 2014) and their presence is consistent with the hydrothermal signature of the sediment microbial community. However, it should be stressed that all PLFAs with larger $\delta^{13}C$ differences between sites were comparatively rare and never individually exceeded 5 % of total abundance. The few PLFAs that had wide ranges in their $\delta^{13}C$ signatures provide further evidence of limited chemosynthetic activity at all sites and is consistent with the presence of bacteria associated with methane and sulphur cycling. Lower PLFA carbon isotope signatures with small ranges (e.g. -60 ‰ to -50 ‰) could also be indicative of methane cycling, but most PLFAs at all sites had $\delta^{13}C$ of > -40 ‰. Microbial signatures, whilst supporting the suggestion of chemosynthetic activity, are not indicative of chemosynthetic OM being the dominant source of organic matter to food webs at any site (hypothesis four). It is not possible to assess from PLFA data the relative importance of chemoautotrophic and photosynthetic OM sources, since PLFAs degrade quickly and therefore surface FA abundances are inevitably underestimated in deep water samples. Several algal biomarkers were present in the samples, such as 20:5ω3 (Colaço et al. 2007) but their abundances were low (1.6 %), which is consistent with the expected degradation rates during sinking.

5.5.2 *Siboglinids*

Both species of siboglinid (*Sclerolinum contortum* from Hook Ridge and *Siboglinum* sp. from the non-vent sites) were clearly subsisting upon chemosynthetically derived organic matter, as evidenced by their morphology and strongly ^{15}N-depleted isotopic signatures (see values with $\delta^{15}N$ of < -2 ‰; Figure 5.4.3a). Low $\delta^{15}N$ signatures have also been observed in other siboglinids in a range of hydrothermal settings, such as *Riftia pachyptila* at the East Pacific Rise hard substratum vents (Rau

1981), which is consistent with our observations. Nitrogen values for both species ($\delta^{15}N$ *Sclerolinum* = -5.3 ‰ ± 1.0, *Siboglinum* = -8.9 ‰ ± 0.8) clearly indicated reliance upon locally fixed nitrogen sources, such as N_2 (Rau 1981, Dekas et al. 2009, Dekas et al. 2014, Wu et al. 2014, Yamanaka et al. 2015) or strong internal fractionation of nitrate (Naraoka et al. 2008, Liao et al. 2014, Bennett et al. 2015) rather than utilisation of organic nitrogen sources within the sediment ($\delta^{15}N$ = 5.7 ‰ ± 0.7). These values were also in contrast to the rest of the non-chemosynthetic obligate species, which generally had much heavier $\delta^{15}N$ values. This supports hypothesis three, confirming that the siboglinid species were subsisting upon chemosynthetic OM, most likely supplied by their endosymbionts. Diazotrophy, facilitated by sulphate-reducing bacteria is one possible explanation (Weber & Jørgensen 2002, Dhillon et al. 2003, Desai et al. 2013, Frank et al. 2013), which is consistent with the low $\delta^{15}N$ and $\delta^{34}S$ signatures of both siboglinid species (Figure 5.4.3a; Figure 5.4.3b). An alternative hypothesis is that the low $\delta^{15}N$ signatures may be explained by dissimilatory nitrate reduction to ammonium (Naraoka et al. 2008, Liao et al. 2014, Bennett et al. 2015). Unfortunately, bulk faunal isotopic signatures are inadequate to address this question, which would require analysis of the functional genes in the *Siboglinum* endosymbionts.

Carbon isotopic signatures in chemosynthetic primary production depend upon the mode of fixation and the initial ^{13}C of available DIC. *Sclerolinum contortum* $\delta^{13}C$ (-20.5 ‰ ± 1.0 ‰) was depleted in $\delta^{13}C$ relative to Southern Ocean DIC by around 10 ‰ (Henley et al. 2012, Young et al. 2013), giving it a signal within the fractionation range of the reverse tricarboxyclic acid cycle (Yorisue et al. 2012). Regional measurements of surface ocean DIC $\delta^{13}C$ have an average isotopic signature of -10.4 ‰ (Henley et al. 2012, Young et al. 2013) but the concentration and isotopic composition of DIC can undergo considerable alteration at sedimented vents (Walker et al. 2008). Therefore, without measurements of $\delta^{13}C$ in pore fluid DIC, it was not possible to determine which fixation pathway(s) were being used by *S. contortum* endosymbionts.

Sulphur isotopic signatures in *S. contortum* were very low, and quite variable ($\delta^{34}S$ -26.7 ‰ ± 3.5 ‰). *Sclerolinum* endosymbionts may have been utilising sulphide re-

dissolved from hydrothermal precipitates. Mineral sulphide has been observed to be supporting food webs around inactive vents in the Manus Basin (Erickson et al. 2009) and similar material was present at Hook Ridge that ranged between -28.1 ‰ to +5.1 ‰ (Petersen et al. 2004), consistent with the relatively high $\delta^{34}S$ variability in *S. contortum*. These precipitates at Hook Ridge are thought to originate from a previous period of high-temperature venting at this site (Klinkhammer et al. 2001). Alternatively, sulphide supplied as a result of microbial sulphate reduction (Canfield 2001) may have been the primary source of organic sulphur, similar to that of solemyid bivalves from reducing sediments near a sewage pipe outfall (mean $\delta^{34}S$ ranged -30 ‰ to -20 ‰; Vetter and Fry (1998)). Sulphate reduction can also be associated with anaerobic oxidation of methane (Whiticar & Suess 1990, Canfield 2001, Dowell et al. 2016), suggesting that methanotrophic pathways could also have been important at Hook Ridge. (e.g. abundance of *Methylohalomonas*, 2.1 % – 4.3 % of sequences at all sites). Although endosymbiont composition data are not available for the Southern Ocean population, *Sclerolinum contortum* is also known from hydrocarbon seeps in the Gulf of Mexico (Eichinger et al. 2013, Eichinger et al. 2014, Georgieva et al. 2015) and the Håkon Mosby mud volcano in the Arctic ocean, where *S. contortum* $\delta^{13}C$ ranged between -48.3 ‰ to -34.9 ‰ (Gebruk et al. 2003) demonstrating that this species may be capable of occupying several reducing environments and using a range of chemosynthetic fixation pathways, including sulphide oxidation and methanotrophy (Eichinger et al. 2014, Georgieva et al. 2015). However, without more detailed information on endmember isotopic signatures and the possible extent of preservation effects in faunal isotopic data, it is difficult to be certain in this case.

Siboglinum sp. $\delta^{13}C$ values (mean -41.4 ‰, range -45.7 ‰ to -38.1 ‰, n = 8) corresponded very closely to published values of thermogenic methane (-43 ‰ to -38 ‰) from the Bransfield Strait (Whiticar & Suess 1990). This suggested that methanotrophy was the likely carbon source for this species. Biogenic methane typically has much lower $\delta^{13}C$ values (Whiticar 1999, Yamanaka et al. 2015), indicating a hydrothermal/ thermogenic source of methane in the Bransfield Strait. Sulphur isotopic signatures were also very low in *Siboglinum* sp. ($\delta^{34}S$ -22.9 ‰, one sample from 15 pooled individuals from the off-axis site), the lowest measurement

of $\delta^{34}S$ reported for this genus (Schmaljohann & Flügel 1987, Rodrigues et al. 2013). The low $\delta^{13}C$, $\delta^{15}N$ and $\delta^{34}S$ signatures of *Siboglinum* sp. suggest that its symbionts may have included methanotrophs (Thornhill et al. 2008), sulphate reducers and diazotrophic/ denitrifying bacteria (Boetius et al. 2000, Canfield 2001, Dekas et al. 2009). Methanotrophy in *Siboglinum* spp. has been previously documented at seeps in the NE Pacific (Bernardino & Smith 2010) and Norwegian margin ($\delta^{13}C$ = -78.3 ‰ to -62.2 ‰) (Schmaljohann et al. 1990) and in Atlantic mud volcanoes ($\delta^{13}C$ range -49.8 ‰ to -33.0 ‰) (Rodrigues et al. 2013). Sulphur isotopic signatures in *Siboglinum* spp. from Atlantic mud volcanoes ranged between -16.8 ‰ to 6.5 ‰ (Rodrigues et al. 2013) with the lowest value still being 6 ‰ greater than that of Bransfield strait specimens. Rodrigues et al. (2013) also reported a greater range in $\delta^{15}N$ than observed in the Bransfield siboglinids ($\delta^{15}N$ -1.3 ‰ to 12.2 ‰ and -10.2 ‰ to -7.6 ‰ respectively). This suggests that, in comparison to *Siboglinum* spp. in Atlantic Mud volcanoes, which seemed to be using a mixture of organic matter sources (Rodrigues et al. 2013), the Bransfield specimens relied much more heavily upon a single OM source, suggesting considerable trophic plasticity in this genus worldwide.

Off-vent methanotrophy, using thermogenic methane, potentially illustrates an indirect dependence upon hydrothermalism (Whiticar & Suess 1990). Sediment methane production is thought to be accelerated by the heat flux associated with mixing of hydrothermal fluid in sediment (Whiticar & Suess 1990) and thus, sediment and *Siboglinum* isotopic data suggest that the footprint of hydrothermal influence may be much larger than previously recognised, giving rise to transitional environments (Bell et al. 2016a, Levin et al. 2016). Clear contribution of methane-derived carbon to consumer diets was limited predominately to neotanaids, consistent with the relatively small population sizes (64 ind. m^2 – 159 ind. m^2) of *Siboglinum* sp. observed in the Bransfield Strait (Bell et al. 2016b). However, it is worth noting here that the carbon isotopic data should be interpreted with respect to potential preservation shifts. Although there were not any significant shifts between the pilot study of formalin and ethanol preserved material (see methods section 5.3.4), this does not necessarily mean that there were no substantial shifts from the original isotopic ratios of the samples. Since ethanol has a documented

capacity to shift carbon signatures (Fanelli et al. 2010; Rennie et al., 2012), it is possible that the isotopic signatures of *Siboglinum* were not consistent with the reports of thermogenic methane in Bransfield Strait sediments. The low $\delta^{34}S$ values observed would still strongly suggest some degree of AOM but, when coupled with the potential preservation shift, this may have arisen from other methane source (e.g. biogenic) that would not suggest a relationship to the hydrothermal system in the strait.

5.5.3 *Organic Matter Sources*

Pelagic salps, collected from an Agassiz trawl at Hook Ridge (1647 m), were presumed to most closely represent a diet of entirely surface-derived material and were more depleted in $\delta^{13}C$ and more enriched in ^{34}S than sediments (Table 5.4.3a). Salp samples had a mean $\delta^{13}C$ of -27.4 ‰, which was also lighter than the majority of macrofauna, both at Hook Ridge and the non-vent sites (Figure 5.4.3a) and similar to other suspension feeding fauna in the Bransfield Strait (Elias-Piera et al. 2013). This suggests that fauna with more depleted $\delta^{34}S$/ more enriched $\delta^{13}C$ values are likely to have derived at least a small amount of their diet from chemosynthetic sources, both at vents and background regions. Carbon and sulphur isotopic measurements indicated mixed sources for most consumers between chemosynthetic OM and surface-derived photosynthetic OM. Non-vent sediments were more enriched in ^{34}S than vent sediments, an offset that probably resulted from greater availability of lighter sulphur sources such as sulphide oxidation at Hook Ridge. As with the discussion of the potential sources of methane, these data should be interpreted in the context of potential preservation effects. The pilot study detailed here, and the fact that the local fauna had carbon isotopic signatures broadly similar to local suspension feeders (salps, which were freeze-dried) and Southern Ocean phytoplankton ($\delta^{13}C$ approximately -27 to – 26 ‰; Young et al., 2013), does generally suggest fairly limited preservation interference but it is still important to acknowledge this potential confounding factor.

Samples of bacterial mat could not be collected during JC55 (Tyler et al. 2011) and without these endmember measurements, it was not possible to quantitatively

model resource partitioning in the Bransfield Strait using isotope mixing models (Phillips et al. 2014). Bacterial mats from high-temperature vents in the Southern Ocean had $\delta^{34}S$ values of 0.8 ‰ (Reid et al. 2013) and at sedimented areas of the Loki's Castle hydrothermal vents in the Arctic Ocean has $\delta^{34}S$ values of -4.9 ‰ (Bulk sediment; Jaeschke et al. 2014). Therefore it is probable that low faunal $\delta^{34}S$ values represent a contribution of chemosynthetic OM (from either siboglinid tissue or free-living bacteria). Inorganic sulphur can also be a source to consumers when sulphide deposits are utilised by free living bacteria ($\delta^{34}S$ ranged -7.3 ‰ to 5.4 ‰; Erickson et al. (2009)) and sulphide crusts have been found at Hook Ridge ($\delta^{34}S$ -28.1 ‰ to 5.1 ‰; Petersen et al. (2004)). There were several species (e.g. Tubificid oligochaetes) that had moderately depleted $\delta^{34}S$ signatures, such as *Limnodriloides* sp. ($\delta^{34}S$ 7.6 ‰ at vents, -1.2 ‰ at non-vents, Figure 5.4.3b) further supporting the hypothesis of different trophic positions between vent/ non-vent regions (hypothesis two). This provides evidence of coupled anaerobic oxidation of methane/ sulphate reduction but overall, the contribution of $\delta^{34}S$-depleted bacterial production did not seem widespread (further rejecting hypothesis four).

Without samples of all OM sources (and more certainty regarding preservation effects) we cannot quantitatively assert that faunal utilisation of chemosynthetic OM was low in the Bransfield Strait. Although isotopic data were consistent with several OM sources, it seemed unlikely that chemosynthetic OM was a dominant source of OM to the vast majority of taxa. The apparently limited consumption of chemosynthetic OM suggested that either it was not widely available (e.g. patchy or low density of endosymbiont-bearing fauna (Bell et al. 2016b)), or that the ecological stress associated with feeding in areas of in situ production was a significant deterrent to many species (Bernardino et al. 2012, Levin et al. 2013). Owing to the sampling procedure, this study can only consider spatial differences between replicate deployments and it is possible, given the high habitat heterogeneity in SHVs, that substantial variability between cores of a single deployment may be existed but could not be described by this study.

5.5.4 *A-priori vs. a-posteriori trophic groups*

Morphology did not prove to be an accurate predictor of trophic associations, suggesting that faunal behaviour is potentially more important in determining dietary composition than morphology (e.g. having/ lacking jaws). Peracarid species that possessed structures adapted to a motile, carnivorous lifestyle were assigned to a carnivore/ scavenger guild (Bell et al. 2016b) and were distributed throughout the food web both at vents and background regions, indicating more diverse feeding strategies than expected. Taxa presumed to be deposit feeders (largely annelids) also had a surprisingly large range of $\delta^{15}N$ values. This may reflect the consumption of detritus from both 'fresh' and more recycled sources as observed in other non-vent sedimented deep-sea habitats (Iken et al. 2001, Reid et al. 2012) or variability in trophic discrimination related to diet quality (Adams & Sterner 2000). The result is high $\delta^{15}N$ values in taxa without predatory morphology (e.g. oligochaetes) (Bell et al. 2016a). Tubificid oligochaetes had higher $\delta^{15}N$ values at the vent sites, suggesting that they fed upon more recycled organic matter, possibly owing to greater microbial activity at vent sites. Bacterial biomass was very variable at the vent sites (86 mg C m^{-2} – 535 mg C m^{-2}, compared with 136 mg C m^{-2} – 197 mg C m^{-2} at non-vent sites; Table 5.4.2a) and so it is possible that at Hook Ridge 1 bacterial assemblages could have had a greater influence upon $\delta^{15}N$ of organic matter.

Neotanaids from the off-axis site had the lowest $\delta^{13}C$ and $\delta^{15}N$ values of any non-siboglinid taxon (Figure 5.4.4a), suggesting a significant contribution of methane-derived carbon. The clustering of the neotanaids together with endosymbiont-bearing taxa is far more likely to be an artifact of the cluster linkage method, introduced by consumption of low $\delta^{13}C$ methanotrophic sources (e.g. *Siboglinum* tissue), rather than suggesting symbionts in these fauna (Larsen 2006, Levin et al. 2009).

Several taxa (e.g. neotanaids from the off-axis site and ophiuroids at Hook Ridge) had low $\delta^{15}N$ values relative to sediment OM, suggesting preferential consumption of chemosynthetic OM (Rau 1981, Dekas et al. 2014). In these taxa, it is likely that the widespread, but patchy bacterial mats or *Sclerolinum* populations at Hook Ridge

(Aquilina et al. 2013) were an important source of organic matter to fauna with low $\delta^{15}N$ values (e.g. ophiuroids). Fauna from the non-vent sites with low $\delta^{15}N$ were likely subsisting in part upon siboglinid tissue (*Siboglinum* sp.). There were no video transects over the off-axis site but footage of the Three Sisters, which was similar in macrofaunal composition (Bell et al. 2016b), did not reveal bacterial mats (Aquilina et al. 2013), hence it is unlikely that these were a significant resource at non-vent sites.

It is clear that some fauna can exhibit a degree of trophic plasticity, depending upon habitat (supporting hypothesis two). This is consistent with other SHVs where several taxa (e.g. *Prionospio* sp. – Polychaeta: Spionidae) had different isotopic signatures, depending upon their environment (Levin et al. 2009), demonstrating differential patterns in resource utilisation. Alternatively, there could have been different $\delta^{15}N$ baselines between sites, though if these differences were significant, we argue that it likely that more species would have had significant differences in tissue $\delta^{15}N$.

5.5.5 *Impact of hydrothermal activity on community trophodynamics*

Standard ellipse area was lower at Hook Ridge than at non-vent sites (Table 5.4.5a), analogous to trends in macrofaunal diversity and abundance in the Bransfield Strait (Bell et al. 2016b) and changes in SEA.B along a gradient of methane flux at vent and seep ecosystems in the Guaymas Basin (Portail et al. 2016). This demonstrates that at community level, ellipse area is associated with other macrofaunal assemblage characteristics. This concurrent decline in niche area and alpha diversity is consistent with the concept that species have finely partitioned niches and greater total niche area permits higher biodiversity (McClain & Schlacher 2015). Productivity-diversity relationships, whereby higher productivity sustains higher diversity, have also been suggested for deep-sea ecosystems (McClain & Schlacher 2015, Woolley et al. 2016) but in the absence of measurements of in situ organic matter fixation rates at Hook Ridge, it is unclear whether such relationships exist in the Bransfield Strait. Sediment organic carbon content was similar between Hook Ridge 1 and non-vent sites but was slightly lower at Hook Ridge 2 (Bell et al. 2016b),

which is not consistent with variation in niche area. The decline in alpha diversity and niche area is consistent with the influence of disturbance gradients created by hydrothermalism that result in an impoverished community (McClain & Schlacher 2015, Bell et al. 2016b). We suggest that, in the Bransfield Strait, the environmental toxicity at SHVs (from differences in temperature and porewater chemistry) causes a concomitant decline in both trophic and species diversity (Bell et al. 2016b), in spite of the potential for increased localised production. However, we acknowledge that, owing to the high small-scale habitat heterogeneity apparent from video imagery over the vent area, that it is likely that the contribution of chemosynthetic organic matter varies widely over 10s of metres at Hook Ridge. There may also have been considerable variability at scales of < 1 m that could not be investigated using the samples available to this study.

Community-based trophic metrics (Layman et al. 2007) indicated that, although measures of dispersion within sites were relatively similar between vents and background areas (Table 5.4.5a), trophic diversity, particularly in terms of range of carbon sources (dCr) and total hull area (TA) were higher at background sites. It was expected that trophic diversity would be greater at Hook Ridge but the greater dCr at non-vent sites (owing to the methanotrophic source) meant that the isotopic niches at these sites were larger. Range in nitrogen values (dNr) was also greater at non-vents, driven by the more heavily depleted $\delta^{15}N$ values of *Siboglinum* sp. It is of course debatable whether this assemblage isotopic niche really corresponds to the assemblage's actualised trophic niche (i.e. does isotopic variability directly relate to actual behavioural/ diet differences) and is therefore still possible that, although the niche space was smaller at the vent sites, the potential for different trophic strategies was still greater than at non-vent sites. Differences in eccentricity are more heavily influenced by the spread of all isotopes used to construct the niche space (where E = 0 corresponds to an equal influence of both carbon and nitrogen) whereas theta (the angle of the long axis) determines which, if any, isotope is most influential in determining ellipse characteristics (Reid et al. 2016). For the non-vent sites, the dominant isotope was carbon, owing to the relatively light $\delta^{13}C$ of methanotrophic source utilised by *Siboglinum*. Some sites, particularly the Axe, had several fauna with heavy $\delta^{13}C$ values (Figure 5.4.5a), which could be explained by

either contamination from marine carbonate (~0 ‰), as specimens were not acidified, or a diet that included a heavier source of carbon, such as sea ice algae (Henley et al. 2012).

5.6 Conclusions

In this study, we demonstrate the influence of sediment-hosted hydrothermal venting upon trophodynamics and microbial populations. Low activity vent microbiota were more similar to the non-vent site than to high activity populations, illustrating the effect of ecological gradients upon deep-sea microbial diversity. Despite widespread bacterial mats, and populations of vent-endemic macrofauna, utilisation of chemosynthetic OM amongst non-specialist macro- and megafauna seemed relatively low, with a concomitant decline in trophic diversity with increasing hydrothermal activity. Morphology was also not indicative of trophic relationships, demonstrating the effects of differential resource availability and behaviour. We suggest that, because these sedimented hydrothermal vents are insufficiently active to host large populations of vent-endemic megafauna, the transfer of chemosynthetic organic matter into the metazoan food web is more limited than in other similar environments. However, through the supply of thermogenic methane to off-axis areas, we demonstrate that hydrothermal circulation can have a much larger spatial extent than previously considered for benthic food webs.

5.7 Acknowledgements

JBB was funded by a NERC PhD Studentship (NE/L501542/1). This work was funded by the NERC ChEsSo consortium (Chemosynthetically-driven Ecosystems South of the Polar Front, NERC Grant NE/DOI249X/I). Elemental analyses were funded by the NERC Life Sciences Mass Spectrometry Facility (Proposal no. EK234-13/14). We thank Barry Thornton and the James Hutton Laboratory, Aberdeen for processing the PLFA samples. We also thank Will Goodall-Copestake for assistance in processing the 16S sequence data. We are grateful to the Master and Crew of RRS *James Cook* cruise 055 for technical support and the Cruise Principal Scientific Officer Professor Paul Tyler.

5.8 Ethics Statement

In accordance with the Antarctic Act (1994) and the Antarctic Regulations (1995), necessary permits (S5-4/2010) were acquired from the South Georgia and South Sandwich Islands Government.

5.9 Author contributions

Conceived and designed the sampling programme: WDKR, DAP, AGG, CJS & CW. Sample laboratory preparation and isotopic analyses: JBB, JN & CJS. Microbial sequencing: DAP. Statistical analyses: JBB. Produced figures: JBB. Wrote the paper: JBB, CW & WDKR, with contributions and comments from all other authors.

5.10 References

Adams TS, Sterner RW (2000) The effect of dietary nitrogen content on trophic level ^{15}N enrichment. Limnology & Oceanography 45:601-607

Aquilina A, Connelly DP, Copley JT, Green DR, Hawkes JA, Hepburn L, Huvenne VA, Marsh L, Mills RA, Tyler PA (2013) Geochemical and Visual Indicators of Hydrothermal Fluid Flow through a Sediment-Hosted Volcanic Ridge in the Central Bransfield Basin (Antarctica). Plos One 8:e54686

Aquilina A, Homoky WB, Hawkes JA, Lyons TW, Mills RA (2014) Hydrothermal sediments are a source of water column Fe and Mn in the Bransfield Strait, Antarctica. Geochimica et Cosmochimica Acta 137:64-80

Bell JB, Aquilina A, Woulds C, Glover AG, Little CTS, Reid WDK, Hepburn LE, Newton J, Mills RA (2016a) Geochemistry, faunal composition and trophic structure at an area of weak methane seepage on the southwest South Georgia margin. Royal Society Open Science 3

Bell JB, Woulds C, Brown LE, Little CTS, Sweeting CJ, Reid WDK, Glover AG (2016b) Macrofaunal ecology of sedimented hydrothermal vents in the Bransfield Strait, Antarctica. Frontiers in Marine Science 3:32

Bemis K, Lowell R, Farough A (2012) Diffuse Flow On and Around Hydrothermal Vents at Mid-Ocean Ridges. Oceanography 25:182-191

Bennett SA, Dover CV, Breier JA, Coleman M (2015) Effect of depth and vent fluid composition on the carbon sources at two neighboring deep-sea hydrothermal vent fields (Mid-Cayman Rise). Deep Sea Research Part I: Oceanographic Research Papers 104:122-133

Bernardino AF, Levin LA, Thurber AR, Smith CR (2012) Comparative Composition, Diversity and Trophic Ecology of Sediment Macrofauna at Vents, Seeps and Organic Falls. Plos ONE 7:e33515

Bernardino AF, Smith CR (2010) Community structure of infaunal macrobenthos around vestimentiferan thickets at the San Clemente cold seep, NE Pacific. Marine Ecology-an Evolutionary Perspective 31:608-621

Biomatters (2014) Geneious.

Bligh EG (1959) A rapid method of total lipid extration and purification. Canadian Journal of Biochemistry and Phsiology 37:911-917

Boetius A, Ravenschlag K, Schubert CJ, Rickert D, Widdel F, Gieseke A, Amman R, Jørgensen BB, Witte U, Pfannkuche O (2000) A marine microbial consortium apparently mediating anaerobic oxidation of methane. Nature 407:623-626

Bondoso J, Albuquerque L, Lobo-da-Cunha A, da Costa MS, Harder J, Lage OM (2014) Rhodopirellula lusitana sp. nov. and Rhodopirellula rubra sp. nov., isolated from the surface of macroalgae. Syst Appl Microbiol 37:157-164

Boschker HT, Middelburg JJ (2002) Stable isotopes and biomarkers in microbial ecology. FEMS Microbiology Ecology 40:85-95

Boschker HT, Vasquez-Cardenas D, Bolhuis H, Moerdijk-Poortvliet TW, Moodley L (2014) Chemoautotrophic carbon fixation rates and active bacterial communities in intertidal marine sediments. PLoS One 9:e101443

Canfield DE (2001) Isotope fractionation by natural populations of sulfate-reducing bacteria. Geochimica Et Cosmochimica Acta 65:1117-1124

Clarke KR, Somerfield PJ, Gorley RN (2008) Testing of null hypotheses in exploratory community analyses: similarity profiles and biota-environment linkage. Journal of Experimental Marine Biology and Ecology 366:56-69

Colaço A, Desbruyères D, Guezennec J (2007) Polar lipid fatty acids as indicators of trophic associations in a deep-sea vent system community. Marine Ecology 28:15-24

Connolly RM, Schlacher TA (2013) Sample acidification significantly alters stable isotope ratios of sulfur in aquatic plants and animals. Marine Ecology Progress Series 493:1-8

Dählmann A, Wallman K, Sahling H, Sarthou G, Bohrmann G, Petersen S, Chin CS, Klinkhammer GP (2001) Hot vents in an ice-cold ocean: Indications for phase separation at the southernmost area of hydrothermal activity, Bransfield Strait, Antarctica. Earth and Planetary Science Letters 193:381-394

Dekas AE, Chadwick GL, Bowles MW, Joye SB, Orphan VJ (2014) Spatial distribution of nitrogen fixation in methane seep sediment and the role of the ANME archaea. Environ Microbiol 16:3012-3029

Dekas AE, Poretsky RS, Orphan VJ (2009) Deep-sea archaea fix and share nitrogen in methane-consuming microbial consortia. Science 326:422-426

Desai MS, Assig K, Dattagupta S (2013) Nitrogen fixation in distinct microbial niches within a chemoautotrophy-driven cave ecosystem. Isme Journal 7:2411-2423

Dhillon A, Teske A, Dillon J, Stahl DA, Sogin ML (2003) Molecular Characterization of Sulfate-Reducing Bacteria in the Guaymas Basin. Applied and environmental microbiology 69:2765-2772

Dong L-J, Sun Z-K, Gao Y, He W-M (2015) Two-year interactions between invasive Solidago canadensis and soil decrease its subsequent growth and competitive ability. Journal of Plant Ecology:rtv003

Dowell F, Cardman Z, Dasarathy S, Kellerman M, Lipp JS, Ruff SE, Biddle JF, McKay L, MacGregor BJ, Lloyd KG, Albert DB, Mendlovitz H, Hinrichs KU, Teske A (2016) Microbial communities in methane- and short chain alkane- rich hydrothermal sediments of Guaymas Basin. Frontiers in microbiology

Eichinger I, Hourdez S, Bright M (2013) Morphology, microanatomy and sequence data of *Sclerolinum contortum* (Siboglindae, Annelida) of the Gulf of Mexico. Organisms Diversity & Evolution 13:311-329

Eichinger I, Schmitz-Esser S, Schmid M, Fisher CR, Bright M (2014) Symbiont-driven sulfur crystal formation in a thiotrophic symbiosis from deep-sea hydrocarbon seeps. Environ Microbiol Rep 6:364-372

Elias-Piera F, Rossi S, Gili JM, Orejas C (2013) Trophic ecology of seven Antarctic gorgonian species. Marine Ecology Progress Series 477:93-106

Erickson KL, Macko SA, Van Dover CL (2009) Evidence for a chemotrophically based food web at inactive hydrothermal vents (Manus Basin). Deep Sea Research Part II: Topical Studies in Oceanography 56:1577-1585

Fanelli E, Cartes JE, Enric J, Papiol V, Rumolo P, Sprovieri M (2010) Effects of preservation on the δ13C and δ15N values of deep sea macrofauna. Journal of Experimental Marine Biology and Ecology 395:93-97

Frank KL, Rogers DR, Olins HC, Vidoudez C, Girguis PR (2013) Characterizing the distribution and rates of microbial sulfate reduction at Middle Valley hydrothermal vents. ISME J 7:1391-1401

Fry B, Jannasch HW, Molyneaux SJ, Wirsen CO, Muramoto JA, King S (1991) Stable Isotope Studies of the Carbon Nitrogen and Sulfur Cycles in the Black Sea and the Cariaco Trench. Deep-Sea Research Part A Oceanographic Research Papers 38:S1003-S1020

Gebruk A, Krylova E, Lein A, Vinogradov G, Anderson E, Pimenov N, Cherkashev G, Crane K (2003) Methane seep community of the Håkon Mosby mud volcano

(the Norwegian Sea): composition and trophic aspects. Sarsia: North Atlantic Marine Science 88:394-403

Georgieva M, Wiklund H, Bell JB, Eilersten MH, Mills RA, Little CTS, Glover AG (2015) A chemosynthetic weed: the tubeworm *Sclerolinum contortum* is a bipolar, cosmopolitan species. BMC Evolutionary Biology 15:280

Gollner S, Govenar B, Fisher CR, Bright M (2015) Size matters at deep-sea hydrothermal vents: different diversity and habitat fidelity patterns of meio- and macrofauna. Marine Ecology Progress Series 520:57-66

Hayes JM (2001) Fractionation of carbon and hydrogen isotopes in biosynthetic processes. Reviews in Mineralogy & Geochemistry 43:225-277

Henley SF, Annett AL, Ganeshram RS, Carson DS, Weston K, Crosta X, Tait A, Dougans J, Fallick AE, Clarke A (2012) Factors influencing the stable carbon isotopic composition of suspended and sinking organic matter in the coastal Antarctic sea ice environment. Biogeosciences 9:1137-1157

Hothorn T, van de Wiel MA, Zeilis A (2015) Package 'Coin': Conditional Inference Procedures in a Permutation Test Framework. cranr-projectorg

Hugler M, Sievert SM (2011) Beyond the Calvin cycle: autotrophic carbon fixation in the ocean. Annual review of marine science 3:261-289

Iken K, Brey T, Wand U, Voight J, Junghans P (2001) Trophic relationships in the benthic community at Porcupine Abyssal Plain (NE Atlantic): a stable isotope analysis. Progress in Oceanography 50:383-405

Inskeep WP, Jay ZJ, Macur RE, Clingenpeel S, Tenney A, Lovalvo D, Beam JP, Kozubal MA, Shanks WC, Morgan LA, Kan J, Gorby Y, Yooseph S, Nealson K (2015) Geomicrobiology of sublacustrine thermal vents in Yellowstone Lake: geochemical controls on microbial community structure and function. Frontiers in microbiology 6:1044

Jackson AL, Inger R, Parnell AC, Bearhop S (2011) Comparing isotopic niche widths among and within communities: SIBER - Stable Isotope Bayesian Ellipses in R. The Journal of animal ecology 80:595-602

Jaeschke A, Eickmann B, Lang SQ, Bernasconi SM, Strauss H, Fruh-Green GL (2014) Biosignatures in chimney structures and sediment from the Loki's Castle low-temperature hydrothermal vent field at the Arctic Mid-Ocean Ridge. Extremophiles 18:545-560

Kallmeyer J, Boetius A (2004) Effects of Temperature and Pressure on Sulfate Reduction and Anaerobic Oxidation of Methane in Hydrothermal Sediments of Guaymas Basin. Applied and environmental microbiology 70:1231-1233

Kharlamenko VI, Zhukova NV, Khotimchenko SV, Svetashev VI, Kamenev GM (1995) Fatty-acids as markers of food sources in a shallow-water hydrothermal ecosystem (Kraternaya Bight, Yankich island, Kurile Islands). Marine Ecology Progress Series 120:231-241

Klinkhammer GP, Chin CS, Keller RA, Dahlmann A, Sahling H, Sarthou G, Petersen S, Smith F (2001) Discovery of new hydrothermal vent sites in Bransfield Strait, Antarctica. Earth and Planetary Science Letters 193:395-407

Klouche N, Basso O, Lascourréges J-F, Cavol J-L, Thomas P, Fauque G, Fardeau M-L, Magot M (2009) Desulfocurvus vexinensis gen. nov., sp. nov., a sulfate-reducing bacterium isolated from a deep subsurface aquifer. International Journal of Systematic and Evolutionary Microbiology 30:3100-3104

Koranda M, Kaiser C, Fuchslueger L, Kitzler B, Sessitsch A, Zechmeister-Boltenstern S, Rickhter A (2013) Fungal and bacterial utilization of organic substrates depends on substrate complexity and N availability. In: Dieckmann U (ed). International Institute for Applied Systems Analysis, Laxenburg, Austria

Larsen K (2006) Tanaidacea (Crustacea; Peracarida) from chemically reduced habitats—the hydrothermal vent system of the Juan de Fuca Ridge, Escabana Trough and Gorda Ridge, northeast Pacific. Zootaxa 1164:1-33

Layman CA, Arrington DA, Montaña CG, Post DM (2007) Can Stable Isotope Ratios Provide For Community-Wide Measures of Trophic Structure? Ecology 88:42-48

Levin LA, Baco AR, Bowden D, Colaço A, Cordes E, Cunha MR, Demopoulos A, Gobin J, Grupe B, Le J, Metaxas A, Netburn A, Rouse GW, Thurber AR, Tunnicliffe V, Van Dover C, Vanreusel A, Watling L (2016) Hydrothermal Vents and Methane Seeps: Rethinking the Sphere of Influence. Frontiers in Marine Science 3:72

Levin LA, Mendoza GF, Konotchick T, Lee R (2009) Macrobenthos community structure and trophic relationships within active and inactive Pacific hydrothermal sediments. Deep Sea Research Part II: Topical Studies in Oceanography 56:1632-1648

Levin LA, Michener RH (2002) Isotopic evidence for chemosynthesis-based nutrition of macrobenthos: The lightness of being at Pacific methane seeps. Limnology and Oceanography 47:1336-1345

Levin LA, Orphan VJ, Rouse GW, Rathburn AE, Ussler W, III, Cook GS, Goffredi SK, Perez EM, Waren A, Grupe BM, Chadwick G, Strickrott B (2012) A hydrothermal seep on the Costa Rica margin: middle ground in a continuum of reducing ecosystems. Proceedings of the Royal Society B-Biological Sciences 279:2580-2588

Levin LA, Ziebis W, Mendoza GF, Bertics VJ, Washington T, Gonzalez J, Thurber AR, Ebbed B, Lee RW (2013) Ecological release and niche partitioning under stress: Lessons from dorvilleid polychaetes in sulfidic sediments at methane seeps. Deep-Sea Research Part II-Topical Studies in Oceanography 92:214-233

Liao L, Wankel SD, Wu M, Cavanaugh CM, Girguis PR (2014) Characterizing the plasticity of nitrogen metabolism by the host and symbionts of the hydrothermal vent chemoautotrophic symbioses Ridgeia piscesae. Mol Ecol 23:1544-1557

Macko SA, Estep MLF (1984) Microbial alteration of stable nitrogen and carbon isotopic compositions of organic matter. Organic Geochemistry 6:787-790

Main CE, Ruhl HA, Jones DOB, Yool A, Thornton B, Mayor DJ (2015) Hydrocarbon contamination affects deep-sea benthic oxygen uptake and microbial community composition. Deep Sea Research Part I: Oceanographic Research Papers 100:79-87

Martens CS (1990) Generation of short chain organic acid anions in hydrothermally altered sediments of the Guaymas Basin, Gulf of California. Applied Geochemistry 5:71-76

McClain CR, Schlacher TA (2015) On some hypotheses of diversity of animal life at great depths on the sea floor. Marine Ecology:12288

McKay L, Klokman VW, Mendlovitz HP, LaRowe DE, Hoer DR, Albert D, Amend JP, Teske A (2015) Thermal and geochemical influences on microbial biogeography in the hydrothermal sediments of Guaymas Basin, Gulf of California. Environmental Microbiology Reports:n/a-n/a

Mincks SL, Smith CR, Jeffreys RM, Sumida PYG (2008) Trophic structure on the West Antarctic Peninsula shelf: Detritivory and benthic inertia revealed by δ13C and δ15N analysis. Deep Sea Research Part II: Topical Studies in Oceanography 55:2502-2514

Naraoka H, Naito T, Yamanaka T, Tsunogai U, Fujikura K (2008) A multi-isotope study of deep-sea mussels at three different hydrothermal vent sites in the northwestern Pacific. Chemical Geology 255:25-32

Nichols PD, Guckbert JB, White DC (1986) Determination of monounsaturated fatty acid double-bond position and geometry for microbial monocultures and complex consortia by capillary GC-MS of their dimethyl disulphide adducts. Journal of Microbiological Methods 5:49-55

Ondov BD, Bergman NH, Phillippy AM (2011) Interactive metagenomic visualization in a Web browser. BMC Bioinformatics 30:385

Parnell AC, Inger R, Bearhop S, Jackson AL (2010) Source partitioning using stable isotopes: coping with too much variation. PLoS One 5:e9672

Petersen S, Herzig PM, Schwarz-Schampera U, Hannington MD, Jonasson IR (2004) Hydrothermal precipitates associated with bimodal volcanism in the Central Bransfield Strait, Antarctica. Mineralium Deposita 39:358-379

Phillips DL, Inger R, Bearhop S, Jackson AL, Moore JW, Parnell AC, Semmens BX, Ward EJ (2014) Best practices for use of stable isotope mixing models in food-web studies. Canadian Journal of Zoology 92:823-835

Portail M, Olu K, Dubois SF, Escobar-Briones E, Gelinas Y, Menot L, Sarrazin J (2016) Food-Web Complexity in Guaymas Basin Hydrothermal Vents and Cold Seeps. PLoS One 11:e0162263

R Core Team (2013) R: A Language and environment for statistical computing. R Foundation for Statistical Computing, Vienna, Austria http://www.R-project.org/.

Rau GH (1981) Low $^{15}N/^{14}N$ in hydrothermal vent animals: ecological implications. Nature 289:484-485

Reid WDK, Sweeting CJ, Wigham BD, McGill RAR, Polunin NVC (2016) Isotopic niche variability in macroconsumers of the East Scotia Ridge (Southern Ocean) hydrothermal vents: what more can we learn from an ellipse? Marine Ecology Progress Series:13-24

Reid WDK, Sweeting CJ, Wigham BD, Zwirglmaier K, Hawkes JA, McGill RAR, Linse K, Polunin NVC (2013) Spatial Differences in East Scotia Ridge Hydrothermal Vent Food Webs: Influences of Chemistry, Microbiology and Predation on Trophodynamics. Plos One 8

Reid WDK, Wigham BD, McGill RAR, Polunin NVC (2012) Elucidating trophic pathways in benthic deep-sea assemblages of the Mid-Atlantic Ridge north and south of the Charlie-Gibbs Fracture Zone. Marine Ecology Progress Series 463:89-103

Rennie MD, Ozersky T, Evans DO (2012) Effects of formalin preservation on invertebrate stable isotope values over decadal time scales. Canadian Journal of Zoology 90:1320-1327

Rodrigues CF, Hilário A, Cunha MR (2013) Chemosymbiotic species from the Gulf of Cadiz (NE Atlantic): distribution, life styles and nutritional patterns. Biogeosciences 10:2569-2581

Sahling H, Wallman K, Dählmann A, Schmaljohann R, Petersen S (2005) The physicochemical habitat of *Sclerolinum sp.* at Hook Ridge hydrothermal vent, Bransfield Strait, Antarctica. Limnology & Oceanography 50:598-606

Schlesner H (2015) Blastopirellula. Bergey's Manual of Systematics of Archaea and Bacteria. John Wiley & Sons, Ltd

Schmaljohann R, Faber E, Whiticar MJ, Dando PR (1990) Co-existence of methane- and sulphur-based endosymbioses between bacteria and invertebrates at a site in the Skagerrak. Marine Ecology Progress Series 61:11-124

Schmaljohann R, Flügel HJ (1987) Methane-oxidizing bacteria in Pogonophora. Sarsia 72:91-98

Sellanes J, Zapata-Hernández G, Pantoja S, Jessen GL (2011) Chemosynthetic trophic support for the benthic community at an intertidal cold seep site at Mocha Island off central Chile. Estuarine, Coastal and Shelf Science 95:431-439

Soto LA (2009) Stable carbon and nitrogen isotopic signatures of fauna associated with the deep-sea hydrothermal vent system of Guaymas Basin, Gulf of California. Deep Sea Research Part II: Topical Studies in Oceanography 56:1675-1682

Southward A, J., Southward EC, Brattegard T, Bakke T (1979) Further Experiments on the value of Dissolved Organic Matter as Food for *Siboglinum fjiordicum*

(Pogonophora). Journal of Marine Biological Asociation of the United Kingdom 59:133-148

Southward EC, Gebruk A, Kennedy H, Southward AJ, Chevaldonne P (2001) Different energy sources for three symbiont-dependent bivalve molluscs at the Logatchev hydrothermal site (Mid-Atlantic Ridge). Journal of Marine Biological Asociation of the United Kingdom 81:655-661

Sweetman AK, Levin LA, Rapp HT, Schander C (2013) Faunal trophic structure at hydrothermal vents on the southern Mohn's Ridge, Arctic Ocean. Marine Ecology Progress Series 473:115

Tarasov VG, Gebruk AV, Mironov AN, Moskalev LI (2005) Deep-sea and shallow-water hydrothermal vent communities: Two different phenomena? Chemical Geology 224:5-39

Teske A, Callaghan AV, LaRowe DE (2014) Biosphere frontiers of subsurface life in the sedimented hydrothermal system of Guaymas Basin. Frontiers in microbiology 5:362

Teske A, Hinrichs KU, Edgcomb V, de Vera Gomez A, Kysela D, Sylva SP, Sogin ML, Jannasch HW (2002) Microbial Diversity of Hydrothermal Sediments in the Guaymas Basin: Evidence for Anaerobic Methanotrophic Communities. Applied and environmental microbiology 68:1994-2007

Thornhill DJ, Wiley AA, Campbell AL, Bartol FF, Teske A, Halanych KM (2008) Endosymbionts of *Siboglinum fjordicum* and the Phylogeny of Bacterial Endosymbionts in Siboglinidae (Annelida). Biological Bulletin 214:135-144

Thornton B, Zhang Z, Mayes RW, Högberg MN, Midwood AJ (2011) Can gas chromatography combustion isotope ratio mass spectrometry be used to quantify organic compound abundance? Rapid Communications in Mass Spectrometry 25:2433-2438

Tyler PA, Connelly DP, Copley JT, Linse K, Mills RA, Pearce DA, Aquilina A, Cole C, Glover AG, Green DR, Hawkes JA, Hepburn L, Herrera S, Marsh L, Reid WD, Roterman CN, Sweeting CJ, Tate A, Woulds C, Zwirglmaier K (2011) RRS *James Cook* cruise JC55: Chemosynthetic Ecosystems of the Southern Ocean. BODC Cruise Report

Valls M, Olivar MP, Fernández de Puelles ML, Molí B, Bernal A, Sweeting CJ (2014) Trophic structure of mesopelagic fishes in the western Mediterranean based

on stable isotopes of carbon and nitrogen. Journal of Marine Systems 138:160-170

Vetter RD, Fry B (1998) Sulfur contents and sulfur-isotope compositions of thiotrophic symbioses in bivalve molluscs and vestimentiferan worms. Marine Biology 132:453-460

Walker BD, McCarthy MD, Fisher AT, Guilderson TP (2008) Dissolved inorganic carbon isotopic composition of low-temperature axial and ridge-flank hydrothermal fluids of the Juan de Fuca Ridge. Marine Chemistry 108:123-136

Wang Q, Garrity GM, Tiedje JM, Cole JR (2007) Naïve Bayesian Classifier for Rapid Asssignment of rRNA sequences into the New Bacterial Taxonomy. Applied Environmental Microbiology 73:5261-5267

Weber A, Jørgensen BB (2002) Bacterial sulfate reduction in hydrothermal sediments of the Guaymas Basin, Gulf of California, Mexico. Deep-Sea Research I 49:827-841

Whitaker D, Christmann M (2013) Package 'clustsig'. cranr-projectorg

Whiticar MJ (1999) Carbon and Hydrogen isotope systematics of bacterial formation and oxidation of methane. Chemical Geology 161:291-314

Whiticar MJ, Suess E (1990) Hydrothermal hydrocarbon gases in the sediments of the King George Basin, Bransfield Strait, Antarctica. Applied Geochemistry 5:135-147

Woolley SNC, Tittensor DP, Dunstan PK, Guillera-Arroita G, Lahoz-Monfort JJ, Wintle BA, Worm B, O'Hara TD (2016) Deep-sea diversity patterns are shaped by energy availability. Nature

Wu Y, Cao Y, Wang C, Wu M, Aharon O, Xu X (2014) Microbial community structure and nitrogenase gene diversity of sediment from a deep-sea hydrothermal vent field on the Southwest Indian Ridge. Acta Oceanologica Sinica 33:94-104

Yamanaka T, Sakata S (2004) Abundance and distribution of fatty acids in hydrothermal vent sediments of the western Pacific Ocean. Organic Geochemistry 35:573-582

Yamanaka T, Shimamura S, Nagashio H, Yamagami S, Onishi Y, Hyodo A, Mampuku M, Mizota C (2015) A Compilation of the Stable Isotopic Compositions of Carbon, Nitrogen, and Sulfur in Soft Body Parts of Animals Collected from

Deep-Sea Hydrothermal Vent and Methane Seep Fields: Variations in Energy Source and Importance of Subsurface Microbial Processes in the Sediment-Hosted Systems. In: Ishibashi J, Okino K, Sunamura M (eds) Subseafloor Biosphere Linked to Hydrothermal Systems. SpringerOpen, Tokyo

Yorisue T, Inoue K, Miyake H, Kojima S (2012) Trophic structure of hydrothermal vent communities at Myojin Knoll and Nikko Seamount in the northwestern Pacific: Implications for photosynthesis-derived food supply. Plankton and Benthos Research 7:35-40

Young JN, Bruggeman J, Rickaby REM, Erez J, Conte M (2013) Evidence for changes in carbon isotopic fractionation by phytoplankton between 1960 and 2010. Global Biogeochemical Cycles 27:505-515

Chapter 6: Hydrothermal activity, functional diversity and chemoautotrophy are major drivers of seafloor carbon cycling.

Scientific Reports (In Review)

James B. Bell[1, 2]*, Clare Woulds[1] & Dick van Oevelen[3]

[1]School of Geography, University of Leeds, Leeds, LS2 9JT, UK.
[2]Life Sciences, Natural History Museum, Cromwell Rd, London SW7 5BD, UK
[3]Department of Estuarine and Delta Systems, Royal Netherlands Institute for Sea Research (NIOZ) and Utrecht University, Yerseke, the Netherlands

Keywords: Sedimented Hydrothermal Vent; Chemosynthesis; Modelling; Biogeochemistry

6.1 Abstract

Hydrothermal vents are highly dynamic ecosystems and are unusually energy rich in the deep-sea. In situ hydrothermal-based productivity combined with sinking photosynthetic organic matter in a soft-sediment setting creates geochemically diverse environments, which remain poorly studied. Here, we use new field observations to develop the first quantitative ecosystem model of a deep-sea chemosynthetic ecosystem from the most southerly hydrothermal vent system known. We find evidence of widespread chemosynthetic production at vent sites and elsewhere. This demonstrates a substantially broader spatial extent and importance of hydrothermal activity to deep-seafloor food webs than previously recognised (1000s of square kilometres as opposed to 10s). Differences between relative abundance of faunal functional groups, resulting from environmental variability, were clear drivers of differences in biogeochemical cycling. Endosymbiont-bearing fauna were very important in supporting the transfer of chemosynthetic carbon into the food web, particularly to higher trophic levels. Based on our observation of the unexpectedly wide spatial extent of chemosynthetic production, we propose that these ecosystems contribute significantly to global deep-sea organic matter cycling, particularly for deep-sea benthos not adapted to living at high temperature vents. This has implications for global seafloor carbon budgets and the importance of chemosynthesis.

6.2 Introduction

6.2.1 Sedimented Hydrothermal Vents

Following the discovery of hydrothermal vents on the East Pacific Rise in the late 1970s, it has become clear that chemosynthesis represents a vital carbon fixation pathway in the deep-sea (Dubilier et al. 2008, Middelburg 2011), supporting a unique diversity of fauna (Connelly et al. 2012). Hydrothermal vents have a diverse range of geological and geochemical drivers, resulting in several distinct types in soft and hard substratum settings but so far, the vast majority of research has focussed upon hard substratum vent systems. Sedimented hydrothermal vents

(SHVs), where hydrothermal fluid vents through soft-sediment are geochemically very rich, with high concentrations of chemosynthetic substrates (Bernardino et al. 2012). They have been discovered in diverse geological settings, both on the periphery of high-temperature vents (Grassle & Petrecca 1994, Southward et al. 2001, Sweetman et al. 2013), and as independent environments (Levin et al. 2009, Aquilina et al. 2013, Aquilina et al. 2014), meaning that they are globally distributed and a potentially important source of food to deep-sea fauna, particularly those not endemic to hydrothermal vents.

Food webs at SHVs are supported by in situ chemosynthetic-based productivity and surface-derived organic matter and the soft-sediment setting allows for colonisation by both vent-endemic fauna and typical deep-sea soft-sediment fauna (Levin & Mendoza 2007, Bernardino et al. 2012, Sweetman et al. 2013, Bell et al. 2016d). The combination of organic matter sources and differences in relative abundance of functional groups between sites of variable hydrothermal activity create potential for a wide range of possible trophic activities. In such a complex setting it is challenging to determine the contribution of the various food sources and differences relating to hydrothermal activity based on empirical observations alone. These deep-sea ecosystems, owing to their extreme isolation, are some of the most poorly studied areas on the planet and the present study represents the first attempt to quantitatively describe seafloor carbon cycling in these settings.

Typical chemosynthetic substrates at SHVs include hydrogen sulphide and methane and, owing to thermal decomposition of sediments, the concentration of these substrates can be several orders of magnitude higher than at unsedimented hydrothermal vents (Bernardino et al. 2012). Chemosynthetic production occurs through several pathways, such as sulphide oxidation or anaerobic oxidation of methane and there is now also evidence of diverse microbial lineages associated with other pathways, such as iron reduction (Teske et al. 2014, Bell et al. 2016c). Fauna living in these habitats have access to both chemosynthetic and photosynthetic energy sources, while their distribution and behaviour reflect a balance between their ability to tolerate the high temperature, reducing conditions introduced by the influx of hydrothermal fluid and selectivity of the relative

amounts of organic matter present (Bernardino et al. 2012, Bell et al. 2016d). The environmental gradients between SHVs and background sediments therefore create a range of assemblage compositions, trophic structures and pathways for in situ productivity (Soto 2009, Bernardino et al. 2012, Levin et al. 2012, Sweetman et al. 2013, Bell et al. 2016c, Bell et al. 2016d). We report here for the first time how this affects energy transfers within food webs and the extent to which chemosynthetic production effectively subsidises the diet of non-specialist fauna.

6.2.2 Measuring food web interactions

Stable isotopes have been used widely to study chemosynthetic activity in deep-sea food webs, but their interpretation is often complicated by variability and uncertainty in factors such as trophic discrimination factors and the range of OM sources available (Reid et al. invited review in prep.). Owing to the small number of SHVs that have been studied and the multiple scales of variability within each site, quantitative estimates of the contribution of chemosynthetic OM to the faunal food web are lacking. Stable isotope mixing models have been implemented for some Arctic SHVs (Sweetman et al. 2013), which found wide ranges of chemosynthetic organic matter contribution to different taxa but generally, the lack of data (e.g. for trophic discrimination factors) has precluded the use of these tools to quantify trophic interactions and biogeochemical cycling (Phillips et al. 2014, Reid et al. invited review in prep.). In this study, we take advantage of an extensive, multidisciplinary dataset available for the sedimented vent system at Hook Ridge in the Bransfield Strait (62˚S), in the Southern Ocean, which hosts the most southerly known vent field worldwide (Klinkhammer et al. 2001). We designed three linear inverse models (LIMs), one each for two sites along a gradient of variable hydrothermal activity (low activity: Hook Ridge 1 and high activity: Hook Ridge 2) and a non-vent site (Bransfield Off-Vent) to quantify carbon flows in the benthic food web. LIMs are especially suited for environments where repeated or very detailed measurements are not practical (e.g. the deep-sea) and represent a powerful tool to address uncertainty in these settings. A comprehensive dataset was implemented in the LIMs including: organic and inorganic geochemistry (Dählmann et al. 2001, Aquilina et al. 2013, Aquilina et al. 2014, Bell et al. 2016c, Bell et al.

2016d); microbial composition and stable isotopic signatures (Bell et al. 2016c); faunal composition and stable isotopic signatures (Bell et al. 2016c, Bell et al. 2016d); sediment community respiration rates (Woulds et al. in prep.) as well as more general data for the Bransfield Strait and other deep-sea food webs (Wefer et al. 1988, Wefer & Fischer 1991, Masque et al. 2002, Howe et al. 2007, van Oevelen et al. 2011a). Here we apply a LIM approach for two sites of variable hydrothermal activity and one off-vent site to address the following hypotheses that hydrothermal activity: 1) supports in situ production that subsidises the diet of local fauna; 2) creates structural differences between food-web networks and 3) increases faunal trophic diversity.

6.3 Results

6.3.1 Contribution of Chemosynthetic OM to the food web

Chemosynthetic OM constituted 0.2 % (± 0.07) of the net total OM inputs at the off-vent site, compared with 30.6 % (± 7.97) at Hook Ridge 1 (HR1) and 13.8 % (± 1.95) at Hook Ridge 2 (HR2) (Fig. 6.3.1a). The net total OM input to each site ranged between 2.31 – 3.52 mmol C m^{-2} $d^{-1}$and net contribution of in situ chemosynthetic primary production varied substantially between sites (Figure 6.3.1a; Table 6.3.1a). Other OM inputs were direct POC deposition and inputs from suspension feeders. The models suggested that at the off-vent site, direct POC deposition was significantly higher than at either Hook Ridge 1 or 2 (Table 6.3.1a) (97.4 and 97.5 % of BOV solutions greater than Hook Ridge 1 & 2 respectively). Net suspension feeding was highest at Hook Ridge 2 (Table 6.3.1a) and was the only site where suspension feeding represented the dominant input of OM. POC deposition was the dominant mode of OM delivery at BOV and HR1.

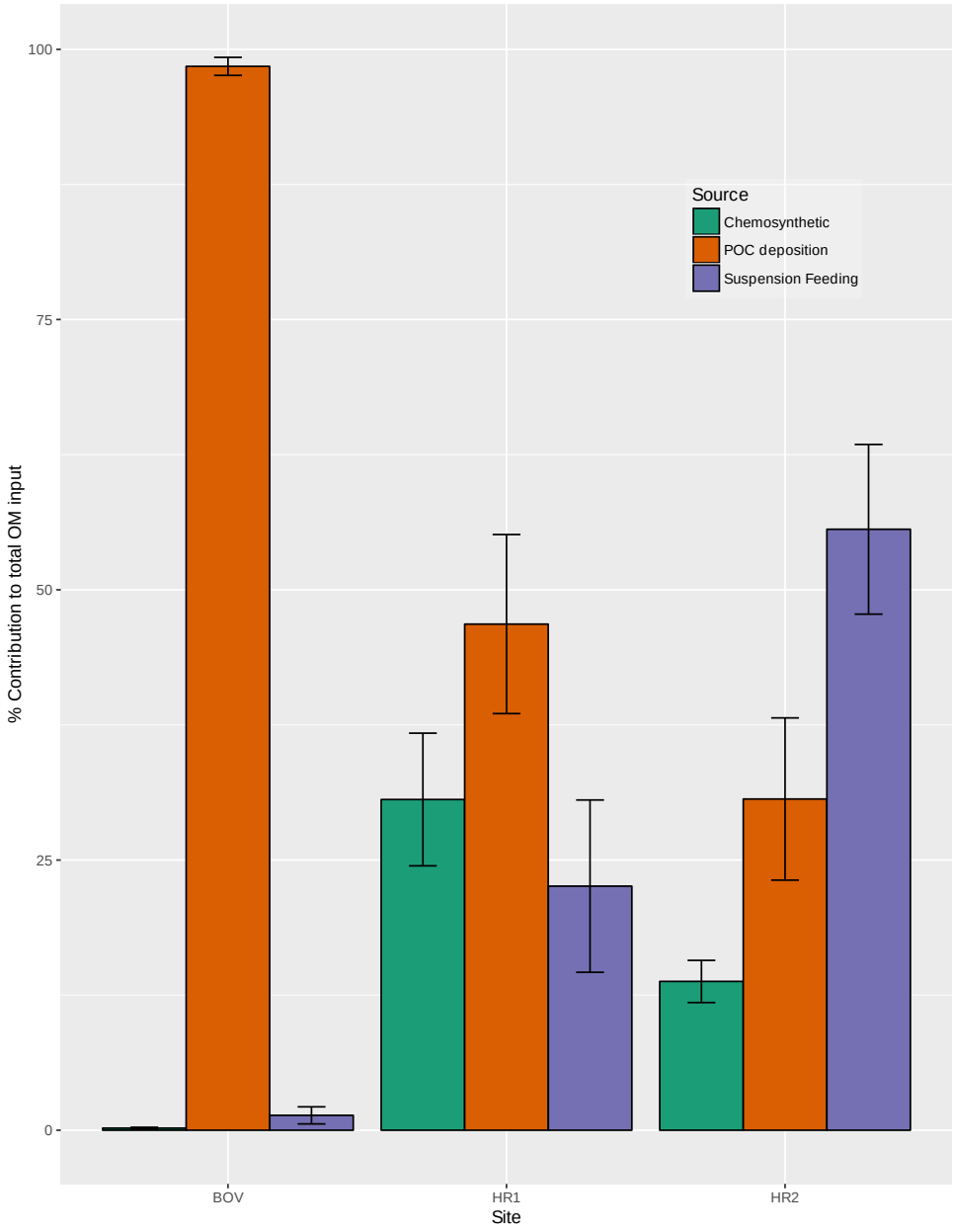

Fig. 6.3.1a – Percentage contribution of OM inputs at each site (± 1 S.D.).

Variable	Carbon flux (mmol C m^{-2} d^{-1} ± S.D.)		
	BOV	HR1	HR2
Inputs			
POC deposition	2.43 (± 0.57)	1.09 (± 0.26)	1.08 (± 0.27)
Net Suspension Feeding	0.03 (± < 0.01)	0.53 (± 0.22)	1.96 (± 0.33)
Net Chemosynthesis	< 0.01 (± < 0.01)	0.70 (± 0.12)	0.48 (± 0.05)
Net Total OM Input	2.46 (± 0.57)	2.31 (± 0.30)	3.52 (± 0.20)
Gross Total OM Input	2.72 (± 0.54)	3.72 (± 0.30)	4.77 (± 0.20)
Internal C Processing			
Faunal Detritus Production	4.02 (± 0.96)	3.54 (± 0.57)	3.08 (± 0.20)
Total C Respiration	2.21 (± 0.48)	2.71 (± 0.14)	2.82 (± 0.04)
Outputs			
Burial of Organic C	0.05 (± 0.01)	0.08 (± 0.02)	0.10 (± 0.03)
DOC Efflux	0.11 (± 0.07)	0.14 (± 0.08)	0.15 (± 0.08)
External Predation	0.33 (± 0.09)	0.79 (± 0.23)	1.70 (± 0.17)

Table 6.3.1a. – Selected variables from each model (mean ± 95 % confidence intervals). Net fluxes are corrected for relevant constraints (e.g. respiration or uptake efficiency), which also accounts for HR1 where total respiration is higher than the net OM inputs (because OM inputs are already adjusted for bacterial and metazoan respiration).

Respiration was the dominant fate of organic carbon in each model (Table 6.3.1a), accounting for 59.0 – 81.7 % of total OM input at each site, though there were clear differences in the proportion accounted for by each compartment. Mean total respiration was slightly higher at the vent sites than at the off-vent site (Table 6.3.1a; Figure 6.3.1b). Heterotrophic bacterial respiration accounted for 89.2 % of the total at the off-vent site but only 49.6 – 66.7 % at the vent sites. Macrofaunal respiration accounted for 30.1 and 41.8 % of total respiration at HR1 and HR2

respectively, compared with 10.4 % at the off-vent site. Megafaunal respiratory demands were comparatively limited (0.4 – 8.6 % of total at each site). Respiration represented a loss of C from the system as DIC but 39.6 – 74.1 % of this was recycled as in situ production at the vent sites. Detritus production (by all microbial and faunal compartments) exceeded total input of allochthonous POC (direct input plus net suspension feeding) at both BOV and HR1 (pairwise comparisons: > 99.9 % of solutions greater for detritus production) but at HR2, faunal recycling rates were comparable to POC input (Table 6.3.1a) (Means 3.07 and 3.04 mmol C m^{-2} d^{-1} respectively).

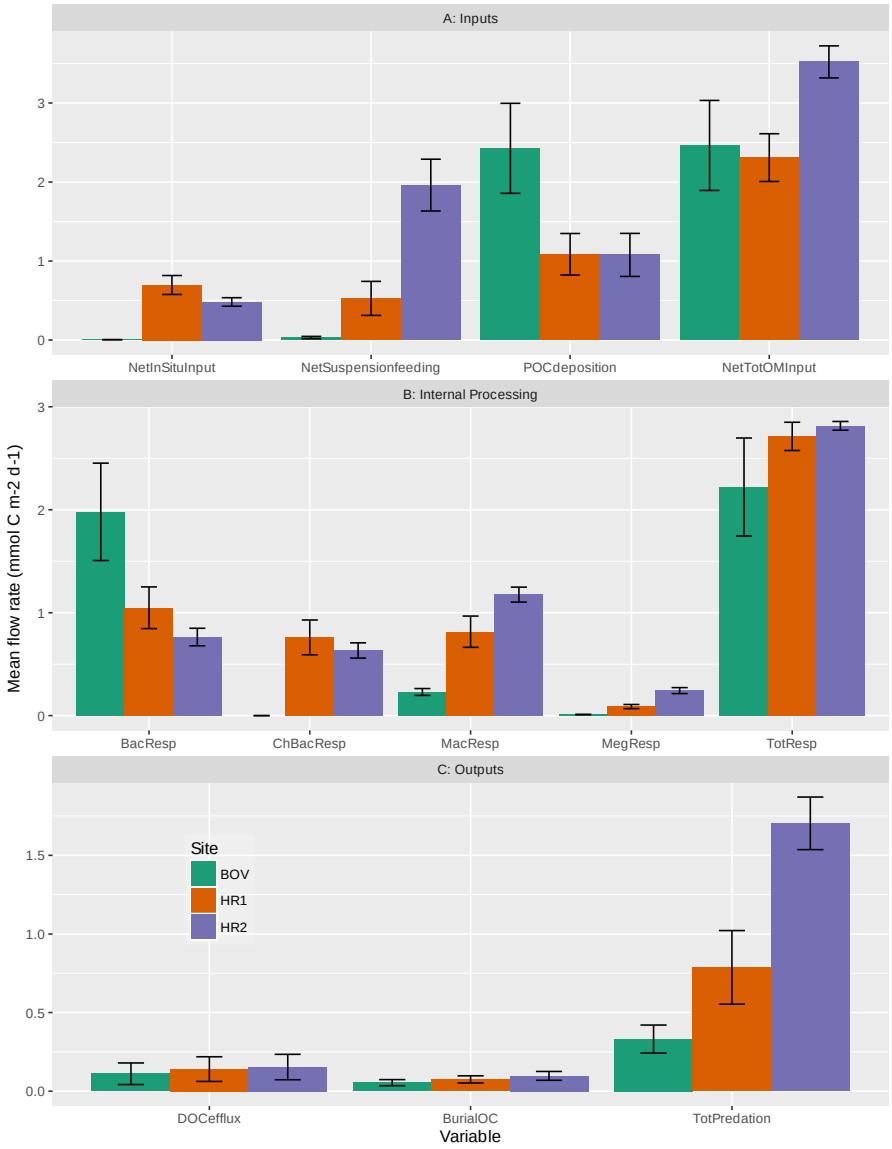

Fig. 6.3.1b – Comparison of selected variables of external and internal cycling values (± 1 s.d.)

Several compartments had their dietary composition fixed by the model structure (e.g. Endosymbiont-bearing siboglinids could only receive organic matter via in situ chemosynthetic OM fixation owing to their lack of feeding organs) but others were able to vary their diet according to isotopic variability and stock size. Diet composition varied between sites particularly for predators/ scavengers (Figure 6.3.1c) (Chi-sq: $\chi^2 = 172.77$; $p < 0.001$). Deposit feeder diet was generally dominated by detritus (35.6 – 100 %; Figure 6.3.1c) but also included heterotrophic and chemosynthetic bacterial carbon in varying amounts (0 – 62.0 % and 0 – 20.2 % respectively). Predator/ scavenging (MacPS) faunal diet composition was the most different between sites and included significant proportions of bacterial carbon (9.1 – 89.3 % of diet; Figure 6.3.1c), overlapping with deposit feeder diets, particularly at BOV. Predator/ scavenger diet at the vent sites was dominated by predation upon macrofaunal deposit feeders (41.7 and 63.9 % of diet at HR1 and HR2 respectively), but was also comprised of significant amounts of other sources (e.g. MacES at HR1; 20.5 % of diet or MacSF at HR2; 27.0 % of diet; Figure 6.3.1c). Predator/ scavengers at Hook Ridge 1 had the greatest trophic diversity and did not seem to be as dependent upon a single source to the same extent as at other sites. This suggests that trophic diversity amongst higher trophic level fauna at SHVs may be highest at intermediate levels of hydrothermal activity.

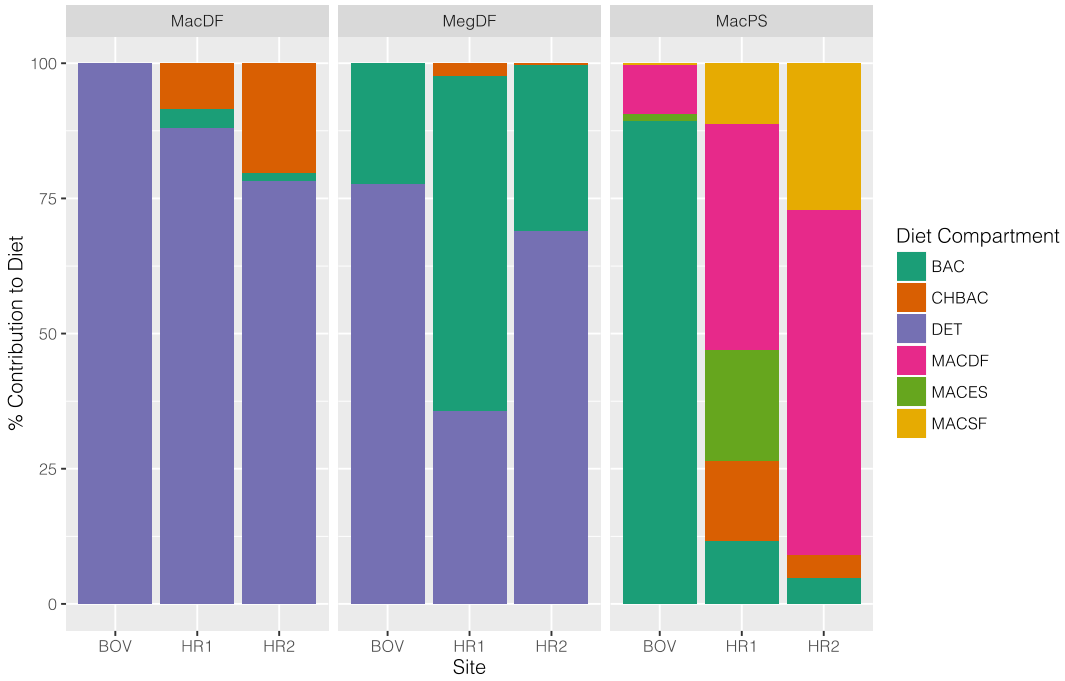

Fig. 6.3.1c – Percentage diet composition of deposit feeders and predators/ scavengers at each site, along a gradient of hydrothermal activity.

DOC efflux and organic carbon burial rates were broadly similar between all sites and the major C loss (other than respiration) was external predation by motile megafaunal predators (e.g. fish) that were not included within the model. Mean external predation rates were highest at HR2 and lowest at BOV (Table 6.3.1a) and were significantly different between all sites (pairwise comparisons all > 98 % of solutions greater in one model).

6.3.2 Food Web Structure

Mean food web structures were different between each site, both in terms of the dominant flows and also the overall structure of the network (Figure 6.3.2a). Some of these differences were owing to changes in stock sizes of individual functional groups between sites (e.g. MacES absent from HR2), meaning that some flows were absent or differed in magnitude. Bacterial respiration was the dominant biological process (1.98 mmol C m^{-2} d^{-1} ± 0.47) at the non-hydrothermally influenced site (BOV) and, whilst it was still an active flow at HR1 and HR2 (1.05 mmol C m^{-2} d^{-1} ±

0.20 and 0.76 mmol C m^{-2} d^{-1} ± < 0.09 respectively), other flow magnitudes were greater (e.g. macrofaunal deposit feeding at HR1 = 1.92 mmol C m^{-2} d^{-1} ± 0.51 or macrofaunal suspension feeding at HR2 = 2.57 mmol C m^{-2} d^{-1} ± 0.36).

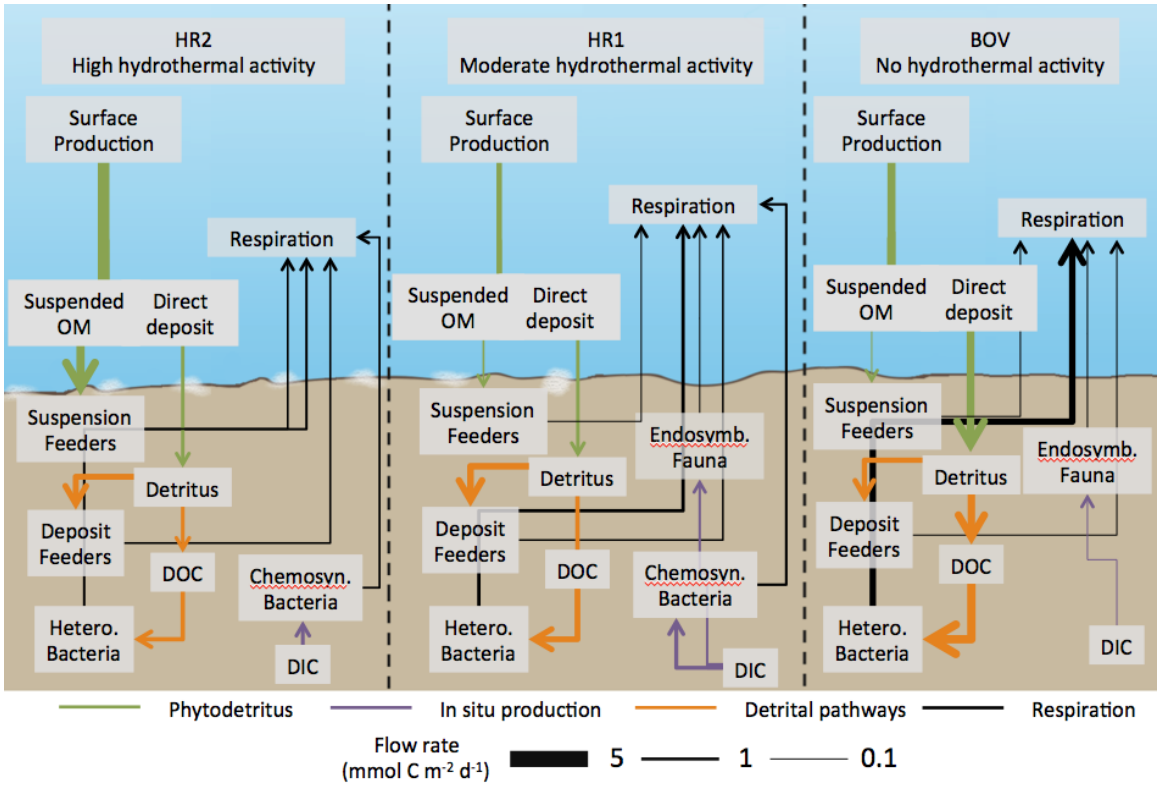

Fig. 6.3.2a – Selected mean carbon flows between food web compartments at each site. White patches = bacterial mat. See supplement 6-4 for full details of exchanges between compartments

6.3.3 Network Indices

Mean total system throughflow (TST) was greater at the vent sites (12.70 – 13.03 mmol C m^{-2} d^{-1}, compared with 11.56 mmol C m^{-2} d^{-1} at BOV) but the non-vent site had a higher proportion of recycled flows (Corrected Finn Cycling Index = 0.20 ± 0.06), as compared to HR1 and HR2 (0.19 ± 0.04 and 0.10 ± 0.01 respectively). BOV was the most strongly internally structured network (compartmentalisation index 0.33) though differences were generally small between all three sites (HR1: 0.32 & HR2: 0.30), indicating that the network was marginally more partitioned at the off-vent site. Average Mutual Information (AMI), a measure the amount of constraint upon each flow, was lowest at the off-vent site (1.91 ± 0.06) and highest at HR1

(2.00 ± 0.03), suggesting that at the off-vent site, despite the higher degree of compartmentalisation, exchanges between compartments were more flexible.

6.4 Discussion

Our study provides the first quantitative estimate of the contribution of chemosynthetic OM to the food web along a gradient of hydrothermal activity at SHVs. Predictions of the contribution of chemosynthetic OM are most consistent with the stock sizes of chemosynthetic primary producers at each site, ranging from 0.2 – 30.6 % of net total OM inputs. This highlights the importance of chemosymbiotic metazoa in mediating carbon flows at hydrothermal vents and clearly demonstrates that variability over several spatial scales can result in significant differences in the importance of various OM sources. At Hook Ridge 1, where chemosynthetic production represented 30.6 % of the total OM inputs, this resource was widely utilised. This was due to the increased availability as well as the wider diversity of the sources. Chemosynthetic bacterial mat was available at both Hook Ridge sites but at HR1, the vent-endemic *Sclerolinum contortum* provided an additional means to route in situ production directly into metazoan biomass, thus providing trophic support to predatory/scavenging fauna that may not otherwise have been able to feed directly upon locally produced OM. Thus, it is clear that symbiont-hosting megafauna can provide an important means towards integrating chemosynthetic production into the wider food web, and subsidising the diet of non-specialist fauna. *Sclerolinum* was also highly patchy, even (qualitatively) within replicate drops (cores spaced up to ~50 cm apart), meaning that contribution of chemosynthetic OM was likely similarly patchy. This has clear relevance to trophodynamics in other marine chemosynthetic ecosystems and suggests that patch-scale abundance of endosymbiont-bearing fauna is likely to considerably influence the transfer of chemosynthetic carbon into seafloor food webs (Figure 6.4a).

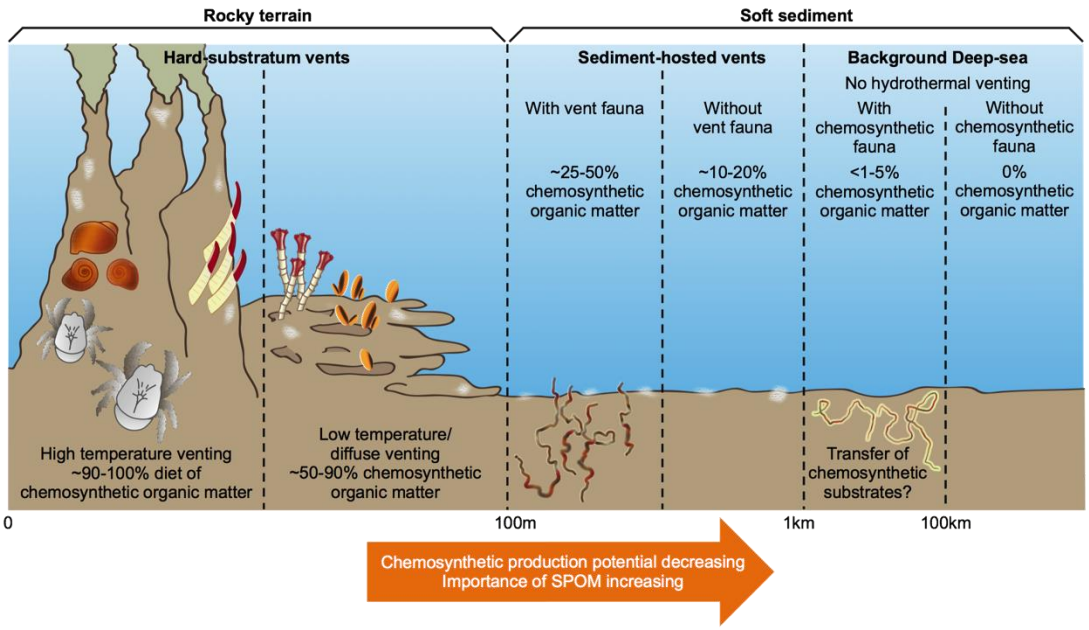

Fig. 6.4a – Differences in the contribution of chemosynthetic organic matter to different hydrothermal vent types, with representative taxa included for reference. SPOM = Surface-derived Particulate Organic Matter. White patches = bacterial mats

At the off-vent site, net chemosynthetic production was very low (< 0.01 mmol C m^{-2} d^{-1}), owing to the small population sizes (64 – 159 ind. m^2) of endosymbiont-bearing fauna (*Siboglinum* sp.) at these sites (Bell et al. 2016d). Chemosynthetic OM contributed the largest proportion of total OM inputs at Hook Ridge 1 (Figure 6.3.1a), a site where dense (but patchy) populations of vent endemic species (*Sclerolinum contortum*) were observed that fix inorganic carbon into organic matter in situ (Georgieva et al. 2015, Bell et al. 2016c, Bell et al. 2016d). At Hook Ridge 2, chemosynthetic OM contribution was lower (13.8 %), owing in part to the absence of populations of *Sclerolinum* sp. at this site. Chemosynthetic bacterial production was broadly similar at the vent sites (HR1: 0.50 ± 0.11 and HR2: 0.48 ± 0.05 mmol C m^{-2} d^{-1}). Bacterial biomass at Hook Ridge 1 was also much higher than in non-vent areas (Bell et al. 2016c), indicating greater potential for bacterial activity at the vent sites. Bacterial biomass however is not necessarily a good proxy of activity, since bacterial populations can be relatively dormant and so biomass specific metabolic rates were not implemented in the model (van Oevelen et al. 2006a, van Oevelen et al. 2009).

Total OM input (chemosynthetic and surface-derived OM) was highest at HR2 (Figure 6.3.1a) but the model results also indicated that direct POC deposition was highest at the off-vent site (Figure 6.3.2a). Available estimates of OM export from the surface ocean in the Bransfield Strait vary widely (0.7 – 27.1 mmol C m^{-2} d^{-1}) (Wefer et al. 1988, Masque et al. 2002, Howe et al. 2007) and so the model predictions are comparatively consistent between sites. These estimates are likely to represent a time-averaged signal as it is based on the amount of surface-derived OM required to support the observed stock sizes, which is likely to turn over at a lower rate to the natural variability in POC deposition. POC flux at the vent sites was similar but only ~45 % of that of the off-vent site. The spatial separation between sites is likely too small (~100 km between BOV and Hook Ridge) to account for these differences in direct POC flux. At the vent sites however, more surface-derived organic carbon was routed (rather than as direct POC deposition) through suspension feeding fauna, particularly at HR2. The off-vent site by comparison had a very small contribution of suspension feeding OM input, as these taxa were largely absent at this site. If direct POC deposition was genuinely different between sites, a possible reason was that BOV, being situated towards the base of a continental slope, could have received additional input from material sliding down the basin margin. The vent sites were elevated above the surrounding seafloor so were less likely to receive additional OM inputs in this way (Bell et al. 2016d). It is also possible that the location of the vent sites on a mid-basin ridge, and the input of hydrothermal fluid, could have created local scale hydrodynamic conditions that influenced POC deposition rates. Differences in hydrodynamic regime between the basin axis and margins may also explain the relatively high abundance of suspension feeding fauna at HR2 (Bell et al. 2016d).

Despite a lower overall faunal biomass at vent sites, particularly Hook Ridge 2 (Bell et al. 2016c, Bell et al. 2016d), these sites had higher mean total respiration than the off-vent site (Figure 6.3.2a). These differences were predominately a result of differences in temperature between sites (highest at Hook Ridge 2 ~48°C (Dählmann et al. 2001), compared with ~-1°C at the off-vent site), meaning that total respiration was higher and faunal compartments accounted for a greater proportion of total respiration. Total respiration was also higher, that total OM inputs at HR2,

which we attribute to increased bacterial activity and an elevated significance of the role of OM recycling in the hydrothermal sites, relative to the off-vent site. We note that meiofaunal assemblages would likely have contributed to some of the observed differences in SCOC and so the models probably over-estimated bacterial, macro- and megafaunal respiration rates. LIM models from the Hausgarten Observatory (2500m depth, Arctic Ocean ~79°N, ~7°E) (van Oevelen et al. 2011a) indicated that meiofaunal respiration accounted for approximately 0.68 % of total respiration, hence it is unlikely that meiofaunal respiration was sufficient to explain differences between sites. Respiration rates at Hausgarten were dominated by microbial activity (93 %) (van Oevelen et al. 2011a), similar to the off-vent site, where bacterial respiration accounted from 89.2 % of mean total respiration (Table 6.3.1a). This provides strong independent confirmation that the models presented here are behaving consistently with previous applications of this framework in other deep-sea ecosystems. Total bacterial respiration (heterotrophic and chemoautotrophic) rates were 1.98 (± 0.47), 1.81 (± 0.19) and 1.40 (± 0.08) mmol C m^{-2} d^{-1} at BOV, HR1 and HR2 respectively, despite the higher bacterial biomass at the vent sites. Bacterial respiration accounted for just 66.7 and 49.6 % at HR1 and HR2 respectively, with faunal respiration accounting for 30.0 – 41.8 % of total respiration at the vent sites, compared with just 10.4 % at BOV. Bacterial respiration and OM recycling are usually very dominant processes in non-hydrothermally influenced seafloor ecosystems (van Oevelen et al. 2011a, van Oevelen et al. 2012), often with little transfer of OM to metazoa (Pozzato et al. 2013) but these models demonstrate that this can be quickly overturned in higher energy systems in the deep-sea.

Network analyses indicated that the proportion of flows that were cycled within the food web was highest at the non-vent site (cFCI = 0.20), despite this site having the most compartmentalised network with the fewest links. Network compartmentalisation provides a means to investigate the extent to which in situ production was incorporated into the wider food web and was lowest at the most active vent site (HR2). This suggests that chemosynthetic carbon was generally well assimilated into the wider food web (rather than representing a spatially concurrent, yet isolated, set of trophic interactions). It also implies that the vent sites were generally more likely to be inhabited by more opportunistic fauna, with

the off-vent site, being more stable, being inhabited by fauna with more finely partitioned niches. This corresponds to cycling efficiency, which declined with increasing hydrothermal activity, to 0.10 at HR2. The increase in temperature associated with higher hydrothermal advection caused an increase in bacterial and faunal respiration, and thus likely contributed to these differences in carbon cycling efficiency. It is also possible that the lower diversity at the most active vent sites meant that the food web was less efficient at processing the inputs of organic matter or that chemosynthetic OM was less efficiently recycled. Burial rates of organic carbon were higher at the vent sites but were not significantly different between sites (pairwise comparisons 11.6 – 27.8 % smaller in one site), meaning that the differences in processing efficiency are most likely to be attributable to respiration differences.

Particularly in predatory/ scavenging fauna (the group that had the most trophic resources available), the impact of hydrothermal activity elicited considerable differences in diet (Figure 6.3.1c). At the off-vent site, predators predominately consumed bacteria and deposit feeders but also included a small contribution from endosymbiont-bearing fauna (1.5 %). This is consistent with more detailed stable isotopic observations of a peracarid taxa (Neotanaidae) at this site, which had notably depleted carbon isotopic signatures, consistent with consumption of the methanotrophic *Siboglinum* sp. (Bell et al. 2016c). Additionally, many of the predatory polychaete fauna were small syllid polychaetes, which have been suggested to exhibit bacterivory (Levin et al. 2009, Bell et al. 2016b, Bell et al. 2016d). However, the values associated with flow from bacterial carbon to predator/ scavengers at the off-vent site had relatively high variability (0.20 mmol C m^{-2} d^{-1} ± 0.09), so these estimates should be treated with some caution. Predator/ scavengers at Hook Ridge 1 had the most trophically diverse diet and this in part is reflects the number of resources available (HR1 was the only site to include both chemosynthetic bacteria and endosymbiont-bearing fauna, as well as other macrofaunal functional groups). This contrasted with community bulk stable isotopic data (Bell et al. 2016c), where isotopic niche area (analogous to trophic diversity) was lower at the vent sites. This was likely a product of differences in observational techniques but also the larger differences in carbon isotopic

signatures of sources at the non-vent sites. Deposit feeders were the main source of food for predator/ scavengers at both vent sites (41.7 – 63.9 %, Figure 6.3.1c) and differences in the remainder of diet were generally consistent with stock sizes at each site (e.g. greater density of suspension feeders at HR2). Though we did not explicitly investigate predator trophic position, it is likely that the increased consumption of macrofaunal sources at vent sites would have resulted in a higher trophic position for predator/scavengers than at the off-vent site. This distinction is not clear from the bulk stable isotopic data (Bell et al. 2016c), perhaps because of confounding factors such as different nitrogen isotopic baselines between sites, preservation effects and unknown variability in trophic fractionation (Reid et al. invited review in prep.) that can complicate interpretation of trophodynamics at hydrothermal vents. It should also be noted that deep-sea hydrothermal sediments are highly heterogeneous on scales of 10s of cm, and that the importance of hydrothermal OM to diet, particularly for the more sessile individuals, will likely have varied substantially over similar scales. This demonstrates the value of the approach used here, as a means to circumvent the considerable uncertainty associated with food web measurements, particularly for the deep-sea.

The models presented here provide the first quantitative estimates of carbon biogeochemical cycles in deep-sea settings that have a combination of in situ and surface derived organic matter inputs. It remains challenging to use these results for an estimate of the contribution of SHVs to global benthic biogeochemical cycling, because the global extent of individual vent fields is largely unknown, both in the Bransfield Strait and in other systems in the Pacific, such as Middle Valley or Guaymas Basin. Additionally, many hydrothermal vent fields have peripheral areas of hydrothermal sediment (Southward et al. 2001, Levin et al. 2009, Sweetman et al. 2013) of unknown size. Furthermore, vast areas of the global submarine ridge system remain unexplored. However, the large range of settings that could house SHVs indicates that their global extent may be significant. Moreover, our results may also be representative for other sedimented chemosynthetic ecosystems, such as cold seeps or mud volcanoes or even trophic subsidies in shallow water commercial species (Higgs et al. In Press). Cold seeps in particular are widespread in the global ocean (Boetius & Wenzhöfer 2013), suggesting considerable impacts upon benthic

biogeochemical cycling as a result of differences in functional diversity. In situ productivity and hydrothermal input were associated with clear differences in the relative abundance of faunal functional groups (Bell et al. 2016c, Bell et al. 2016d) and carbon processing patterns (e.g. transfer pathways of OM into food web and differences in respiration), raising significant questions about benthic biogeochemical cycling, as it is clear that in terms of carbon cycling, sedimented chemosynthetic ecosystems are very distinct from non-chemosynthetic deep-sea ecosystems. Recent research has shown that animal distribution is strongly partitioned according to species thermal niches (Bates et al. 2010) and here we demonstrate that this has a major concomitant effect upon carbon processing patterns, through the resultant effects upon the distribution of endosymbiont-hosting metazoa (Figure 6.4a). This has important implications for other seafloor chemosynthetic ecosystems, where the transition between non-chemosynthetic areas and areas of high densities of endosymbiont-bearing metazoa can be very patchy (Bernardino et al. 2012). It is virtually impossible to provide a substantiated estimate of the importance of chemosynthetic activity in seafloor sediments without much more extensive data concerning the distribution of SHVs and the spatial extent of hydrothermal influence (Levin et al. 2016). This is a clear gap in current knowledge and we suggest that future hydrothermal vent research cruises should consider incorporating wider spatial coverage into their study design, to better capture this within-field variability and gradients of chemosynthetic OM utilisation (Figure 6.4a).

The presence of chemosynthetic production at non-hydrothermally influenced sites raises important questions about the spatial scales over which hydrothermal vents (or other seafloor chemosynthetic ecosystems) contribute to energy flows within ecosystems (Levin et al. 2016). Although the contribution was very small at the off-vent site (0.2 %), populations of *Siboglinum* sp. were much wider spread than populations of *Sclerolinum contortum* at Hook Ridge (Bell et al. 2016c, Bell et al. 2016d). In the Bransfield Strait, *Siboglinum* sp. was found at all non-Hook Ridge sites (Bell et al. 2016c). Although these fauna generally occurred at low densities (25 – 135 ind. m^2, compared with 32 – 4520 ind. m^2 of *Sclerolinum contortum* at Hook Ridge (Bell et al. 2016d)), their greater spatial extent could have resulted in

comparable levels of total contribution of chemosynthetic carbon to the benthic food web across the Bransfield Strait. *Siboglinum* is a globally distributed genus and these results suggest that it, and other similar taxa, may have far greater impacts upon benthic food webs throughout the deep-ocean than previously recognised. However, it is not clear from the isotopic data from which source the requisite methane (i.e. thermo- or biogenic) was supplied so implicating hydrothermal activity in this suggestion may be unsubstantiated at this time.

6.5 Conclusions

We have developed the first quantitative ecosystem model of seafloor chemosynthetic ecosystems and show that the partitioning and processing of organic matter within the sediment is strongly influenced by the production and availability of chemosynthetic OM. We suggest that vent-endemic fauna are highly important for mediating transfer of local production into the food web, particularly for predatory or scavenging fauna. Contribution of chemosynthetic carbon was much more strongly influenced by the thermal niche of metazoan primary producers (not found at the more active site) than the levels of hydrothermal input and can vary substantially within vent fields. We also show that sediment hydrothermal vents make chemosynthetic carbon much more widely available than previous recognised and suggest that it may have very significant capacity to influence benthic food webs at large scales, even in areas that are very distant from a vent field.

6.6 Materials and Methods

6.6.1 Study Site

The Bransfield Strait is a slow spreading basin (max. depth ~1900 m) located between the West Antarctic Peninsula and the South Shetland Islands (~62˚20 S, 57˚00 W). Along the basin axis there are three raised volcanic edifices (~1000 – 1300 m depth) and at one of these, Hook Ridge, hydrothermal activity and chemosynthetic communities have been observed, making this the most southerly

hydrothermal vent site currently known (Klinkhammer et al. 2001, Sahling et al. 2005, Aquilina et al. 2013, Bell et al. 2016d). The sites studied here are at roughly the same depth to eliminate depth as factor from our analysis (Table 6.6.1a) Hook Ridge 1 was less hydrothermally active than Hook Ridge 2 (hydrothermal advection 9 and 34 cm yr^{-1} respectively) but had greater porewater sulphide (Aquilina et al. 2013). At Hook Ridge 1 there were populations of an endosymbiont-bearing siboglinid tubeworm *Sclerolinum contortum* (Georgieva et al. 2015, Bell et al. 2016c, Bell et al. 2016d). Bacterial mats were widespread at both sites but patchy (Aquilina et al. 2013), indicating that the flux of sulphide (and other chemosynthetic substrates) to the sediment-water interface was probably similarly patchy. The off-vent site, and others around the Bransfield Strait, received inputs of thermogenic methane that supported small populations of a different endosymbiont-bearing siboglinid species (*Siboglinum* sp.) (Whiticar & Suess 1990, Bell et al. 2016c, Bell et al. 2016d).

Site	Depth (m)	Hydrothermally active?	Approx. Temp. (°C)	Chemosynthetic macrofauna?	Chemosynthetic Substrates
Off-Vent (BOV)	1150	No	-1	*Siboglinum* sp.	CH_4
Hook Ridge 1 (HR1)	1174	Yes (9 cm yr^{-1}) Low activity	24	*Sclerolinum contortum*	H_2S, CH_4
Hook Ridge 2 (HR2)	1054	Yes (34 cm yr^{-1}) High Activity	48	No	H_2S, CH_4

Table 6.6.1a. Description of sites (Dählmann et al. 2001, Aquilina et al. 2013, Aquilina et al. 2014, Georgieva et al. 2015, Bell et al. 2016c, Bell et al. 2016d).

6.6.2 Megafauna

Macrofaunal, microbial and geochemical data specific to these sites are published in separate papers (Aquilina et al. 2013, Aquilina et al. 2014, Bell et al. 2016c, Bell et al. 2016d). As the methodology for collecting megafaunal assemblage data has not been published yet, it is given here. Seafloor images were collected during Seabed High-Resolution Imaging Platform (SHRIMP) tows conducted during RRS *James Cook* cruise 55 (JC55) (Tyler et al. 2011). These images were extracted from video footage at a rate of 1 per 10 seconds and analysed for megafaunal abundance in ImageJ (Rasband 2013). A subset of suitable non-overlapping images were selected (Bell et al. 2016a) from two areas of Hook Ridge, close to megacore deployment positions (Bell et al. 2016c, Bell et al. 2016d), totaling a minimum of 150 m^2 of seafloor imagery per site. There was no SHRIMP tow for the control site on JC55, so density was estimated from measurements at another non-vent site (the Three Sisters), which had comparable macrofaunal composition and density, and sediment organic carbon content (Bell et al. 2016d). Each image was scaled using the SHRIMP parallel lasers (10 cm apart) and the abundance and areal extent of the fauna; the vast majority being ophiuroids (cf. *Ophionotus* sp. & *Opioperla* sp.) and holothurians (cf. *Peniagone* sp.), were measured to give density and area per m^2. Biomass was calculated using fixed relationships between area and dry weight for each group, measured from Agassiz trawl samples collected from Hook Ridge (Tyler et al. 2011).

6.6.3 Model Structure and Data Availability

The food web model underlying the LIM was set up as a number of compartments (e.g. detritus, macrofaunal endosymbiont-bearing fauna, megafaunal deposit feeders) and each was connected to other compartments by a number of flows (van Oevelen et al. 2006b, van Oevelen et al. 2011a, van Oevelen et al. 2012) that reflected their feeding mode(s) and production of detritus or DOC. Compartment biomass was given as the sum of the average carbon masses per taxa, multiplied by density per square metre, using data for dry mass and percentage carbon of faunal tissue collected during preparation and analysis of stable isotopic samples (Bell et al. 2016c). Carbon stable isotopic data were averaged for each compartment (Bell et al.

2016c) and used to constrain possible diet composition. By imposing a number of constraints using available data (e.g. biomass or respiration; Table 6.6.3b), the magnitude of every flow is constrained to a finite and ecologically feasible range of possible values. In addition to the explicit constraints, data provided for each component for biomass and respiration provided implicit constraints upon the magnitude of flows in and out of a given stock (Table 6.6.3a). External compartments were in some instances given a range of possible values (e.g. POC flux) but others were constrained only by processes occurring between internal compartments (e.g. external predation). The resultant models were used to create large numbers of independently valid solutions, from which the mean and error distribution of each of the unknown flows were calculated (van Oevelen et al. 2009).

Compartment	Code	Depth (bsf)	References (Rates & Stocks)
Internal (exchanges between these compartments determined by permissible flows)			
Detritus	Det	0 – 10 cm	(Aquilina et al. 2013, Bell et al. 2016c, Bell et al. 2016d)
Dissolved Organic Carbon	DOC	0 – 10 cm	Stock size not defined a-priori, assumed non-limiting
Heterotrophic Bacteria	Bac	0 – 1 cm	(Bell et al. 2016c)
Chemosynthetic Bacteria	ChBac	0 – 1 cm	(Bell et al. 2016c)
Macrofauna with Endosymbionts	MacES	0 – 10 cm	(Bell et al. 2016c, Bell et al. 2016d)
Macrofaunal Deposit Feeders	MacDF	0 – 10 cm	(Bell et al. 2016c, Bell et al. 2016d)
Macrofaunal Suspension Feeders	MacSF	0 – 10 cm	(Bell et al. 2016c, Bell et al. 2016d)

Macrofaunal Predators/ Scavengers	MacPS	0 – 10 cm	(Bell et al. 2016c, Bell et al. 2016d)
Megafaunal Deposit Feeders	MegDF	0 cm	This study
Megafaunal Suspension Feeders	MegSF	0 cm	This study
External (inputs to and losses from internal compartments)			
Buried Detritus	Det_s	> 10 cm	(Dunne et al. 2007)
Megafaunal Predation	Predation	Above sediment surface	Loss only, rate not directly constrained a-priori
Biomass specific Respiration + Maintenance Respiration	Respiration	0 – 10 cm	(Mahaut et al. 1995, Bell et al. 2016d)
Dissolved Inorganic Carbon	DIC	Not relevant	Stock size not defined a-priori, assumed non-limiting
Dissolved Organic Carbon in the water column	DOC_w	Above sediment surface	Loss only, rate proportional to total respiration (Burdige et al. 1999)
Particulate flux of detritus from the water column	Det_w	Above sediment surface	(Wefer et al. 1988, Wefer & Fischer 1991, Masque et al. 2002, Howe et al. 2007, Bell et al. 2016c)

Table 6.6.3a. Compartments used in the models. For compartments where stocks/ rates were not defined in the model set up there were no available data (e.g. DIC). Therefore, flows in and out of these compartments were only indirectly determined by constraints upon other compartments. Detritus is termed as any non-living organic material including faecal material, dead bacterial or metazoan tissue and

extra polymeric substances like mucus. No data were available to discriminate lability of detrital OM.

Where site specific data were not available, we used constraints (e.g. bacterial growth efficiency) that encompassed a typical range from a wider variety of studies to constrain the flows in the network that encompass a typical range from a wider variety of studies (Table 6.6.3b). This approach is consistent with previous implementations of this modelling framework in the deep-sea, where such data are rarely available for specific environments (van Oevelen et al. 2011a, van Oevelen et al. 2011b, van Oevelen et al. 2012). Bacterial growth efficiency was estimated using a range of values from other deep-sea systems (van Oevelen et al., 2011b; 2012) but the range of possible values was the same for vent and non-vent sites. Bacterial biomass was estimated for the more active vent site (HR2) from isotopically labeled samples (Woulds et al. in prep.), since comparable natural PLFA data were not available (Bell et al. 2016c). At other sites, natural bacterial biomass was 45 – 60 % of that measured in pulse-chase experiments and we used an estimate, based on bacterial biomass from labeled samples collected at HR2 (Bell et al. 2016c, Woulds et al. in prep.).

Constraint	Unit	Value	Ref.
Deposition of Organic Carbon	mmol C m^{-2} d^{-1}	[0.70, 27.17]	(Wefer et al. 1988, Wefer & Fischer 1991, Masque et al. 2002, Howe et al. 2007)
Total Sediment Community Oxygen Consumption	mmol C m^{-2} d^{-1}	[0.81, 2.86][a] [1.62, 2.86][b, c]	(Woulds et al. in prep.)
Relative DOC efflux	-	[0, 0.1]	(Burdige et al. 1999)
Q10	-	2	(Childress et al. 1990, Isaksen & Jørgensen 1996, van Oevelen et al. 2006a)

Temperature limits = $Q10^{((Temp°C-20)/10)}$	-	0.20[a][-1°C], 1.30[b] [24°C], 7.00[c] [48°C]	(Dählmann et al. 2001, van Oevelen et al. 2011a)
Burial efficiency of Organic C	-	[0.01, 0.03]	(Dunne et al. 2007)
Bacterial Growth Efficiency	-	[0.05, 0.45]	(del Giorgio & Cole 1998)
Viral lysis of Bacteria (fraction of bacterial production)	-	[0.30, 0.80]	(Fischer et al. 2003, Mei & Danovaro 2004, van Oevelen et al. 2006b)
Efficiency of Chemosynthetic OM fixation	-	[0.10, 0.50]	(Sorokin 1972, Howarth 1984, Dale et al. 2010)
Macrofaunal Growth	-	[Tlim*0.01, Tlim*0.05]	(van Oevelen et al. 2006b)
Macrofaunal Net Growth Efficiency	-	[0.30, 0.70]	(van Oevelen et al. 2006b)
Macrofaunal Assimilation Efficiency	-	[0.20, 0.75]	(van Oevelen et al. 2006b)
Macrofaunal Faecal Production	-	[0.25, 0.80]	(van Oevelen et al. 2006b)
Macrofaunal Maintenance Respiration	mmol C m^{-2} d^{-1}	Tlim*0.01*Biomass	(van Oevelen et al. 2006b)
Macrofaunal Respiration	mmol C m^{-2} d^{-1}	[0.5, 1.5]* Biomass* Biomass-specific respiration*Tlim	(Mahaut et al. 1995, Bell et al. 2016d)
Megafaunal Growth	-	[Tlim*0.0027, Tlim*0.014]	(van Oevelen et al. 2006b)
Megafaunal Net Growth Efficiency	-	[0.50, 0.70]	(van Oevelen et al. 2006b)

Megafaunal Assimilation Efficiency	-	[0.20, 0.75]	(van Oevelen et al. 2006b)
Megafaunal Faecal Production	-	[0.25, 0.80]	(van Oevelen et al. 2006b)
Megafaunal Maintenance Respiration	mmol C m^{-2} d^{-1}	Tlim*0.001*Biomass	(van Oevelen et al. 2006b)
Megafaunal Respiration	mmol C m^{-2} d^{-1}	[0.5, 1.5]* Biomass* Biomass-specific respiration*Tlim	(Mahaut et al. 1995, Bell et al. 2016d)

Table 6.6.3b. Constraints implemented for each model. Parameters contained within [ ] represent minimum and maximum values that encompass uncertainty in the data. Parameters used marked by [a, b] or [c] were used specifically for the off-vent site and the low and high activity vent sites respectively. Faunal respiration was calculated separately for each functional group.

6.6.4 LIM Implementation

Each of these models were implemented into the LIM framework in the R statistical environment (R Core Team 2013) in the package LIM (Soetaert & van Oevelen 2008, van Oevelen et al. 2009) using the data outlined above and a series of equality (a = b) and inequality (a > b) constraints. The model structure (constraints and flows) was the same for each site so the differences observed resulted from differences in biomass, respiration and stable isotopic signatures.

6.6.5 Model Solutions

To determine the number of model iterations required to achieve a representative series of mean flows for each site, we compared the means of several flows between data from a series of model solutions with different numbers of iterations. Each model was sampled for 300, 3 000, 30 000 and 200 000 iterations to compare

change in mean and standard deviation with increasing replication for a subset of flows of varying magnitude. Each set of solutions was begun from the same set of approximated flow means for both the preliminary tests and the final solutions. The minimum number of solutions required was determined at the point where the mean and standard deviations had converged to within 2 % of the final value given by the most sampled dataset. Most flows were within this range within 1 000 iterations, but some flows that had higher standard deviation required more than 30 000 iterations to converge. The minimum number of iterations required to reach convergence (± 2 %), for all of the 5 flows sampled, was approximately 46 000, 37 000 and 13 000 for the off-vent site and the low and high hydrothermal activity sites respectively. In the final set of model outcomes presented here, we used approximately double the greatest number of iterations required (BOV Flow 6 – Macrofaunal deposit feeders to detritus). Thus the final set of solutions consisted of 100 000 iterations for each of the three models from which means and standard deviations for each flow were calculated (van Oevelen et al. 2009). The reason for using this likelihood approach (van Oevelen et al. 2009, van Oevelen et al. 2011a) is that the fitted LIM still had an infinitely large number of possible solutions, each one corresponding to an independently valid solution (individual flow values are not necessarily exchangeable between solutions).

We calculated network summary statistics for each of the model solutions using the R package 'NetIndices' (Allesina & Ulanowicz 2004, Latham 2006, Kones et al. 2009, van Oevelen et al. 2011b, De Smet et al. 2016). These indices were calculated to compare network structure (i.e. the degree of compartmentalisation, number of links or average mutual information) and the proportion of flows that were recycled (Finn cycling index) at each site. Average Mutual Information (AMI) measures the average constraint upon a each flow and tends towards lower values in more mature ecosystems (Latham 2006)

Since this approach results in a large solution set ($n = 10^5$), conventional comparison tests were highly sensitive to very small differences between variables. Several results had very high significance values but with negligible effect sizes (Cohen's D), such as differences in POC deposition (pairwise Wilcoxon test between HR1 and

HR2: $p < 2 \times 10^{-16}$, Cohen's D estimate = 0.03) (Cohen 1992). Data were also not normally distributed and had unequal variance between models. Therefore, we compared variables by calculating the fraction of solutions from a particular solution set that were larger than either of the other two. We define differences where > 95 % of solutions from one solution were greater than another as being significant and > 98 % as being highly significant (van Oevelen et al. 2011b).

6.6.6 Model Solutions and Error Distribution

The quality of the final model solution sets was evaluated using the coefficient of variation (CoV, standard deviation divided by mean) for each flow. CoV provides a simple indication of residual uncertainty within the solution space and flows with a CoV of 1 or more (i.e. standard deviation equals or exceeds the mean) can be considered as still having considerable uncertainty. Mean CoV across all flows for BOV (31 flows), HR1 (38 flows) and HR2 (37 flows) was 0.41, 0.44 and 0.29 respectively, indicating that error distribution each of the models was generally quite low. Maximum CoV values were 0.70, 0.90 and 0.95 respectively but 60.5 – 80.4 % of flows had CoV values of < 0.5 and 10.5 – 51.4 % of flows have CoV values of < 0.2, demonstrating that the majority of values had quite small errors, relative to their means.

6.6.7 Model limitations

Despite a large dataset, data for some compartments used in some other LIM studies (e.g. van Oevelen et al. 2011a) were not available. Meiofaunal data were lacking entirely and as such were excluded from the model. Transfers between bacteria and metazoa were mediated by meiofaunal activity to some degree but we could not explicitly investigate this activity. Detailed data on the composition of detritus were also not available and thus detritus was considered a single compartment, with no consideration given to OM lability (van Oevelen et al. 2011a). This also meant that it was not possible to directly compare the model with certain measurements from the isotope tracing experiment, since the detrital compartment was different between this and the tracer study (Woulds et al. in prep.). Additionally, stable isotopic data

were used to inform dietary proportions but were averaged for whole compartments so may have contributed increased uncertainty to some of the results (such as bacteria to macrofaunal predator/ scavengers at the off-vent site).

6.7 Acknowledgements

We thank Alison Manson for preparation of the conceptual figure and the shipboard party and cruise PI (Prof. Paul Tyler) during JC55 for their assistance in sample collection. We are also grateful to Graeme Swindles and Lee Brown who provided some editorial suggestions to the final manuscript.

6.8 Author Contributions

JBB & CW collected the data. JBB & DvO wrote the model. JBB prepared the figures. JBB wrote the paper with comments from CW & DvO.

6.9 Competing financial interests

This work was funded by the UK Natural Environmental Research Council. This work was funded by a NERC PhD Studentship (NE/L501542/1) and the NERC ChEsSo consortium (Chemosynthetically-driven Ecosystems South of the Polar Front, NERC Grant NE/DOI249X/I). NERC were not involved in the writing of this manuscript or in the decision to publish this research and all authors declare no conflicts of interest.

6.10 Supplementary Information

Supplementary Figure 1 (Supplement 6-4). Mean flow rates between compartments at each site.

6.11 References

Allesina S, Ulanowicz RE (2004) Cycling in ecological networks: Finn's Index revisited. Computational Biology and Chemistry 28:227-233

Aquilina A, Connelly DP, Copley JT, Green DR, Hawkes JA, Hepburn L, Huvenne VA, Marsh L, Mills RA, Tyler PA (2013) Geochemical and Visual Indicators of Hydrothermal Fluid Flow through a Sediment-Hosted Volcanic Ridge in the Central Bransfield Basin (Antarctica). Plos One 8:e54686

Aquilina A, Homoky WB, Hawkes JA, Lyons TW, Mills RA (2014) Hydrothermal sediments are a source of water column Fe and Mn in the Bransfield Strait, Antarctica. Geochimica et Cosmochimica Acta 137:64-80

Bates AE, Lee RW, Tunnicliffe V, Lamare MD (2010) Deep-sea hydrothermal vent animals seek cool fluids in a highly variable thermal environment. Nat Commun 1:14

Bell JB, Alt CHS, Jones DOB (2016a) Benthic megafauna on steep slopes at the northern Mid-Atlantic Ridge. Marine Ecology:maec 12319

Bell JB, Aquilina A, Woulds C, Glover AG, Little CTS, Reid WDK, Hepburn LE, Newton J, Mills RA (2016b) Geochemistry, faunal composition and trophic structure at an area of weak methane seepage on the southwest South Georgia margin. Royal Society Open Science 3

Bell JB, Reid WDK, Pearce DA, Glover AG, Sweeting CJ, Newton J, Woulds C (2016c) Hydrothermal activity lowers trophic diversity in Antarctic sedimented hydrothermal vents. Biogeosciences Discussions

Bell JB, Woulds C, Brown LE, Little CTS, Sweeting CJ, Reid WDK, Glover AG (2016d) Macrofaunal ecology of sedimented hydrothermal vents in the Bransfield Strait, Antarctica. Frontiers in Marine Science 3:32

Bernardino AF, Levin LA, Thurber AR, Smith CR (2012) Comparative Composition, Diversity and Trophic Ecology of Sediment Macrofauna at Vents, Seeps and Organic Falls. Plos ONE 7:e33515

Boetius A, Wenzhöfer F (2013) Seafloor oxygen consumption fuelled by methane from cold seeps. Nature Geoscience 6:725-734

Burdige DJ, Berelson WM, Coale KH, McManus J, Johnson KS (1999) Fluxes of dissolved organic carbon from California continental margin sediments. Geochimica Et Cosmochimica Acta 63

Childress JJ, Cowles DL, Favuzzi JA, Mickel TJ (1990) Metabolic rates of benthic deep-sea decapod crustaceans decline with increasing depth primarily due to the decline in temperature. Deep-Sea Research 37:929-949

Cohen J (1992) A power primer. Psychological Bulletin 112:155-159

Connelly DP, Copley JT, Murton BJ, Stansfield K, Tyler PA, German CR, Van Dover CL, Amon D, Furlong M, Grindlay N, Hayman N, Huehnerbach V, Judge M, Le Bas T, McPhail S, Meier A, Nakamura K-i, Nye V, Pebody M, Pedersen RB, Plouviez S, Sands C, Searle RC, Stevenson P, Taws S, Wilcox S (2012) Hydrothermal vent fields and chemosynthetic biota on the world's deepest seafloor spreading centre. Nature Communications 3:1-9

Dählmann A, Wallman K, Sahling H, Sarthou G, Bohrmann G, Petersen S, Chin CS, Klinkhammer GP (2001) Hot vents in an ice-cold ocean: Indications for phase separation at the southernmost area of hydrothermal activity, Bransfield Strait, Antarctica. Earth and Planetary Science Letters 193:381-394

Dale AW, Sommer S, Haeckel M, Wallmann K, Linke P, Wegener G, Pfannkuche O (2010) Pathways and regulation of carbon, sulfur and energy transfer in marine sediments overlying methane gas hydrates on the Opouawe Bank (New Zealand). Geochimica Et Cosmochimica Acta 74:5763-5784

De Smet B, van Oevelen D, Vincx M, Vanaverbeke J, Soetaert K (2016) Lanice conchilega structures carbon flows in soft-bottom intertidal areas. Marine Ecology Progress Series 552:47-60

del Giorgio PA, Cole JJ (1998) Bacterial Growth Efficiency in Natural Aquatic Systems. Annual Review of Ecology and Systematics 29:503-541

Dubilier N, Bergin C, Lott C (2008) Symbiotic diversity in marine animals: the art of harnessing chemosynthesis. Nature Reviews Microbiology 6:725-740

Dunne JP, Sarmiento JL, Gnanadesikan A (2007) A synthesis of global particle export from the surface ocean and cycling through the ocean interior and on the seafloor. Global Biogeochemical Cycles 21:n/a-n/a

Fischer UR, Wieltschnig C, Kirshner AKT, Velimirov B (2003) Does virus-induced lysis contribute significanty to bacterial mortality in the oxygenated sediment

layer of shallow oxbow lakes. Applied and environmental microbiology 69:5281-5289

Georgieva M, Wiklund H, Bell JB, Eilersten MH, Mills RA, Little CTS, Glover AG (2015) A chemosynthetic weed: the tubeworm *Sclerolinum contortum* is a bipolar, cosmopolitan species. BMC Evolutionary Biology 15:280

Grassle JF, Petrecca RF (1994) Soft-sediment hydrothermal vent communities of Escanaba Trough. In: Zierenberg RA, Reiss CA (eds) Geological, hydrothermal, and biological studies at Escanaba Trough, Gorda Ridge, offshore Northern California. US Geological Survey, Denver, CO

Higgs ND, Newton J, Attrill MJ (In Press) Caribbean Spiny Lobster Fishery is Underpinned by Trophic Subsidies from Chemosynthetic Primary Production. Current Biology

Howarth RW (1984) The ecological significance of sulfur in the energy dynamics of salt marsh and coastal marine sediments. Biogeochemistry 1:5-27

Howe JA, Wilson CR, Shimmield TM, Diaz RJ, Carpenter LW (2007) Recent deep-water sedimentation, trace metal and radioisotope geochemistry across the Southern Ocean and Northern Weddell Sea, Antarctica. Deep Sea Research Part II: Topical Studies in Oceanography 54:1652-1681

Isaksen MF, Jørgensen BB (1996) Adaptation of Psychrophilic and Psychrotrophic Sulfate-Reducing Bacteria to Permanently Cold Marine Environments. Applied Environmental Microbiology 62:408-414

Klinkhammer GP, Chin CS, Keller RA, Dahlmann A, Sahling H, Sarthou G, Petersen S, Smith F (2001) Discovery of new hydrothermal vent sites in Bransfield Strait, Antarctica. Earth and Planetary Science Letters 193:395-407

Kones JK, Soetaert K, van Oevelen D, Owino JO (2009) Are network indices robust indicators of food web functioning? A Monte Carlo Approach. Ecological Modelling 220:370-382

Latham LG (2006) Network flow analysis algorithms. Ecological Modelling 192:586-600

Levin LA, Baco AR, Bowden D, Colaço A, Cordes E, Cunha MR, Demopoulos A, Gobin J, Grupe B, Le J, Metaxas A, Netburn A, Rouse GW, Thurber AR, Tunnicliffe V, Van Dover C, Vanreusel A, Watling L (2016) Hydrothermal Vents and Methane Seeps: Rethinking the Sphere of Influence. Frontiers in Marine Science 3:72

Levin LA, Mendoza GF (2007) Community structure and nutrition of deep methane-seep macrobenthos from the North Pacific (Aleutian) Margin and the Gulf of Mexico (Florida Escarpment). Marine Ecology 28:131-151

Levin LA, Mendoza GF, Konotchick T, Lee R (2009) Macrobenthos community structure and trophic relationships within active and inactive Pacific hydrothermal sediments. Deep Sea Research Part II: Topical Studies in Oceanography 56:1632-1648

Levin LA, Orphan VJ, Rouse GW, Rathburn AE, Ussler W, III, Cook GS, Goffredi SK, Perez EM, Waren A, Grupe BM, Chadwick G, Strickrott B (2012) A hydrothermal seep on the Costa Rica margin: middle ground in a continuum of reducing ecosystems. Proceedings of the Royal Society B-Biological Sciences 279:2580-2588

Mahaut ML, Sibuet M, Shirayama Y (1995) Weight-dependent respiration rates in deep-sea organisms. Deep-Sea Research I 42:1575-1582

Masque P, Isla E, Sanchez-Cabeza JA, Palanques A, Bruach JM, Puig P, Guillén J (2002) Sediment accumulation rates and carbon fluxes to bottom sediments at the Western Bransfield Strait (Antarctica). Deep Sea Research Part II 49:921-933

Mei ML, Danovaro R (2004) Virus production and life strategies in aquatic sediments. Limnology & Oceanography 49:459-470

Middelburg JJ (2011) Chemoautotrophy in the ocean. Geophysical Research Letters 38:n/a-n/a

Phillips DL, Inger R, Bearhop S, Jackson AL, Moore JW, Parnell AC, Semmens BX, Ward EJ (2014) Best practices for use of stable isotope mixing models in food-web studies. Canadian Journal of Zoology 92:823-835

Pozzato L, Van Oevelen D, Moodley L, Soetaert K, Middelburg JJ (2013) Sink or link? The bacterial role in benthic carbon cycling in the Arabian Sea's oxygen minimum zone. Biogeosciences 10:6879-6891

R Core Team (2013) R: A Language and environment for statistical computing. R Foundation for Statistical Computing, Vienna, Austria http://www.R-project.org/.

Rasband WS (2013) ImageJ. Book 1.47. U.S. National Institutes of Health, Bethesda, Maryland, USA

Reid WDK, Bell JB, Sweeting CJ, Woulds C, Wigham BD (invited review in prep.) Elucidating trophodynamics at hydrothermal vents using stable isotope analysis.

Sahling H, Wallman K, Dählmann A, Schmaljohann R, Petersen S (2005) The physicochemical habitat of *Sclerolinum sp.* at Hook Ridge hydrothermal vent, Bransfield Strait, Antarctica. Limnology & Oceanography 50:598-606

Soetaert K, van Oevelen D (2008) LIM: Linear Inverse Model examples and solutions methods. R Package v1.2

Sorokin YI (1972) The bacterial population and the processes of hydrogen sulphide oxidation in the Black Sea. Journal de Conseil International pour l'Exploration de la Mer 34:423-454

Soto LA (2009) Stable carbon and nitrogen isotopic signatures of fauna associated with the deep-sea hydrothermal vent system of Guaymas Basin, Gulf of California. Deep Sea Research Part II: Topical Studies in Oceanography 56:1675-1682

Southward EC, Gebruk A, Kennedy H, Southward AJ, Chevaldonne P (2001) Different energy sources for three symbiont-dependent bivalve molluscs at the Logatchev hydrothermal site (Mid-Atlantic Ridge). Journal of Marine Biological Asociation of the United Kingdom 81:655-661

Sweetman AK, Levin LA, Rapp HT, Schander C (2013) Faunal trophic structure at hydrothermal vents on the southern Mohn's Ridge, Arctic Ocean. Marine Ecology Progress Series 473:115

Teske A, Callaghan AV, LaRowe DE (2014) Biosphere frontiers of subsurface life in the sedimented hydrothermal system of Guaymas Basin. Frontiers in microbiology 5:362

Tyler PA, Connelly DP, Copley JT, Linse K, Mills RA, Pearce DA, Aquilina A, Cole C, Glover AG, Green DR, Hawkes JA, Hepburn L, Herrera S, Marsh L, Reid WD, Roterman CN, Sweeting CJ, Tate A, Woulds C, Zwirglmaier K (2011) RRS *James Cook* cruise JC55: Chemosynthetic Ecosystems of the Southern Ocean. BODC Cruise Report

van Oevelen D, Bergman MJN, Soetaert K, Bauerfeind E, Hasemann C, Klages M, Schewe I, Soltwedel T, Budaeva NE (2011a) Carbon flows in the benthic food web at the deep-sea observatory HAUSGARTEN (Fram Strait). Deep Sea Research Part I 58:1069-1083

van Oevelen D, Middleburg JJ, Soetaert K, Moodley L (2006a) The fate of bacterial carbon in an intertidal sediment: Modeling an in situ isotope tracer experiment. Limnology & Oceanography 51:1302-1314

van Oevelen D, Soetaert K, Garcia R, de Stigter HC, Cunha MR, Pusceddu A, Danovaro R (2011b) Canyon conditions impact carbon flows in food webs of three sections of the Nazaré canyon. Deep Sea Research Part II: Topical Studies in Oceanography 58:2461-2476

van Oevelen D, Soetaert K, Heip C (2012) Carbon flows in the benthic food web of the Porcupine Abyssal Plain: The (un)importance of labile detritus in supporting microbial and faunal carbon demands. Limnology & Oceanography 57:645-664

van Oevelen D, Soetaert K, Middelburg JJ, Herman PMJ, Moodley L, Hamels I, Moens T, Heip CHR (2006b) Carbon flows through a benthic food web: Integrating biomass, isotope and tracer data. Journal of Marine Research 64:453-482

van Oevelen D, Van den Meersche K, Meysman FJR, Soetaert K, Middelburg JJ, Vézina AF (2009) Quantifying Food Web Flows Using Linear Inverse Models. Ecosystems 13:32-45

Wefer G, Fischer G (1991) Annual primary production and export flux in the Southern Ocean from sediment trap data. Marine Chemistry 35:597-613

Wefer G, Fischer G, Fuetterer D, Gersonde R (1988) Seasonal particle flux in the Bransfield Strait, Antarctica. Deep-Sea Research 35:891-898

Whiticar MJ, Suess E (1990) Hydrothermal hydrocarbon gases in the sediments of the King George Basin, Bransfield Strait, Antarctica. Applied Geochemistry 5:135-147

Woulds C, Bell JB, Brown L, Pancost RD, Bouillon S, Tyler PA (in prep.) An isotope tracing experiment in Southern ocean hydrothermal sediments.

7. Discussion

This project has synthesised a number of themes and approaches in the study of chemosynthetic ecosystems, focusing upon sedimented ecosystems and the interactions between sediment geochemistry and patterns in biological composition and behaviour in the Southern Ocean. I have studied two distinct sedimented chemosynthetic ecosystems, which are united by their physical structure and the diffuse, patchy nature of the chemosynthetic substrates that they provide. The behaviour of these substrates, and concomitant patterns in environmental toxicity, is highly important for structuring ecosystem form and function and has received very little attention in the Southern Ocean prior to this project. Sedimented vents in particular are globally poorly studied and this project contributes valuable insight into their community structure, trophodynamics and ecosystem function. These ecosystems are a part of a continuum of the wide range of deep-sea habitats, most of which are soft sediment, and so it is possible to draw a number of parallels between the ecological processes that occur in different seafloor settings.

Chapters 3-6 have been sorted according to site-specific and methodological approaches, with the Bransfield Strait sedimented vent system comprising the main focus of the present project. The results and implications of each chapter are discussed separately in their respective chapters but here I will provide an overview of how they can be considered as a cohesive single project, as well as highlighting some of the additional considerations or limitations that did not accompany the published manuscripts.

7.1 Influence of environmental toxicity upon benthic communities

Sedimented chemosynthetic ecosystems are all characterised by gradients in productivity and physiological stress (Bernardino et al. 2012). This has concomitant effects upon food webs (section 7.2) but also assemblage composition, biomass and species diversity (Chapter 3; 4, Levin et al. 2000, Levin & Mendoza 2007, Levin et al. 2009, Levin et al. 2010, Bell et al. 2016b, Bell et al. 2016d). A major theme of this

project has been to examine how these environmental gradients act upon benthic communities in the Southern Ocean.

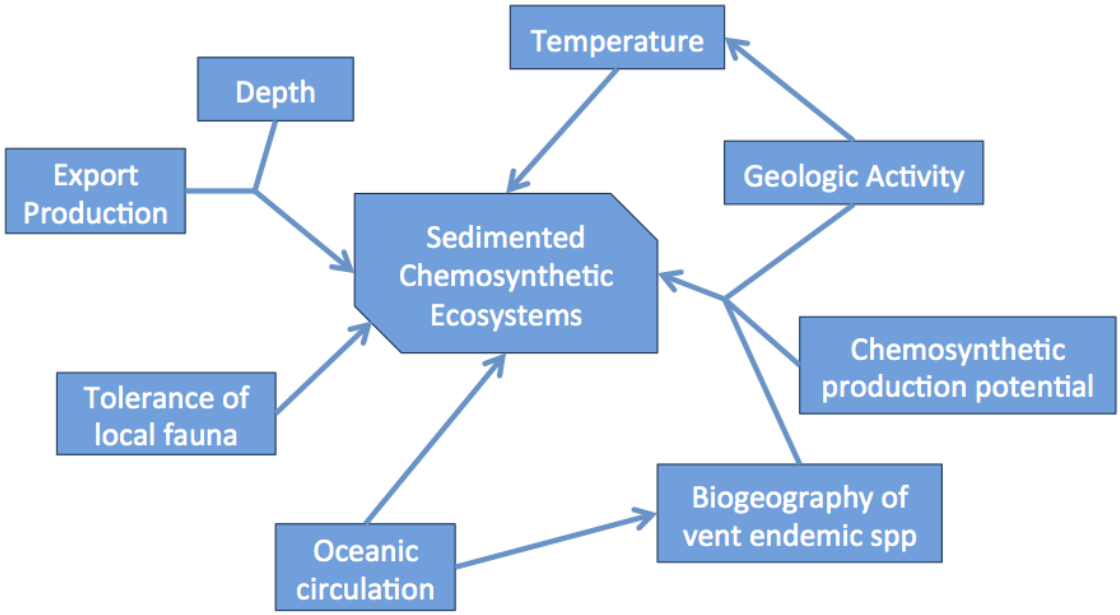

Figure 7.1a – Factors affecting the ecology SCEs

7.1.1 Local scale composition shifts

In the Bransfield Strait, biodiversity and abundance declined towards the most hydrothermally active areas, suggesting that the local fauna were generally not well suited to the relatively high temperature conditions (Chapter 4, Clarke et al. 2009, Clarke & Crame 2010, Bell et al. 2016d), and that the in situ production of organic matter was insufficient to offset the metabolic costs associated with living in a more physiologically stressful environment (Chapter 5; 6, Levin et al. 2013, Bell et al. 2016c, Bell et al. submitted). Quantitatively examining these gradients of ecological distance can be challenging, owing to wide variation in factors such as the spread of chemosynthetic substrates; biogeography and local oceanographic regimes; in situ production rates and the inherent biological and geochemical patchiness (Figure 7.1a) that is common in deep-seafloor habitats (Chapter 3; 4, Gage & Tyler 1991, Levin 2005, Clarke et al. 2009, Bell et al. 2016b, Bell et al. 2016d, Levin et al. 2016a). The sampling design during JC55 in the Bransfield Strait allowed this project to compare assemblages in several geochemical conditions at a range of spatial scales, both between vent and non-vent sites, but also between variable levels of

hydrothermal activity. This demonstrated that in these settings, the importance of environmental distance outweighs the spatial separation between sites and that assemblage composition varied more within Hook Ridge than between all non-vent sites throughout the basin (Figure 4.5.1a).

7.1.2 Regional scale composition shifts

Assemblage data from the South Georgia shelf, whilst generally comparable throughout the sampling area, provided an opportunity to test wider patterns in biodiversity and assemblage composition (Figure 3.6.1a). Family-level composition of South Georgian benthos was found to be intermediate between other fauna from the Antarctic shelf and Pacific seeps. This is consistent with their geochemical environment (elevated levels of methane, but insufficient to support seep-endemic metazoa) (Chapter 3, Bell et al. 2016b), though the lack of seep-endemic fauna may also have been a result of bathymetric patterns in their distribution . In the sea of Okhotsk, seep-endemic fauna were not found shallower than 370m depth (Sahling et al. 2003). Despite the widespread diffuse source of methane, albeit at low concentrations (Figure 3.5.4a), endosymbiont-hosting metazoa were not observed in the reducing sediments on the South Georgia margin. Given the global distribution of *Siboglinum* spp. (Southward et al. 1979, Thornhill et al. 2008, Rodrigues et al. 2013) and the comparable conditions to off-vent regions of the Bransfield Strait (Chapter 3, Aquilina et al. 2013, Bell et al. 2016b), it was perhaps surprising that these, or similar fauna were not observed here. This was possibly owing to bathymetric limitations (Sahling et al. 2003), though *Siboglinum* spp. have been found at shallower depths than the South Georgia sites (and at similar latitudes) (George 1976), or insufficient flux of methane to surface sediments.

7.1.3 Ecological responses to reducing conditions

Species diversity was also influenced by environmental conditions. Geochemical conditions did not vary significantly across the South Georgia sampling area, meaning that the influence of environmental distance upon diversity could not be tested here. However, the broad range of geochemical conditions presented in the

Bransfield Strait meant that significant differences could be observed throughout the basin. Geochemical data were coalesced into an index (the hydrothermal index, Table 4.5.4a) in a bid to fit these parameters to gradients in abundance and diversity in a way that the noisy geochemical data could not individually explain (Brown et al. 2010) and mitigate the lower spatial resolution available for geochemical data. The 'hydrothermal index' approach used here is consistent with other attempts to fit environmental parameters to ecological data (Brown et al. 2010, Robertson et al. 2015) but, given that these were either too specific to a particular environment or required data that were lacking from the available datasets, I chose to develop a new proxy index that captured the most relevant parameters to test the response of ecological data to the environmental trends. Concentration of chloride, hydrogen sulphide and methane were selected as representative of both the amount of hydrothermal input and the concentration of chemosynthetic substrates. It was necessary to capture both of these components, since they were apparently not directly correlated (Aquilina et al. 2013, Aquilina et al. 2014). Diversity, abundance and species richness all followed fairly similar patterns, initially declining fairly rapidly (Figure 4.5.4a) and leveling out at HI values of > 1. Owing to the normalisation approach used (to scale the varying concentration values equally), this index should be considered a relative measure that is only directly comparable within individual studies (though the patterns observed could be comparable to other studies, or be simply combined for a possible future meta-analysis). The value of this approach is to provide a simple framework to elucidate ecological responses to complex physico-chemical changes in habitat but some caveats should be acknowledged. Temperature data was notably lacking, having not been collected during JC55. Chlorinity was selected as a proxy for hydrothermal fluid advection rates, and thus temperature, as hydrothermal fluid and bottom water are very different in terms of chloride ion content and can thus be used to estimate mixing between the two fluid endmembers (Ginsburg et al. 1999, Aquilina et al. 2013). Although the amount of sediment porewater accounted for by hydrothermal fluid should be proportional to temperature, using this proxy for separate sites assumes that the temperature of the hydrothermal endmember was equal at a given depth below seafloor across the vent site. The incorporation of a temperature proxy makes this particular approach specific to such environments where temperature is a

consideration (i.e. hydrothermal sediments and mud volcanoes) and other comparable sedimented chemosynthetic ecosystems (e.g. seeps) would not be expected to exhibit temperature variability. In these cases, alternative measures for fluid advection rates might be considered if necessary but it is also possible that the concentration of chemosynthetic substrates or dissolved oxygen depletion/ redox conditions alone would be sufficient to adequately explain ecological patterns. The main challenge associated with fitting ecological variables to fluxes of chemosynthetic substrates is that they can represent both a cost and a reward (Levin et al. 2013). These substrates support primary production and (should) increase the amount of organic matter available, but they are also toxic (Figure 7.1.3a). Hydrogen sulphide for example, once oxidised forms sulphuric acid, concurrently reducing porewater oxygen content and sediment pH, meaning that although more food may be available, inhabiting these environments comes with an associated metabolic cost (Levin et al. 2013). Alvinellid polychaetes at hydrothermal vents invest significant quantities of energy into mucus production (as much as 25%, Juniper & Martineu 1995, Martineu et al. 1997, Levesque et al. 2005). This mucus is necessary to capture and remove toxic sulphides and heavy metals from body tissue and, although it is a substantial cost, is still energetically economic, given the paucity of food in the surrounding area and the potential for local production. However, in the Bransfield Strait where export production was high and apparently exceeded chemosynthetic primary production rates at all sites (Figure 6.3.1a), the metabolic costs associated with occupying areas of in situ production may be more of a deterrent. As demonstrated in chapter 4, this has potential to introduce extrinsic factors into shaping the ecosystem dynamics, such as biogeography or variation in surface primary productivity. The response of ecological variables along the gradient of hydrothermal activity in the Bransfield Strait was substantially different to those in Pacific sediments (Figure 4.6.1a) (Chapter 4, Bernardino et al. 2012, Bell et al. 2016d), providing clear evidence of regional variability and further complicating our understanding of ecosystem dynamics around sedimented chemosynthetic ecosystems. It is clear therefore that when estimating future changes (e.g. ecological responses to the changing extent of reducing sediments), that regional factors should not be overlooked. A wider research effort is integral to

determining how these factors (e.g. seafloor temperature or supply of allochthonous OM) interact to determine local ecological shifts.

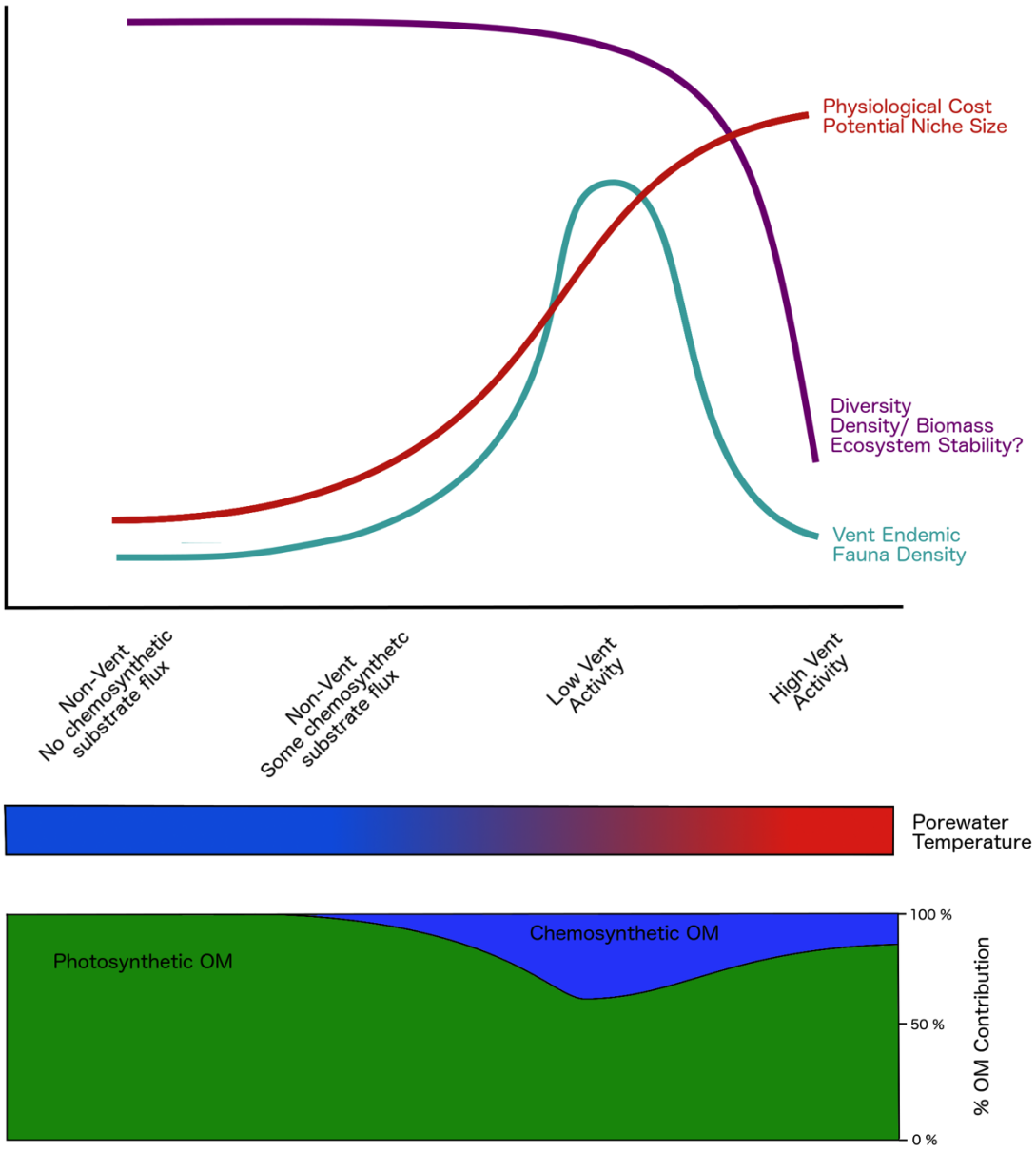

Figure 7.1.3 a – Environmental and ecological shifts in soft-sediment benthic habitats along a gradient of hydrothermal activity in the Bransfield Strait.

7.2 Importance of chemosynthesis in benthic food webs

7.2.1 Spatial extent of chemosynthetic contribution to benthic food webs

Here I present a number of methodological approaches to examine the contribution of chemosynthetic organic matter to the benthic food web in and around sedimented vents and reducing sediments. These results have suggested that chemoautotrophy may be widespread in the Southern Ocean (Wood & Jung 2008), but that in most areas, the contribution of this source is probably quite limited. Hydrothermal products and related trophic activity was detected in every non-Hook Ridge site in the Bransfield Strait, including those over 100km from the basin axis and along the full length of the axis surveyed. Owing to the diffuse nature of chemosynthetic substrates, it is challenging to accurately determine the spatial extent of sedimented chemosynthetic ecosystems (e.g. seeps). At Hook Ridge, even between the two sites visited, the differences in sediment geochemistry, temperature and hydrothermal advection (Bohrmann et al. 1998, Dählmann et al. 2001, Aquilina et al. 2013, Aquilina et al. 2014) resulted in some substantial differences in the contribution of chemosynthetic OM (Chapter 6, Bell et al. submitted) and notable differences in diversity, abundance and assemblage composition (Chapter 4, Bell et al. 2016d). This sub-km scale heterogeneity, coupled with the unknown spatial extent of the chemosynthetic substrate input, means that it is very difficult to constrain the total contribution of chemosynthetic carbon over a given area (Chapter 4; 6, Bell et al. 2016b, Bell et al. submitted).

These results have demonstrated that symbiont-bearing metazoa adopt an important functional role in these ecosystems, by mediating a significant amount of carbon transfer into the food web (Chapter 6, Bell et al. submitted). *Sclerolinum contortum* (Georgieva et al. 2015) was very abundant at the less active Hook Ridge site (HR1), suggesting that species-level autecological constraints, such as thermal niches (Bates et al. 2010) or tolerance to porewater toxicity (Sahling et al. 2005), could be a very important factor for determining the importance of chemosynthetic carbon transfer for benthic food webs. Macrofauna with endosymbionts represented an important OM source, particularly for higher trophic level consumers that were

not adapted to consumption of bacterial sources (Chapter 6, Bell et al. submitted). *S. contortum* fragments were observed at Hook Ridge 2 but no complete specimens were found meaning that it was likely that very patchy populations may have existed in this area that were not captured by the sampling programme during JC55 (sampling effort equal at Hook Ridge sites).

7.2.2 The role of endosymbiont-bearing fauna

Another siboglinid species, *Siboglinum* sp. was widely distributed around the Bransfield Strait and was apparently fixing thermogenic methane (Chapter 4; 5, Whiticar & Suess 1990, Bell et al. 2016c, Bell et al. 2016d). The production of thermogenic methane from the degradation of sediment organic matter is accelerated by the heat flux associated with sediment hydrothermalism (Whiticar & Suess 1990). Although the organic matter production rates were very low at the off-vent site (net production: < 0.01 mmol C m^{-2} d^{-1}, ~ 0.2 % of the total OM input at this site) compared with Hook Ridge (0.48 – 0.70 mmol C m^{-2} d^{-1}), their much greater spatial extent, meant that production rates could have been have been comparable over the entire basin (Chapter 6, Bell et al. submitted). Assuming that *Siboglinum* production rates at the off-axis site were representative of elsewhere in the basin and that it was distributed throughout the basin (approx. 17,000 km^2, compared with ~100 km^2 for Hook Ridge), total fixation of methane-derived carbon was approximately 76 kmol C d^{-1}, compared with 48-70 kmol C d^{-1} for *Sclerolinum* production at Hook Ridge (or 6.4 kg C d^{-1} across the strait, compared with 4.0 – 5.8 kg C d^{-1} at Hook Ridge). These estimates, in spite of their significant assumptions and caveats concerning the distribution and activity of siboglinids, raise significant questions about benthic food webs and of the transfer of carbon in and around sedimented vent sites. *Siboglinum* is a widely distributed genus and, whilst it does appear to exhibit a certain amount of trophic plasticity (Chapter 5, George 1976, Southward et al. 1979, Thornhill et al. 2008, Rodrigues et al. 2013, Bell et al. 2016c), there is evidence that it could be a very important genus for mediating certain carbon cycling pathways across a wide ocean depth range. *Siboglinum* spp. can remobilise carbon (either from reduced organic compounds or dissolved OM) and provide a means to reintroduce it in a format that is accessible to other metazoa. By

routing chemosynthetic carbon directly through metazoan tissue, it may be possible that in situ production becomes more accessible to a wider range of fauna. Despite bacterial production being comparable between the two vent sites, and higher than *Sclerolinum* net fixation rates at Hook Ridge 1, proportional contribution of chemosynthetic carbon at this site was more than double that of Hook Ridge 2 (30.6 % at HR1 compared with 13.8 % at HR2). The results from vent and non-vent areas of the Bransfield Strait demonstrate that chemosynthetic activity be clearly traced through assemblages at a range of scales and contributes significantly to regional species distribution and diversity. It is clear that endosymbiont-bearing fauna are key in mediating transfers of chemosynthetic carbon into benthic food webs and controls that act upon their distribution have significant implications for the wider communities.

7.2.3 Source isotope measurements of chemosynthetic OM uptake

Despite the lack of seep-endemic metazoa, there was still evidence of limited chemosynthetic activity on the South Georgia margin, with observable contributions to bulk isotopic signatures across a range of fauna, particularly in sulphur isotopic signatures (Figure 3.5.2c) (Chapter 3, Bell et al. 2016b). As at the site of higher hydrothermal activity in the Bransfield Strait (Hook Ridge 2), bacterial activity apparently was the only known means by which chemosynthetic OM could enter the food web. Much of this activity was apparently occurring below 20 cmbsf (Chapter 3, Bell et al. 2016b) and so seemingly beyond the reach of the benthos collected (sampled down to 10 cmbsf), particularly so for the less motile species. However, sulphur isotopic signatures (and to a lesser extent, carbon) provided evidence of incorporation of methane-derived organic matter (MDOM). Had stable isotope mixing models been possible in this case, there would likely have been a considerable disparity between estimates of the contribution of MDOM based upon carbon and sulphur isotopic measurements. This clearly emphasises the value of using multiple isotopic tracers in food web studies and warrants further investigation to understand the drivers behind this discrepancy. One possible cause for this disparity is that the range of values associated with the two sources of $\delta^{34}S$ is greater than those for $\delta^{13}C$, and thus it would be expected that differences in isotopic

signatures between taxa would be more substantial in the isotope with the greater range of source values. The possible range of $\delta^{34}S$ values was greater than for $\delta^{13}C$ but it is not likely that the difference in the ranges would have been sufficient to elicit the faunal measurements observed (Table 7.2a). Differences in the isotopic ranges of the available endmembers for carbon and sulphur are likely to have contributed to some of the disparity between carbon and sulphur measurements but suggest further mechanisms for the partitioning of carbon and sulphur in diet. One possible mechanism for this would be differences in the relative availability and lability of sulphur and carbon sources. It seems likely that phytodetritus was the main carbon source for the vast majority of the benthos but, supposing that this material was poor in organic sulphur, relative to MDOM sources, it might be expected that organisms could gain more of their sulphur from in situ production and more carbon from sinking phytodetritus, thus weighting the two signatures to varying degrees. To properly address this suggestion would require detailed measurements of total organic carbon (TOC) and sulphur (TOS) in both surface-derived and in situ organic matter sources, as well as some information on the physiology of the benthos, ideally confirmed by some experimental studies. Taxa with particularly low $\delta^{34}S$ signatures (< 0 ‰) were largely deposit feeding annelids that may have ingested free-living methanotrophic microbes (Figure 3.5.2c). Another possible suggestion is that the resident fauna fractionated their TOC and TOS by different amounts during assimilation. Trophic discrimination for carbon and sulphur is generally considered to be fairly minimal (<~1 ‰), hence their use as source identifiers. However, it is also known that trophic discrimination factors (TDFs) vary according to several factors, including the quality of the organic source (Caut et al. 2009), meaning that some disparity between carbon and sulphur isotopic values is certainly not unrealistic. Tri-isotopic measurements will continue to prove of significant value to stable isotope research, but there is an obvious need to develop more complete understanding of processes individually affecting carbon and sulphur isotopic signatures respectively, and of updated analytic methods than can capture differences observable from the increased dimensionality of tri-isotope data (e.g. in isotopic niche space and ellipses).

	South Georgia Shelf		Bransfield Strait	
Source	$\delta^{13}C$ (‰)	$\delta^{34}S$ (‰)	$\delta^{13}C$ (‰)	$\delta^{34}S$ (‰)
Phytodetritus	-25	+20	-24	+20
Methane-derived OM	-65	-30	-42	-30
Potential Source Range	40	50	18	50
Observed Faunal Range	7.8	21.2	27.6*	45.6

Table 7.2a – Approximate isotopic values associated with organic matter sources on the South Georgia shelf and non-vent areas of the Bransfield Strait (Whiticar & Suess 1990, Canfield 2001, Young et al. 2013, Geprägs et al. 2016). *In the Bransfield Strait, the larger faunal $\delta^{13}C$ range may be explained by potential inputs of enriched $\delta^{13}C$ ice algae that were not directly captured during the JC55 sampling campaign. Total range not given as presumed skewed by some unusual $\delta^{13}C$ measurements from the Axe. Sulphide oxidation not given as not considered active at non-vent areas of the Bransfield Strait.

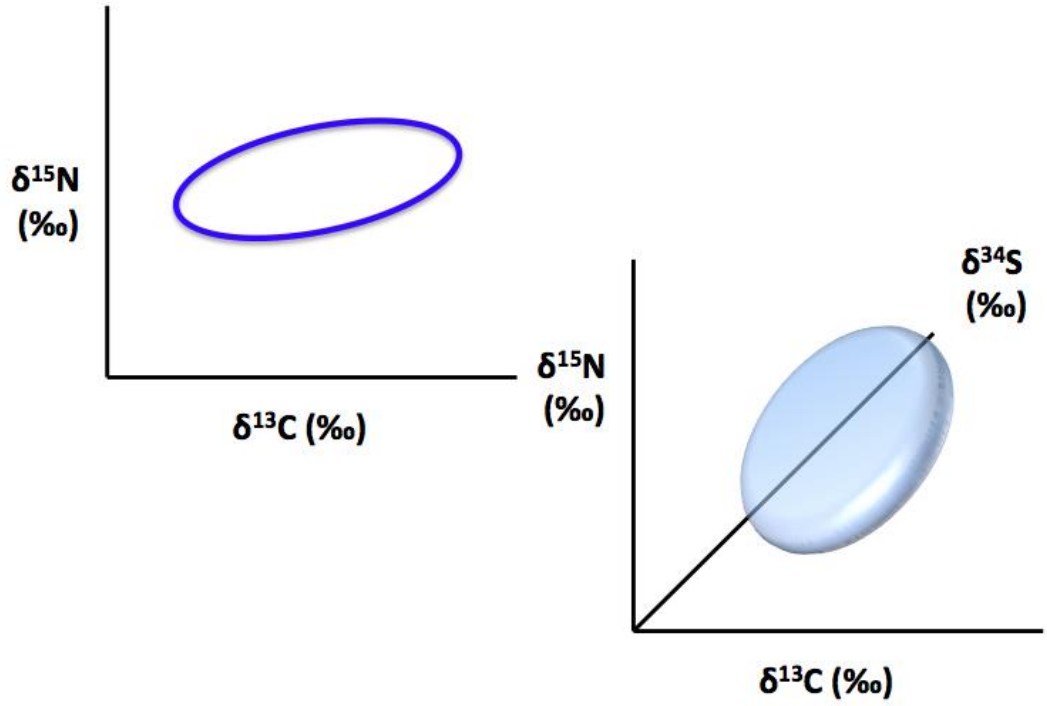

Figure 7.2.3a – Incorporating additional dimensions into established isotope analytic techniques.

7.3 Methodological considerations

7.3.1 Scale Dependency

Although informative in several ways, interpretation of stable isotopic data was confounded by unknown variability in endmembers and trophic discrimination factors. This meant that for calculating certain ecosystem processes, such as the importance of chemosynthetic OM, I adopted a linear inverse modelling approach, which incorporates the known uncertainty directly into the analysis and is a robust framework for reconstructing ecosystem flow networks. Certain aspects of the resultant models (e.g. non-vent bacterial respiration) were quite representative of other applications of this framework (van Oevelen et al. 2011a) but this was also the first time such an approach has been taken for deep-sea ecosystems with in situ production as a consideration. Therefore, as a means to further validate these results, some comparisons can be made with a ship-board isotope tracing experiment from some of the same sites (Woulds et al. in prep.). Respiration rates estimated by the model were comparable to tracer observations, but since the tracer observations were used to constrain upper and lower bounds on this aspect of the model, this is not surprising. The tracer experiment specifically considered the fate of (labeled) labile algal material, whereas the LIMs were limited to considering detritus as a single pool, presumably with varying degrees of lability from pre-aged during sinking, to refractory. However, DIC fixation rates were measured and so can be directly compared with the model results from Hook Ridge 2. Bacterial uptake at HR2 was estimated by the model at 1.11 mmol C m^{-2} d^{-1} (± 0.12) but was below detection limits in the labelling experiments. This discrepancy is likely owing to the extreme patchiness that is characteristic of these sorts of environments, which was observed at both bacterial and metazoan levels (Chapter 4; 5, Aquilina et al. 2013, Bell et al. 2016c, Bell et al. 2016d). Bacterial uptake of DIC is also likely to have been higher in situ, as the tracer experiments were incubated at typical Southern Ocean seafloor temperatures (~0-1˚C), rather than their respective in situ temperatures given in the LIMs. These temperatures were unknown at the time (Woulds et al. in prep.), which will likely have resulted in lower observed metabolic rates and faunal activity. The LIMs represent an averaged signal across the total replicate cores (6

from each vent site & 4 from the off-vent site), whereas the tracer experiment much better captures the potential noise between replicate cores. Thus, although the estimates of DIC fixation are comparable, the LIM estimates should be considered a mean value for the total area sampled (scale of ~100 – 1000 m^2). This also means that variability within the distribution of each flow values is quite scale dependent and would likely have been significantly higher at smaller spatial scales (Levin 1992). Particularly for highly heterogeneous environments, such as SHVs (Figure 4.5.1a), the choice of scale may significantly bias results (Levin 1992). In this case, data were pooled from as many cores as possible (4 – 6 replicate deployments per site) (Chapter 4; 5, Bell et al. 2016c, Bell et al. 2016d), in order to give the 'most accurate' measure that could be derived through this approach, but this is only the most accurate for the scale concerned (i.e. spatial separation of replicate sampling points). By selecting different levels of replication to inform stock sizes, it would be possible to use this approach to study this potential source of bias, and may represent a valuable insight into design of future LIM studies and into the patchiness that is inherent in the deep-sea. That said, the lack of intra-site specificity available for many of the constraints in the Bransfield Strait (e.g. Export production or SCOC) would probably mask, to some extent, any changes that could be attributed to patterns in scale dependence.

The macrofaunal sampling procedure, if treated differently, may also have yielded some interesting differences, given the tiny scales over which hydrothermal fluid flux can vary in sedimented vent systems. It is common practice to pool replicate cores from a single deployment, since these are considered to be pseudoreplicates (and generally, would yield too small a sample to be meaningful). However, in this case, had the samples been kept separate, there may have been some interesting differences observed even at the scale of the diameter of the coring device (ca. 50 cm). Future studies may consider either keeping separate cores from a deployment apart for subsequent analysis or using a larger coring device (e.g. a box core) and then examining the surface patchiness once the sample is recovered.

7.3.2 Constraining the food web

Despite the LIM approach proving to agree reasonably well with field manipulations, several criticisms of these models can be made. For instance, several of the data sources available did not effectively constrain the model. POC deposition rates in the Bransfield Strait vary widely spatially and sub-annually (Wefer et al. 1988, Wefer & Fischer 1991), resulting in upper and lower boundaries that accommodated a very wide range of possible fluxes (0.7 – 27.2 mmol C m^{-2} d^{-1}). However, the predicted range in POC deposition values between sites was still relatively narrow, suggesting that the models were still able to conserve a realistic set of values, despite the lack of constraint. This is because the constraints used in each LIM variously interact, either explicitly or implicitly to reduce the size of the solution space, and can thus mitigate increased uncertainty for particular variables, provided that these represent a minority of cases. These values also are informed by the stock sizes of the various organic compartments in the model (i.e. what is the required rate of input of A, B and C to sustain an assemblage of size X? see Equation 7.3.2a), and thus can be considered an averaged signal, over timescales that are equivalent to biomass turnover times. Total sediment community oxygen consumption was constrained by respiration rates measured during the tracing experiment but may not have very accurately represented true respiration rates, since the tracing experiment incubations were all performed at the same temperature, which is very unlikely to have been representative of the seafloor conditions at each site. Some suitable data were available from the Hakon-Mosby mud volcano in the Arctic Ocean (Felden et al. 2010) but ultimately these data were not included, as respiration rates were much higher than observed in the Bransfield Strait (Woulds et al. in prep.) and so were considered to be unrealistic for this particular set of models.

$$TotOM \geq \Sigma((I * A_e) - (R_m * B) - (R_e * B) - (G * NGE))$$

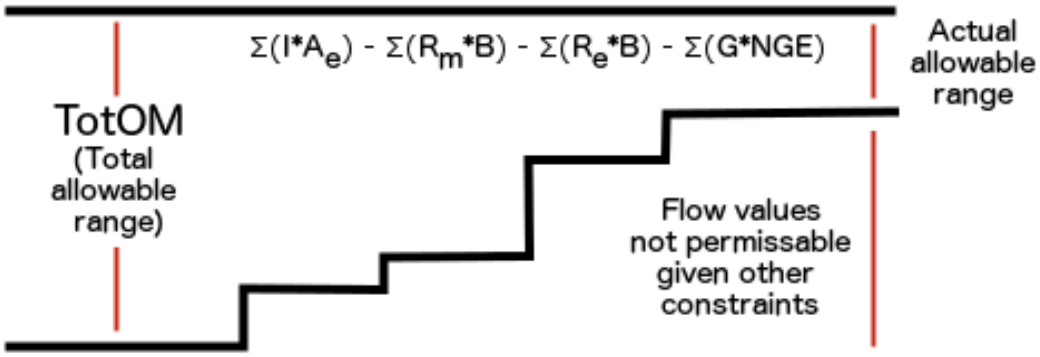

Equation 7.3.2a – Mass balance equation used by LIM to estimate total OM inputs to each model with conceptual graphic representation of effect of constraints. A_e = Assimilation Efficiency; B = Biomass; G = Growth; I = Intake; NGE = Net Growth Efficiency; R_e = Respiration through energy expenditure; R_m = Maintenance Respiration (i.e. minimum energy required to sustain cellular processes); TotOM = Total organic matter input.

A further criticism that could be made is that some of the external compartments were not explicitly constrained (e.g. DOC or External Predation), owing to a lack of appropriate data. In a LIM framework, if two or more of the equalities or inequalities (a.k.a. the constraints) are contradictory, the model will be unsolvable. The risk associated with having some compartments or flows poorly constrained is that this permits a larger solution space (the total extent of allowable solutions, where the number of dimensions is equal to the number of flows), and thus is likely to be less representative of the true situation (Figure 7.3.2a). Conversely, a model with a high number of equations that constrain the solution space is much more likely to either become over-determined (more equations than unknowns and only one solution possible) or simply unsolvable. As a consequence of this, and lack of data, it is usually the case that the ranges implemented for a specific constraint (e.g. efficiency of chemosynthetic carbon fixation from DIC to OM, 10 – 50 % in this case) are probably wider than are realistic for a particular ecosystem. The parsimony approach mitigates this concern to some degree, since all the constraints variously interact with each other, either directly or indirectly, and so even if a particular flow could have a wide range of values, the effective range (< ± 1 s.d. of the solution space

mean) should be much narrower (Figure 7.3.2a). Some constraints upon input and output rates to/from the DOC compartment existed (e.g. detrital dissolution or bacterial uptake) but no limits could be placed upon the initial stock size, thus the models lacked any data specific to the Bransfield Strait. At best, this just increases the uncertainty in between independent solutions. At worst, these externals may have acted to mitigate other, more constrained areas of the model that may otherwise have been contradictory. Despite these concerns, this approach still represented a valid way to address much of the uncertainty associated with SHV food webs and has demonstrated substantial variability in network structure associated with functional differences between assemblages. A possible future application of this framework would be to look at changes in network structure that may result from changing ocean temperatures and chemistry, particularly at cold seeps and peripheral areas, where temperature increases will also likely increase the flux of methane to the seafloor.

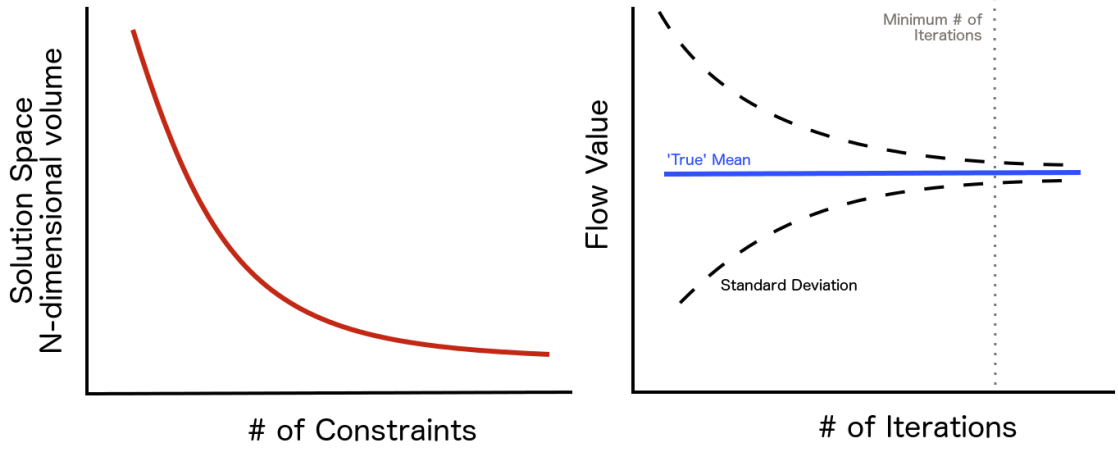

Figure 7.3.2a – Generalised changes in LIM characteristics with increasing numbers of constraints and iterations.

External predation, which could also not be captured during the tracer experiment, was the least well constrained of any compartment and varied widely between sites. This was likely owing to the fact that, once the model had accounted for C consumption through growth, respiration and production of detritus (constrained fluxes), any amount of left over faunal biomass could simply be partitioned as a loss to megafaunal predators, without causing a model imbalance. At both Hook Ridge 1 and the off-vent site, external predation accounted for a relatively small loss

compared to respiration and thus is unlikely to have very significantly influenced the carbon processing patterns suggested by their respectively models. However, at Hook Ridge 2, external predation was much higher (Woulds et al., in prep.) and this could feasibly be a product of the model attempting to unjustifiably partition left over carbon fluxes. If external predation was over-estimated in this case, it is therefore also possible that other mean estimates of fluxes from faunal compartments (e.g. detritus production) would have been under-estimated (or that the total input was over-estimated). These results in particular should be interpreted with caution and are likely to be an over-estimate. Possible other routes for this flux may have been increased detrital production and/or burial of organic carbon. Burial efficiency of organic carbon was constrained to 1 – 3 % of total OM inputs (Dunne et al. 2007), as in previous applications of this approach, but it is quite possible that hydrothermal activity also influences this flux, though no directly applicable measurements were found. Despite these concerns, the LIM framework is well suited to handling this uncertainty but it is still important, particularly where constraints are limited or not specific to the ecosystem of interest, to evaluate the possible sources of error in the model and acknowledge where confidence in the results is justified. This approach substantially increased the available information from what could be provided by the observed data alone (Chapter 4; 5, Bell et al. 2016c, Bell et al. 2016d), particularly given the complications associated with interpretation of the stable isotopic data.

7.4 Implications of this research

7.4.1 Southern Ocean Ecosystems

The research presented here into the Bransfield Strait SHVs is arguably the most comprehensive study of a sedimented vent system worldwide (Chapter 4; 5; 6, Bell et al. 2016c, Bell et al. 2016d, Woulds et al. in prep., Bell et al. submitted). It combines a suite of contemporary analyses that have considered the processes affecting ecological variability in terms of composition, trophodynamics, metabolic activity and biogeochemical cycling, for both microbial and metazoan groups. The Bransfield Strait studies, coupled with the South Georgia shelf study (Chapter 3, Bell

et al. 2016b) also provide valuable data on the distribution of fauna in the Southern Ocean, particularly with respect to reducing conditions. Thus, this project has significantly advanced our understanding of seafloor ecosystems from the Southern Ocean, as well as underpinning an improved process understanding of the factors affecting ecosystem variability in sedimented chemosynthetic ecosystems worldwide. One of the major differences between Southern Ocean SHVs and elsewhere pertains to temperature and this has important implications for the management of marine ecosystems in the Southern Ocean. Whilst the high-temperature, hard substratum vents on the East Scotia Ridge (ESR) appear relatively typical of other similar systems, at least at a process level, if not in terms of faunal composition (Marsh et al. 2012, Rogers et al. 2012, Reid et al. 2013), the SHV complex in the Bransfield Strait is demonstrably distinct from comparable systems in the Pacific. Production of chemosynthetic OM was clearly a highly important food source at the ESR vents, supporting vastly increased densities of megafauna compared with the surrounding area (Marsh et al. 2012, Rogers et al. 2012), whereas this was apparently not the case in the Bransfield Strait. Although total OM inputs were slightly higher at the vent sites (Woulds et al., in prep.), the expected concomitant changes in faunal density/ biomass were not observed, suggesting that the increased metabolic costs (total respiration higher at vent sites) associated with the vent habitat meant that this extra source of OM had no net benefit (or maybe even a net loss) for faunal energetic budgets. Additionally, aside from *S. contortum*, no vent-endemic fauna were observed and many of the more abundant taxa were found elsewhere in the strait, just at much lower relative abundances (Chapter 4, Bell et al. 2016d). It seems likely that the Bransfield Strait SHVs (at least in the areas sampled during JC55) were simply too low in productivity to support large vent endemic fauna and provide a valuable increase to local OM stocks. Therefore, in terms of environmental management, if hydrothermal vents are considered important for their contribution to regional biodiversity and in supporting unique assemblages with substantial inputs of OM, then the Bransfield Strait SHVs, whilst potentially an important site for geodiversity, are arguably not important to the vast majority of the benthos in the Bransfield Strait. This is not to say that these ecosystems are not valuable. For example, Hook Ridge is putatively an important source of water column Fe and Mn (Aquilina et al. 2014) and, particularly in the

context of Southern Ocean surface ocean iron deficiency, provides important ecosystem services to the surface ocean and the wider climate, but the extent to which these services would continued to be provided in the absence of the resident fauna is debatable (Aquilina et al. 2014, Chapter 3, Bell et al. 2016b).

7.4.2 Spatial extent of hydrothermal activity

One suggestion made here which raises a number of questions about benthic carbon cycling, is the surprisingly large footprint that hydrothermal circulation around Hook Ridge may have had. If the limited evidence for isotopic data being subject only to small shifts in $\delta^{13}C$ signatures is genuinely representative of the wider sample set, then it is possible that hydrothermal contribution to the food web was traceable, taxonomically and isotopically, throughout the basin. Although the importance of this chemosynthetic OM was undoubtedly very low, compared to the diets of fauna at Hook Ridge, the extent of the production was much greater and occurred at distances in excess of 100km from the site of active hydrothermal flux. Since very little is known about the true spatial footprint of any seafloor chemosynthetic environment, sedimented vents included, these results raise the question of just how important is chemosynthesis to benthic food webs? Even in shallow waters, it is being realised that chemosynthetic OM is far more widely utilised than previously recognised (Higgs et al. 2016) and this places serious uncertainties upon our understanding of seafloor biogeochemical cycling and of the OM sources underpinning benthic food webs. Oceanic trenches are one suggested place where chemosynthesis may be much more prevalent than previously recognised, particularly in oligotrophic areas where measurements of sediment community oxygen consumption are apparently not reconcilable with suggested inputs of surface-derived OM. Hadal seeps have previously been identified in the Japan Trench (Juniper & Sibuet 1987) and hydrothermal vents are common around subduction zones. It is therefore perhaps not unreasonable to suggest that chemosynthetic activity has significant potential to underpin these isolated and ultra-deep food webs. Interest in hadal biology is currently constrained by technical capacity but this could certainly be a fruitful area of future research.

This project has also demonstrated that, in addition to the surprising extent of chemosynthetic activity, it significantly influences biogeochemical cycling (Figure 6.3.2a). This is the first time that this has been studied in SCEs and, whilst a number of parallels can be drawn with other deep-sea ecosystems, the food webs within SCEs are quite distinct and uncharacteristic of other areas of the deep-seafloor in the way that energy enters the system, how it is partitioned within the system and how effectively it is utilised. In the Bransfield Strait, the energetic costs associated with vent habitats mean than carbon is used less efficiently (this may also be a contributing factor to the lower biomass observed). Temperature is usually not a consideration for most deep-sea ecosystems, although it is widely acknowledged to be a major driver of sediment community oxygen consumption. However, in hydrothermal sediments (or other similar systems e.g. mud volcanoes), it is clear that temperature is an important factor in controlling biological energy budgets. This places these ecosystems into the framework of the metabolic theory of ecology (MTE) (Gillooly et al. 2001, McClain et al. 2012) and starts to address the uncertainty, at the level of individual faunal groups and whole ecosystems, of how deep-sea ecosystems respond to differences in temperature. The limited evidence available for individual level responses suggest that MTE relatively poorly explains their characteristics, both in terms of metabolic and growth rates, compared with other deep-sea invertebrates (McClain et al. 2012). Environmental toxicity may also be considered as a controlling factor in ecosystem dynamics (Chapter 3, Bell et al. 2016b) and although we were not able to gather as detailed data for the South Georgia shelf as for the Bransfield Strait during this project, largely owing to time constraints, there was still substantial geochemical and biological evidence of differences between this area and background sediments (Chapter 3, Bell et al. 2016b). In this case, even comparatively minor changes to sediment geochemistry resulted in major shifts in assemblage composition, and physical habitat structure (Belchier et al. 2004). Chemosynthesis is clearly an important process in deep-sea ecosystems and has the potential to fundamentally restructure the physiology, behaviour and composition of resident biota.

8. Conclusions

In this project, I have significantly advanced the understanding of the ecology of sedimented chemosynthetic ecosystems in the Southern Ocean, and drawn a number of parallels with comparable ecosystems from elsewhere in the global ocean. This project has developed several contemporary themes in marine ecology, such as: highlighting the importance of biogeographic constraints in the distribution of faunal communities around SCEs; demonstrating the widespread influence of chemosynthetic organic matter production and elucidating the impacts of hydrothermal circulation upon functional diversity and carbon processing patterns in seafloor environments.

The evidence of biogeographic or regional factors in controlling community responses to habitat variability is important since it underscores the case for considering multiple levels of extrinsic processes when designing and implementing management strategies for sedimented chemosynthetic ecosystems. These ecosystems provide several important services, some of which are mediated by their biological communities and should not be overlooked when predicting future climactic changes. Furthermore, this project presents evidence that the extent of SCEs may be seriously under-estimated, adding to a growing body of research that is questioning the importance of chemosynthetic activity on the seafloor. Contemporary isotopic and analytic techniques, such as those demonstrated in this thesis, will be of critical value to further developing understanding of these processes and the dynamics of seafloor ecosystems.

9. References

Introduction, methods and discussion only. Reference lists for individual papers are given at the end of their respective chapters

Amon DJ, Glover AG, Wiklund H, Marsh L, Linse K, Rogers AD, Copley JT (2013) The discovery of a natural whale fall in the Antarctic deep sea. Deep Sea Research Part II: Topical Studies in Oceanography 92:87-96

Anderson MJ (2001) A new method for non-parametric multivariate analysis of variance. Austral Ecology 26:32-46

Aquilina A, Connelly DP, Copley JT, Green DR, Hawkes JA, Hepburn L, Huvenne VA, Marsh L, Mills RA, Tyler PA (2013) Geochemical and Visual Indicators of Hydrothermal Fluid Flow through a Sediment-Hosted Volcanic Ridge in the Central Bransfield Basin (Antarctica). Plos One 8:e54686

Aquilina A, Homoky WB, Hawkes JA, Lyons TW, Mills RA (2014) Hydrothermal sediments are a source of water column Fe and Mn in the Bransfield Strait, Antarctica. Geochimica et Cosmochimica Acta 137:64-80

Barnard JL, Karaman GS (1991) The families and genera of marine gammaridean Amphipoda (except marine gammaroids). Part 2. Records of the Australian Museum, Supplement 13:419-866

Baselga A, Orme D, Villeger S (2013) Package 'betapart'. cranr-projectorg

Bates AE, Lee RW, Tunnicliffe V, Lamare MD (2010) Deep-sea hydrothermal vent animals seek cool fluids in a highly variable thermal environment. Nat Commun 1:14

Beesley PL, Ross GJB, Glasby C (2000) Polychaetes & Allies: The Southern Synthesis. *Fauna of Australia Vol. 4A Polychaeta, Myzostomida, Pogonophora, Echiura, Spincula*. CSIRO, Melbourne

Belchier M, Purves M, Marlow T, Szlakowski J, Collins M, Hawkins S, Mitchell R, Xavier J, Black A (2004) FPRV *Dorada* cruise DOSG04: South Georgia Groundfish Survey, 6th January - 10th February 2004. A report to the Government of South Georgia and the South Sandwich Islands

Bell JB (2014) Greenhouse gas deposits in the deep sea. Geology Today 30

Bell JB, Alt CHS, Jones DOB (2016a) Benthic megafauna on steep slopes at the northern Mid-Atlantic Ridge. Marine Ecology:maec 12319

Bell JB, Aquilina A, Woulds C, Glover AG, Little CTS, Reid WDK, Hepburn LE, Newton J, Mills RA (2016b) Geochemistry, faunal composition and trophic structure at an area of weak methane seepage on the southwest South Georgia margin. Royal Society Open Science 3

Bell JB, Reid WDK, Pearce DA, Glover AG, Sweeting CJ, Newton J, Woulds C (2016c) Hydrothermal activity lowers trophic diversity in Antarctic sedimented hydrothermal vents. Biogeosciences Discussions

Bell JB, Woulds C, Brown LE, Little CTS, Sweeting CJ, Reid WDK, Glover AG (2016d) Macrofaunal ecology of sedimented hydrothermal vents in the Bransfield Strait, Antarctica. Frontiers in Marine Science 3:32

Bell JB, Woulds C, van Oevelen D (submitted) Hydrothermal activity, functional diversity and chemoautotrophy are major drivers of seafloor carbon cycling.

Berg IA, Kockelkorn D, Ramos-Vera WH, Say RF, Zarzycki J, Hugler M, Alber BE, Fuchs G (2010) Autotrophic carbon fixation in archaea. Nat Rev Microbiol 8:447-460

Bernardino AF, Levin LA, Thurber AR, Smith CR (2012) Comparative Composition, Diversity and Trophic Ecology of Sediment Macrofauna at Vents, Seeps and Organic Falls. Plos ONE 7:e33515

Bohrmann G, Chin C, Petersen S, Sahling H, Schwarz-Schampera U, Greinert J, Lammers S, Rehder G, Dählmann A, Wallmann K, Dijkstra S, Schenke HW (1998) Hydrothermal activity at Hook Ridge in the Central Bransfield Basin, Antarctica. Geo-Marine Letters 18:277-284

Breitsprecher K, Thorkelson DJ (2009) Neogene kinematic history of Nazca–Antarctic–Phoenix slab windows beneath Patagonia and the Antarctic Peninsula. Tectonophysics 464:10-20

Brown LE, Milner AM, Hannah DM (2010) Predicting river ecosystem response to glacial meltwater dynamics: a case study of quantitative water sourcing and glaciality index approaches. Aquatic Sciences 72:325-334

Canfield DE (2001) Isotope fractionation by natural populations of sulfate-reducing bacteria. Geochimica Et Cosmochimica Acta 65:1117-1124

Caut S, Angulo E, Courchamp F (2009) Variation in discrimination factors (Δ15N and Δ13C): the effect of diet isotopic values and applications for diet reconstruction. Journal of Applied Ecology 46:443-453

Chikaraishi Y, Ogawa NO, Kashiyama Y, Takano Y, Suga H, Tomitani A, Miyashita, H., Kitazato H, Ohkouchi N (2009) Determination of aquatic food-web structure based in compound-specific nitrogen isotopic composition of amino acids. Limnology & Oceanography: Methods 7:740-750

Clarke A (2008) Antarctic marine benthic diversity: patterns and processes. Journal of Experimental Marine Biology and Ecology 366:48-55

Clarke A, Crame JA (1992) The Southern Ocean Benthic Fauna and Climate Change: A Historical Perspective. Philosophical Transactions of the Royal Society B-Biological Sciences 338:299-309

Clarke A, Crame JA (2010) Evolutionary dynamics at high latitudes: speciation and extinction in polar marine faunas. Philosophical transactions of the Royal Society B-Biological sciences 365:3655-3666

Clarke A, Griffiths HJ, Barnes DKA, Meredith MP, Grant SM (2009) Spatial variation in seabed temperatures in the Southern Ocean: Implications for benthic ecology and biogeography. Journal of Geophysical Research 114:1-11

Corliss JB, Ballard RD (1977) Oases of Life in the Cold Abyss. National Geographic Magazine 152:441-453

Dählmann A, Wallman K, Sahling H, Sarthou G, Bohrmann G, Petersen S, Chin CS, Klinkhammer GP (2001) Hot vents in an ice-cold ocean: Indications for phase separation at the southernmost area of hydrothermal activity, Bransfield Strait, Antarctica. Earth and Planetary Science Letters 193:381-394

Dubilier N, Bergin C, Lott C (2008) Symbiotic diversity in marine animals: the art of harnessing chemosynthesis. Nature Reviews Microbiology 6:725-740

Dunne JP, Sarmiento JL, Gnanadesikan A (2007) A synthesis of global particle export from the surface ocean and cycling through the ocean interior and on the seafloor. Global Biogeochemical Cycles 21:n/a-n/a

Fauchald K (1977) The Polychaete Worms: Definitions and Keys to the Orders, Families and Genera, Natural History Museum of Los Angeles County

Fauchald K, Jumars PA (1979) The Diet of Worms: A Study of Polychaete Feeding Guilds. Oceanography and Marine Biology: An Annual Review 17:193-284
Felden J, Wenzhoefer F, Feseker T, Boetius A (2010) Transport and consumption of oxygen and methane in different habitats of the Hakon Mosby Mud Volcano (HMMV). Limnology and Oceanography 55:2366-2380
Fox J, Weisberg S (2011) An R companion to applied regression. SAGE Publications, California
Fry B (2006) Stable Isotope Ecology. In: Fry B (ed). Springer
Gage JD, Tyler PA (1991) Deep-Sea Biology: A Natural History of Organisms at the Deep-Sea Floor. Cambridge University Press
Gebruk A, Chevaldonne P, Shank TM, Lutz RA, Vrijenhoek RC (2000) Deep-sea hydrothermal vent communities of the Logatchev area (14°45'N, Mid-Atlantic Ridge): diverse biotopes and high biomass. Journal of the Marine Biological Association of the United Kingdom 80:383-393
George JD (1976) Ecology of the Pogonophore, *Siboglinum fiordicum* Webb, in a shallow-water fjord community. In: Keegan BF, Boaden PJS, Ceidigh PO (eds) Biology of Benthic Organisms: 11th European Symposium on Marine Biology. Elsevier, Galway
Georgieva M, Wiklund H, Bell JB, Eilersten MH, Mills RA, Little CTS, Glover AG (2015) A chemosynthetic weed: the tubeworm *Sclerolinum contortum* is a bipolar, cosmopolitan species. BMC Evolutionary Biology 15:280
Geprägs P, Torres ME, Mau S, Kasten S, Römer M, Bohrmann G (2016) Carbon cycling fed by methane seepage at the shallow Cumberland Bay, South Georgia, sub-Antarctic. Geochemistry, Geophysics, Geosystems 17:1401-1418
German CR, Ramirez-Llodra E, Baker MC, Tyler PA, and the ChEss Scientific Steering C (2011) Deep-Water Chemosynthetic Ecosystem Research during the Census of Marine Life Decade and Beyond: A Proposed Deep-Ocean Road Map. PLoS ONE 6:e23259
Gillooly JF, Brown JH, West GB, Savage VM, Charnov EL (2001) Effects of size and temperature on metabolic rate. Science 293:2248-2251
Ginsburg GD, Milkov AV, Soloviev VA, Egorov AV, Cherkashev GA, Vogt PR, Crane K, Lorenson TD, Khutorsky MD (1999) Gas hydrate accumulation at the Håkon Mosby Mud Volcano. Geo-Marine Letters 19:57-67
Habicht KS, Canfield DE (1997) Sulfur isotope fractionation during bacterial sulfate reduction in organic-rich sediments. Geochimica Et Cosmochimica Acta 61:5351-5361
Hauquier F, Ingels J, Gutt J, Raes M, Vanreusel A (2011) Characterisation of the nematode community of a low-activity cold seep in the recently ice-shelf free Larsen B area, Eastern Antarctic Peninsula. PLoS One 6:e22240
Higgs ND, Newton J, Attrill MJ (2016) Caribbean Spiny Lobster Fishery is Underpinned by Trophic Subsidies from Chemosynthetic Primary Production. Current Biology
House CH, Schopf JW, Stetter KO (2003) Carbon isotopic fractionation by Archaeans and other thermophilic prokaryotes. Organic Geochemistry 34:345-356
Hugler M, Petersen JM, Dubilier N, Imhoff JF, Sievert SM (2011) Pathways of carbon and energy metabolism of the epibiotic community associated with the deep-sea hydrothermal vent shrimp Rimicaris exoculata. PLoS One 6:e16018
Hugler M, Sievert SM (2011) Beyond the Calvin cycle: autotrophic carbon fixation in the ocean. Annual review of marine science 3:261-289

Jannasch J, Mottl MJ (1985) Geomicrobiology of Deep-Sea Hydrothermal Vents. Science 229:717-725
Jumars PA, Dorgan KM, Lindsay SM (2015) Diet of worms emended: an update of polychaete feeding guilds. Annual review of marine science 7:497-520
Juniper SK, Martineu P (1995) Alvinellids and Sulfides at Hydrothermal Vents of the Eastern Pacific: A Review. American Zoologist 35:174-185
Juniper SK, Sibuet M (1987) Cold seep benthic communities in Japan subduction zones: spatial organisation, trophic strategies and evidence for temporal evolution. Marine Ecology Progress Series 40:115-126
Kastner M, Kvenvolden KA, Lorenson TD (1998) Chemistry, isotopic composition, and origin of a methane-hydrogen sulfide hydrate at the Cascadia Subduction Zone. Earth and Planetary Science Letters 156:173-183
Kawagucci S, Ueno Y, Takai K, Toki T, Ito M, Inoue K, Makabe A, Yoshida N, Muramatsu Y, Takahata N, Sano Y, Narita T, Teranishi G, Obata H, Nakagawa S, Nunoura T, Gamo T (2013) Geochemical origin of hydrothermal fluid methane in sediment-associated fields and its relevance to the geographical distribution of whole hydrothermal circulation. Chemical Geology 339:213-225
Kilgallen NH (2007) Taxonomy of the Lysianassoidea of the Northeast Alantic and Mediterranean: An Interactive Identification Key and Studies on Problematic Groups. PhD Thesis
Kim D, Kim D-Y, Park J-S, Kim Y-J (2005) Interannual variation of particle fluxes in the eastern Bransfield Strait, Antarctica: A response to the sea ice distribution. Deep Sea Research Part I: Oceanographic Research Papers 52:2140-2155
Klinkhammer GP, Chin CS, Keller RA, Dahlmann A, Sahling H, Sarthou G, Petersen S, Smith F (2001) Discovery of new hydrothermal vent sites in Bransfield Strait, Antarctica. Earth and Planetary Science Letters 193:395-407
Kvenvolden KA (1993) Gas Hydrates - Geological Perspective and Global Change. Reviews of Geophysics 31:173-187
Levesque C, Limén H, Juniper SK (2005) Origin, composition and nutritional quality of particulate matter at deep-sea hydrothermal vents on Axial Volcano, NE Pacific. Marine Ecology Progress Series 289:43-52
Levin LA (2005) Ecology of Cold Seep Sediments: Interactions of Fauna with flow, chemistry and microbes. Oceanography and Marine Biology: An Annual Review 43:1-46
Levin LA, Baco AR, Bowden D, Colaço A, Cordes E, Cunha MR, Demopoulos A, Gobin J, Grupe B, Le J, Metaxas A, Netburn A, Rouse GW, Thurber AR, Tunnicliffe V, Van Dover C, Vanreusel A, Watling L (2016a) Hydrothermal Vents and Methane Seeps: Rethinking the Sphere of Influence. Frontiers in Marine Science 3:72
Levin LA, James DW, Martin CM, Rathburn AE, Harris LH, Michener RH (2000) Do methane seeps support distinct macrofaunal assemblages? Observations on community structure and nutrition from the northern California slope and shelf. Marine Ecology Progress Series 208:21-39
Levin LA, Mendoza GF (2007) Community structure and nutrition of deep methane-seep macrobenthos from the North Pacific (Aleutian) Margin and the Gulf of Mexico (Florida Escarpment). Marine Ecology 28:131-151

Levin LA, Mendoza GF, Gonzalez JP, Thurber AR, Cordes EE (2010) Diversity of bathyal macrofauna on the northeastern Pacific margin: the influence of methane seeps and oxygen minimum zones. Marine Ecology 31:94-110
Levin LA, Mendoza GF, Grupe BM (2016b) Methane seepage effects on biodiversity and biological traits of macrofauna inhabiting authigenic carbonates. Deep Sea Research Part II: Topical Studies in Oceanography
Levin LA, Mendoza GF, Grupe BM, Gonzalez JP, Jellison B, Rouse G, Thurber AR, Waren A (2015) Biodiversity on the Rocks: Macrofauna Inhabiting Authigenic Carbonate at Costa Rica Methane Seeps. PLoS One 10:e0131080
Levin LA, Mendoza GF, Konotchick T, Lee R (2009) Macrobenthos community structure and trophic relationships within active and inactive Pacific hydrothermal sediments. Deep Sea Research Part II: Topical Studies in Oceanography 56:1632-1648
Levin LA, Ziebis W, Mendoza GF, Bertics VJ, Washington T, Gonzalez J, Thurber AR, Ebbed B, Lee RW (2013) Ecological release and niche partitioning under stress: Lessons from dorvilleid polychaetes in sulfidic sediments at methane seeps. Deep-Sea Research Part II-Topical Studies in Oceanography 92:214-233
Levin SA (1992) The Problem of Pattern and Scale in Ecology. Ecology 73:1943-1967
Marsh L, Copley JT, Huvenne VAI, Linse K, Reid WDK, Rogers AD, Sweeting CJ, Tyler PA (2012) Microdistribution of Faunal Assemblages at Deep-Sea Hydrothermal Vents in the Southern Ocean. PloS ONE 7:e48348
Marsh L, Copley JT, Tyler PA, Thatje S (2015) In hot and cold water: differential life-history traits are key to success in contrasting thermal deep-sea environments. The Journal of animal ecology
Martineu P, Juniper SK, Fisher CR, Massoth GJ (1997) Sulfide binding in the Body Fluids of Hydrothermal Vent Alvinellid Polychaetes. Physiological Zoology 70:578-588
McClain CR, Allen AP, Tittensor DP, Rex MA (2012) Energetics of Life on the deep seafloor. Proceedings of the National Academy of Sciences of the United States of America 109:15366-15731
Oksanen J, Blanchet GG, Kindt R, Legendre P, Minchin PR, O'Hara RB, Simpson GL, Solymos P, Stevens HH, Wagner H (2013) Package 'vegan'. cranr-projectorg
Parnell AC, Jackson AL (2013) Package 'siar'. cranr-projectorg
Phillips DL, Gregg JW (2003) Source partitioning using stable isotopes: coping with too many sources. Oecologia 136:261-269
Phillips DL, Inger R, Bearhop S, Jackson AL, Moore JW, Parnell AC, Semmens BX, Ward EJ (2014) Best practices for use of stable isotope mixing models in food-web studies. Canadian Journal of Zoology 92:823-835
Poore GCB (2001) Isopoda Valvifera: Diagnoses and Relationships of the Families. Journal of Crustacean Biology 21:205-230
R Core Team (2013) R: A Language and environment for statistical computing. R Foundation for Statistical Computing, Vienna, Austria http://www.R-project.org/.
Reed AJ, Morris JP, Linse K, Thatje S (2013) Plasticity in shell morphology and growth among deep-sea protobranch bivalves of the genus *Yoldiella* (Yoldiidae) from contrasting Southern Ocean regions. Deep Sea Research Part I: Oceanographic Research Papers 81:14-24

Reid WDK, Bell JB, Sweeting CJ, Woulds C, Wigham BD (invited review in prep.) Elucidating trophodynamics at hydrothermal vents using stable isotope analysis.

Reid WDK, Sweeting CJ, Wigham BD, Zwirglmaier K, Hawkes JA, McGill RAR, Linse K, Polunin NVC (2013) Spatial Differences in East Scotia Ridge Hydrothermal Vent Food Webs: Influences of Chemistry, Microbiology and Predation on Trophodynamics. Plos One 8

Robertson BP, Gardner JPA, Savage C (2015) Macrobenthic–mud relations strengthen the foundation for benthic index development: A case study from shallow, temperate New Zealand estuaries. Ecological Indicators 58:161-174

Rodrigues CF, Hilário A, Cunha MR (2013) Chemosymbiotic species from the Gulf of Cadiz (NE Atlantic): distribution, life styles and nutritional patterns. Biogeosciences 10:2569-2581

Rogers AD, Alker BJ, Aquilina A, Clarke A, Connelly DP, Copley J, Dinley J, German C, Graham AG, Green D, Hawkes JA, Hepburn L, Huvenne VA, James R, Linse K, Marsh L, Reid WDK, Roterman CN, Sweeting CJ, Thatje S, Zwirglmaier K (2010) RRS James Cook Cruise 42: Chemosynthetic Ecosystems of the Southern Ocean. Cruise Report

Rogers AD, Tyler PA, Connelly DP, Copley JT, James R, Larter RD, Linse K, Mills RA, Garabato AN, Pancost RD, Pearce DA, Polunin NVC, German CR, Shank T, Boersch-Supan PH, Alker BJ, Aquilina A, Bennett SA, Clarke A, Dinley RJJ, Graham AGC, Green DRH, Hawkes JA, Hepburn L, Hilario A, Huvenne VAI, Marsh L, Ramirez-Llodra E, Reid WDK, Roterman CN, Sweeting CJ, Thatje S, Zwirglmaier K (2012) The Discovery of New Deep-Sea Hydrothermal Vent Communities in the Southern Ocean and Implications for Biogeography. PLoS Biology 10:e1001234

Römer M, Torres M, Kasten S, Kuhn G, Graham AGC, Mau S, Little CTS, Linse K, Pape T, Geprägs P, Fischer D, Wintersteller P, Marcon Y, Rethemeyer J, Bohrmann G (2014) First evidence of widespread active methane seepage in the Southern Ocean, off the sub-Antarctic island of South Georgia. Earth and Planetary Science Letters 403:166-177

Roterman CN, Copley JT, Linse KT, Tyler PA, Rogers AD (2013) The biogeography of the yeti crabs (Kiwaidae) with notes on the phylogeny of the Chirostyloidea (Decapoda: Anomura). Proceedings of the Royal Society B-Biological Sciences 280

Rozemarjin K, Christoffer S, Anders KJ, Endre W (2011) Ecology of twelve species of Thyasiridae (Mollusca: Bivalvia). Mar Pollut Bull 62:786-791

Sahling H, Galkin SV, Salyuk A, Greinert J, Foerstel H, Piepenburg D, Suess E (2003) Depth-related structure and ecological significance of cold-seep communities - a case study from the Sea of Okhotsk. Deep-Sea Research Part I-Oceanographic Research Papers 50:1391-1409

Sahling H, Wallman K, Dählmann A, Schmaljohann R, Petersen S (2005) The physicochemical habitat of *Sclerolinum sp.* at Hook Ridge hydrothermal vent, Bransfield Strait, Antarctica. Limnology & Oceanography 50:598-606

Schwedt A, Kreutzmann AC, Polerecky L, Schulz-Vogt HN (2011) Sulfur respiration in a marine chemolithoautotrophic beggiatoa strain. Frontiers in microbiology 2:276

Soetaert K, van Oevelen D (2008) LIM: Linear Inverse Model examples and solutions methods. R Package v1.2

Southward A, J., Southward EC, Brattegard T, Bakke T (1979) Further Experiments on the value of Dissolved Organic Matter as Food for *Siboglinum fjiordicum* (Pogonophora). Journal of Marine Biological Asociation of the United Kingdom 59:133-148

Southward EC, Gebruk A, Kennedy H, Southward AJ, Chevaldonne P (2001) Different energy sources for three symbiont-dependent bivalve molluscs at the Logatchev hydrothermal site (Mid-Atlantic Ridge). Journal of Marine Biological Asociation of the United Kingdom 81:655-661

Sweetman AK, Levin LA, Rapp HT, Schander C (2013) Faunal trophic structure at hydrothermal vents on the southern Mohn's Ridge, Arctic Ocean. Marine Ecology Progress Series 473:115

Thornhill DJ, Wiley AA, Campbell AL, Bartol FF, Teske A, Halanych KM (2008) Endosymbionts of *Siboglinum fjordicum* and the Phylogeny of Bacterial Endosymbionts in Siboglinidae (Annelida). Biological Bulletin 214:135-144

Tyler PA, Connelly DP, Copley JT, Linse K, Mills RA, Pearce DA, Aquilina A, Cole C, Glover AG, Green DR, Hawkes JA, Hepburn L, Herrera S, Marsh L, Reid WD, Roterman CN, Sweeting CJ, Tate A, Woulds C, Zwirglmaier K (2011) RRS *James Cook* cruise JC55: Chemosynthetic Ecosystems of the Southern Ocean. BODC Cruise Report

van Oevelen D, Bergman MJN, Soetaert K, Bauerfeind E, Hasemann C, Klages M, Schewe I, Soltwedel T, Budaeva NE (2011a) Carbon flows in the benthic food web at the deep-sea observatory HAUSGARTEN (Fram Strait). Deep Sea Research Part I 58:1069-1083

van Oevelen D, Soetaert K, Garcia R, de Stigter HC, Cunha MR, Pusceddu A, Danovaro R (2011b) Canyon conditions impact carbon flows in food webs of three sections of the Nazaré canyon. Deep Sea Research Part II: Topical Studies in Oceanography 58:2461-2476

van Oevelen D, Soetaert K, Heip C (2012) Carbon flows in the benthic food web of the Porcupine Abyssal Plain: The (un)importance of labile detritus in supporting microbial and faunal carbon demands. Limnology & Oceanography 57:645-664

van Oevelen D, Van den Meersche K, Meysman FJR, Soetaert K, Middelburg JJ, Vézina AF (2009) Quantifying Food Web Flows Using Linear Inverse Models. Ecosystems 13:32-45

Vérard C, Flores K, Stampfli G (2012) Geodynamic reconstructions of the South America–Antarctica plate system. Journal of Geodynamics 53:43-60

Walker BD, McCarthy MD, Fisher AT, Guilderson TP (2008) Dissolved inorganic carbon isotopic composition of low-temperature axial and ridge-flank hydrothermal fluids of the Juan de Fuca Ridge. Marine Chemistry 108:123-136

Wefer G, Fischer G (1991) Annual primary production and export flux in the Southern Ocean from sediment trap data. Marine Chemistry 35:597-613

Wefer G, Fischer G, Fuetterer D, Gersonde R (1988) Seasonal particle flux in the Bransfield Strait, Antarctica. Deep-Sea Research 35:891-898

Whitaker D, Christmann M (2013) Package 'clustsig'. cranr-projectorg

Whiticar MJ, Suess E (1990) Hydrothermal hydrocarbon gases in the sediments of the King George Basin, Bransfield Strait, Antarctica. Applied Geochemistry 5:135-147

Winogradsky S (1887) Über Schwefelbakterien. Botanische Zeitung 45:489-610

Wood WT, Jung WY Modeling the extent of the Earth's methane hydrate cryosphere. Proc Proceedings of the 6th International Conference on Gas Hydrates. University of British Columbia

Woulds C, Bell JB, Brown L, Pancost RD, Bouillon S, Tyler PA (in prep.) An isotope tracing experiment in Southern ocean hydrothermal sediments.

Young JN, Bruggeman J, Rickaby REM, Erez J, Conte M (2013) Evidence for changes in carbon isotopic fractionation by phytoplankton between 1960 and 2010. Global Biogeochemical Cycles 27:505-515